Expanding the catalytic activity of amine dehydrogenases

Rational enzyme engineering via computational analysis and application in organic synthesis

Tseliou, V.

Publication date
2020

Document Version
Final published version

License
Other

[Link to publication](#)

EXPANDING THE CATALYTIC ACTIVITY OF AMINE DEHYDROGENASES: RATIONAL ENZYME ENGINEERING VIA COMPUTATIONAL ANALYSIS AND APPLICATION IN ORGANIC SYNTHESIS

VASILEIOS TSELIOU

Expanding the catalytic activity of amine dehydrogenases: rational enzyme engineering via computational analysis and application in organic synthesis
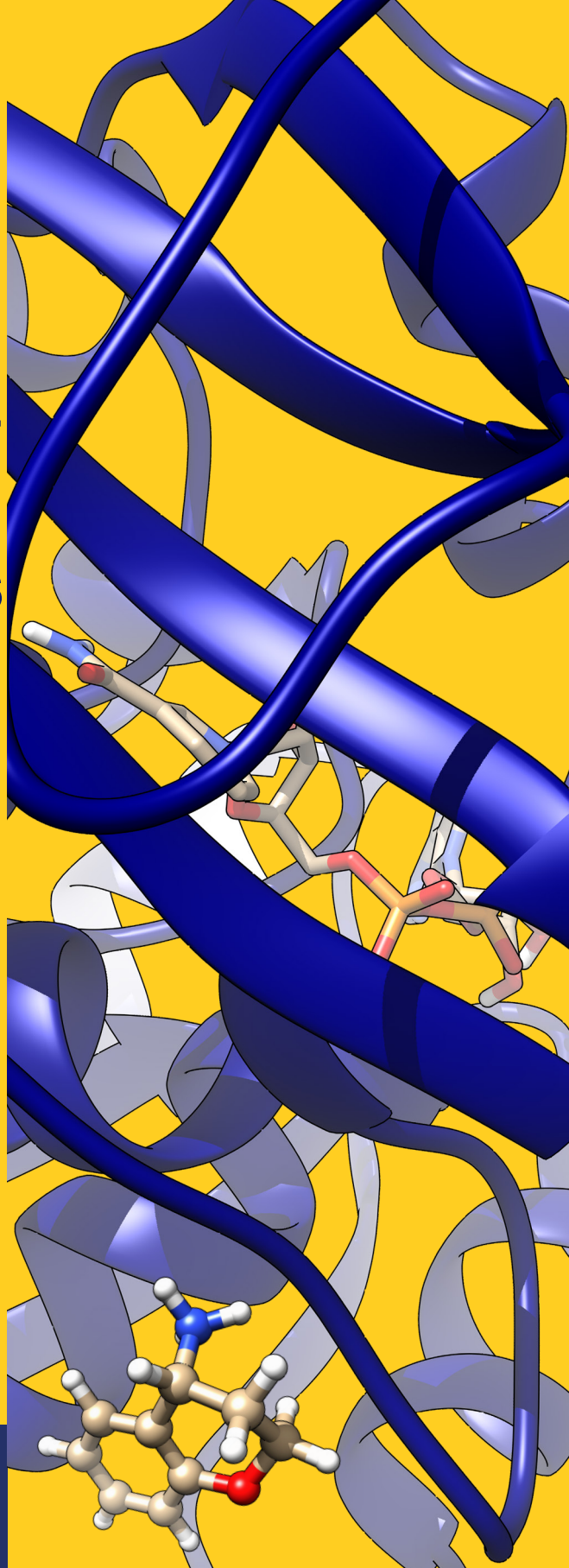
Tseliou Vasileios

2020

Expanding the catalytic activity of amine dehydrogenases: rational enzyme engineering via computational analysis and application in organic synthesis

ACADEMISCH PROEFSCHRIFT

ter verkrijging van de graad van doctor

aan de Universiteit van Amsterdam

op gezag van de Rector Magnificus

prof. dr. ir. K.I.J. Maex

ten overstaan van een door het College voor Promoties ingestelde commissie,

in het openbaar te verdedigen

op dinsdag 12 mei 2020, te 12:00 uur

door

Vasileios Tseliou

geboren te Rodos

Promotiecommissie:

| Promotores: | dr. F. G. Mutti | Universiteit van Amsterdam |
| | Prof. dr. J. H. van Maarseveen | Universiteit van Amsterdam |

Overige leden:	Prof. dr. R. Wever	Universiteit van Amsterdam
	Prof. dr. T.N. Grossmann	VU Amsterdam
	Prof. dr. S. Brul	Universiteit van Amsterdam
	dr. I.V. Pavlidis	University of Crete
	dr. M. A. Fernández Ibáñez	Universiteit van Amsterdam

Faculteit der Natuurwetenschappen, Wiskunde en Informatica (FNWI)

'Η Ιθάκη σ' έδωσε τ'ωραίο ταξίδι.

Χωρίς αυτήν δεν θα 'βγαινες στον δρόμο.

Αλλά δέν έχει να σε δώσει πια.

Κι αν πτωχική την βρείς, η Ιθάκη δεν σε γέλασε.

Έτσι σοφός που έγινες, με τόση πείρα,

ήδη θα κατάλαβες οι Ιθάκες τι σημαίνουν.'

Κωνσταντίνος Π. Καβάφης (1863-1933)

'Ithaka gave you the beautiful journey.

without her you wouldn't have set out.

But there's nothing else to give you anymore.

And if you find her poor, Ithaka won't have fooled you.

Wise as you will have become, so full of experience,

you'll have understood by then what these Ithakas mean.'

Constantine P. Cavafy (1863-1933)

Table of Contents

List of abbreviations

AADH	Amino acid dehydrogenase
AAP	4-aminoantipyrine
ADH	Alcohol dehydrogenase
AlaDH	Alanine dehydrogenase
AmDH	Amine dehydrogenase
API	Active pharmaceutical ingredient
Cb-FDH	Formate dehydrogenase from *Candida boidinii*
CTA	Chromotropic acid
DCM	Dichloromethane
DKR	Dynamic kinetic resolution
DMSO	Dimethyl sulfoxide
E. coli	*Escherichia coli*
ee	Enantiomeric excess
EtOAc	Ethyl acetate
FAD	Flavin adenine dinucleotide
FDA	Food and drug administration
FDH	Formate dehydrogenase
GC	Gas cromatography
GDH	Glucose Dehydrogenase
GST	Glutathione S-transferase
HEPES	4-(2-hydroxyethyl)-1-piperazineethanesulfonic acid
HPLC	High pressure liquid chromatography
HRP	Horseradish peroxidase
IPTG	Isopropyl β-D-thiogalactoside
IS	Internal standard
KPi	Phosphate buffer
KR	Kinetic resolution
LB	Lysogeny broth medium
LDH	Lactate Dehydrogenase
LE-AmDH	Variant of L-lysine ε-dehydrogenase from *Geobacillus stearothermophilus*
LysEDH	L-lysine ε-dehydrogenase from *Geobacillus stearothermophilus*
MAO	Monoamine oxidase
MD	Molecular dynamics

MOPS	3-(N-morpholino)propanesulfonic acid
MTBE	Methyl tert-butyl ether
MW	Molecular weight
N.a.	Not applicable
N.d	Not detected
N.m	Not measured
NAD$^+$	Nicotinamide adenine dinucleotide
NADP$^+$	Nicotinamide adenine dinucleotide phosphate
Ni-NTA	Nickel-nitrilotriacetic acid
NOx	NADH-oxidase from *Streptococcus mutans*
NPC	Non protein control
OD$_{600}$	Optical density at 600 nm
ONC	Overnight culture
PLP	Pyridoxal phosphate
rac	Racemic
RF	Response factor
rpm	Revolutions per minute
SDS-PAGE	Sodium dodecyl sulfate polyacrylamide gel electrophoresis
TFA	Trifluoroacetic acid
THF	Tetrahydrofuran
Tris	Tris(hydroxymethyl)aminomethane
UV-Vis	Ultraviolet-visible spectroscopy
WT	Wild type
ωTA	ω-transaminase

Chapter 1

Introduction: Substrate scope and applications of amine dehydrogenases in asymmetric synthesis of α-chiral amines

A modified version of this chapter is in preparation for submission as review

1.1 Towards greener production of a-chiral amines

Chiral amines are ubiquitously present in many active pharmaceutical ingredients (APIs) and agrochemicals (**Figure 1**). They have also been applied as chiral auxiliaries, resolving agents, catalysts as well as intermediates for the production of a large number of fine and bulk chemicals.[1-3] Although a number of amines are present in APIs in racemic form, recent regulations on drug toxicity,
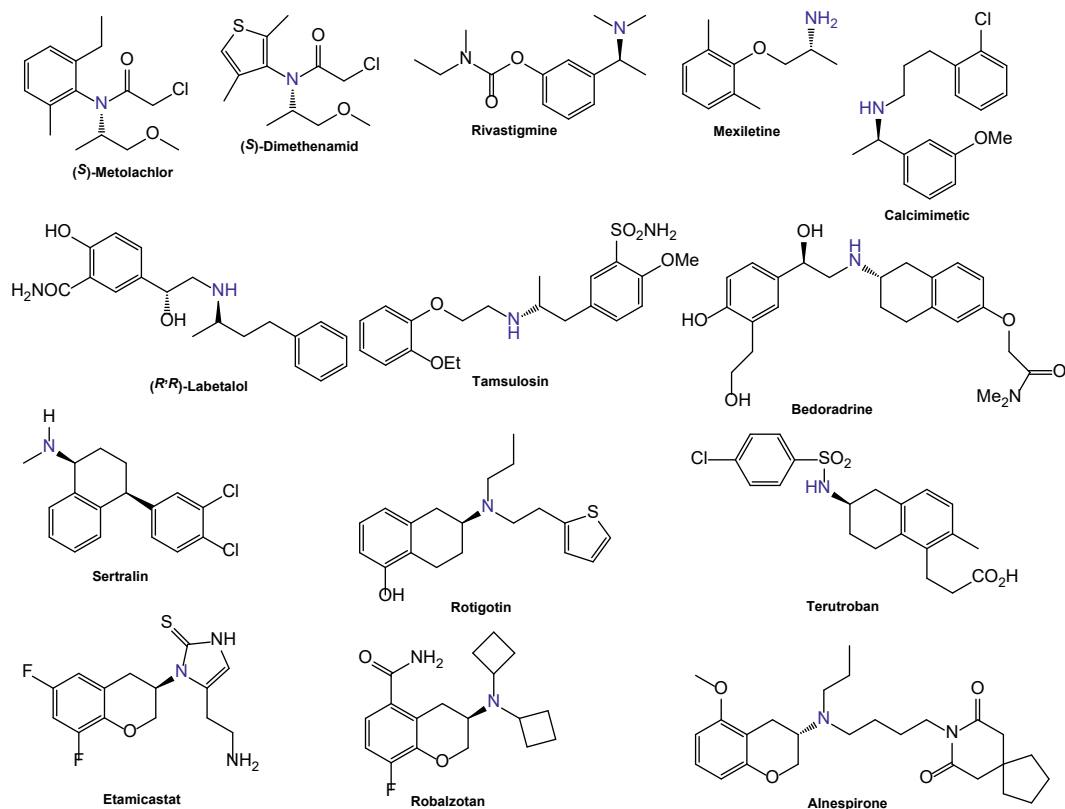
Figure 1.   Chiral amine based active pharmaceutical ingredients (APIs) and agrochemicals

safety and efficiency, have raised the need for the introduction of a 'chiral switch policy' by the U.S. Food and Drug Administration (FDA).[4] To fulfil these regulations, thus producing amines of high optical purity, pharmaceutical industries have been performing environmental-unfriendly processes which consume a lot of energy and generate copious amount of waste. It is estimated that during these processes the total mass of the waste can reach up to 100 times the mass of the

final product[5] (E factor more than 100) leading therefore to the need for the development of greener processes.[6] Towards this aim, new stereoselective and environmentally friendly catalysts for the synthesis of enantiomerically pure amines have been the subject of extensive investigation for the past couple of decades.[7,8] As a consequence, considerable advancements have been made in the discovery of the new enzymes or in optimization (via engineering) of existing biocatalysts that can be applied either for the asymmetric synthesis or for deracemization of a-chiral amines.[9-13] These newly discovered or evolved biocatalysts feature impressive stereoselectivities and high catalytic activities. Moreover, they operate under mild reaction conditions, display high atom economy and as such, they can be considered a 'green alternative' to the existing methodologies.

Stereoselective conversion of ketones into a-chiral primary amines is a well-studied chemical transformation that can be accomplished by a formal reductive amination using ω-transaminases (ωTAs). These PLP (pyridoxal 5'-phosphate)-depended enzymes have been applied both in laboratory and at industrial scale and have been proven to be useful biocatalyst for the preparation of valuable compounds.[14] However, they usually require supra-stoichiometric amounts of an amino donor and often multiple enzymes (and cofactors) to drive the equilibrium towards amine formation through the removal of the undesired by-product(s). To eliminate most of these disadvantages, the use of oxidoreductases with cofactor recycling has been proven to increase the atom economy. For instance, amine dehydrogenases (AmDHs), imine reductases (IREDs) and reductive aminases (RedAms) have all been applied for the efficient synthesis of a-chiral primary, secondary and tertiary amines in combination with FDH (formate dehydrogenase) or GDH (glucose dehydrogenase) for nicotinamide adenine dinucleotide (NAD) cofactor regeneration.[9,15] IREDs commonly catalyze the asymmetric reduction of cyclic pro-chiral imines; however, it has been also reported that IREDs catalyze the reductive amination of carbonyl compounds with amines thus giving access to secondary and tertiary amines[16] in a similar fashion as observed for the RedAms.[17]

In a large number of IRED catalyzed reactions, however, the enantiomeric excess of the obtained amines was moderate.[9] P450s have also been shown to catalyze C-H amination of sulfonic azides to sulfamates or sulfonamide products.[9] However, direct C-H amination of non-functionalized hydrocarbons have been only recently enabled by creating cytochrome P411, which requires tosyl azide as nitrogen source.[18] This strategy is limited to benzylic C-H amination and requires a deprotection step to remove the tosyl group. Other enzymatic methodologies for the synthesis of chiral amines involve the use of ammonia lyases, Pictet-Spenglerases or berberine bridge enzymes, all of which are active towards a restricted yet valuable type of compounds.[19-24] Classical routes to obtain a-chiral amines is via kinetic resolution (KR) or dynamic kinetic resolution (DKR) using hydrolases[25] or deracemization using monoamine oxidases.[13] The applicability of KR has also been demonstrated using ω-transaminases,[26] whole cells coexpressing AmDHs and an NADH oxidase[27] or alanine dehydrogenase[28] or using a reductive aminase.[29]

Because of their exquisite enantioselectivity, high atom economy and their intrinsic ability to utilize cheap ammonia as nitrogen donor for the synthesis of a-chiral primary amines, AmDHs have attracted considerable attention during the past decade. Since the pioneer work of Bommarius and coworkers that resulted in the first engineered AmDH in 2012,[30] fourteen AmDH members are now available. These AmDHs have been obtained either by enzyme engineering or discovered as native (i.e., wild-type) enzymes using metagenomic data.[31] Therefore, the toolbox of available AmDHs can now give access to approximately eighty valuable a-chiral amines with high conversions and excellent enantioselectivities. The applicability of AmDHs have been demonstrated for the kinetic resolution of racemic amines as well as these enzymes have been incorporated in novel cascades for the amination of alcohols; the AmDHs were applied either in purified form,[32] or as immobilized enzymes[33] or as whole cell systems.[34] Recent reports also described the application of AmDHs towards the synthesis of secondary or tertiary amines.[31,35] With the recent discoveries of native Amine dehydrogenases and engineering

of new members with different properties, this family is expected to expand further during the forthcoming years. This chapter focuses exclusively on the reactions catalyzed by the available AmDHs until to date and in biocatalytic processes of synthetic purpose. Major emphasis is given on the substrate scope and in the reactions' conditions under which the reported activities were achieved.

Table 1. Current pool of available AmDHs

Entry	Name	Originated from	Parental enzyme	Crystal structure of parental	Crystal structure that the evolution was based on	Mutations of the parental scaffold	Preferred Co-factor
1	**Bs-AmDH**	*Bacillus stearothermophilus*	L-Leucine Dehydrogenase (Leu-DH)	-	1C1D (homolog from *Rhodococcus sp. M4* Phe-DH)	K68S/E114V/ N261L/V291C	NADH
2	**Bb-AmDH**	*Bacillus badius*	L-Phenylalanine Dehydrogenase (Phe-DH)	-	1C1D (homolog from *Rhodococcus sp. M4* Phe-DH)	K77S/N276L	NADH
3	**cFL(1,2)-AmDH**	*Chimera (domain shuffling between AmDHs from entries 1 and 2)*		-		K77S/N270L (cFL1) K77S/N270L/N271L (cFL2)	NADH
4	**Rs-AmDH**	*Rhodococcus sp. M4*	L-Phenylalanine dehydrogenase	1C1D, 1BW9, 1C1X, 1BXG		K66Q/ S149G/N262C	NADH
5	**Cal-AmDH**	*Caldalkalibacillus thermarum*	L-Phenylalanine dehydrogenase	-		K68S/N266L	NADH
6	**Es-AmDH-M0, M3**	*Exiguobacterium sibiricum*	L-Leucine Dehydrogenase	-		K77S/N270L (M0) K77S/N270L/A122G/ T143G (M3)	NADH
7	**Lf-AmDH (M0-M3)**	*Lysinibacillus fusiformis*	L-Leucine Dehydrogenase	-		K68S/N261L (M0), K68S/N261L/A113G (M1), K68S/N261L/A113G/ T134A (M2), K68S/N261L/A113G/ T134G (M3)	NADH
8	**Bsp-AmDH-M0, M3**	*Bacillus sphaericus*	L-Leucine Dehydrogenase	1LEH		K68S/N261L (M0) K68S/N261L/A113G/ T134G (M3)	NADH
9	**LE-AmDHs (v1-v14)**	*Geobacillus sterothemophilus*	L-Lysine-ε-Dehydrogenase	-		F173A (v1), F173G (v2), V172A/F173G (v3), V172G/F173G (v4), V172G/F173A (v5), V172A/F173A	NADH

Ent ry	Name	Originated from	Parental enzyme	Crystal structure of parental	Crystal structure that the evolution was based on	Mutations of the parental scaffold	Preferred Co-factor
						(v6), R242M/F173A (v7), R242W/F173A (v8), V130A/F173V (v9), V130G/F173V (v10), V130A/F173A (v11), V130G/F173A (v12), R242M/F173V (v13), R242M (v14)	
10	Pm-AmDH-4-4	Petrotoga mobilis	Diaminopenta noate Dehydrogena se	6G1M/6 G1H		N135V/N163V/R161 M/H264L (Pm-AmDH-4-4)	NADH
11	MsmeA mDH	Mycobacteri um smegmatis	native	6IAQ		-	NADH/NA DPH
12	MicroA mDH	Microbacteri um sp.	native	-		-	NADH/NA DPH
13	CfusAm DH	Cystobacter fuscus	native	6IAU		-	NADH/NA DPH
14	ApauA mDH	Aminomonas paucivorans	native	-		-	NADH

1.2 Engineered AmDHs from L-AADHs for the asymmetric synthesis of amines

1.2.1 Evolution of *Bacillus stearothermophilus* Leu-DH to *Bs*-AmDH

The evolution of a L-leucine dehydrogenase (Leu-DH) by Bommarius and co-workers represents the first example of a highly enantioselective engineered amine dehydrogenase (AmDH) for the reductive amination of ketones. This AmDH was engineered from an L-amino acid dehydrogenase (L-AADH) from *Bacillus stearothermophilus*.[30] Despite the fact that the apo crystal structure of the closely related Leu-DH from *Bacillus sphaericus* (76% sequence identity) was available (1LEH)[36] (**Table 1,** entry 8), the authors based their work on the holo crystal structure of a L-phenylalanine dehydrogenase (Phe-DH) from *Rhodococcus sp. M4*[37] (1C1D, 1BW9, **Table 1** entry 4) as the two enzymes showed a nearly identical secondary structure (38% sequence identity). A first library of variants was constructed using saturation mutagenesis of the residue K68. The researchers based their work on the analysis of the crystal structure of 1C1D (L-Phe-DH), thus excluding the catalytically essential amino acid residues K80

and D115 as earlier suggested by Sekimoto and coworkers.[38] In particular, K68 residue interacts with the carboxyl group of the natural substrate (L-phenylalanine) in the crystal structure. The best variant K68M showed activity towards the reductive amination of 4-methyl-2-pentanone **41a** (0.2 mU mg^{-1}) and the oxidative deamination of **41b** (3.4 mU mg^{-1}). Further mutagenesis was performed by using the CASTing approach.[39] Single site libraries were also constructed using NNK codons. Following this procedure, a set of different libraries was constructed and screened for the desirable activity using **41a**. By combing the beneficial mutations of each round of mutagenesis the most active variant was finally obtained after 11 rounds of mutagenesis. This variant contained four mutations (*Bs*-AmDH: K68S/E114V/N261L/V291C, **Table 1** entry 1). It is worth to mention that among the beneficial mutations, were also the residues: K68 and N261 that are directly involved in the interaction with the carboxyl group of the natural substrate. Substitution of Lys (K) with either Met (M) or Ser (S) and of Asn (N) with Val (V) or Leu (L), produced the most active variants. As a consequence, the quadruple variant *Bs*-AmDH showed 690 mU mg^{-1} activity towards reductive amination of **41a** as well as 2640 mU mg^{-1} in the oxidative deamination direction of its corresponding amine, with K_M of 15 mM and 57.5 mM for the ketone and amine, respectively. The enantioselectivity of *Bs*-AmDH was measured in the oxidative deamination direction using as substrates the enantiopure amines. *Bs*-AmDH exhibited 586.3 mU mg^{-1} for (*R*)-**41b** and 1.6 mU mg^{-1} for (*S*)-**41b**, thereby retaining the enantioselective properties of the parental enzyme (Leu-DH). The *Bs*-AmDH was further tested in the reductive amination of cyclohexanone (**27a**, 123.4 ± 3.5 mU mg^{-1}), ethyl-pyruvate (**76a**, 13.2 ± 5.8 mU mg^{-1}), methyl-acetoacetate (**77a**, 4.5 ± 0.6 mU mg^{-1}), ethyl-3-oxohexanoate (**78a**, 14 ± 1.2 mU mg^{-1}) and acetophenone (**13a**, 58.8 ± 1.7 mU mg^{-1}) as shown in **Table 2**. The assay was performed with 20 mM of substrate. Apart from the oxidative deamination of **41b**, the same variant also showed measurable activity levels towards **27b** (56.0 mU mg^{-1}). Finally large scale amination of **41a** (10 mM) was performed for 48 h using 26 mg of enzyme in

175 mL reaction (0.15 mg/ mL, 3.7 µM) and GDH/glucose recycling system (**Scheme 1A**), thus resulting in 85% conv. and 99.8% *ee*.

1.2.2 Evolution of *Bacillus badius* Phe-DH to *Bb*-AmDH

After the evolution of *Bs*-AmDH, Bommarius and coworkers further developed a second AmDH by transposition of the mutations of *Bs*-AmDH to a L-phenylalanine dehydrogenase (Phe-DH) scaffold.[40] The authors used the closely related scaffold of the Phe-DH from *Bacillus badius*[41] that shares 48% sequence identity with the one of Leu-DH from *Bacillus stearothermophilus*. Therefore, both enzymes share similar structure with the Phe-DH from *Rhodococcus sp. M4*.[37,42] The analogous substitutions in Phe-DH scaffold were identified by sequence alignment to be K77, N276. Transposition of the previously reported beneficial mutations Lys (K) to Met (M) and Asn (N) to Val (V), directly generated an active variant with AmDH activity towards **41a** (0.0722 s⁻¹, for reductive amination) and **41b** (0.0037 s⁻¹, for oxidative deamination) as well as for *para*-fluorophenyl-acetone **2a** (0.128 s⁻¹, for reductive amination). Nevertheless, the authors decided to create a library by simultaneously mutating these two residues (K77 and N276) using DDK codons (encoding 15 amino acids). In total 21 active variants were identified and among them, the K77S/N276L variant (*Bb*-AmDH **Table 1** entry 2) was selected due to its high activity for the reductive amination of **2a**. As expected, the *Bb*-AmDH showed (*R*)-enantioselectivity. Thermostability measurements revealed a melting point of 59.9 °C. Initially the substrate scope of the *Bb*-AmDH was evaluated in the oxidative deamination using (*R*)-**13b** (1.9 mU mg⁻¹) and **41b** (166.3 mU mg⁻¹). The k_{cat} for *rac* **2b** was determined to be 1.92 s⁻¹ (**Table 2**). A variety of substrates (20 mM) were tested for the reductive amination reaction including **41a** (77 mU mg⁻¹), phenoxy-2-propanone (**62a**, 540.8 mU mg⁻¹), 2-hexanone (**36a**, 155.7 mU mg⁻¹), 3-hexanone (**54a**, 1.6 mU mg⁻¹), 3-pentanone (**53a**, 1.3 mU mg⁻¹), cyclopentanone (**24a**, 0.9 mU mg⁻¹), **27a** (27.5 mU mg⁻¹), **76a** (18.4 mU mg⁻¹), benzaldehyde (**21a**, 31.4 mU mg⁻¹), 2-methylcyclohexanone (**28a**, 19.3 mU mg⁻¹), 3-methylcyclohexanone (**29a,** 41.1 mU mg⁻¹) and 3-methylbutan-2-one (**44a**,

72.7 mU mg^{-1}). It is worth to mention that the *Bb*-AmDH exhibited approximately 100-fold higher activity for 2-hexanone compared with 3-hexanone. The *Bb*-AmDH showed the highest activity with compounds **2a** and **62a** followed by the linear ketones (e.g**. 36a**, **41a**). Despite the fact that *Bb*-AmDH can now provide access to **2b**, which was impossible with *Bs*-AmDH, it completely lost its activity towards the amination of **13a**. Four years later the *Bb*-AmDH was used in a systematic study performed by Knaus *et al*.[43] In this study among the other AmDHs used, the authors reported that *Bb*-AmDH converted 50 mM of **2a** (93%) as well as 50 mM of phenylacetaldehyde (**10a**, 34%) using 50 µM of the *Bb*-AmDH and 14 µM of *Cb*-FDH after 48 h in ammonium formate buffer (1 M, pH 8.5) (**scheme 1A**). All specific activities or conversions are reported in **Table 2**.

1.2.3 Generation of a chimeric amine dehydrogenase from *Bs*-AmDH and *Bb*-AmDH

One year after the development of the *Bb*-AmDH, Bommarius and co-workers generated an improved variant following a novel approach. Using the previously generated *Bs*-AmDH[30] (derived from a Leu-DH) and *Bb*-AmDH[40] (derived from a Phe-DH) and by employing domain shuffling using overlap PCR they created the cFL1-AmDH.[44] The residues used from Bb-AmDH were from 1-149 while from *Bs*-AmDH were 140-344. The new chimera (cFL1-AmDH **Table 1 entry 3**) retains the substrate binding domain of *Bb*-AmDH and the cofactor binding domain of *Bs*-AmDH. The new enzyme not only maintained its substrate binding ability towards the original substrates, but now accepts new benzylic carbonyl substrates. Moreover, the enantioselective properties of the enzyme remained intact (as its parent enzymes) and therefore displayed (*R*)-stereoselectivity. Interestingly the cFL1-AmDH showed an increased temperature optimum (T_{opt}) of 60 °C (10 °C higher than its parent enzymes). The cFL1-AmDH contains the mutations K77S (from *Bb*-AmDH) and N270L (from *Bs*-AmDH). The sequence of cFL1-AmDH revealed two adjacent asparagines at positions 270 and 271. In order to examine any influence of the N271 the authors mutated also the N271 to L, generating in this way the cFL2-AmDH (**Table 1** entry 3). cFL2-AmDH showed

a higher k_{cat} for **2a** (2.52 s^{-1}) compared with cFL1-AmDH (1.24 s^{-1}) but the turnover number was lower for compound **13a** (0.24 s^{-1} for cFL1 and 0.1 s^{-1} for cFL2). The T_{opt} was further increased another 10 °C for cFL2-AmDH, indicating an influence of the asparagine residues in the thermal stability of the enzyme. Nevertheless, the authors tested the cFL1-AmDH for the reductive amination of eight ketones and for the oxidative deamination of three amines (**Table 2**) using 20 mM of substrate in 5 M NH₄Cl buffer pH 9.5 at 60 °C. The enzyme was found to be capable of aminating **2a** (1725 mU mg^{-1}), **13a** (301 mU mg^{-1}), a-tetralone (**23a**, 107 mU mg^{-1}), adamantly methyl ketone (**20a**, 69 mU mg^{-1}) and pinacolone (**45a**, 133 mU mg^{-1}). In the oxidative deamination the enzyme showed activity towards the (*R*)-a-methylbenzylamine (**13b**, 19 mU mg^{-1}) and methoxy-isopropylamine (**79b**, 40 mU mg^{-1}). Overall cFL1-AmDH showed 2.3-fold decrease in activity for the amination of **2a** but 5.1-fold increase in activity for the amination of **13a** compared with *Bs*-AmDH under the same reaction conditions. Notably, *Bb*-AmDH showed no activity towards **13a**. In contrast the oxidative deamination of **13b** proceeded better using *Bs*-AmDH than cFL1-AmDH with almost 10-fold higher activity under the same conditions. The applicability of cFL1-AmDH was further demonstrated three years later by Knaus *et al*.[43] The authors used this enzyme to aminate a wide panel of pro-chiral ketones and aldehydes at 50 mM scale. In total fourteen compounds were tested in the reductive amination direction using 30–130 µM of cFL1-AmDH, 14 µM of *Cb*-FDH in ammonium formate buffer (1 M, pH 8.5) at 30 °C (**Table 2**). Amination of **2a** proceeded with 93% conversion using 30 µM of enzyme after 24 h, while higher loading of *Bb*-AmDH was required (50 µM) to reach the conversion of 93% after 48 h. In general, cFL1-AmDH showed the highest activity towards 2-heptanone (**37a**) among all of the linear ketones tested (98% conv., 30 µM, for 24 h **Table 2**), and towards **2a** (93% conv., 30 µM, for 24h **Table 2**) among all of the aromatic ketones tested. Lower conversion were obtained for amination of **13a** (34%) despite the higher biocatalyst loading (130 µM) and longer reaction time (48 h). This conversion value for substrate **13a** was the highest observed by testing all of the AmDHs developed until 2013.

1.2.4 Generation of *Rs*-AmDH from *Rhodococcus sp. M4* Phe-DH

In all of the above mentioned cases, the parental scaffolds (i.e., wild-type L-AADH) of the engineered AmDHs possessed high sequence and structural similarity with the Phe-DH from *Rhodococcus sp. M4*.[37] Therefore, the expected development of a new AmDH starting precisely from this scaffold was published a year later in 2015 by Li and coworkers.[45] The fact that the structure of the wild type Phe-DH was available[37] (PDB:1C1D) and the reported mechanism known,[42] in combination with the gained knowledge from the previous works by Bommarius and coworkers (i.e., *Bb*-AmDH shares 32% identity with *Rs*-PheDH), provided a solid background for the generation of this new AmDH. The analogous mutations of K68 and N261 of the *Bs*-AmDH that were known to play a crucial role in the binding of substrates with a carboxylic group, were identified to be the K66 and the N262 in the PDB 1C1D scaffold. By performing a double site saturation mutagenesis using NNK codons, the authors found six active double variants for the deamination of target compounds: amphetamine (**1b**) and 4-phenyl-2-butylamine (**60b**). Among them, four variants showed activity in the amination direction for at least one of the **1a** and **60a** (phenylacetone and 4-phenyl-2-butanone), while only two of the variants (K66Q/N262L and K66Q/N262C) showed activity with both ketones. To investigate the importance of these two single mutations, three single mutants: K66Q, N262L, and N262C were prepared. The only active variant proved to be K66Q with lower activity towards the amination of both ketones indicating synergistic effects in the double variants. Finally, the authors decided to make another round of evolution starting from the most active double variant (K66Q/N262C), by mutating 20 amino acid residues within 6 Å of the active site using NNK codons. A triple variant (K66Q/S149G/N262C, *Rs*-AmDH, **Table 1** entry 4) was found to be the only variant possessing increased deamination activity towards compounds **1b** and **60b**; therefore, it was further screened for the reductive amination of a number of ketones (**Table 2**). As expected, the enzyme aminated **1a** (0.7 s^{-1}) and **60a** (0.72 s^{-1}) and the products were obtained with (*R*) configuration. Asymmetric amination of 15 mM of **60a** using 4 mg/mL (102.8 µM) of AmDH at 30 °C for 60 h

resulted in 95% conversion. Apart from the reported substrates **1a** and **60a**, *Rs*-AmDH was later applied for the reductive amination of linear and aromatic ketones;[43] these data are summarized in **Table 2**. In general, *Rs*-AmDH showed very high conversions for the amination of phenylacetone and derivatives with conversions above or equal to 98% using 50-130 µM of enzyme and 50 mM of substrate for 24-48 h (for details see **Table 2**). Bulky-bulky ketones like compounds 1-phenyl-butan-2-one (**57a**), 1-phenyl-pentan-2-one (**58a**) and 1-phenyl-pentan-3-one (**59a**) were also accepted with conversions of more than 70%. *Rs*-AmDH seems to be active on the linear ketone **37a** and 2-octanone (**38a**) with 99% and 93% conversions, respectively, by using 50 µM of enzyme for 48 h reaction time. Although both cFL1-AmDH and *Rs*-AmDH seem to be the most active AmDHs developed up to that time, none of them is able to aminate aromatic compounds in which the aromatic ring is adjacent to the carbonyl moiety (e.g., propiophenone **64a**, butyrophenone **65a** and valerophenone **66a**) to any synthetically useful extent.

1.2.5 Generation of *Es*-AmDH from *Exiguobactertium sibiricum* Leu-DH

In 2014, the Xu's group identified an L-amino acid dehydrogenase (L-Leucine dehydrogenase) from *Exiguobactertium sibiricum*[46] (*Es*-LeuDH, Uniprot B1YLR3) by using a genome mining approach. The newly discovered scaffold shares 68% sequence identity with *Bacillus sphaericus* LeuDH (**Table 1**, entry 8), (PDB:1LEH).[36] The *Es*-LeuDH showed high activity for trimethyl-pyruvic acid and therefore used for the preparation of L-*tert*-Leucine. However, the *Es*-LeuDH showed undetectable levels of activity towards ketones. Inspired by the engineered strategy of Bommarius and co-workers, a year later Chen *et al*. introduced the same mutations (K77S/N270L) in the scaffold of *Es*-LeuDH creating in this way the *Es*-AmDH[47] (**Table 1**, entry 6). *Es*-AmDH exhibited moderate level of activity for **13a** (98.5 mU mg^{-1}) and was found to be more active for cyclic ketones (**Table 2**). For instance, **27a** (868 mU mg^{-1}), **28a** (403 mU mg^{-1}) and **29a** (2465 mU mg^{-1}) were all well accepted by the enzyme with the latest to be the best cyclic ketone substrate for *Es*-AmDH. In contrast, the enzyme showed low levels of activity for

24a (6.5 mU mg^{-1}) and cycloheptanone (**32a**, 287 mU mg^{-1}). *Es*-AmDH proved to be a versatile catalyst for the reductive amination of branched linear ketones. The highest specific activity was observed for the 3-methyl-2-pentanone (**42a**, 3628 mU mg^{-1}) followed by **44a** (2559 mU mg^{-1}), **45a** (760 mU mg^{-1}) and **41a** (490 mU mg^{-1}). In general, lower specific activities were observed for the linear ketones compared with branched ketones with the highest one to be 796 mU mg^{-1} for 2-pentanone (**35a**). The enzyme showed a preference for 2-butanone (**34a**, 137 mU mg^{-1}) instead of **36a** (83 mU mg^{-1}).

1.2.6 Generation of Cal-AmDH from *Caldalkalibacillus thermarum* Phe-DH

Two years after the generation of *Rs*-AmDH, Ahir *et al.* used a genome mining approach to identify and then mutate a Phe-DH from *Caldalkalibacillus thermarum* (UniProt Accession Code: F5L9G2)[48] in order to create the *Cal*-AmDH[49] (**Table 1**, entry 5) possessing a similar but increased catalytic profile compared with *Bb*-AmDH. *Cal*-PheDH shares 63% sequence identity with *Bb*-PheDH[41] and 48% with *Bs*-PheDH.[50] The only reported difference between *Cal*-PheDH and *Bb*-PheDH in the active site is in position 303, in which there is an alanine (*Cal*-PheDH) instead of a serine (*Bb*-PheDH).[49] Following an identical approach as before, the authors choose the two highly conserved residues (K68 and N266) for double site saturation mutagenesis. Interestingly, the best variant (*cal*-AmDH) bears the same two mutations (K22S/N266L) (**Table 1**, entry 5) as observed in all AmDHs created up to the time of this study. An interesting feature of *Cal*-AmDH is the increased thermal stability compared with Bb-AmDH, which is 27 °C higher. This property was retained from the wild type Phe-DH from *Caldalkalibacillus thermarum*. In this work the kinetic parameters of Cal-AmDH (**Table 1** entry 5) and *Bb*-AmDH (**Table 1** entry 2) were determined from a number of substrates (**2a**, *meta*-fluoro-phenylacetone, **3a**, **62a**, **60a**, **13a**, **41a, Table 2**). *Cal*-AmDH showed an approximately 2-fold increased turnover number for the amination of **2a** compare with *Bb*-AmDH. On the other hand, both enzymes showed a very similar k_{cat} value for the rest of the substrates. The specific activities were measured with both enzymes for 18 structurally diverse compounds in 2 M

ammonium formate buffer (pH 9.6) at 25 °C using a less than 10 mM substrate concentration (depending on the solubility) and all results are summarized in **Table 2**. *Cal*-AmDH showed the highest activity for *para*-methyl-phenylacetone (**7a**) among all of the substrates tested with a specific activity of 1600.86 mU mg^{1}. *Bb*-AmDH showed 5.74-fold decrease in its specific activity for the same substrate. For the *ortho*-methoxy substituted phenylacetone (**4a**), the *Cal*-AmDH showed a specific activity of 276.87 mU mg^{-1} while for the *meta*-methoxy substituted analog **5a** the specific activity was reduced to 55.36 mU mg^{-1}. The opposite behaviour was observed with *Bb*-AmDH, which showed 142.79 mU mg^{-1} and 294.38 mU mg^{-1} for **4a** and **5a** respectively. *Cal*-AmDH proved to be a better catalyst for the *meta*-trifluoromethyl substituted phenylacetone (**9a**) compared with *Bb*-AmDH (27.67 mU mg^{-1} for *Cal*-AmDH and 12.45 mU mg^{-1} for *Bb*-AmDH), which were the lowest specific activities that the enzymes displayed among all of the tested phenylacetone derivatives. For the rest of the substrates tested, both enzymes showed specific activities lower to 45 mU mg^{-1}. *Cal*-AmDH showed severe inhibition profiles with IC$_{50}$ values of 10-15 mM for (*R*)-**60b** and 1-6 mM for (*R*)-**13b**. The applicability of *Cal*-AmDH and *Bb*-AmDH was demonstrated either as lyophilized lysate or lyophilized whole cells in the presence or absence of water immiscible cosolvents for the reductive amination of **62a** at 200 mM scale. The best conversion (97%) was observed with lyophilized lysate (10 mg/mL) and GDH (3 mg mL^{-1}) in an ammonium chloride buffer (2 M, pH 9.6) containing NAD^{+} (1 mM), glucose (240 mM, 1.2 equiv) at 37 °C for 24 h reaction time. Under the same conditions, *Bb*-AmDH converted 71% of **62a**. The cosolvents significantly increased the conversion, thereby implying an improved general stability offered by this biocatalyst preparation under the reaction conditions, even considering potential mass-transfer limitations in the biphasic system.

1.2.7 Generation of *Lf*-AmDH and *Bsp*-AmDH from Leu-DHs

After the development of *Es*-AmDH,[47] the same research group identified and mutated native Leu-DHs originated from *Lysinibacillus fusiformis*[51] (*Lf*-LeuDH, Uniprot D7WWB4) and *Bacillus sphaericus*[52] (*Bsp*-LeuDH, Uniprot Q76GS2). After

the introduction of the same two mutations in both Leu-DHs (K68S/N261L), the *Lf*-AmDH (**Table 1** entry 7, M0) and *Bsp*-AmDH (**Table 1** entry 8, M0) were obtained and showed activity towards a number of ketones. Without any further mutations, both enzymes were tested for the reductive amination of acetone (**33a**),as well as **34a**, **45a**, **44a**, **35a**, **42a**, **36a** and **37a** using 20 mM of substrate in ammonium chloride buffer (2 M pH 9.5, **Table 2**). Both variants showed a similar substrate preference in the initial screening. *Lf*-AmDH *and Bsp*-AmDH accepted short aliphatic ketones like **34a** (169 and 202 mU mg^{-1}, respectively) and **35a** (927 and 1030 mU mg^{-1}, respectively). In contrast, these AmDHs showed significantly reduced activity with longer aliphatic ketones. For instance, **36a** was accepted (111 and 89 mU mg^{-1} for *Lf*-AmDH *and Bsp*-AmDH respectively) as well as **37a**, but no other bulkier aliphatic ketone (**38a,** 2-nonanone **39a,** 2-decanone **40a**). *Lf*-AmDH *and Bsp*-AmDH showed impressive specific activities for **44a** (2646 and 3078 mU mg^{-1}, respectively) and **42a** (3077 and 3662 mU mg^{-1}, respectively). These substrates were also the most well accepted by *Es*-AmDH with similar specific activities (**44a**, 2559 mU mg^{-1} and **42a**, 3628 mU mg^{-1}), (**Table 2**). Despite the promising results obtained by *Bsp*-AmDH and the availability of the crystal structure of the parental *Bsp*-LeuDH[36] (1LEH) the authors decided to introduce further mutations into *Lf*-AmDH by creating an homology model based on 1LEH (86% sequence identity). Docking of **37a** into the active site of *Lf*-AmDH model, revealed that residues A113, E114, T134 and V294 may be potential targets for mutagenesis since they provide steric hindrance for more bulky linear ketones. First a single site saturation mutagenesis protocol was applied using *Lf*-AmDH for the position 113, resulting in *Lf*-AmDH-M1 (K68S/N261L/A113G) with improved (ca. 13-fold increased) activity for **36a** (1470 mU mg^{-1}) and acceptance of **37a** (430 mU mg^{-1}). However, the *Lf*-AmDH-M1 showed ca. 4 fold decreased activity towards **35a** (220 mU mg^{-1}) possibly due to the larger active site. Improved variants *Lf*-AmDH-M2 (K68S/N261L/A113G/T134A) and LfAmDH-M3 (K68S/N261L/A113G/T134G) were generated after mutations of the residues surrounding the substrate-binding pocket site of *Lf*-AmDH-M1. The new *Lf*-AmDH-M2 and M3 showed 340 and 670 mU mg^{-1} specific activity for **35a**, 1560

and 2240 mU mg^{-1} specific activity for **36a** and 1400 and 2590 mU mg^{-1} specific activity for **37a**, respectively, indicating that the two introduced glycine residues in the *Lf*-AmDH-M3 enhanced its catalytic performance towards linear ketones. The Lf-AmDH-M2 and M3 were found to capable of aminating linear ketones up to 2-decanone (2.5 mU mg^{-1}). Analytical scale synthesis of a-chiral amines using the developed *Lf*-AmDHs (1.5 mg mL^{-1}, 40 μM) at 50 mM substrate concentration (**35a-39a**), at 30 °C for 24 h reaction time showed that all of the amine dehydrogenases quantitatively aminated **36a,** while only *Lf*-AmDH-M1and M3 reached ≥99% conversion for **37a** (**Table 2**). The most challenging substrate **39a** was converted only by *Lf*-AmDH-M2 (12%) and M3 (22%) while for **38a** conversion was observed also using *Lf*-AmDH-M1 (45%), *Lf*-AmDH-M2 (61%) and *Lf*-AmDH-M3 (80%). A different behavior was observed for the less bulky **35a**. The highest conversion was observed for *Lf*-AmDH-M0 (>99%) followed by *Lf*-AmDH-M3 (98%), *Lf*-AmDH-M2 (97%) and finally *Lf*-AmDH-M1 (86%). All amine products were obtained with *R* configuration. Circular dichroism measurements showed that *Lf*-AmDH-M0 to M3 have a T_m of 68.5 °C, 67.9 °C, 70 °C, 68.1 °C, respectively. Finally the authors validated the mutations A113G and T134G of *Lf*-AmDH-M3 by transposition into the *Es*-AmDH (A122G/T143G) and *Bsp*-AmDH (A113G/T134G). The new variants: *Es*-AmDH-M3 and *Bsp*-AmDH-M3 (**Table 1**, entry 6 and entry 8, respectively), were tested for the acceptance of bulkier ketones. *Es*-AmDH-M3 showed a specific activity of 460 mU mg^{-1}, 1430 mU mg^{-1} and 1480 mU mg^{-1} for **35a**, **36a** and **37a** respectively. *Bsp*-AmDH-M3 showed even higher specific activities of 760 mU mg^{-1} for **35a**, 2360 mU mg^{-1} for **36a**, and 2800 mU mg^{-1} for **37a**. It is worth to mention that *Bsp*-AmDH was not active at all towards **37a**.

1.2.8 Generation of LE-AmDHs from ε-deaminating *L*-Lysine dehydrogenase

All of the AmDHs discussed so far have been engineered from similar L-amino acid dehydrogenases (L-AADHs) (deaminating at the a-amino group) using an identical approach. As all parental enzymes displayed high sequence identity, the two highly conserved residues (i.e., lysine and aspartate) were mutated to serine or glutamine and leucine or cysteine, respectively. Therefore, all AmDH

members (**Table 1**, entries: 1-8) displayed similar catalytic properties. In order to create AmDHs with different catalytic profile (i.e., substrate scope, enantioselectivity) we have recently engineered the ε-deaminating *L*-lysine dehydrogenase from *Geobacillus stearothermophilus* (LysEDH).[53] The folding of LysEDH is significantly different from the almost identical folding of members 1-8 (**Table 1**). The *wild type* LysEDH was found to be capable of aminating 6-oxo-heptanoic acid (**71a**, 44% analytical yield) and 6-oxo-hexanoic acid (**72a**, 90% analytical yield).[54] Notably, in contrast with all AmDHs engineered so far, the amine **71b** was obtained with (*S*)-configuration confirming our hypothesis that the hydride of NADH must be transferred towards the *Si*-face of the prochiral carbonyl moiety as observed in the homology model. After the examination of the residues that interact with the natural substrate (L-Lysine) in the active site of LysEDH, we designed a library of 14 variants potentially active towards non functionalized ketones (i.e., that lack of the terminal carboxyl group). Initial screening with a number of structurally diverse ketones revealed that the best variant bears the mutation F173A (LE-AmDH-v1, **Table 1** entry 9). LE-AmDH-v1 (90 μM) was tested with a number of ketones (10-100 mM) using FDH (16 μM) for 48 h reaction time and at different temperatures. For comparison purposes, conversions reported in **Table 2** have been determined for substrate concentration of 50 mM at 50 °C. The T_m of LE-AmDH-v1 was found to be 69 °C when measured in the presence of NAD^+ and longer term stability measurements showed that the enzyme retained its initial activity for 7 days upon incubation at room temperature. The LE-AmDH-v1 showed approximately 20 fold decreased IC_{50} value for enzymatic assays performed in the presence of (*R*)-**13b** as inhibitor, compared with cFL1-AmDH. Furthermore, determination of the inhibition constant (K_I) for both enzymes revealed that cFL1-AmDH is ca. 38-fold more inhibited that LE-AmDH-v1. This support the fact that although cFL1-AmDH possess a slightly higher k_{cat} (0.128 s^{-1}) than LE-AmDH-v1 (0.095 s^{-1}), the latest converted >99% of **13a** while cFL1-AmDH converted only 34% of the same compound into the corresponding amine product, under the same reaction conditions. This feature of LE-AmDH-v1 enabled high substrate loading of **13a**

(100 mM), thus resulting in 80% conversion after 48 h reaction time and using the same amount of enzyme (90 µM). Apart from **13a**, LE-AmDH-v1 was found to be the first AmDH capable of aminating **64a** (95% conv.), **65a** (65% conv.), **66a** (26% conv.), a-chromanone (**22a**, 55% conv.), a-tetralone (**23a**, 50% conv.) as well as fluoro-substituted acetophenones (**14a**, **16a**, **17a**) with >95% conversion in all cases. Best substrate for LE-AmDH-v1 was **21a**, which was converted with >99% even at 200 mM scale (k_{cat}: 0.72 s^{-1}). An interesting property of LE-AmDH-v1 is its enantioselective preferences for different substrates. For example, 6-oxoheptanoic acid was obtained with >99% conv. and >99% ee for the (*S*)-configured amino acid indicating that LE-AmDH-v1 has an (*S*)-selective binding cavity where R242 interacts with the carboxyl-moiety of the substrate. In contrast, non-functionalized aromatic and aliphatic ketones—thus lacking the terminal carboxylic group—are accommodated in another (*R*)-selective binding cavity that has been created by the introduction of the F173A mutation. Notably, all of the non-functionalized aromatic ketones were aminated with >99% - >99.9% ee and (*R*)-configuration. The only exceptions were substrates **35a** and **41a** which were obtained with 89% and 97% ee, respectively. For these substrates multiple binding poses can be generated in the active site of the enzyme resulting in lower ee values. These findings were explained by *in silico* studies using molecular dynamic simulations of the docked enzyme-substrate binding possesses, using a number of different substrates.

1.2.9 Discovery of Pm-AmDH-4 and engineering for the acceptance of 2-pentanone

In 2016, Mayol *et al*. explored metabolic databases[55,56] for reactions transforming ketones to amines (a-keto acids were excluded) to identify a 2,4 diaminopimilate dehydrogenase (2,4-DAPDH) from *Clostridium sticklandii*[57,58] (UniprotKB identifier: E3PY99). This enzyme was used in a sequence driven approach to identify 169 enzymes sharing at least 30% sequence identity over the 80% of the target gene (2,4-DAPDH). In total, 26 candidates were chosen, based on the sequence diversity and availability of the genomic DNA and 20 of them were successfully

cloned. The enzymes were tested towards a panel of compounds including: **35a**, **36a**, 4-oxo-pentanoic acid (**68a**), and 5-oxo-hexanoic acid (**70a**); six of the enzymes were found to be active towards **68a**. One out of the three that were found to possess the highest specific activities towards **72a,** namely AmDH-4 from *Petrotoga mobilis*, was chosen. AmDH-4 is originated from a thermophilic organism (possibly will be a thermostable nezyme) and showed some activity towards **70a** thus suggesting higher substrate promiscuity.[59] Indeed, the enzyme showed an increased catalytic profile at 90 °C for **68a**. *Pm*-AmDH-4 converted almost quantitatively 10 mM of **68a** with 0.1 mg mL⁻¹ of catalyst loading, 0.4 mM of cofactor using the FDH/formate recycling system (3 U mL⁻¹). The reaction was performed in HCOONH₄/NH₄OH 5 M buffer pH 8.5 at 50 °C for 24h. The enzyme was claimed by the authors to be a wild type AmDH, because it can aminate ω-substituted ketones without introducing any mutation. The same feature was observed in the wild type (ε-deaminating) LysEDH. However, neither *Pm*-AmDH-4[59] nor LysEDH[54] showed activity to any of non-functionalized ketones tested (**13a**, **27a** and **45a** for *Pm*-AmDH-4 and **13a**, **22a**, **37a** and **38a** for LysEDH) and therefore, in our opinion, they cannot be considered as native AmDHs. Three years later,[31] crystallization of the *Pm*-AmDH-4 allowed for rational engineering of the enzyme. The best variant was obtained by introducing four mutations (N135V/N163V/R161M/H264L). The new enzyme (**Table 1**, entry 10, *Pm*-AmDH-4-4) can now be included in the AmDH toolbox as it is active for the reductive amination of **35a** (104 mU mg⁻¹) which is structurally related with the natural substrate **68a**. Notably, *Pm*-AmDH-4-4 produced the 2-aminopentane (**35b**) with *S* configuration representing the first (*S*)-selective AmDH developed up that date. The *Pm*-AmDH-4 was not tested with any other ketone as substrate; therefore, its substrate scope remains unexplored.

1.3 Native AmDHs for the asymmetric synthesis of amines
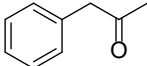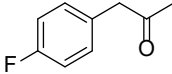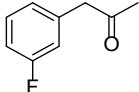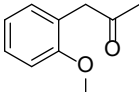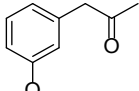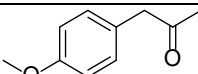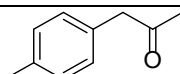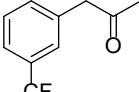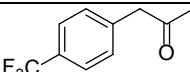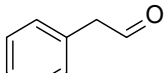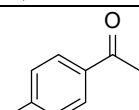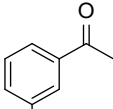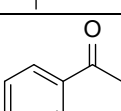
The first reported examples of native amine dehydrogenases arise from 1967 to 1971 by Eady and Large, when used whole cell extracts from *Pseudomonas* AMI to oxidize aliphatic monoamines or diamines, histamine and ethanolamine.[60,61]
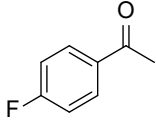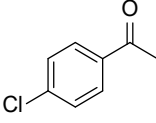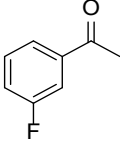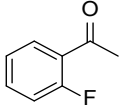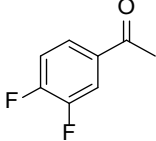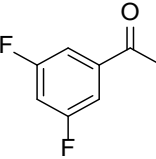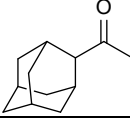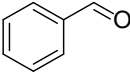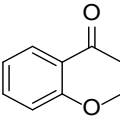
Whether this enzyme is an AmDH remains questionable since it requires either phenazine ethosulfate (PES) or phenazine methosulfate (PMS) as electron acceptor and is unable to utilize oxygen, NAD or NADP. Thirty years later, in 2000 Itoh *et al.*, discovered NADH dependent enzyme from *Streptomyces virginiae*[62] IFO 1282, which was able to catalyze oxidative deamination of amines, amino acids and amino alcohols. This enzyme was also found active in the reductive amination of ketones (**35a**-**37a, 13a** and **60a**), keto-alcohols, keto-acids and aldehydes. Unfortunately, no other reports based on this AmDH were published since then, and both DNA and amino acid sequences were never determined or published.
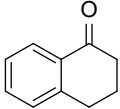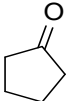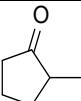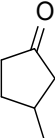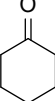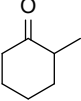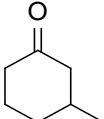
Earlier this year, native AmDHs were discovered in the same work in which *Pm*-AmDH-4 was engineered to accept 2-pentanone by Mayol *et al.*[31] As before, a sequence-driven search was performed, this time using as template the *Pm*-AmDH-4. The resulted 23 enzymes were characterized as potential AmDHs and screened for the oxidative deamination of (2*R*, 4*S*)−2,4-diaminopentanoate and 4-aminopentanoate as well as for the non-functionalized substrates: 2-pentylamine (**35b**), a-methylbenzylamine (**13b**) and cyclohexylamine (**27b**). From the 23 enzymes only one originated from *Mycobacterium smegmatis* (*Msme*AmDH, **Table 1**, entry 11, Uniprot: A0A0D6I8P6), was found to be active for the oxidative deamination of **27b** (6 mU mg^{-1}) and for the reductive amination of **29a** and **37a**. Subsequently, the *Msme*AmDH was used as starting template to discover other native AmDHs (nat-AmDHs). Searching criteria were defined in order for the new enzymes to show >38% sequence identity with *Msme*AmDH and activity towards at least one of the above mentioned substrates. This approach resulted in another three nat-AmDHs (**Table 1** entries: 12-14, *Cfus*AmDH, *Micro*AmDH and *Apau*AmDH). All of the four nat-AmDHs (**Table 1**, entries 11-14) were screened against a number of carbonyl compounds (10 mM), (**Table 2**). In general, *Msme*AmDH, *Cfus*AmDH (Uniprot: S9Q235) and *Micro*AmDH (Uniprot: C3UMY1) showed a similar carbonyl acceptor spectrum, with a preference for cycloalkanones and accepted both NADH and NADPH. In contrast, *Apau*AmDH (Uniprot: E3CZE3) showed a specificity for NADH and a
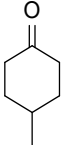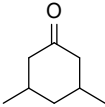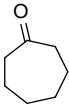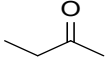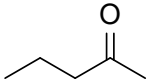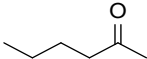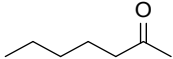
preference for aliphatic aldehydes albeit with moderate specific activities. *Apau*AmDH did not accept any of the cycloalkanones tested with the exception of **27a**. In all cyclic ketones used (**27-29a**, 4-methyl-cyclohexanone **30a**, 3,5-dimethyl-cyclohexanone **31a**, **24a,** 2-methyl-cyclopentanone **25a**, 3-methyl-cyclopentanone **26a**, cyclohexyl-ethanone **47a** and cyclohexen-2-one **67a**), *Msme*AmDH showed highest specific activity with NADPH rather than NADH with the exception being substrate **27a**. The same feature was observed for *Micro*AmDH and *Cfus*AmDH, although for the last two the discrepancies in their specific activities using either NAD$^+$ or NADP$^+$ were lower than *Msme*AmDH. The best nat-AmDH among all nat-AmDHs for the amination of cyclic ketones under the same reaction conditions was *Micro*AmDH, which showed the highest specific activities for **27a**, **28-31a**, **24-26a, 47a and 67a**. The same behavior was observed for the linear ketones (**53a**, **54a**, **35a**, **42a**, 3-hydroxy-butanone **48a** and 4-hydroxybutan-2-one **49a**), since *Micro*AmDH was found to be better for the amination of these compounds compared with the other enzymes. All reported activities are summarized in **Table 2**. The discovered AmDHs reported in this study showed a preference towards the synthesis of (*S*)-configured amines with *ee* values from 68% to ≥98.5%, depending on the substrate. Notably, these nat-AmDHs are evolutionary unrelated with the engineered AmDHs described in the previous sections but highly related with each other.
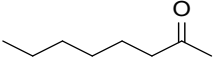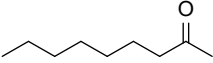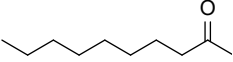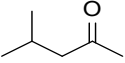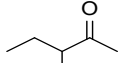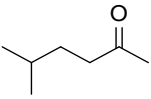
Table 1: Substrate scope of available AmDHs
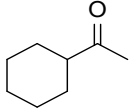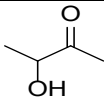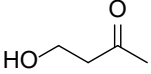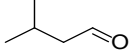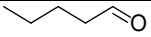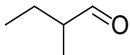
Compound	Structure	Reductive Amination (1-84a) AmDH (activity)[a]	Oxidative Deamination (1-84b) AmDH (activity)[a]	Kinetic resolution (*rac* 1-84b) (Conv. %, ee % -S-)
1a	(phenylacetone)	**4** (0.7 s^{-1})		
2a	(4-F-phenylacetone)	**2** (6.85 s^{-1}, 93%$_{50/50/48}$, 4000 mU mg^{-1}) **3** (1725 mU mg^{-1}, 93%$_{50,30,24}$) **5** (11.33 s^{-1})	**2** (*rac* 1.92 s^{-1})	**3** (51, >99)[c]
3a	(3-F-phenylacetone)	**2** (4.04 s^{-1}) **5** (3.46 s^{-1})		
4a	(2-O-phenylacetone)	**2** (142.79 mU mg^{-1}) **3** (>99%$_{50,130,48}$) **5** (276.87 mU mg^{-1})		
5a	(3-OMe-phenylacetone)	**2** (294.38 mU mg^{-1}) **4** (98%$_{50,50,24}$) **5** (55.36 mU mg^{-1})	**3** (19 mU mg^{-1})	
6a	(4-OMe-phenylacetone)	**4** (>99%$_{50,50,24}$)		
7a	(4-Me-phenylacetone)	**4** (98%$_{50,130,48}$) **5** (1600.86 mU mg^{-1})		
8a	(3-CF$_3$-phenylacetone)	**4** (98%$_{50,130,48}$)		
9a	(4-CF$_3$-phenylacetone)	**2** (12.45 mU mg^{-1}) **5** (27.67 mU mg^{-1})		
10a	(phenylacetaldehyde)	**2** (34% $_{50/50/48}$)		
11a	(4'-methylacetophenone)	**3** (9% $_{50,130,48}$)		**3** (50, >99)[b], (51, >99)[c]
12a	(3'-methylacetophenone)	**3** (39% $_{50,50,48}$)		**3** (50, >99)[b], (52, >99)[c]
13a	(acetophenone)	**1** (58.8 mU mg^{-1}) **3** (301 mU mg^{-1}, 34% $_{50,130,48}$) **6** (98.5 mU mg^{-1}) **9** (0.11 s^{-1}, >99%$_{50,90,48}$)	**2** (*R*, 1.9 mU mg^{-1}) **3** (*R*, 19 mU mg^{-1}, *rac* 0.016 s^{-1})	**3** (50, >99)[b], (50, >99%)[c]
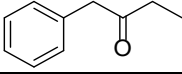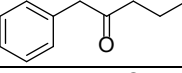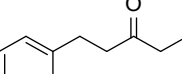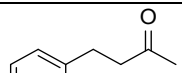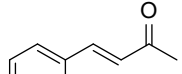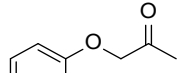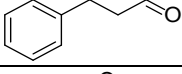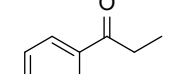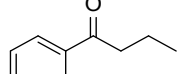
Compound	Structure	Reductive Amination (1-84a) AmDH (activity)[a]	Oxidative Deamination (1-84b) AmDH (activity)[a]	Kinetic resolution (*rac* 1-84b) (Conv. % , ee % -*S*-)
14a		**3** (22% 50,130,48) **9** (92% 50,90,48)		**3** (40, 66)[b], (51, >99)[c]
15a		**4** (33% 50,100,48)		
16a		**3** (43% 50,50,48) **9** (96% 50,90,48)		
17a		**9** (98% 50,90,48)		
18a				**3** (50, >99)[b], (50, >99) [c]
19a				**3** (22, 28)[b]
20a		**3** (69 mU mg^{-1})		
21a		**2** (31.4 mU mg^{-1}) **3** (0% 50,30,24) **4** (0% 50,50,24) **2** (1.29 mU mg^{-1}) **5** (1.68 mU mg^{-1}) **9** (0.72 s^{-1}, >99% 50,90,48) **11**_NADH_ (16.4 mU mg^{-1}) **11**_NADPH_ (3 mU mg^{-1}) **12**_NADH_ (0 mU mg^{-1}) **12**_NADPH_ (0 mU mg^{-1}) **13**_NADH_ (0 mU mg^{-1}) **13**_NADPH_ (0 mU mg^{-1}) **14** (6.4 mU mg^{-1})		
22a		**9** (55% 50,90,48)		
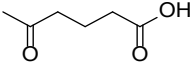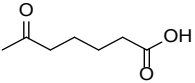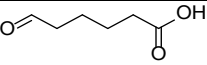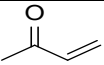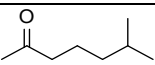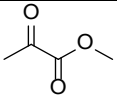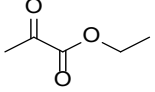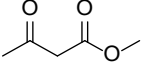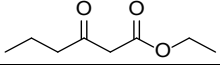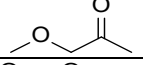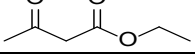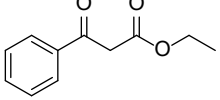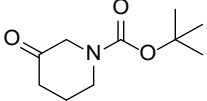
Compound	Structure	Reductive Amination (1-84a) AmDH (activity)[a]	Oxidative Deamination (1-84b) AmDH (activity)[a]	Kinetic resolution (*rac* 1-84b) (Conv. % , ee % -S-)
23a		*2* (0.96 mU mg^{-1}) *3* (107 mU mg^{-1}) *5* (3.22 mU mg^{-1}) *9* (50% $_{50,90,48}$)		
24a		*2* (0.9 mU mg^{-1}) *6* (11.8 mU mg^{-1}) *11*$_{NADH}$ (2.3 mU mg^{-1}) *11*$_{NADPH}$ (5.6 mU mg^{-1}) *12*$_{NADH}$ (14.9 mU mg^{-1}) *12*$_{NADPH}$ (60.6 mU mg^{-1}) *13*$_{NADH}$ (40.1 mU mg^{-1}) *13*$_{NADPH}$ (41.5 mU mg^{-1}) *14* (0 mU mg^{-1})		
25a		*11*$_{NADH}$ (0 mU mg^{-1}) *11*$_{NADPH}$ (63.2 mU mg^{-1}) *12*$_{NADH}$ (31.9 mU mg^{-1}) *12*$_{NADPH}$ (90.3 mU mg^{-1}) *13*$_{NADH}$ (9.4 mU mg^{-1}) *13*$_{NADPH}$ (15.2 mU mg^{-1}) *14* (0 mU mg^{-1})		
26a		*11*$_{NADH}$ (0 mU mg^{-1}) *11*$_{NADPH}$ (7.7 mU mg^{-1}) *12*$_{NADH}$ (0 mU mg^{-1}) *12*$_{NADPH}$ (23.3 mU mg^{-1}) *13*$_{NADH}$ (14.1 mU mg^{-1}) *13*$_{NADPH}$ (23.9 mU mg^{-1}) *14* (0 mU mg^{-1})		
27a		*1* (123 mU mg^{-1}) *2* (27.5 mU mg^{-1}) *2* (11.26 mU mg^{-1}) *5* (12.26 mU mg^{-1}) *6* (868 mU mg^{-1}) *9* (84% $_{50,90,48}$) *11*$_{NADH}$ (196.2 mU mg^{-1}) *11*$_{NADPH}$ (25.1 mU mg^{-1}) *12*$_{NADH}$ (614.5 mU mg^{-1}) *12*$_{NADPH}$ (388.6 mU mg^{-1}) *13*$_{NADH}$ (233.2 mU mg^{-1}) *13*$_{NADPH}$ (60.2 mU mg^{-1}) *14* (9.8 mU mg^{-1})	*1* (56 mU mg^{-1})	
28a		*2* (19.3 mU mg^{-1}) *6* (403 mU mg^{-1}) *11*$_{NADH}$ (37.3 mU mg^{-1}) *11*$_{NADPH}$ (175.2 mU mg^{-1}) *12*$_{NADH}$ (337 mU mg^{-1}) *12*$_{NADPH}$ (252.6 mU mg^{-1}) *13*$_{NADH}$ (19.6 mU mg^{-1}) *13*$_{NADPH}$ (25.5 mU mg^{-1}) *14* (0 mU mg^{-1})		
29a		*2* (41.1 mU mg^{-1}) *6* (2465 mU mg^{-1}) *11*$_{NADH}$ (38 mU mg^{-1}) *11*$_{NADPH}$ (160.9 mU mg^{-1}) *12*$_{NADH}$ (160.7 mU mg^{-1}) *12*$_{NADPH}$ (206.5 mU mg^{-1}) *13*$_{NADH}$ (33.8 mU mg^{-1}) *13*$_{NADPH}$ (63.6 mU mg^{-1}) *14* (0 mU mg^{-1})		
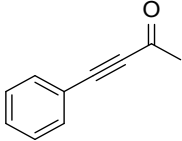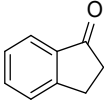
Compound	Structure	Reductive Amination (1-84a) AmDH (activity)[a]	Oxidative Deamination (1-84b) AmDH (activity)[a]	Kinetic resolution (*rac* 1-84b) (Conv. % , ee % -*S*-)
30a	(4-methylcyclohexanone)	**11**$_{NADH}$ (9.3 mU mg⁻¹) **11**$_{NADPH}$ (85.2 mU mg⁻¹) **12**$_{NADH}$ (60.1 mU mg⁻¹) **12**$_{NADPH}$ (170.1 mU mg⁻¹) **13**$_{NADH}$ (18.8 mU mg⁻¹) **13**$_{NADPH}$ (35.0 mU mg⁻¹) **14** (0 mU mg⁻¹)		
31a	(3,5-dimethylcyclohexanone)	**11**$_{NADH}$ (0 mU mg⁻¹) **11**$_{NADPH}$ (9.7 mU mg⁻¹) **12**$_{NADH}$ (0 mU mg⁻¹) **12**$_{NADPH}$ (61.6 mU mg⁻¹) **13**$_{NADH}$ (0 mU mg⁻¹) **13**$_{NADPH}$ (0 mU mg⁻¹) **14** (0 mU mg⁻¹)		
32a	(cycloheptanone)	**6** (287 mU mg⁻¹)		
33a	(acetone)	**7**$_{MO}$ (0.36 mU mg⁻¹) **8** (1.2 mU mg⁻¹)		
34a	(2-butanone)	**2** (3.68 mU mg⁻¹) **3** (8% 50,30,24) **4** (4% 50,50,24) **5** (8.26 mU mg⁻¹) **6** (137 mU mg⁻¹) **7**$_{MO}$ (169 mU mg⁻¹) **8** (202 mU mg⁻¹)		
35a	(2-pentanone)	**3** (75% 50,130,48) **6** (796 mU mg⁻¹, 0.84 s⁻¹) **6**$_{M3}$ (460 mU mg⁻¹) **7**$_{MO}$ (927 mU mg⁻¹, 30.6 s⁻¹, >99% 50,40,24) **7**$_{M1}$ (220 mU mg⁻¹, 86% 50,40,24) **7**$_{M2}$ (340 mU mg⁻¹, 97% 50,40,24) **7**$_{M3}$ (670 mU mg⁻¹, 98% 50,40,24) **8** (1030 mU mg⁻¹, 32.4 s⁻¹) **8**$_{M3}$ (760 mU mg⁻¹) **9** (81% 50,90,48) **10**$_{4-4}$ (104 mU mg⁻¹) **11**$_{NADH}$ (0 mU mg⁻¹) **11**$_{NADPH}$ (9 mU mg⁻¹) **12**$_{NADH}$ (0 mU mg⁻¹) **12**$_{NADPH}$ (51.2 mU mg⁻¹) **13**$_{NADH}$ (5.3 mU mg⁻¹) **13**$_{NADPH}$ (11 mU mg⁻¹) **14** (0 mU mg⁻¹)		**3** (37, 59)[c]
36a	(2-hexanone)	**2** (155.7 mU mg⁻¹) **3** (92% 50,30,24) **5** (30.08 mU mg⁻¹) **6** (82.8 mU mg⁻¹) **6**$_{M3}$ (1430 mU mg⁻¹) **7**$_{MO}$ (111 mU mg⁻¹, 99% 50,40,24) **7**$_{M1}$ (1470 mU mg⁻¹, >99% 50,40,24) **7**$_{M2}$ (1560 mU mg⁻¹, >99% 50,40,24) **7**$_{M3}$ (2240 mU mg⁻¹, >99% 50,40,24) **8** (89 mU mg⁻¹) **8**$_{M3}$ (2360 mU mg⁻¹) **9** (71% 50,90,48)		
37a	(2-heptanone)	**2** (11.11 mU mg⁻¹) **3** (98% 50,30,24) **4** (99% 50,50,24)	**3** (0.198 s⁻¹)	**3** (50, >99)[b], (50, >99) [c]

Compound	Structure	Reductive Amination (1-84a) AmDH (activity)[a]	Oxidative Deamination (1-84b) AmDH (activity)[a]	Kinetic resolution (*rac* 1-84b) (Conv. % , ee % -S-)
		5 (42.42 mU mg^{-1}) *6*$_{M3}$ (1480 mU mg^{-1}) *7*$_{MO}$ (0 mU mg^{-1}, 4% $_{50,40,24}$) *7*$_{M1}$ (430 mU mg^{-1}, 99% $_{50,40,24}$) *7*$_{M2}$ (1400 mU mg^{-1}, >99% $_{50,40,24}$) *7*$_{M3}$ (2590 mU mg^{-1}, >99% $_{50,40,24}$) *8* (0 mU mg^{-1}) *8*$_{M3}$ (2800 mU mg^{-1})		
38a		*3* (50% $_{50,30,48}$) *4* (93% $_{50,50,48}$) *7*$_{MO}$ (0 mU mg^{-1}, 0% $_{50,40,24}$) *7*$_{M1}$ (45% $_{50,40,24}$) *7*$_{M2}$ (61% $_{50,40,24}$) *7*$_{M3}$ (80% $_{50,40,24}$) *8* (0 mU mg^{-1})		
39a		*7*$_{MO}$ (0 mU mg^{-1}, 0% $_{50,40,24}$) *7*$_{M1}$ (0% $_{50,40,24}$) *7*$_{M3}$ (12% $_{50,40,24}$) *7*$_{M3}$ (22% $_{50,40,24}$) *8* (0 mU mg^{-1})		
40a		*7*$_{MO}$ (0 mU mg^{-1}) *7*$_{M1}$ (0 mU mg^{-1}) *7*$_{M3}$ (2.5 mU mg^{-1}) *7*$_{M3}$ (2.5 mU mg^{-1})		
41a		*1* (690 mU mg^{-1}, 85% conv$_{10,4,48}$) *2* (77 mU mg^{-1}, 0.03 s^{-1}) *3* (96% $_{50,130,48}$) *4* (91% $_{50,130,48}$) *5* (0.06 s^{-1}) *6* (490 mU mg^{-1}) *9* (53% $_{50,90,48}$)	*1* (2640 mU mg^{-1}) *2* (166.3 mU mg^{-1})	*3* (50, >99)[c]
42a		*6* (3628 mU mg^{-1}) *7*$_{MO}$ (3077 mU mg^{-1}) *8* (3662 mU mg^{-1}) *11*$_{NADH}$ (18.6 mU mg^{-1}) *11*$_{NADPH}$ (129 mU mg^{-1}) *12*$_{NADH}$ (54.4 mU mg^{-1}) *12*$_{NADPH}$ (245.6 mU mg^{-1}) *13*$_{NADH}$ (120.6 mU mg^{-1}) *13*$_{NADPH}$ (109.6 mU mg^{-1}) *14* (0 mU mg^{-1})		
43a		*7*$_{MO}$ (~1 mU mg^{-1}) *7*$_{M1}$ (>1000 mU mg^{-1}) *7*$_{M2}$ (>1000 mU mg^{-1}) *7*$_{M3}$ (>1000 mU mg^{-1})		
44a		*2* (72.7 mU mg^{-1}) *6* (2559 mU mg^{-1}) *7*$_{MO}$ (2646 mU mg^{-1}) *8* (3078 mU mg^{-1})		
45a		*3* (133 mU mg^{-1}) *6* (760 mU mg^{-1}) *7*$_{MO}$ (637 mU mg^{-1}) *8* (681 mU mg^{-1})		
46a		*6* (11.8 mU mg^{-1})		

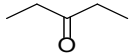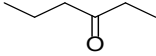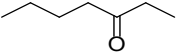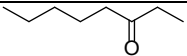| Compound	Structure	Reductive Amination (1-84a) AmDH (activity)[a]	Oxidative Deamination (1-84b) AmDH (activity)[a]	Kinetic resolution (*rac 1-84b*) (Conv. % , ee % -*S*-)
47a		**2** (0.044 s⁻¹) **5** (0.007 s⁻¹) **11**$_{NADH}$ (0 mU mg⁻¹) **11**$_{NADPH}$ (2.1 mU mg⁻¹) **12**$_{NADH}$ (0 mU mg⁻¹) **12**$_{NADPH}$ (64.0 mU mg⁻¹) **13**$_{NADH}$ (0 mU mg⁻¹) **13**$_{NADPH}$ (0 mU mg⁻¹) **14** (0 mU mg⁻¹)		
48a		**11**$_{NADH}$ (0 mU mg⁻¹) **11**$_{NADPH}$ (177.7 mU mg⁻¹) **12**$_{NADH}$ (0 mU mg⁻¹) **12**$_{NADPH}$ (324 mU mg⁻¹) **13**$_{NADH}$ (43.1 mU mg⁻¹) **13**$_{NADPH}$ (72.7 mU mg⁻¹) **14** (0 mU mg⁻¹)		
49a		**6** (4.5 mU mg⁻¹) **11**$_{NADH}$ (0 mU mg⁻¹) **11**$_{NADPH}$ (10.3 mU mg⁻¹) **12**$_{NADH}$ (0 mU mg⁻¹) **12**$_{NADPH}$ (11.0 mU mg⁻¹) **13**$_{NADH}$ (3.1 mU mg⁻¹) **13**$_{NADPH}$ (6.1 mU mg⁻¹) **14** (0 mU mg⁻¹)		
50a		**3** (>99% 50,30,24) **4** (99% 50,130,48)		
51a		**11**$_{NADH}$ (0 mU mg⁻¹) **11**$_{NADPH}$ (26.8 mU mg⁻¹) **12**$_{NADH}$ (0 mU mg⁻¹) **12**$_{NADPH}$ (57.8 mU mg⁻¹) **13**$_{NADH}$ (85 mU mg⁻¹) **13**$_{NADPH}$ (125.1 mU mg⁻¹) **14** (33.9 mU mg⁻¹)		
52a		**11**$_{NADH}$ (16.4 mU mg⁻¹) **11**$_{NADPH}$ (75.2 mU mg⁻¹) **12**$_{NADH}$ (159.4 mU mg⁻¹) **12**$_{NADPH}$ (97.6 mU mg⁻¹) **13**$_{NADH}$ (397.9 mU mg⁻¹) **13**$_{NADPH}$ (131.6 mU mg⁻¹) **14** (129.6 mU mg⁻¹)		
53a		**2** (1.3 mU mg⁻¹) **11**$_{NADH}$ (0 mU mg⁻¹) **11**$_{NADPH}$ (48.1 mU mg⁻¹) **12**$_{NADH}$ (0 mU mg⁻¹) **12**$_{NADPH}$ (190.2 mU mg⁻¹) **13**$_{NADH}$ (3.1 mU mg⁻¹) **13**$_{NADPH}$ (5.8 mU mg⁻¹) **14** (0 mU mg⁻¹)		
54a		**2** (1.6 mU mg⁻¹) **11**$_{NADH}$ (0 mU mg⁻¹) **11**$_{NADPH}$ (6.8 mU mg⁻¹) **12**$_{NADH}$ (0 mU mg⁻¹) **12**$_{NADPH}$ (28.1 mU mg⁻¹) **13**$_{NADH}$ (0 mU mg⁻¹) **13**$_{NADPH}$ (0 mU mg⁻¹) **14** (0 mU mg⁻¹)		
55a		**3** (57% 50,90,48) **4** (32% 50,100,48)		
56a		**2** (4.70 mU mg⁻¹) **5** (3.30 mU mg⁻¹)		

Compound	Structure	Reductive Amination (1-84a) AmDH (activity)[a]	Oxidative Deamination (1-84b) AmDH (activity)[a]	Kinetic resolution (*rac* 1-84b) (Conv. %, ee % -S-)
57a		*4* (99% 50,130,48)		
58a		*4* (71% 50,100,48)		
59a		*4* (87% 50,100,48)		
60a		*2* (0.005 s^{-1}) *4* (0.72 s^{-1}, >99% 50,50,24) *5* (0.007 s^{-1})		*3* (25, 33)[b], 51, >99) [c]
61a		*2* (0.62 mU mg^{-1}) *5* (2.13 mU mg^{-1})		
62a		*2* (540.8 mU mg^{-1}, 0.39 s^{-1}) *5* (0.35 s^{-1})		
63a		*2* (15.27 mU mg^{-1}) *4* (96% 50,100,48) *5* (17.06 mU mg^{-1})		
64a		*3* (8% 50,90,48) *4* (0% 50,100,48) *9* (95% 50,90,48)		
65a		*3* (0% 50,90,48) *4* (1% 50,100,48) *9* (65% 50,90,48)		
66a		*3* (2% 50,90,48) *4* (2% 50,100,48) *9* (26% 50,90,48)		
67a		*2* (1.15 mU mg^{-1}) *5* (1.93 mU mg^{-1}) *11*$_{NADH}$ (2.3 mU mg^{-1}) *11*$_{NADPH}$ (7.4 mU mg^{-1}) *12*$_{NADH}$ (34.0 mU mg^{-1}) *12*$_{NADPH}$ (37.1 mU mg^{-1}) *13*$_{NADH}$ (4.3 mU mg^{-1}) *13*$_{NADPH}$ (3.6 mU mg^{-1}) *14* (0 mU mg^{-1})		
68a		*10*$_{wt}$ (51.9 mU mg^{-1})		
69a		*11*$_{NADH}$ (119.2 mU mg^{-1}) *11*$_{NADPH}$ (88.1 mU mg^{-1}) *12*$_{NADH}$ (541 mU mg^{-1})		

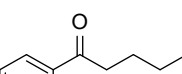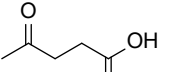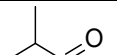| Compound	Structure	Reductive Amination (1-84a) AmDH (activity)[a]	Oxidative Deamination (1-84b) AmDH (activity)[a]	Kinetic resolution (*rac* 1-84b) (Conv. % , ee % -*S*-)
		12$_{NADPH}$ (269.8 mU mg^{-1}) **13**$_{NADH}$ (955 mU mg^{-1}) **13**$_{NADPH}$ (73.8 mU mg^{-1}) **14** (514 mU mg^{-1})		
70a		**10**$_{wt}$ (N.R.)		
71a		**9** (>99% $_{50,90,48}$)		
72a		**9** (>99% $_{50,90,48}$)		
73a		**11**$_{NADH}$ (2.7 mU mg^{-1}) **11**$_{NADPH}$ (7.9 mU mg^{-1}) **12**$_{NADH}$ (0 mU mg^{-1}) **12**$_{NADPH}$ (0 mU mg^{-1}) **13**$_{NADH}$ (0 mU mg^{-1}) **13**$_{NADPH}$ (0 mU mg^{-1}) **14** (0 mU mg^{-1})		
74a		**7**$_{MO}$ (0 mU mg^{-1}) **7**$_{M1}$ (~2 mU mg^{-1}) **7**$_{M2}$ (~80 mU mg^{-1}) **7**$_{M3}$ (~90 mU mg^{-1})		
75a		**6** (1.4 mU mg^{-1})		
76a		**1** (13.2 mU mg^{-1}) **2** (18.4 mU mg^{-1})		
77a		**1** (4.5 mU mg^{-1})		
78a		**1** (14 mU mg^{-1})		
79a			**3** (40 mU mg^{-1})	
80a		**2** (0.36 mU mg^{-1}) **5** (1.69 mU mg^{-1})		
81a		**2** (3.71 mU mg^{-1}) **5** (9.77 mU mg^{-1})		
82a		**2** (0.46 mU mg^{-1}) **5** (0.86 mU mg^{-1})		

Compound	Structure	Reductive Amination (1-84a) AmDH (activity)[a]	Oxidative Deamination (1-84b) AmDH (activity)[a]	Kinetic resolution (*rac* 1-84b) (Conv. % , ee % -*S*-)
83a	O (phenyl propynyl ketone)	**2** (<0.1 mU mg⁻¹) **5** (<0.1 mU mg⁻¹)		
84a	O (indanone)	**9** (>99% ₂₀,₉₀,₄₈) **11**_NADH_ (0 mU mg⁻¹) **11**_NADPH_ (0 mU mg⁻¹) **12**_NADH_ (0 mU mg⁻¹) **12**_NADPH_ (12 mU mg⁻¹) **13**_NADH_ (0 mU mg⁻¹) **13**_NADPH_ (0 mU mg⁻¹) **14** (0 mU mg⁻¹)		

[a] Activities reported here are expressed as: i) k_{cat} (s⁻¹), ii) specific activity (mU mg⁻¹) or iii) conversion (%). In the case of reported conversion, the subscripts after % means: 1) substrate concentration in mM; 2) enzyme concentration in µM and 3) time (h). Conversions reported for LE-AmDH-v1 (No 9) have been obtained at 50 °C, while for the rest of the AmDHs at 30 °C. The number in front of the activity (1-14) refers to the AmDH based on the numbering of Table 1. WT refers to the wild type enzyme; M0-M3 refers to the variants as described in Table 1 and NADH or NADPH refers to the form of cofactor used for the determination of the activity.

[b] The kinetic resolution was performed using 5-10 mM of substrate, 120 mg_DCW mL⁻¹ of lyophilized cFL1-AmDH-NOx bi-enzymatic system in Tris/HCl buffer (100 mM, pH 8.5) for 24 h at 37 °C

[c] The kinetic resolution was performed using 20 mM of substrate, 30 mg_DCW mL⁻¹ of lyophilized cFL1-AmDH/AlaDH bi-enzymatic system in glycine buffer (100 mM, pH 10.0) for 24h at 37 °C N.R.: Not reported (the exact number)

Compounds 1-84a are shown in the Table 2. Compounds 1-84b are the aminated products of compounds 1-84a.

1.4 Applicability of AmDHs

Because of the availability of (*R*)-stereoselective members, AmDH family has been successfully applied for the preparation of (*S*)-configured amines via kinetic resolution of racemates. This strategy requires a driving force towards the oxidative deamination direction that is provided either by an oxidase or by an alanine dehydrogenase, which consume the hydride produced by the AmDH oxidative step to re-oxidise NADH to NAD⁺. NAD⁺ is then use by the AmDH for another catalytic cycle (**Scheme 1B**). The inherent high AmDHs' enantioselectivity enabled this process to reach the theoretical maximum of 50% yield with excellent *ee* of the remaining amine (>99% *S*). AmDHs combined with

(*S*)-selective ω-transaminases have also been involved in deracemization cascades. They have been applied either in the enantioselective amination step (**Scheme 1C**) or in the enantioselective deamination step (**scheme 1D**). The challenging simultaneous execution of oxidative and reductive steps has been enabled by the use of AmDHs and ADHs (**scheme 1E**) for the asymmetric amination of alcohols using enzymes in purified form, immobilized or as whole cells. Finally, AmDHs have been applied in a thermodynamically favored biocatalytic network employing in total five different enzymes (**Scheme 1G**).
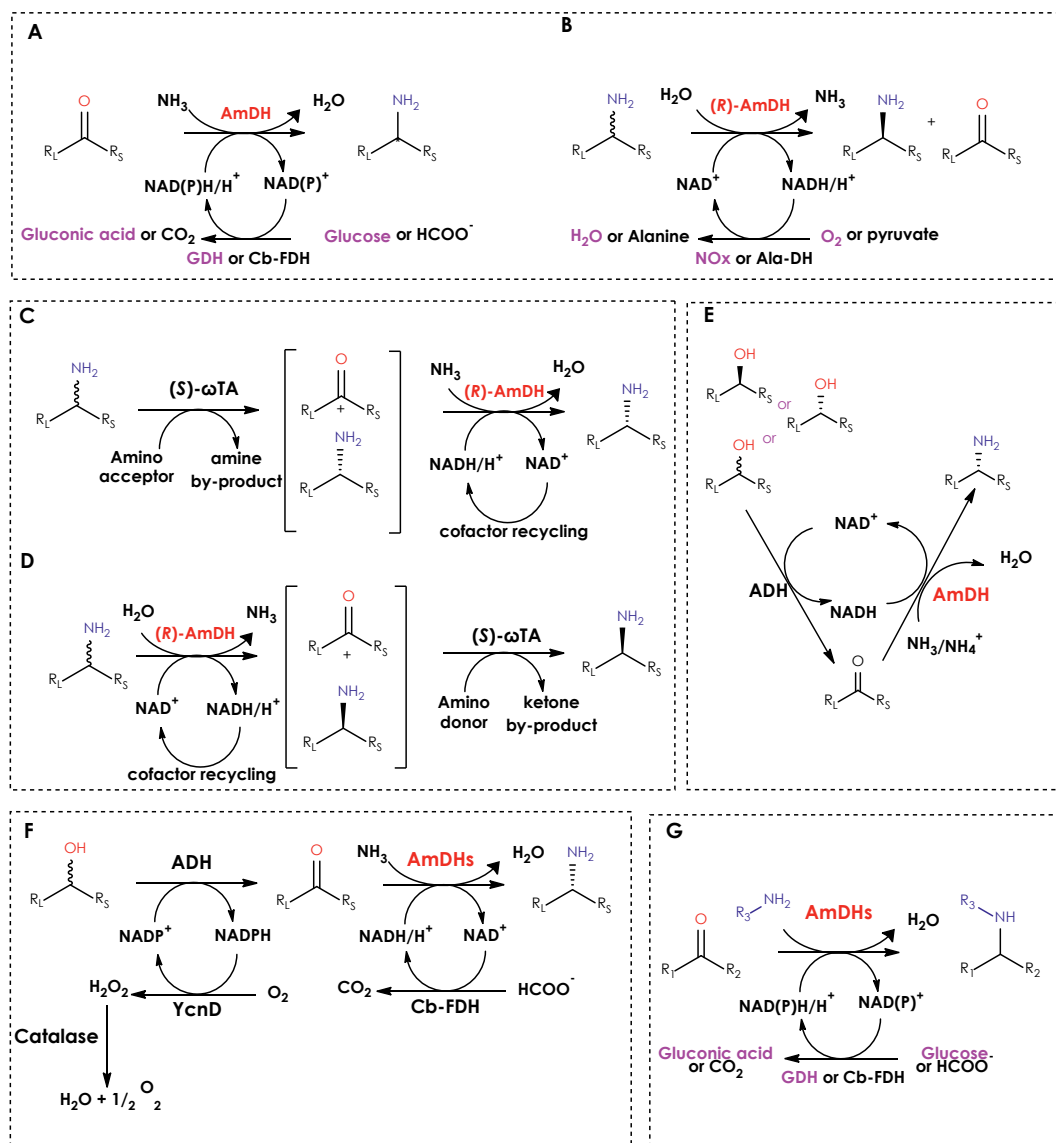
Scheme 1. Reactions and/or biocatalytic cascades in which AmDHs have been implemented so far. (A) Reductive amination of carbonyl compounds with cofactor recycling; (B) kinetic resolution of racemic amines with cofactor recycling; (C) and (D) deracemization cascades employing *R* selective AmDHs and *S* selective ω-transaminases; (E) Hydrogen borrowing cascade for the asymmetric amination of alcohols (F) biocatalytic network for the amination of alcohols utilizing alcohol dehydrogenases and amine dehydrogenases with orthogonal cofactor recycling systems (G) application of AmDHs for the synthesis of secondary and tertiary amines.

R_L: Large substituent, R_s: Small substituent

1.4.1 Kinetic resolution and deracemization of *racemic* amines

AmDHs cover already a respectable substrate scope (**Table 2**) but one of the major limitations relies on the enantioselectivity that the majority of the members display. Apart from the recently discovered nat-AmDHs, the rest of the AmDHs exhibit (*R*)-enantioselectivity and thus are unable to give access to the (*S*)-enantiomer via asymmetric amination. However, the scarce availability of (*S*)-selective AmDHs can be overcome by performing kinetic resolution (KR) of racemic amines using the available (*R*)-selective AmDHs. This strategy is particularly attractive since amine racemates, as starting materials, can be available. KR has been demonstrated using ωTAs,[26] the recently discovered reductive aminases (RedAms)[29] and has been extensively studied using monoamine oxidases (MAOs).[13,63] The applicability of the AmDHs in the kinetic resolution is a less studied reaction with only a few examples reported so far. For instance, Hyunwoo *et al.*[27] have been used whole cells co-expressing cFL1-AmDH and an NADH oxidase (NOx) from *Lactobacillus brevis*.[64] The authors first examined a panel of substrates for the oxidative deamination reaction to ensure that the enzyme was active in this direction. Most well accepted substrates were *rac*-**13b** (0.016 s^{-1}) and *rac*-2-aminoheptane (**37b,** 0.198 s^{-1}). These two substrates were chosen for optimization of the reaction's conditions. Determination of the optimum pH, revealed a preference for pH 10.0 for AmDHs, while NOx found more active at pH 7.5. The AmDH-NOx coupled assay did not proceeded well when tested for the kinetic resolution of *rac*-**37b** irrespectively of pH of the reaction buffer giving a maximum of 26% *ee* of the amine product after 24 h due to strong product inhibition. Indeed, the enzyme's initial activity for the deamination of *rac*-**37b** decreased by 40% when 2 mM of 2-heptanone was present in the reaction mixture. In contrast, the activity of NOx was not affected by the presence of the ketone. To overcome the moderate activity of the coupled AmDH-NOx assay, the authors used whole cells co-expressing the cFL1-AmDH and NOx (cloned in different expression vectors). Both *rac*-**13b** and **37b** were successfully resolved at 10 mM scale using 20 mg mL^{-1} at pH 8.5 after

24 h without any addition of the cofactor. Higher substrate loading of 20 mM, 30 mM, 40 mM and 50 mM for *rac*-**37b** resulted in *ee* values of (*S*)-**37b** of >99%, 87%, 48% and 30%, respectively. The minimum amounts of whole cells required to resolved 50 mM of *rac*-**37b** and 20 mM of *rac*-**13b** were 60 and 100 mg$_{DCW}$ mL^{-1}, respectively. The whole cell system was further applied for the KR of a panel of racemic amines (*para*-methyl-a-methylbenzylamine **11b**, *meta*-methyl-a-methylbenzylamine **12b**, *meta*-fluoro-a-methylbenzylamine **14b**, 3,4-difluoro-a-methylbenzylamine **18b**, 3,5-difluoro-a-methylbenzylamine **19b, 37b** and **60b**) using 5-10 mM of substrate, 120 mg$_{DCW}$ mL^{-1} in Tris/ HCl buffer (100 mM, pH 8.5) for 24 h at 37 °C. **11b**, **12b** and **18b** were successfully resolved at 10 mM scale, under the assay conditions. The KR of **14b** proceeded with 77% *ee* at 5 mM scale. Similar results were obtained for **19b** since the obtained *ee* after 24 h was 77% (5 mM) and significantly lower (28%) at 10 mM substrate concentration. Finally, resolution of *rac*-**60b** proceeded with moderate *ee* of 51%. All results are summarized in **Table 2**.

Two years later in 2019, Patil and coworkers developed another biocatalytic cascade utilizing an AmDH and an alanine dehydrogenase (Ala-DH) as shown in **Scheme 1B**.[28] In this study cFL1-AmDH (**Table 1**, entry 3) and *Rs*-AmDH (**Table 1**, entry 4) were used. In the initial set of reactions the authors tested various racemic amines for the oxidative deamination potential of these AmDHs. The cFL1-AmDH showed the highest activity towards **37b** and Rs-AmDH towards **60b**. Both enzymes also displayed high activity for *para*-fluorophenyl-propan-2-amine (**2b**) and *meta*-methyl-a-methylbenzylamine (**12b**). Nevertheless, the authors chose **37b** and **13b** as substrates to optimize the AmDH/Ala-DH system. The pH optimum of Ala-DH was determined at 10.0, which is identical to the pH optimum of cFL1-AmDH (pH 10.0) and very close to the one of *Rs*-AmDH (pH 9.5). Thus, the kinetic resolution using cFL1-AmDH/Ala-DH and *Rs*-AmDH/Ala-DH was carried at pH 10.0 and 9.5, respectively. Increasing the concentration of pyruvate correlated with a consistent increase in the oxidative deamination reaction reaching its maximum rate when the molar ratio between substrate and pyruvate was equal or higher to 1:2. Using this molar ratio, 50 mM of *rac*-**37b** were

successfully resolved by both enzymes using 1 mg mL^{-1} AmDH, 1 mg mL^{-1} of Ala-DH in 100 mM glycine buffer (pH 9.5-10.0). In contrast, under the same reaction conditions, the resolution of 50 mM of *rac*-**13b** proceeded with 43% *ee* for the reaction catalyzed by cFL1-AmDH, possibly due to substrate or product inhibition as we have also shown later this year for this AmDH.[54] Therefore, the authors decided to study the inhibition effects of *rac*-**37a** and alanine on *Rs*-AmDH as well as the effects of *rac*-**37b** and **13b** and their corresponding ketones (**37a** and **13a**) on Ala-DH. *Rs*-AmDH retained 61% and 65% of its original activity in the presence of 15 mM *rac* **37a** and 50 mM alanine, respectively. Moreover, the relative activity of Ala-DH was 63% and 84% in the presence of 10 mM *rac*-**37b** and *rac*-**13b**, respectively. As shown in the past by the same group, the authors decided to overcome these inhibitory effects by using whole cells expressing the AmDHs and Ala-DH. Using 10 mg$_{DCW}$ mL^{-1} of cells, 10 mM of *rac*-**37b** and *rac*-**13b** were successfully resolved into the corresponding (*S*)-configured amines (*ee* > 99%) without any addition of cofactor due to efficient cofactor regeneration in whole cells. The most challenging *rac*-**13b** was successfully resolved at 50 mM or 100 mM using 30 mg$_{DCW}$ mL^{-1} or 40 mg$_{DCW}$ mL^{-1} of whole cells co-expressing cFL1-AmDH and Ala-DH, respectively. Moreover, 30 mg$_{DCW}$ mL^{-1} was enough resolve 100 mM of *rac*-**37b**. The applicability of the whole cell system was further investigated with various substrates (**2b**, **11b**, **12b**, **14b**, **18b**, **35b**, 4-methyl-2-pentylamine **41b** and **60b**) using 20 mM of substrate, 30 mg$_{DCW}$ mL^{-1} of the cFL1-AmDH/Ala-DH system, 40 mM pyruvate (1:2, substrate: pyruvate) in 100 mM glycine buffer pH 10.0 at 37 °C for 24 h. In all cases, the kinetic resolution proceeded with >99% ee for the (*S*)-configured amine with the exception of **35b** which resulted in 37% conv. into the corresponding ketone with 59% *ee*.

Recently Sanghan and coworkers established a deracemization protocol employing the (*R*)-selective AmDHs (cFL1-AmDH or Rs-AmDH) in tandem with enantiocomplementary (*S*)-selective ω-TA (or vice versa) in order to access both enantiomers of chiral amines by controlling the direction of the reactions.[65] This one-pot, two-step cascade can be accomplished by enantioselective

deamination of the racemic amine followed by stereoselective amination of the ketone generated according to **scheme 1C and D**. The AmDHs can be applied either in the first step (enantioselective deamination) or in the second step (enantioselective amination). The authors investigated the influence of the pH for the reductive amination reaction catalyzed by AmDHs in the respective activity assay. The highest activity was observed at pH 9.5. The AmDH-FDH system for cofactor recycling was chosen because of its better performance compared with the AmDH-GDH system. This system was used as whole cells co-expressing the AmDH and FDH in different vectors. Among the four ω-TAs tested in the deamination direction, the enzyme from *Polaromonas sp. JS666* (*S*-ω-TA*PO*)[66] showed broader substrate scope and therefore was used for subsequent studies as lyophilized whole cells. With the two individual whole cells systems the deracemization of 11 racemic amines of **Table 2** (**2b**, **11b**, **12b**, **13b**, **14b**, **18b**, 2-hexylamine **36b**, **37b** and **60b**) was attempted according to **Scheme 1C** using 10 mM racemic substrate, 10 mM pyruvate, 0.1 mM PLP, 3.3 mg_{DCW} mL^{-1} ω-TAPO cells and 30 mg_{DCW} mL^{-1} *Rs*-AmDH-FDH cells. Reactions were performed at 37 °C in 100 mM glycine buffer (pH 9.5) and 200 mM ammonium formate for 24 h. The cascade resulted in 4 successful deracemization examples (**60b**, **2b**, **36b**, **37b**) with full conversion and excellent enantioselectivities (>99% *ee*). Excellent *ee* was also observed for the rest of the substrates tested albeit lower conversions (52%-77%) were observed. The authors attributed these results in the low expression of the AmDHs in the whole cell system (AmDH/FDH). Increased expression of the AmDHs was observed when cloned in different vectors. Indeed, the new system resulted in excellent conversions in 8 cases (**2b**, **11b**, **12b**, **14b**, **18b**, **36b, 37b**, **60b**) and excellent enantioselectivity in all cases. Using the approach described in **Scheme 1D**, the authors aimed at deracemizing the same panel of substrates to their corresponding (*S*)-configured amines. A major issue of this cascade, is that the alanine dehydrogenase system used for recycling the pyruvate and regenerating the nicotinamide adenine dinucleotide cofactor performed poorly when both enzymes were combined. Therefore, benzylamine was used as amino donor and an aldehyde reductase

(AHR) from *Sunechocystis sp.*[67] was also added to produce benzyl-alcohol thereby regenerating the NAD^{+} cofactor. In the reductive amination direction, the authors chose the ωTA originated from *Vibrio fluvialis* JS17 (*S*-ω-TAVF).[68] In the initial set of experiments the cascade was performed using *rac* **60b** as substrate. At the end of the reaction, the obtained *ee* was 91% for the (*S*) amine. Notably, addition of 0.2 mM of benzaldehyde (using 20 mM of racemic amine as substrate in the first step) served as driving force towards the desirable direction with >99% conversion and 95.4% ee of (*S*)-**60b**. This deracemization cascade was employed as whole-cell system expressing AmDH-AHR and the (*S*)-ωTA. Addition of 1 mM benzaldehyde with 10 mM of racemic amine as substrate, 0.1 mM PLP as well as 10 and 27 mg$_{DCW}$ mL^{-1} cells of ωTAVF and cFL1-AmDH-AHR, respectively, resulted to full resolution of **14b**, **18b**, **11b**, **12b**, **60b**, **2b**, **36b** and **37b** with >99% conversion.

1.4.2 Biocatalytic cascades for the asymmetric amination of alcohols

Up to date there are a few examples of biocatalytic cascades employing AmDHs for the synthesis of a-chiral amines. The first example has been demonstrated in 2015 when Mutti, Turner and coworkers reported an elegant biocatalytic hydrogen-borrowing amination cascade employing an alcohol dehydrogenase (ADH) for the oxidation of racemic alcohols to the corresponding ketones, and the subsequent reductive amination using an AmDH (**Scheme 1E**).[32] This redox self-sufficient cycle uses ammonium ion/ammonia as the source of the nitrogen and generates only water as the by-product. Moreover, the catalytic amount of nicotinamide adenine dinucleotide coenzyme is internally recycled by the two enzymes. For this study the authors used the *Bb*-AmDH[40] (**Table 1** entry 4) and cFL1-AmDH[44] (**Table 1** entry 3) and two stereo-complementary NAD^{+}-depended ADHs: an (*S*)-selective from *Aromatoleum aromaticum* (AA-ADH)[69] and the (*R*)-selective from *Lactobacillus brevis* (LBv-ADH).[70] After purification of the LBv-ADH and Bb-AmDH, the enzymatic cascade was attempted for the amination of (*R*)-phenyl-propan-2-ol (**1c**). However, low conversions were obtained due to enzyme precipitation in the buffer when both ADH and AmDH were present. The authors speculated that

enzyme precipitation in the dual-enzyme cascade, might have been caused by coordination of free divalent cations, coming from the ADHs, to the imidazole groups of the His-terminal tag of the AmDHs. After cleavage of the tag, the cascade proceeded with 85% conversion and >99% ee (R) after 24 h using the AA-ADH (1.88 mg mL^{-1}) and Bb-AmDH (20 U) (S-**1a**: 20 mM, NAD$^+$: 1 mM, and NH$_4$Cl/NH$_3$: 2 M pH 8.7). High conversions (93%) and >99% ee (R) was also obtained using the LBv-ADH for the amination of (R)-**1a**, only when the buffer of the reaction was reduced to pH 8.0-8.5, indicating that LBv-ADH was not stable in ammonium chloride at pH 8.7. The hydrogen-borrowing cascade was tested for amination with inversion of configuration starting from S configured secondary alcohols and using the AA-DH or for retention of configuration starting from (R)-configured alcohols and using the LBv-ADH. In both cases, most of the substrates were converted to the enantiopure amines with good to excellent conversions. The cascade was also attempted by combining both ADHs in tandem with either *Bb*-AmDH or cFL1-AmDH for the asymmetric amination of racemic amines (**Table 3**, cascade 1). Reaction conditions were: AA-ADH (1.0-2.3 mg mL^{-1}), LBv-ADH (1.0-2.6 mg mL^{-1}), AmDH (20 U) in ammonium formate buffer (pH 8.5, 2 M) containing catalytic NAD$^+$ (1mM). High conversions (>70%) with excellent ee (>99% R) were obtained for substrates **1c**, 1-(1-methoxyphenyl)-propan-2-ol (**5c**), 1-phenyl-butan-2-ol (**57c**) and phenoxy-propan-2-ol (**62c**) using the *Bb*-AmDH as well as 2-hexanol (**36c**), 2-heptanol (**37c**), 2-octanol (**38c**) and 4-methy-pentan-2-ol (**41c**) using the cFL1-AmDH. Notably, the substrate 4-phenyl-butan-2-ol (**60c**) was obtained with 92% conversion and 83% ee although *Bb*-AmDH showed excellent stereoselectivity for the ketone **60a** in previous studies.[43,45] Small aromatic substrates like phenyl-ethanol (**13c**) and derivatives (**11c**, **12c**, **14c**, **16c**, **17c**) resulted in poor conversions (9%-20%) but excellent ee (>99% R). A possible explanation is that the corresponding ketones of these compounds are poor substrates for cFL1-AmDH as demonstrated two years later in a follow-up publication;[43] The reason was the issue of product inhibition as demonstrated earlier this year in another publication.[54]

A few months after the first report by Mutti, Turner and co-workers, Chen *et al*. published the results of an identical cascade using an ADH from *Streptomyces coelicolor*[71] (*Sc*-ADH) and the engineered ,above mentioned, *Es*-AmDH.[47] The *Sc*-ADH was chosen, after screening of 20 available ADHs, because of its ability to convert both isomers of the racemic secondary alcohols into the corresponding ketones and its desirable substrate scope. Optimization studies of the cascade using 2-pentanol (**35c**) as substrate, showed that the best conversion (92%) obtained in NH_4Cl/NH_4OH buffer (2 M, pH 9.5) with 1 mM of NAD^+ at 30 °C after 24h. Using these reaction conditions and both enzymes as lyophilized cell-free extracts (10 mg) substrates: **35c**, **41c**, 3-methyl-pentan2-ol (**42c**), isobutanol (**44c**), 3,3-dimethyl-butanol (**45c**), cyclohexanol (**27c**), 3-methyl-cyclohexanol (**29c**), 2-methyl-cyclohexanol (**28c**), and cycloheptanol (**32c**) were tested at 50 mM scale (**Table 2**, cascade 2). In all cases in which the authors reported information about the absolute configuration of the products (**35b**, **41b**, **44b**, **45b** and **13b**), the *ee* was >99% (*R*). The highest conversion was observed for compound **27c** (97%), following by **35c** (94%), **44c** (93%) and **41c** (73%). The challenging substrate **13c** was poorly converted to the corresponding amine (21%) using the newly developed *Es*-AmDH.

Three years later, this system was further improved by co-immobilizing the AA-ADH and cFL1-AmDH on controlled porosity glass (CPG)-Fe^{III} ion-affinity beads (EziG) by Böhmer *et al*.[33] The co-immobilized dehydrogenases (50 $mg_{enz.}$ g_{beads}^{-1}) were tested for the amination of (*S*)-**1c**, **2c**, **62c**, **36c** and **37c** (20 mM) and the least converted alcohol substrate was **62c** (28%), while using this system, 95% of both **1c** and **37c** were converted**.** In all cases, the obtained *ee* values were >99% for the (*R*)-configured product. Notably, the total turnover numbers were improved from 2 to 15-fold compared with the previous studies with free enzymes in solution. Moreover, the immobilized system enabled recyclability and limited product inhibition phenomenon. In another study, co-immobilization of the cFL1-AmDH and *Cb*-FDH was reported by Thompson *et al*. The authors investigated the AmDH/FDH system in continuous flow. The best activity was obtained with 1:1 molar ratio of AmDH:FDH on EziG™ Amber beads
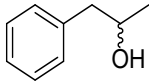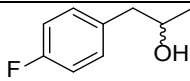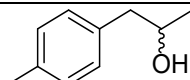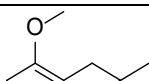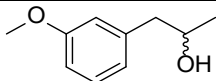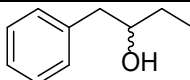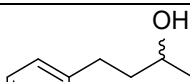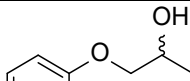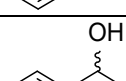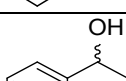
type. The immobilized system converted 64% of 10 mM of **2a** to the corresponding amine after 3 h with a flow rate of 0.2 mL min^{-1} of ammonium formate (1 M, pH 9.0) supplemented with 0.5 mM NAD$^+$. Having successfully demonstrated this process in continuous flow the authors co-immobilized the TeS-ADH[72] variant (W110A/G198D) with cFL1-AmDH. Using a flow rate of 0.02 mL min^{-1}, compound *rac*-**2c** (10 mM) was converted to **2b** using ammonium formate buffer (1 M, pH 9.0) and 1 mM of NAD$^+$. After 10 column volumes the reaction reached steady state (ca. 30% conversion) which was maintained for 20 h.
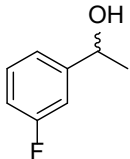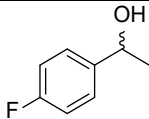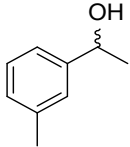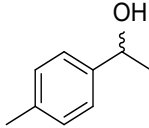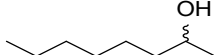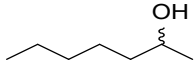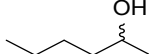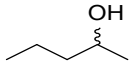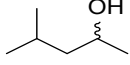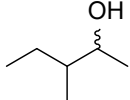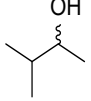
The applicability of the ADH-AmDH bioamination was further investigated earlier this year by Houwman *et al.* using resting *E.coli* cells.[34] The (*S*)-selective AA-ADH and the (*R*)-selective LBv-ADH in combination with cFL1-AmDH were selected for this study. Equal mass production of AA-ADH and cFL1-AmDH was achieved by using a Duet plasmid when the His-tagged cFL1-AmDH precedes the AA-ADH gene in the final DNA construct. The gene of a GST-tagged LBv-ADH was co-expressed in a pET-28b vector in the same host. Using these optimized constructs the authors examined a number of parameters that may affect the whole cell biocatalytic cascade. For instance, they examined the influence of the intracellular NAD$^+$/NADH redox balance which is shifted towards the oxidized form under physiological conditions in the cell. Indeed, addition of glucose (equal to 1:0.6, substrate to glucose molar ratio) led to higher conversion by this system with an optimum cell amount of 60 mg$_{wcw}$ mL^{-1}. A series of toxicity assays were performed to investigate the survival rate of the cells and/or the influence of the toxicity of the compounds (substrates, intermediates and products) in the productivity of the system. Among all compounds tested for their toxicity against *E.coli* cells, using a minimal inhibitory concentration (MIC), the amines showed the highest toxicity levels, even at low quantities resulting in cell death. This toxicity led to large variations of the productivity of the system when the substrate concentration was increased above a critical value. Substrate concentrations below this value resulted in elevated and consistent conversions among different experiments. Notably, addition of hexadecane as co-solvent (10% v v^{-1}) was
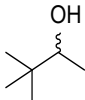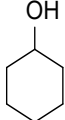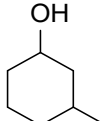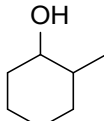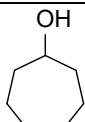
beneficial at higher substrate concentrations (e.g., 20 mM) but detrimental when lower amount of substrate was used (e.g., 1-10 mM) probably due to the side effects of the cosolvent when the amount of amine produced does not reach toxicity levels. Based on the gained knowledge, the authors tested the whole cell cascade for the amination of (*S*)-configured alcohols (**1c**, **35c-38c**) using an *E.coli* strain that expresses the cFL1-AmDH and AA-ADH (cFL1-AA). The amination of racemic alcohols (**1c**, **36c**) was also attempted but using a strain that co-expresses the cFL1-AmDH and AA-ADH in the same vector and also contains another vector encoding for LBv-ADH (cFL1-AA-LBv). Reactions consisted of 1 mL cell suspension in ammonium chloride buffer (60 mg mL^{-1} *E. coli* cells) with 20 mM glucose and 20 mM substrate at 30 °C. The (*S*)-**36c** (20 mM) showed the highest conversion (82%) among the alcohols tested, while using the racemic form of the same substrate, the conversion was slightly lower (64%). A similar scenario was observed for the amination of (*S*)-**1c** (46%) compared with rac-**1c** (21%) possibly due to the elevated toxicity of the *R* enantiomer. The rest of the (*S*)-configured alcohols were converted with 12% (20 mM **37c**), 81% (10 mM, **37c**) and 33% (5 mM, **38c**). In all cases, the (*R*)-configured product was obtained with >99 *ee*.

In 2017, a biocatalytic system employing in total five enzymes (ADH, NADP$^+$-oxidase, catalase, AmDH and FDH) was constructed as an orthogonal two-step oxidation–reduction network comprising a combination of dehydrogenases with divergent cofactor dependence (NAD or NADP) as illustrated in **Scheme 1F**.[73] In the oxidation-reduction step, an ADH oxidizes the alcohol to the carbonyl compound by the transfer of a hydride from the substrate to NADP$^+$. The NADP-oxidase (YcnD) from *Bacillus subtilis*[74] regenerates the NADP$^+$, consuming dioxygen and liberating H$_2$O$_2$ which is disproportionated by catalase to water and dioxygen. In the second cycle, an NAD$^+$ depended AmDH catalyze the reductive amination of the carbonyl compound intermediate in tandem with a formate dehydrogenase from *Candida boidinii* (Cb-FDH) for cofactor recycling. This enzymatic network possesses elevated atom efficiency, since the ammonium formate buffer is both the source of nitrogen and electrons for the reductive amination step, while the first step

requires only molecular oxygen from air (O_2). Furthermore, this system offers a more favorable thermodynamic equilibrium compared to the hydrogen borrowing amination cascade.[32] As the ADH should be NADP$^+$-dependent and non-stereospecific the authors focused on variants of TeS-ADH.[72] The authors decided to use the double variant of TeS-ADH I86A/W110A or a combination of the single variant TeS W110A with LBv-ADH. These TeS-ADH variants have been reported to possess relaxed stereoselctivity as confirmed with computational models by the authors.[73] For the second cycle, the authors used the three (*R*)-selective AmDHs: *Rs*-AmDH, cFL1-AmDH and *Bb*-AmDH. The applicability of this network was demonstrated for the asymmetric amination or racemic compounds (20 mM) shown in **Table 3** (third column). Reaction conditions were: TeS-ADH I86A W110A (52 µM) or TeS-ADH W110A (23 µM) plus LBv-ADH (23 µM), YcnD (10 µM), AmDH (100-126 µM), Cb-FDH (20 µM), catalase (0.2 µM), NAD$^+$ (0.5 mM) and NADP$^+$ (0.5 mM) in HCOONH$_4$ buffer (1 M, pH 8.5) at 30 °C. Results are summarized in **Table 3**. In all cases the (*R*)-configured amine was obtained with excellent *ee*. Quantitative conversions were obtained for **60c**, using a combination of ADHs (TeS W110A + LBv-ADH) and Rs-AmDH or the TeS I68A W110A variant together with cFL1-AmDH for **36c** and **37c**. The latter combination of enzymes showed good conversions (66%-97%) for substrates: **1c**, **2c**, **35c** and **41c.** Similarly, to the hydrogen borrowing cascade, the most challenging racemic alcohols (**11c**, **12c**, **14c** and **16c**) were poorly aminated using the newly developed biocatalytic network due to the lack of a highly active AmDH for the reductive amination of the corresponding ketones.

Table 2. Biocatalytic synthesis of a-chiral amines from racemic alcohols using ADHs and AmDHs.

Compound	Structure	Cascade 1[32] Conv %[a], (ee %)	Cascade 2[47] Conv %[b], (ee %)	Cascade 3[73] Conv %[c], (ee %)
1c		81, >99(R) AADH+ LBv-ADH Bb-AmDH		97, >99(R) TeS I86A/W110A CFL1-AmDH
2c		66, >99(R) AADH+ LBv-ADH Bb-AmDH		91, >99(R) TeS I86A/W110A cFL1-AmDH
7c		47, 97(R) AADH+ LBv-ADH Bb-AmDH		53, >99(R) TeS I86A/W110A Rs-AmDH
5c		78, >99(R) AADH+ LBv-ADH Bb-AmDH		
6c		30, 82(R) AADH+ LBv-ADH Bb-AmDH		91, >99(R) TeS W110A + Lb Rs-AmDH
57c		87, >99(R) AADH+ LBv-ADH CFL1-AmDH		86, >99(R) TeS W110A + Lb Rs-AmDH
60c		92, 83(R) AADH+ LBv-ADH CFL1-AmDH		<99, >99(R) TeS W110A + Lb Rs-AmDH
62c		84, >99(R) AADH+ LBv-ADH CFL1-AmDH		63, >99(R) TeS W110A + Lb Bb-AmDH
13c		16, >99(R) AADH+ LBv-ADH CFL1-AmDH	21, >99(R)	
17c		16, >99(R) AADH+ LBv-ADH CFL1-AmDH		

Compound	Structure	Cascade 1[32] Conv %[a], (ee %)	Cascade 2[47] Conv %[b], (ee %)	Cascade 3[73] Conv %[c], (ee %)
16c	OH, F (meta)	20, >99(R) AADH+ LBv-ADH CFL1-AmDH		29, >99(R) TeS W110A + Lb cFL1-AmDH
14c	OH, F (para)	12, >99(R) AADH+ LBv-ADH CFL1-AmDH		23, >99(R) TeS W110A + Lb cFL1-AmDH
12c	OH	19, >99(R) AADH+ LBv-ADH CFL1-AmDH		21, >99(R) TeS W110A + Lb cFL1-AmDH
11c	OH	9, >99(R) AADH+ LBv-ADH CFL1-AmDH		17, >99(R) TeS W110A + Lb cFL1-AmDH
38c	OH	93, 99(R) AADH+ LBv-ADH CFL1-AmDH		94, >99(R) TeS I86A/W110A cFL1-AmDH
37c	OH	96, 99(R) AADH+ LBv-ADH CFL1-AmDH		>99, >99(R) TeS I86A/W110A cFL1-AmDH
36c	OH	95, >99(R) AADH+ LBv-ADH CFL1-AmDH		>99, >99(R) TeS I86A/W110A cFL1-AmDH
35c	OH	66, >99(R) AADH+ LBv-ADH CFL1-AmDH	94, >99(R)	70, >99(R) TeS I86A/W110A cFL1-AmDH
41c	OH	80, >99(R) AADH+ LBv-ADH CFL1-AmDH	73, >99(R)	92, >99(R) TeS I86A/W110A cFL1-AmDH
42c	OH		57, N.D	
44c	OH		93, >99(R)	

Compound	Structure	Cascade 1[32] Conv %[a], (ee %)	Cascade 2[47] Conv %[b], (ee %)	Cascade 3[73] Conv %[c], (ee %)
45c	OH		29, >99(R)	
27c	OH		97, N.A.	
29c	OH		75, N.D.	
28c	OH		43, N.D.	
32c	OH		35, N.A.	

[a] Conversions reported here were obtained using the following conditions: [substrate]: 20 mM, [AA-ADH]: 1.0-2.3 mg mL^{-1}; [LBv-ADH]: 1.0-2.6 mg mL^{-1}; [AmDH]: 20 U; ammonium formate buffer (pH 8.5, 2 M); [NAD^{+}]: 1 mM: T 30 °C, 48 h, 190 rpm, Volume: 500 µL.

[b] Conversions reported here were obtained using the following conditions: [substrate]: 50 mM, [Sc-ADH]: 10 mg lyophilized cell free extract; [Es-AmDH]: 10 mg lyophilized cell free extract; ammonium chloride buffer (pH 9.5, 2 M); [NAD^{+}] 1 mM: T 30 °C, 24 h , 1000 rpm, Volume: 1000 µL.

[c] Conversions reported here were obtained using the following conditions: [substrate]: 20 mM, [TeS-ADH I86A/W110A]: 52 µM or [TeS-ADH W110A]: 23 µM plus [LBv-ADH]: 23 µM; [cFL1-AmDH]: 126 µM or [Bb-AmDH]: 117 µM or [Rs-AmDH]; 100 µM; [YncD]: 10 µM; [Cb-FDH]: 20 µM; [Catalase]: 0.2 µM; [NADP^{+}]: 0.5 mM in ammonium formate buffer (1 M pH 8.5); T 30 °C, 24 h , 170 rpm.

N.D.: Not determined, N.A.: Not applicable

1.4.3 Synthesis of secondary and tertiary amines by AmDHs.

In 2019, we investigated the catalytic promiscuity of the Rs-AmDH and cFL1-AmDH for the synthesis of secondary and/or tertiary amines when other amino-donors rather than ammonia were present in the reaction mixture.[35] After an extensive screening of these AmDHs with a panel of carbonyl compounds

(ketones and aldehydes) and eleven different amino donors (constituting the buffer of the reaction at 1 M concentration and pH 8.5) we were able to obtain secondary and tertiary amines. The AmDHs (*Rs*-AmDH 103 µM, and cFL1-AmDH 92 µM) were used together with *Cb*-FDH (24 µM) and catalytic amount of NAD$^+$ (1 mM). Conversions of 15% and 40% were obtained with **2a** and cFL1-AmDH using 1 M or 6 M methylamine buffer, respectively. The *Rs*-AmDH catalyzed reaction resulted in 4% conversion using ethylamine and 11% conversion with cyclopropylamine for the same substrate. The cFL1-AmDH also produced secondary amines starting from **36a** (5% conv.), **37a** (32% conv.) and heptanal (41%) in methylamine buffer. The *Rs*-AmDH showed a preference for **21a** producing non chiral secondary amines with methylamine (29% conv.), ethylamine (40% conv.), *n*-propylamine (43% conv.) or even with dimethylamine (3% conv.) and ethyl-methylamine (8% conv.). In all those cases in which the product was chiral, the secondary amines were obtained in an enantioenriched form for the (*R*)-enantiomer. Interestingly in the cases in which a ketone was used as substrate the production of secondary amines were always accompanied with the formation of the corresponding primary amine as by-product with perfect optical purity (*ee* >99% *R*). After a series of mechanistic experiments we concluded that the production of the primary amines was due to a promiscuous formal transamination mechanism through NAD$^+$/NADH redox-mediated iminium isomerization step. In fact, when the secondary imine (intermediate I in **Scheme 2A**) is formed during the catalytic cycle of the AmDHs, isomerization of the imine may takes place due to the action of NADH/NAD$^+$ resulting in imine intermediate II (**Scheme 2A**). The latest is being attacked by a water molecule, due to the particular catalytic environment in the active site of the enzyme, thus generating the primary amine. These findings were further explained with the aid of computational models. Molecular dynamic simulations with the model of cFL1-AmDH docked with intermediate I (**Scheme 1A**) revealed that both pro-(*R*) and pro-(*S*) binding modes can be productive for the biocatalytic reaction to occur, resulting in low *ee* values for the secondary amine product. In contrast, the generated primary amine (last step in **Scheme 2A**) is more stable in the

pro-(R) configuration than in the pro-(S), due to interaction of D125 residue with the amino group of the substrate. Apparently, this binding pose of the primary amine is the only productive one as molecular dynamic simulations revealed. Therefore, although the pro-(S) configuration of the primary amine is an acceptable conformation (in terms of binding energy) the substrate will switch to pro-(R) prior to the reduction by the cofactor, resulting in >99% ee for the (R)-configured primary amine product. Finally, we proposed a catalytic mechanism for the reductive amination catalyzed by the Rs-AmDH and cFL1-AmDH with amine donors differed from ammonia (**Scheme 2B**). This mechanism rationalized the formation of all products observed in the reaction mixture and is based on the catalytic mechanism of Phe-DH from *Rhodococcus sp. M4*.[42]

Later the same year, Mayol and co-workers tested the purified nat-AmDHs with a number of amine donors (methylamine, ethylamine, benzylamine, cyclopentylamine and 3-pentanamine) with 100:1 equivalent of amine donor: substrate molar ratio.[31] Three out of five nat-AmDHs, named: *Msme*AmDH, *MIcro*AmDH, *Mvac*AmDH accepted methylamine using **27a** or **69a** as substrates. The *Micro*AmDH showed even higher specific activity for methylamine (90 mU mg^{-1}) than ammonia (37 mU mg^{-1}) for **27a**. Similarly, for substrate **69a**, *Micro*AmDH showed a specific activity of 851.3 mU mg^{-1} with methylamine and 269.8 mU mg^{-1} with ammonia. The *Msme*AmDH was also found to be active with methylamine for the amination of **27a** (10 mU mg^{-1}) and **69a** (144 mU mg^{-1}). These activity levels are slightly increased for those observed with ammonia using the same substrates. Finally, *Mvac*AmDH which has not been tested for the reductive amination using ammonia for any substrate, showed 12.6 mU mg^{-1} for **27a** and 262.6 mU mg^{-1} for **69a** with methylamine. A pH study using *Micro*AmDH revealed only a minor influence of the pH value on the enzyme specific activity for the amination of isobutyraldehyde using methylamine; in fact, the specific activity was maintained at 70% of its highest value (obtained at pH 9.0) within a pH range between 6.7 and 12.2. Finally, the authors showed that the specific activity for the amination of **69a** remained at the same level when the methylamine

concentration was decreased to 2 equivalents, thus indicating that the activity does not depend on the amount of the pre-formed imine in solution and that the enzyme is able to catalyze both imine formation and reduction. However, the authors were not able to provide data for the enatioselectivity of the obtained secondary amines since all products were not chiral. Moreover, consumption of the cofactor in a spectrophotometric assay may not correlate entirely with the generation of secondary amines; conversely, as it was explained before, a primary amine product can be formed during the catalytic mechanism of the enzymes. Therefore, the product(s) of the reaction should be identified.
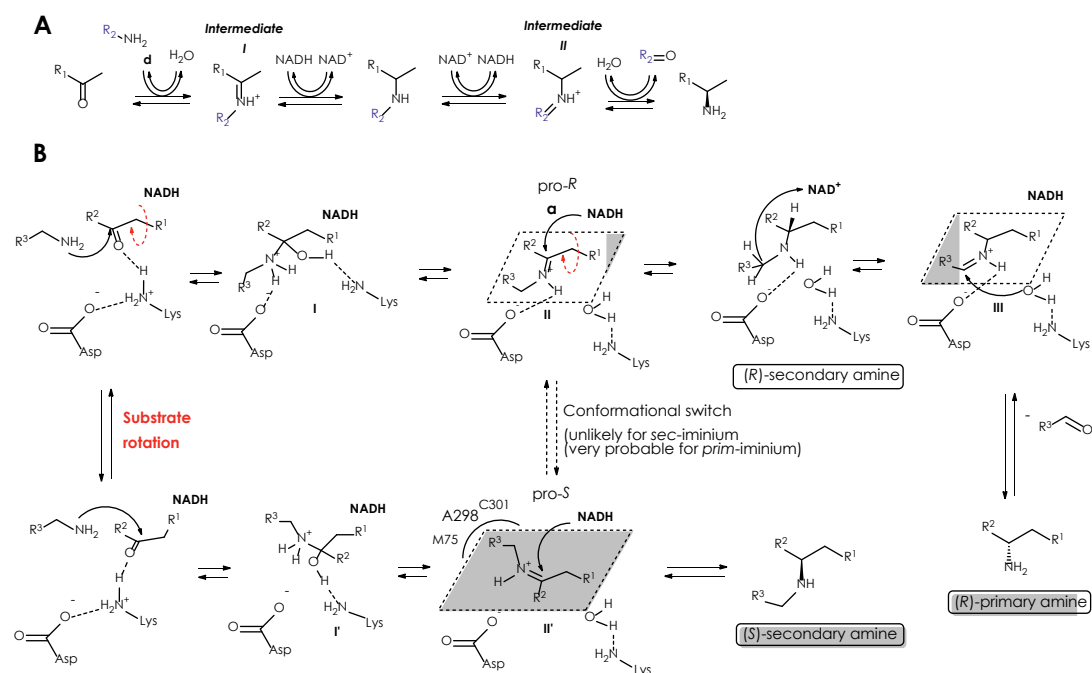
Scheme 2. (A) mechanistic explanation for the promiscuous formation of enantiopure primary amine during the catalytic cycle of the AmDHs for the synthesis of secondary amines, (B) proposed catalytic mechanism for reductive amination catalysed by Rs-AmDH and cFL1-AmDH with amine donors different from ammonia . Two stereocomplementary binding modes are the most probable (either intermediate II or intermediate II'). Reduction of intermediate II' through a hydride shift from NADH forms the secondary amine product in the (*S*)-configuration. Reduction of intermediate II by a hydride shift from NADH forms the secondary amine product in the (*R*)-configuration. However, intermediate II can also be re-oxidised to iminium isomer III. After this formal imine isomerization step, the hydrolysis of intermediate III yields the primary amine product in the (*R*)-configuration.

1.5 Outline of the thesis

This chapter makes evident that the past few years have witnessed tremendous advancements in the amine dehydrogenase catalyzed reactions and, only recently the implementation of AmDHs in state-of-the-art biocatalytic cascades was accomplished. The increased scientific interest for the discovery and engineering of new AmDHs is mainly caused by two factors, both of which are of utmost importance. First, the high atom economy of the AmDHs when combined with recycling enzymes (e.g., FDH or GDH) and second, the exquisite enantioselectivity that the AmDH family members display. These two factors make both the final product as well as the process for amine synthesis compatible with the recent policies related to APIs manufacturing. Despite this accelerated rate of new entries in the AmDH family, this class of enzymes remains underdeveloped. For instance, the diversity of substrate scope and activity among these AmDHs is poor because they were engineered from very similar scaffolds and following an identical strategy. Moreover, accessibility to the (*S*)-configured amines using AmDHs is a major limitation due to the lack of members possessing (*S*)-selectivity. This limitation can be partly overcome by the application of (*R*)-selective AmDHs for the kinetic resolution of racemic mixtures of amines. In addition to that, reductive amination of carbonyl-containing compounds catalyzed by AmDHs with amino donors other than ammonia has not been previously investigated. In terms of catalytic promiscuity, the AmDHs may also give access to secondary or tertiary amines by using alternative amine donors than ammonia. Furthermore, catalytic promiscuity of AmDHs may be exploited starting from scaffolds with different folding for the generation of enzymes with different catalytic activities. Overcoming these limitations is the main objectives of this thesis.

For example, the catalytic promiscuity of previously engineered AmDHs for the synthesis of secondary and tertiary amines is demonstrated in **Chapter 2**. In this study, we have investigated two AmDHs for the synthesis of secondary and tertiary amines using various amino donors. Through the combination of practical

lab experiments and computational simulations, we gained new insights into the catalytic mechanism of these AmDHs, thus revealing new aspects related to their applicability and current limitations in organic synthesis. Extensive computational studies served as a valuable tool to elucidate the chemo-and stereo-selective behaviour of these biocatalysts.

In **Chapter 3** we report new amine dehydrogenases (AmDHs) with expanded substrate scope. These enzymes were created starting from the ε-deaminating L-lysine dehydrogenase that operates through the oxidative deamination of a non-chiral terminal amine group. Via a rationalized approach, we evolved the new enzymes to reveal and harness a stereoselective behaviour that was 'hidden' in the wild-type enzyme. The new enzymes are an important addition to the current enzyme toolbox for the synthesis of chiral amines. They are particularly relevant for the synthesis of key intermediates in the production of important pharmaceuticals displaying exquisite enantioselectivity. The thermostable scaffold used in this study offers also the possibility to reverse the stereoselectivity of the reductive amination (i.e., both (*R*)- or (*S*)-configured amines can be obtained), representing a rare example of substrate-dependent stereo-switchable selectivity. The applicability of the most active AmDH obtained in this study (LE-AmDH-v1) was demonstrated in preparative scale amination reactions.

In **Chapter 4** we applied the LE-AmDH-v1, as developed in the study described in chapter 3, for the kinetic resolution of pharmaceutically relevant racemic mixtures of primary amines in order to access the (*S*)-enantiomer. The AmDH was applied together with NAD-oxidase from *Streptococcus mutans* (NOx), which reduces O_2 by oxidizing the cofactor. Serving as recycling enzyme, it allows for maximizing the atom economy of the whole process. After a series of optimization studies (i.e. pH optimum, type of buffer, temperature, and substrate concentration) we were able to resolve all compounds tested. Moreover, the application of this AmDH in deracemization cascades or with chemical reducing agents (amine boranes) is also reported.

The catalytic promiscuity of the ε-deaminating *L*-lysine dehydrogenase is the subject of **chapter 5**. In this study we exploited the promiscuous formation of alcohols by the wild type enzyme as well as of some variants for the synthesis of primary alcohols and (a)chiral amines. By controlling the conditions of the biocatalytic reaction, some variants could produce exclusively either amines or alcohols. As amine dehydrogenases, these enzymes were highly enantioselective and afforded (*R*)-configured amines with >99% ee. As ADHs, only primary alcohols could be obtained. This bi-funtinal role of the enzymes was harnessed for the direct conversion of benzyl alcohol to benzylamine using two cascades. As a proof of principle, we were able to obtain the amine product confirming an unprecedented 'alcohol aminase' behavior.

Finally, in order to increase the possibility to identify new (*S*)-selective AmDHs in the future, in **Chapter 6**, we describe a novel methodology for screening new (*S*)-selective AmDHs. Expression and purification of the variants can be performed in 96-deep well blocks. The purified variants can be applied in the desirable, reductive amination reaction for the synthesis of (*S*)-configured amines. The products can be then observed using a highly enantioselective colorimetric assay employing an (*S*)-selective monoamine oxidase (MAO) that selectively oxidizes the S configured amines to imines by producing H_2O_2. The latest can be used by horseradish peroxidase (HRP) to conjugate 2,4,6-tribromo-3-hydroxybenzoic acid with 4-aminoantipyrine thereby forming a compound that can be detected spectrophotometrically at 510 nm and by eye (magenta). After a series of optimization studies, the reported methodology is expected to be applied for the screening of potential (*S*)-selective AmDHs that we have created starting from a D-AADH scaffold.

1.6 References

1   France, S., Guerin, D. J., Miller, S. J. & Lectka, T. *Chem. Rev.* **103**, 2985-3012, doi:10.1021/cr020061a (2003).

2   Höhne, M. & Bornscheuer, U. T. *ChemCatChem* **1**, 42-51, doi:10.1002/cctc.200900110 (2009).

3   Nugent, T. C. in *Chiral amine synthesis: Methods, Developments and Applications* (ed T. C. Nugent) (Wiley-VCH, Weinheim, 2010).

4   Gellad, W. F., Choi, P., Mizah, M., Good, C. B. & Kesselheim, A. S. *Am. J. Manag. Care* **20**, E90-E97 (2014).

5   Sheldon, R. A. *Green Chem.* **9**, 1273, doi:10.1039/b713736m (2007).

6   Sanderson, K. *Nature* **469**, 18-20, doi:10.1038/469018a (2011).

7   Bornscheuer, U. T. *et al. Nature* **485**, 185-194, doi:10.1038/nature11117 (2012).

8   Sheldon, R. A. & Woodley, J. M. *Chem. Rev.* **118**, 801-838, doi:10.1021/acs.chemrev.7b00203 (2018).

9   Patil, M. D., Grogan, G., Bommarius, A. & Yun, H. *ACS Catal.* **8**, 10985-11015, doi:10.1021/acscatal.8b02924 (2018).

10   Grogan, G. *Curr. Opin. Chem. Biol.* **43**, 15-22, doi: 10.1016/j.cbpa.2017.09.008 (2018).

11   Sharma, M., Mangas-Sanchez, J., Turner, N. J. & Grogan, G. *Adv. Synth. Catal.* **359**, 2011-2025, doi:10.1002/adsc.201700356 (2017).

12   Kohls, H., Steffen-Munsberg, F. & Höhne, M. *Curr. Opin. Chem. Biol.* **19**, 180-192, doi: 10.1016/j.cbpa.2014.02.021 (2014).

13   Batista, V. F., Galman, J. L., G. A. Pinto, D. C., Silva, A. M. S. & Turner, N. J. *ACS Catal.* **8**, 11889-11907, doi:10.1021/acscatal.8b03525 (2018).

14   Slabu, I., Galman, J. L., Lloyd, R. C. & Turner, N. J. *ACS Catal.* **7**, 8263-8284, doi:10.1021/acscatal.7b02686 (2017).

15   Aleku, G. A. *et al. Nat. Chem.* **9**, 961, doi:10.1038/nchem.2782(2017).

16   Schrittwieser, J. H., Velikogne, S. & Kroutil, W. *Adv. Synth. Catal.* **357**, 1655-1685, doi:10.1002/adsc.201500213 (2015).

17   Sharma, M. *et al. ACS Catal.* **8**, 11534-11541, doi:10.1021/acscatal.8b03491 (2018).

18   Prier, C. K., Zhang, R. K., Buller, A. R., Brinkmann-Chen, S. & Arnold, F. H. *Nat. Chem.* **9**, 629, doi:10.1038/nchem.2783 (2017).

19   Bartsch, S. & Vogel, A. in *Science of Synthesis, Biocatalysis in Organic Synthesis 2* (eds K. Faber, W.-D. Fessner, & N. J. Turner) 291-311 (Georg Thieme Verlag KG, 2015).

20   Li, R. F. *et al. Nat. Chem. Biol.* **14**, 664-670, doi:10.1038/s41589-018-0053-0 (2018).

21   Ilari, A., Bonamore, A. & Boffi, A. in *Science of Synthesis, Biocatalysis in Organic Synthesis 2* (eds K. Faber, W.-D. Fessner, & N. J. Turner) 159-175 (Georg Thieme Verlag KG, 2015).

22   Lichman, B. R., Zhao, J. X., Hailes, H. C. & Ward, J. M. *Nat. Commun.* **8**, 14883, doi:ARTN 14883a10.1038/ncomms14883 (2017).

23   Schrittwieser, J. H. *et al. Angew. Chem. Int. Ed.* **50**, 1068-1071, doi:10.1002/anie.201006268 (2011).

24   Schrittwieser, J. H. *et al. Angew. Chem. Int. Ed.* **53**, 3731-3734, doi:10.1002/anie.201400027 (2014).

25   Mata-Rodríguez, M. & Gotor-Fernández, V. in *Science of Synthesis, Biocatalysis in Organic Synthesis 1* (eds K. Faber, W.-D. Fessner, & N. J. Turner) 189-222 (Georg Thieme Verlag KG, 2015).

26   Bea, H.-S., Seo, Y.-M., Cha, M.-H., Kim, B.-G. & Yun, H. *Biotechnol. Bioprocess Eng.* **15**, 429-434, doi:10.1007/s12257-009-3093-1 (2010).

27   Jeon, H. *et al. Catalysts* **7**, 251, doi:10.3390/catal7090251 (2017).

28   Patil, M. D. *et al. Catalysts* **9**, 600, doi:10.3390/catal9070600 (2019).

29   Aleku, G. A. *et al. ChemCatChem* **10**, 515-519, doi:10.1002/cctc.201701484 (2018).

30   Abrahamson, M. J., Vazquez-Figueroa, E., Woodall, N. B., Moore, J. C. & Bommarius, A. S. *Angew. Chem. Int. Ed.* **51**, 3969-3972, doi:10.1002/anie.201107813 (2012).

31   Mayol, O. *et al. Nat. Catal.* **2**, 324-333, doi:10.1038/s41929-019-0249-z (2019).

32   Mutti, F. G., Knaus, T., Scrutton, N. S., Breuer, M. & Turner, N. J. *Science* **349**, 1525-1529, doi:10.1126/science.aac9283 (2015).

33   Bohmer, W., Knaus, T. & Mutti, F. G. *ChemCatChem* **10**, 731-735, doi:10.1002/cctc.201701366 (2018).

34   Houwman, J. A., Knaus, T., Costa, M. & Mutti, F. G. *Green Chem.* **21**, 3846-3857, doi:10.1039/c9gc01059a (2019).

35   Tseliou, V., Masman, M. F., Bohmer, W., Knaus, T. & Mutti, F. G. *ChemBioChem* **20**, 800-812, doi:10.1002/cbic.201800626 (2019).

36   Baker, P. J., Turnbull, A. P., Sedelnikova, S. E., Stillman, T. J. & Rice, D. W. *Structure* **3**, 693-705, doi:https: 10.1016/S0969-2126(01)00204-0 (1995).

37   Vanhooke, J. L., Thoden, J. B., Brunhuber, N. M. W., Blanchard, J. S. & Holden, H. M. *Biochemistry* **38**, 2326-2339, doi:10.1021/bi982244q (1999).

38   Sekimoto, T., Matsuyama, T., Fukui, T. & Tanizawa, K. *J. Biol. Chem.* **268**, 27039-27045 (1993).

39   Reetz, M. T., Bocola, M., Carballeira, J. D., Zha, D. & Vogel, A. *Angew. Chem.* **117**, 4264-4268, doi:10.1002/ange.200500767 (2005).

40   Abrahamson, M. J., Wong, J. W. & Bommarius, A. S. *Adv. Synth. Catal.* **355**, 1780-1786, doi:10.1002/adsc.201201030 (2013).

41   ASANO, Y. *et al. Eur. J. Biochem.* **168**, 153-159, doi:10.1111/j.1432-1033.1987.tb13399.x (1987).

42   Brunhuber, N. M., Thoden, J. B., Blanchard, J. S. & Vanhooke, J. L. *Biochemistry* **39**, 9174-9187, doi:10.1021/bi000494c (2000).

43   Knaus, T., Böhmer, W. & Mutti, F. G. *Green Chem.* **19**, 453-463, doi:10.1039/C6GC01987K (2017).

44   Bommarius, B. R., Schurmann, M. & Bommarius, A. S. *Chem. Commun.* **50**, 14953-14955, doi:10.1039/c4cc06527a (2014).

45   Ye, L. J. *et al. ACS Catal.* **5**, 1119-1122, doi:10.1021/cs501906r (2015).

46   Li, J., Pan, J., Zhang, J. & Xu, J.-H. *J. Mol. Catal. B: Enzym.* **105**, 11-17, doi:10.1016/j.molcatb.2014.03.010 (2014).

47   Chen, F.-F., Liu, Y.-Y., Zheng, G.-W. & Xu, J.-H. *ChemCatChem* **7**, 3838-3841, doi:10.1002/cctc.201500785 (2015).

48   Xue, Y. *et al. International Journal of Systematic and Evolutionary Microbiology* **56**, 1217-1221, doi: 10.1099/ijs.0.64105-0 (2006).

49   Pushpanath, A., Siirola, E., Bornadel, A., Woodlock, D. & Schell, U. *ACS Catal.* **7**, 3204-3209, doi:10.1021/acscatal.7b00516 (2017).

50   Ohshima, T., Nagata, S. & Soda, K. *Arch. Microbiol.* **141**, 407-411, doi:10.1007/bf00428857 (1985).

51   He, M. *et al. J. Hazard. Mater.* **185**, 682-688, doi:https://doi.org/10.1016/j.jhazmat.2010.09.072 (2011).

52   Omidinia, E. *et al. World J. Microbiol. Biotechnol.* **18**, 593-597, doi:10.1023/a:1016805901112 (2002).

53   Heydari, M., Ohshima, T., Nunoura-Kominato, N. & Sakuraba, H. *Appl. Environ. Microbiol.* **70**, 937-942, doi:10.1128/aem.70.2.937-942.2004 (2004).

54   Tseliou, V., Knaus, T., Masman, M. F., Corrado, M. L. & Mutti, F. G. *Nat. Commun.* **10**, 3717, doi:10.1038/s41467-019-11509-x (2019).

55   Caspi, R. *et al. Nucleic Acids Res.* **40**, D742-D753, doi:10.1093/nar/gkr1014 (2012).

56   Kanehisa, M., Goto, S., Sato, Y., Furumichi, M. & Tanabe, M. *Nucleic Acids Res.* **40**, D109-D114, doi:10.1093/nar/gkr988 (2012).

57   Fonknechten, N. *et al. J. Bacteriol.* **191**, 3162-3167, doi:10.1128/jb.01777-08 (2009).

58   Fukuyama, S. *et al. Journal of Bioscience and Bioengineering* **117**, 551-556, doi: 10.1016/j.jbiosc.2013.11.002 (2014).

59   Mayol, O. *et al. Catal. Sci. Technol.* **6**, 7421-7428, doi:10.1039/c6cy01625a (2016).

60   Eady, R. & Large, P. *Biochem. J* **106**, 245-255 (1968).

61   Eady, R. & Large, P. *Biochem. J* **123**, 757-771 (1971).

62   Itoh, N., Yachi, C. & Kudome, T. *J. Mol. Catal. B: Enzym.* **10**, 281-290, doi:10.1016/s1381-1177(00)00111-9 (2000).

63   Patil, M. D., Grogan, G., Bommarius, A. & Yun, H. *ACS Catal.*, 10985-11015, doi:10.1021/acscatal.8b02924 (2018).

64   Geueke, B., Riebel, B. & Hummel, W. *Enzyme Microb. Technol.* **32**, 205-211, doi: 10.1016/S0141-0229(02)00290-9 (2003).

65   Yoon, S. *et al.* *ChemCatChem* **11**, 1898-1902, doi:10.1002/cctc.201900080 (2019).

66   Shin, G., Mathew, S., Shon, M., Kim, B. G. & Yun, H. *Chem. Commun.* **49**, 8629-8631, doi:10.1039/c3cc43348j (2013).

67   Akhtar, M. K., Turner, N. J. & Jones, P. R. *Proceedings of the National Academy of Sciences* **110**, 87-92, doi:10.1073/pnas.1216516110 (2013).

68   Sung, S. *et al.* *Green Chem.* **20**, 4591-4595, doi:10.1039/c8gc02122h (2018).

69   Höffken, H. W. *et al.* *Biochemistry* **45**, 82-93, doi:10.1021/bi051596b (2006).

70   Schlieben, N. H. *et al.* *J. Mol. Biol.* **349**, 801-813, doi: 10.1016/j.jmb.2005.04.029 (2005).

71   Wang, L.-J. *et al.* *Bioresour. Technol.* **102**, 7023-7028, doi: 10.1016/j.biortech.2011.04.046 (2011).

72   Heiss, C. & Phillips, R. S. *J. Chem. Soc., Perkin Trans. 1*, 2821-2825, doi:10.1039/B001329N (2000).

73   Knaus, T., Cariati, L., Masman, M. F. & Mutti, F. G. *Org. Biomol. Chem.* **15**, 8313-8325, doi:10.1039/c7ob01927k (2017).

74   Morokutti, A. *et al.* *Biochemistry* **44**, 13724-13733, doi:10.1021/bi0510835 (2005).

Chapter 2

Mechanistic insight into the catalytic promiscuity of amine dehydrogenases: asymmetric synthesis of secondary and primary amines

2.1 Abstract

Biocatalytic asymmetric aminations of ketones using amine dehydrogenases (AmDHs) or transaminases, are efficient methods for the synthesis of a-chiral primary amines. A major challenge is the extension of the amination to the synthesis of secondary and tertiary amines. Herein, we show for the first time that AmDHs are capable of accepting other amine donors, hence giving access to enantioenriched secondary amines with conversions up to 43%. Surprisingly, in several cases, we observed the promiscuous formation of enantiopure primary amines along with the expected secondary amines. By conducting practical laboratory experiments and computational experiments, we propose that the promiscuous formation of primary amines along with secondary amines is due to an unprecedented nicotinamide (NAD)-dependent formal transamination catalyzed by AmDHs. In nature, this type of mechanism is commonly performed by pyridoxal 5'-phosphate (PLP) aminotransferase and not by dehydrogenases. Finally, we propose a catalytic pathway that rationalizes the promiscuous NAD-dependent formal transamination activity and explains the formation of the observed mixture of products. This work increases our understanding on the catalytic mechanism of NAD-dependent aminating enzymes such as AmDHs and will aid further research on the rational engineering of oxidoreductases for the synthesis of a-chiral secondary and tertiary amines.

2.2 Introduction

Catalytic enzyme promiscuity is the ability of an enzyme to catalyse alternative chemical reactions by often following catalytic mechanisms that are different from the natural one.[1-8] Although catalytic enzyme promiscuity has been the object of intensive investigation for two decades, the discovery of new promiscuous activities still proceeds at regular pace as witnessed by recent publications.[9-23] Notably, these new biocatalytic activities have been frequently exploited in chemical synthesis.

Amine dehydrogenases (AmDHs) catalyze the reductive amination of carbonyl compounds at the expense of aqueous ammonium/ammonia buffer. All the known AmDHs so far were obtained mainly by protein engineering starting from a-amino acid dehydrogenases such as the leucine dehydrogenases from *Bacillus stereothermophilus*,[24] *Exiguobacterium sibiricum*,[25] *Lysinibacillus fusiformis*[26] and *Bacillus sphaericus*,[26] as well as the phenylalanine dehydrogenases from *Bacillus badius*,[27] *Rhodococcus* sp. M4[28] and *Caldalkalibacillus thermarum*.[29] In all these cases, the mutations of the highly conserved lysine and asparagine residues in the active site, which interact with the two oxygen atoms of the carboxylic moiety of the natural substrate, were essential for switching the substrate specificity from a-keto carboxylic acids to ketones.[24,27-29] A few native amine dehydrogenases have been also identified from *Petrotoga mobilis*, *Fervidobacterium nodosum*, *Clostridium sticklandii*, *Dethiosulfovibrio peptidovorans*, *Staphylothermus hellenicus*, and *Thermosediminibacter oceani*.[30] Several works on the asymmetric biocatalytic reductive amination using the above mentioned amine dehydrogenases (AmDHs) have been published very recently using isolated enzymes, immobilized enzymes or whole cells biocatalysts.[24-40] In particular, our group has shown that AmDHs are efficient catalysts for the reductive amination of prochiral ketones (i.e. TONs > 10^3) and their substrate scope covers already a respectable range of structurally diverse substrates.[34] Biocatalytic reductive amination is also

possible with imine reductases (IReds), which catalyze naturally the asymmetric reduction of cyclic imines.[41,42] In fact, during the past few years, various groups have shown that IReds are also capable of catalyzing the reductive amination of non-cyclic imines although with modest efficiency.[43-46] In a recent study, the reductive amination between ketones and small aliphatic and benzylic amines was carried out with a novel dehydrogenase from *Aspergillus o.* (AspRedAm).[47,48] The enzyme was classified as a "reductive aminase (RedAm)". In a follow-up study two additional RedAms were characterised.[49] Finally, a previous patent from Codexis reported a reductive aminase activity from a library of variants originated from an opine dehydrogenase.[50]

Despite differences in names and apparent reactivity, the catalytic mechanisms of IReds, AmDHs and RedAm are closely related as the actual mechanism is essentially based on the hydride transfer from the nicotinamide coenzyme (NADH or NADPH) to the *in-situ* formed imine intermediate or the already existing cyclic imine in solution. Thus, we hypothesized that the reactivity of AmDHs may not be restricted only to ammonia as amine donor as previously believed and reviewed elsewhere.[42] That was also suggested by a number of oxidoreductases present in nature such as the opine dehydrogenases, which are capable of generating secondary amines by the coupling of an a-amino acid with an a-keto acid.[51-53]

Herein, we show for the first time that the reactivity of AmDHs is indeed not limited to ammonia as the amine donor. The two AmDHs, considered in the present study, can accept other amine donors to enable the formation of secondary and tertiary amines. Surprisingly, in some cases, the reaction was accompanied by the promiscuous formation of primary amines along with the expected secondary and tertiary amines. With the aim of explaining such unprecedented promiscuous activity as well as the stereoselective outcome of the reaction, we performed a study based on an accurate combination between practical laboratory experiments and computational studies. Consequently, herein we

also propose a catalytic cycle for amine dehydrogenases, which explains the promiscuous formation of all products (i.e. secondary and primary amines) as well as the enantiomeric composition of the reaction mixture.

2.3 Results and discussion

2.3.1 Screening of carbonyl compounds and amine donors

The reactivities of *Rs*-AmDH (originated by enzyme engineering from the phenylalanine dehydrogenases from *Rhodococcus sp.* M4)[28,34] and of Ch1-AmDH[32,34] (a chimeric enzyme obtained via domain shuffling of first generation variants) were assayed with eleven different amine donors, which also constituted the buffer system. Four different types of carbonyl compounds were selected: aliphatic ketones, aromatic ketones, aliphatic aldehydes and aromatic aldehydes (**Scheme 1**). We conducted the initial biocatalytic reactions as follows: carbonyl compound (10 mM), amine/ammonium formate buffer (1 M, pH 8.5), N-terminal His$_6$-tagged *Rs*-AmDH (103 µM) or N-terminal His$_6$-tagged Ch1-AmDH (92 µM), NAD$^+$ (1 mM) and N-terminal His$_6$-tagged Cb-FDH (24 µM; for recycling of NADH), at ambient temperature, for 48 h.
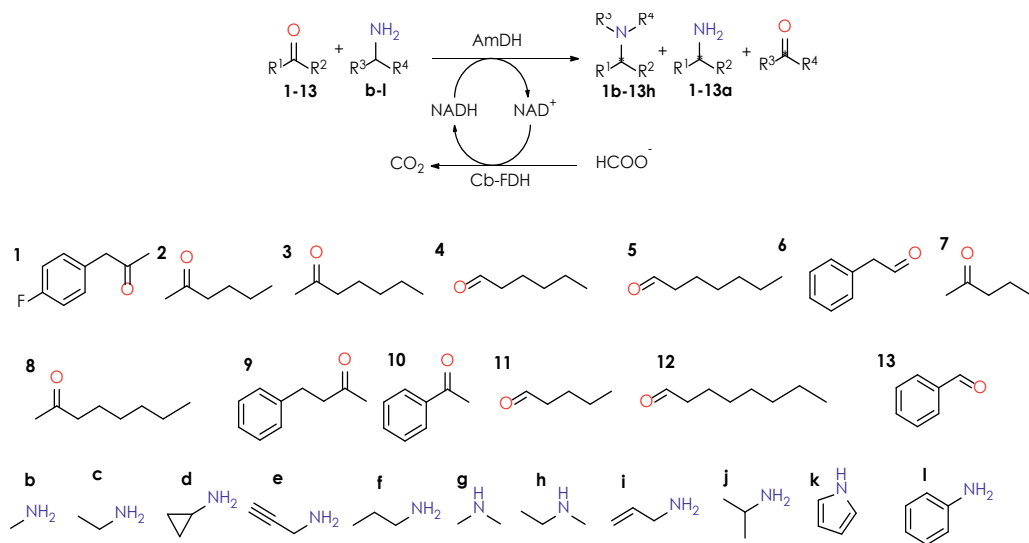
Scheme 1. Biocatalytic reductive amination of carbonyl compounds (1-13, 10 mM) with different amine donors (b-i) catalyzed by amine dehydrogenases (AmDHs). The amine donor was also used as buffer species in water for the reaction (1 M, pH 8.5, formate as counter-anion). The nicotinamide coenzyme (NAD$^+$, 1 mM) was recycled by reduction with formate, which is catalyzed by formate dehydrogenase from *Candida boidinii* (Cb-FDH).

Under the mentioned reactions conditions, both tested AmDHs produced secondary or tertiary amines starting from ketones and aldehydes. All screening results are reported in **Table 1**, whereas selected results are reported in **Table 1**.

Table 1. Reductive amination reactions performed by AmDHs for the synthesis of secondary and tertiary amines. Standard reaction conditions: substrate (10 mM), Ch1-AmDH (92 µM) or *Rs*-AmDH (103 µM), Cb-FDH (24 µM) and buffer constituted by amine donor with formate as counter-anion (1 M, pH 8.5). The reactions were performed at 30 °C, for 48 h using an orbital shaker at 170 rpm.

Substrate	Amine donor	AmDH	Secondary or tertiary amine formation [%]	"Promiscuous " Primary amine formation [%]
1	Methylamine (**b**)	Ch1-AmDH	15	8
		Rs-AmDH	2	N.d.
	Ethylamine (**c**)	Ch1-AmDH	1	7
		Rs-AmDH	4	26
	Cyclopropylamine (**d**)	Ch1-AmDH	4	17
		Rs-AmDH	11	26
	Propargylamine (**e**)	Ch1-AmDH	N.d.	44
		Rs-AmDH	N.d.	66
	N-propylamine (**f**)	Ch1-AmDH	3	N.d.
		Rs-AmDH	N.d.	N.d.
	Dimethylamine (**g**)	Ch1-AmDH	N.d.	N.d.
		Rs-AmDH	N.d.	N.d
	Ethyl-methylamine (**h**)	Ch1-AmDH	N.d.	N.d
		Rs-AmDH	N.d.	N.d
	Allylamine (**i**)	Ch1-AmDH	N.d.	11
		Rs-AmDH	N.d.	14
	Iso-propylamine (**j**)	Ch1-AmDH	N.d.	N.d.
		Rs-AmDH	<1	4
	Pyrrolidine (**k**)	Ch1-AmDH	N.d.	N.d.
		Rs-AmDH	N.d.	N.d.
	Aniline (**l**)	Ch1-AmDH	N.d.	N.d.
		Rs-AmDH	N.d.	N.d.
2	Methylamine (**b**)	*Rs*-AmDH	N.d.	<1
		Ch1-AmDH	5	4
	Ethylamine (**c**)	*Rs*-AmDH	N.d.	5
		Ch1-AmDH	N.d.	N.d.
		Rs-AmDH	N.d.	N.d.

Substrate	Amine donor	AmDH	Secondary or tertiary amine formation [%]	"Promiscuous " Primary amine formation [%]
	Cyclopropylamine (**d**)	Ch1-AmDH	N.d.	N.d.
	Propargylamine (**e**)	*Rs*-AmDH	N.d.	N.d.
		Ch1-AmDH	N.d.	13
	N-propylamine (**f**)	*Rs*-AmDH	N.d.	N.d.
		Ch1-AmDH	N.d.	N.d.
	Dimethylamine (**g**)	*Rs*-AmDH	N.d.	N.d.
		Ch1-AmDH	N.d.	N.d.
	Ethyl-methylamine (**h**)	*Rs*-AmDH	N.d.	N.d.
		Ch1-AmDH	N.d.	N.d.
	Allylamine (**i**)	*Rs*-AmDH	N.d.	N.d.
		Ch1-AmDH	N.d.	<1
	Iso-propylamine (**j**)	*Rs*-AmDH	N.d.	N.d.
		Ch1-AmDH	N.d.	N.d.
	Pyrrolidine (**k**)	*Rs*-AmDH	N.d.	N.d.
		Ch1-AmDH	N.d.	N.d.
	Aniline (**l**)	*Rs*-AmDH	N.d.	N.d.
		Ch1-AmDH	N.d.	N.d.
	Methylamine (**b**)	*Rs*-AmDH	N.d.	6
		Ch1-AmDH	32	26
	Ethylamine (**c**)	*Rs*-AmDH	N.d.	3
		Ch1-AmDH	N.d.	9
	Cyclopropylamine (**d**)	*Rs*-AmDH	N.d.	11
		Ch1-AmDH	N.d.	3
3	Propargylamine (**e**)	*Rs*-AmDH	N.d.	13
		Ch1-AmDH	N.d.	26
	N-propylamine (**f**)	*Rs*-AmDH	N.d.	N.d.
		Ch1-AmDH	N.d.	N.d.
	Allylamine (**i**)	*Rs*-AmDH	N.d.	N.d.
		Ch1-AmDH	N.d.	4
	Iso-propylamine (**j**)	*Rs*-AmDH	N.d.	N.d.
		Ch1-AmDH	N.d.	N.d.
	Aniline (**l**)	*Rs*-AmDH	N.d.	N.d.
		Ch1-AmDH	N.d.	N.d.
4	Methylamine (**b**)	*Rs*-AmDH	24	N.d.
		Ch1-AmDH	N.d.	N.d.
	Ethylamine (**c**)	*Rs*-AmDH	N.d.	N.d.
		Ch1-AmDH	N.d.	N.d.

Substrate	Amine donor	AmDH	Secondary or tertiary amine formation [%]	"Promiscuous" Primary amine formation [%]
	Cyclopropylamine (**d**)	*Rs*-AmDH	N.d.	N.d.
	Propargylamine (**e**)	*Rs*-AmDH	N.d.	N.d.
	N-propylamine (**f**)	*Rs*-AmDH	3	N.d.
		Ch1-AmDH	N.d.	N.d.
	Allylamine (**i**)	*Rs*-AmDH	8	N.d.
	Iso-propylamine (**j**)	*Rs*-AmDH	N.d.	N.d.
		Ch1-AmDH	N.d.	N.d.
	Aniline (**l**)	*Rs*-AmDH	N.d.	N.d.
		Ch1-AmDH	N.d.	N.d.
	Methylamine (**b**)	*Rs*-AmDH	N.d.	N.d.
		Ch1-AmDH	N.d.	N.d.
	Ethylamine (**c**)	*Rs*-AmDH	N.d.	N.d.
		Ch1-AmDH	N.d.	N.d.
	Cyclopropylamine (**d**)	*Rs*-AmDH	<1	N.d.
		Ch1-AmDH	2	N.d.
	Propargylamine (**e**)	*Rs*-AmDH	4	N.d.
5		Ch1-AmDH	41	N.d.
	N-propylamine (**f**)	*Rs*-AmDH	7	N.d.
		Ch1-AmDH	N.d.	N.d.
	Allylamine (**i**)	*Rs*-AmDH	N.d.	N.d.
		Ch1-AmDH	N.d.	N.d.
	Iso-propylamine (**j**)	*Rs*-AmDH	N.d.	N.d.
		Ch1-AmDH	N.d.	N.d.
	Aniline (**l**)	*Rs*-AmDH	N.d.	N.d.
		Ch1-AmDH	N.d.	N.d.
	Methylamine (**b**)	*Rs*-AmDH	29	N.d.
		Ch1-AmDH	14	N.d.
	Ethylamine (**c**)	*Rs*-AmDH	40	N.d.
		Ch1-AmDH	N.d.	N.d.
	Cyclopropylamine (**d**)	*Rs*-AmDH	N.d.	N.d.
		Ch1-AmDH	N.d.	N.d.
6	Propargylamine (**e**)	*Rs*-AmDH	N.d.	N.d.
		Ch1-AmDH	N.d.	N.d.
	N-propylamine (**f**)	*Rs*-AmDH	43	N.d.
		Ch1-AmDH	N.d.	N.d.
	Dimethylamine (**g**)	*Rs*-AmDH	3	N.d.

Substrate	Amine donor	AmDH	Secondary or tertiary amine formation [%]	"Promiscuous " Primary amine formation [%]
		Ch1-AmDH	2	N.d.
	Ethyl-methylamine (**h**)	*Rs*-AmDH	8	N.d.
		Ch1-AmDH	N.d.	N.d.
	Allylamine (**i**)	*Rs*-AmDH	N.d.	N.d.
		Ch1-AmDH	N.d.	N.d.
	Iso-propylamine (**j**)	*Rs*-AmDH	N.d.	N.d.
		Ch1-AmDH	N.d.	N.d.
	Pyrrolidine (**k**)	*Rs*-AmDH	N.d.	N.d.
		Ch1-AmDH	N.d.	N.d.
	Aniline (**l**)	*Rs*-AmDH	N.d.	N.d.
		Ch1-AmDH	N.d.	N.d.
	Methylamine (**b**)	*Rs*-AmDH	N.d.	N.d.
		Ch1-AmDH	2	N.d.
	Ethylamine (**c**)	*Rs*-AmDH	N.d.	N.d.
		Ch1-AmDH	N.d.	N.d.
	Cyclopropylamine (**d**)	*Rs*-AmDH	N.d.	N.d.
		Ch1-AmDH	N.d.	N.d.
	Propargylamine (**e**)	*Rs*-AmDH	N.d.	N.d.
		Ch1-AmDH	N.d.	N.d.
7	*N*-propylamine (**f**)	*Rs*-AmDH	N.d.	N.d.
		Ch1-AmDH	N.d.	N.d.
	Allylamine (**i**)	*Rs*-AmDH	N.d.	N.d.
		Ch1-AmDH	N.d.	N.d.
	Iso-propylamine (**j**)	*Rs*-AmDH	N.d.	N.d.
		Ch1-AmDH	N.d.	N.d.
	Aniline (**l**)	*Rs*-AmDH	N.d.	N.d.
		Ch1-AmDH	N.d.	N.d.
	Methylamine (**b**)	*Rs*-AmDH	9	4
		Ch1-AmDH	N.d.	2
	Ethylamine (**c**)	*Rs*-AmDH	N.d.	<1
		Ch1-AmDH	N.d.	N.d.
	Cyclopropylamine (**d**)	*Rs*-AmDH	10	N.d.
		Ch1-AmDH	N.d.	N.d.
8	Propargylamine (**e**)	*Rs*-AmDH	N.d.	<1
		Ch1-AmDH	N.d.	<1
	N-propylamine (**f**)	*Rs*-AmDH	N.d.	N.d.
		Ch1-AmDH	N.d.	N.d.
	Dimethylamine (**g**)	*Rs*-AmDH	N.d.	N.d.

Substrate	Amine donor	AmDH	Secondary or tertiary amine formation [%]	"Promiscuous " Primary amine formation [%]
		Ch1-AmDH	N.d.	N.d.
	Ethyl-methylamine (**h**)	*Rs*-AmDH	N.d.	N.d.
		Ch1-AmDH	N.d.	N.d.
	Allylamine (**i**)	*Rs*-AmDH	N.d.	N.d.
		Ch1-AmDH	N.d.	N.d.
	Iso-propylamine (**j**)	*Rs*-AmDH	N.d.	N.d.
		Ch1-AmDH	N.d.	N.d.
	Pyrrolidine (**k**)	*Rs*-AmDH	N.d.	N.d.
		Ch1-AmDH	N.d.	N.d.
	Aniline (**l**)	*Rs*-AmDH	N.d.	N.d.
		Ch1-AmDH	N.d.	N.d.
9	Methylamine (**b**)	*Rs*-AmDH	2	N.d.
	Ethylamine (**c**)	*Rs*-AmDH	N.d.	<1
	Cyclopropylamine (**d**)	*Rs*-AmDH	27	N.d.
	Propargylamine (**e**)	*Rs*-AmDH	34	N.d.
	N-propylamine (**f**)	*Rs*-AmDH	N.d.	N.d.
	Allylamine (**i**)	*Rs*-AmDH	9	N.d.
	Iso-propylamine (**j**)	*Rs*-AmDH	N.d.	N.d.
	Aniline (**l**)	*Rs*-AmDH	N.d.	N.d.
		Ch1-AmDH	N.d.	N.d.
10	Methylamine (**b**)	*Rs*-AmDH	N.d.	N.d.
		Ch1-AmDH	N.d.	N.d.
	Ethylamine (**c**)	*Rs*-AmDH	N.d.	N.d.
	Cyclopropylamine (**d**)	*Rs*-AmDH	N.d.	N.d.
	Propargylamine (**e**)	*Rs*-AmDH	N.d.	N.d.
	N-propylamine (**f**)	*Rs*-AmDH	N.d.	N.d.
	Allylamine (**i**)	*Rs*-AmDH	N.d.	N.d.
	Iso-propylamine (**j**)	*Rs*-AmDH	N.d.	N.d.
	Aniline (**l**)	*Rs*-AmDH	N.d.	N.d.
		Ch1-AmDH	N.d.	N.d.
11	Methylamine (**b**)	*Rs*-AmDH	N.d.	N.d.
		Ch1-AmDH	N.d.	N.d.
	Ethylamine (**c**)	*Rs*-AmDH	N.d.	N.d.
		Ch1-AmDH	N.d.	N.d.
	Cyclopropylamine (**d**)	*Rs*-AmDH	N.d.	N.d.
		Ch1-AmDH	N.d.	N.d.
		Rs-AmDH	<1	N.d.

Substrate	Amine donor	AmDH	Secondary or tertiary amine formation [%]	"Promiscuous " Primary amine formation [%]
	Propargylamine (**e**)	Ch1-AmDH	<1	N.d.
	N-propylamine (**f**)	Rs-AmDH	N.d.	N.d.
		Ch1-AmDH	N.d.	N.d.
	Allylamine (**i**)	Rs-AmDH	N.d.	N.d.
		Ch1-AmDH	N.d.	N.d.
	Iso-propylamine (**j**)	Rs-AmDH	N.d.	N.d.
		Ch1-AmDH	N.d.	N.d.
	Aniline (**l**)	Rs-AmDH	N.d.	N.d.
		Ch1-AmDH	N.d.	N.d.
	Methylamine (**b**)	Rs-AmDH	N.d.	N.d.
		Ch1-AmDH	N.d.	N.d.
	Dimethylamine (**g**)	Rs-AmDH	N.d.	N.d.
		Ch1-AmDH	N.d.	N.d.
	Ethyl-methylamine (**h**)	Rs-AmDH	N.d.	N.d.
12		Ch1-AmDH	N.d.	N.d.
	Pyrrolidine (**k**)	Rs-AmDH	N.d.	N.d.
		Ch1-AmDH	N.d.	N.d.
	Aniline (**l**)	Rs-AmDH	N.d.	N.d.
		Ch1-AmDH	N.d.	N.d.
	Methylamine (**b**)	Rs-AmDH	N.d.	N.d.
		Ch1-AmDH	N.d.	N.d.
	Ethylamine (**c**)	Rs-AmDH	N.d.	N.d.
		Ch1-AmDH	N.d.	N.d.
	Cyclopropylamine (**d**)	Rs-AmDH	N.d.	N.d.
		Ch1-AmDH	N.d.	N.d.
	Propargylamine (**e**)	Rs-AmDH	N.d.	N.d.
		Ch1-AmDH	N.d.	N.d.
13	N-propylamine (**f**)	Rs-AmDH	N.d.	N.d.
		Ch1-AmDH	N.d.	N.d.
	Dimethylamine (**g**)	Rs-AmDH	N.d.	N.d.
		Ch1-AmDH	N.d.	N.d.
	Ethyl-methylamine (**h**)	Rs-AmDH	N.d.	N.d.
		Ch1-AmDH	N.d.	N.d.
	Allylamine (**i**)	Rs-AmDH	N.d.	N.d.
		Ch1-AmDH	N.d.	N.d.

Substrate	Amine donor	AmDH	Secondary or tertiary amine formation [%]	"Promiscuous " Primary amine formation [%]
	Iso-propylamine (**j**)	*Rs*-AmDH	N.d.	N.d.
		Ch1-AmDH	N.d.	N.d.
	Pyrrolidine (**k**)	*Rs*-AmDH	N.d.	N.d.
		Ch1-AmDH	N.d.	N.d.
	Aniline (**l**)	*Rs*-AmDH	N.d.	N.d.
		Ch1-AmDH	N.d.	N.d.

N.d.: not detected (the expected product, under assay conditions)

Ch1-AmDH catalyzed the reductive amination between 4'-fluorophenylacetone (**1**) and methylamine (**b**), whereas *Rs*-AmDH accepted ketone **1** in combination with ethylamine (**c**) and cyclopropylamine (**d**) (**Table 2, entries 1, 3, 4**). For these reactions, we were surprised to identify also the formation of the structurally related primary amine, 4'fluoroamphetamine (**1a**), as a second product. Notably, **1a** was obtained in enantiopure form in all the cases (*ee* >99%, *R*). Commercial reagent grade solution of methylamine contains only negligible traces of ammonia, whereas ethylamine and cyclopropylamine do not contain ammonia at all. In addition, the amination of **1** at 4-6 M concentration of methylamine buffer (**b**) resulted in lower conversion into **1a** compared to the same reaction performed at 3 M of **b** (**Figure 1B**). Hence, we ruled out the possibility that the primary amine could have been formed via the enzymatic reaction between the ketone and the ammonia present, eventually, as an impurity. Due to the complexity and the elevated polarity of the components in the reaction mixtures, we succeeded in measuring the enantiomeric excess of the secondary amine products by chromatography in the case of compounds **1b** and **1d**. **1b** was obtained in enantioenriched form (*ee* 72% *R*, **Table 2**, entry 1), whereas **1d** in nearly racemic form (**Table 2**, entry 4). In contrast, the other product -primary amine **1a** - was obtained in enantiopure form as previously observed (for comparison, **Table 2**, entries 1 and 4).

Ch1-AmDH was the most active enzyme for the amination of 2-hexanone (**2**) and 2-heptanone (**3**) with **b** (**Table 2**, entries 5 and 6). Even in this case, the structurally related primary amines 2-aminohexane (**2a**) and 2-aminoheptane (**3a**) were obtained with perfect ee. These results confirm that the formation of primary amines occurs during the catalytic cycle of the AmDHs. Conversely, the amination of aldehydes using the AmDHs and different amine donors under our initial reaction conditions (1 M of amine/amonium buffer, pH 8.5), proceeded with perfect chemoselectivity to afford the expected secondary amines as the sole product up to 43% conversion (**Table 2**, entry 7-11). As a proof of principle, the amination was run also with secondary amines as amine donor (e.g. dimethylamine, ethyl-methylamine), leading to tertiary amines albeit with poor conversions (**Table 2**, entry 12 and 13).

Table 2. Reductive amination reactions performed by AmDHs for the synthesis of secondary and tertiary amines. Standard reaction conditions: substrate (10 mM), Ch1-AmDH (92 µM) or *Rs*-AmDH (103 µM), Cb-FDH (24 µM) and buffer constituted by amine donor with formate as counter-anion (1 M, pH 8.5). The reactions were performed at 30 °C, for 48 h using an orbital shaker at 170 rpm.

Entry	Substrate	Amine donor	AmDH	Secondary/ tertiary amine		Primary amine (1-11a)	
				Conv. (%)	ee (%)	Conv. (%)	ee (%)
1	1	b	Ch1	15	72 (*R*)	8	>99 (*R*)
2	1	b	Ch1	40[a]	64 (*R*)	6	>99 (*R*)
3	1	c	*Rs*	4	N.m.	26	>99 (*R*)
4	1	d	*Rs*	11	1 (*R*)	26	>99 (*R*)
5	2	b	Ch1	5	N.m.	4	>92 (*R*)[b]
6	3	b	Ch1	32	N.m.	26	>99 (*R*)
7	4	b	*Rs*	24	N.a.	N.d.	N.a.
8	5	e	Ch1	41	N.a.	N.d	N.a.
9	6	b	*Rs*	29	N.a.	N.d	N.a.
10	6	c	*Rs*	40	N.a.	N.d	N.a.
11	6	f	*Rs*	43	N.a.	N.d	N.a.
12	6	g	*Rs*	3[c]	N.a.	N.d	N.a.
13	6	h	*Rs*	8[c]	N.a.	N.d	N.a.

[a] Concentration of $MeNH_2/MeNH_3^+$ buffer was increased to 6 M. [b] Unable to determine with precision, due to experimental noise of the GC traces. [c] Measured by GC-MS.
N.d.: not detected (the expected product, under assay conditions, N.m: not measured, N.a.: not applicable

2.3.2 Influence of the enzyme and amine donor concentration

For further studies, we selected the amination of 4'-fluorophenylacetone (**1**) with methylamine (**b**) as test reaction. In the first set of experiments, we kept the buffer concentration constant (1 M, pH 8.5) and we varied the concentration of Ch1-AmDH (4.5–91 µM). As expected, increasing the

enzyme concentration affected positively the overall conversion (**Figure 1A**). Interestingly, the ratio between the formation of secondary (**1b**) and primary (**1a**) amines also varied depending on the enzyme concentration from 1:1.2 (at AmDH 4.5 μM) to 1:1.9 (at AmDH 91 μM).

In a follow-up experiment (**Figure 1B**), we fixed the concentration of Ch1-AmDH (91 μM) and we increased the concentration of the $CH_3NH_2/CH_3NH_3^+$ buffer (200 mM–6 M). Increasing the buffer concentration correlated with a consistent increase in the formation of **1b**. At 6 M buffer concentration, **1b** was finally obtained in 40% conversion (**Figure 1B** and **Table 2** entry 2). The side-reaction that leads to the primary amine product showed a continuous increment of conversion of **1a** (11% conversion) up to a buffer concentration of 3 M. Surprisingly, more elevated concentration of buffer (4, 5, 6 M) reduced the formation of **1a** (6% at 6 M buffer concentration). Hence, the ratio between **1a** and **1b** further increased to 1:6.6. We also monitored a possible variation in the stereoselective outcome of the reaction. The enantiomeric excess of the secondary amine product **1b** was partially affected with a reduction from 72% *ee* (1 M buffer) to 64% *ee* (6 M buffer). In contrast, the optical purity of the primary amine remained perfect (>99%, **Table 2** entries 1 and 2). In all cases, the (*R*)-configured amine (secondary or primary) was the favored enantiomer.
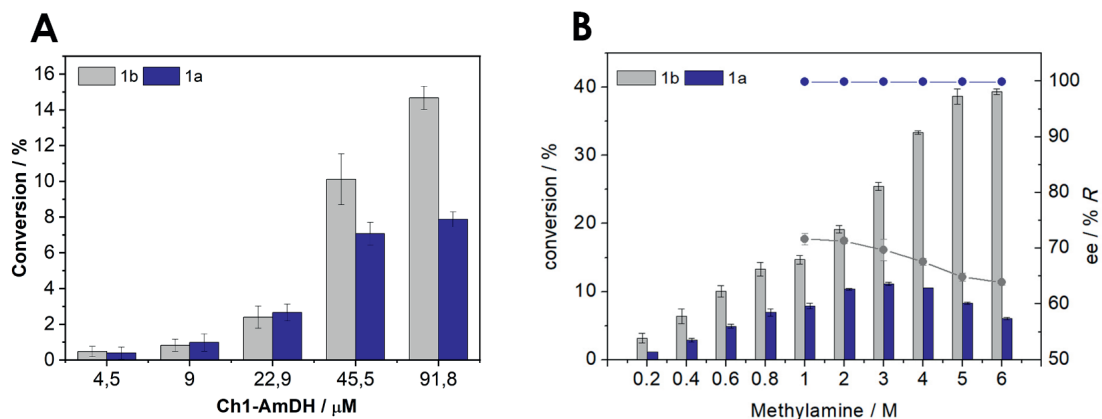
Figure 1. Influence of enzyme and methylamine concentration on the conversion rate. (A) Dependence of enzyme concentration (4.5-91 µM) at fixed concentrations of methylamine buffer (1 M) for the conversion of 4'-fluorophenylacetone (**1**) into primary (**1a**, blue columns) and secondary (**1b**, grey columns) amines catalyzed by Ch1-AmDH. Catalytic amount of NAD^+ (1 mM) was applied and recycled using Cb-FDH (24 µM). Error bars represent the standard deviation calculated from three independent experiments. **(B)** Dependence of CH_3NH_2 concentration (200 mM - 6M) at a fixed concentration of Ch1-AmDH (91 µM) for the conversion of 4'-fluorophenylacetone (**1**) into primary (**1a**, blue columns) and secondary (**1b**, grey columns) amines catalyzed by Ch1-AmDH. Catalytic amount of NAD^+ (1mM) was applied and recycled using Cb-FDH (24 µM). Error bars represent the standard deviation from three independent experiments. Enantiomeric excess (ee) for **1a** (blue) and **1b** (grey) are depicted with circles connected with a solid line.

2.3.3 Initial biochemical and computational studies towards the understanding of the reaction mechanism

Both Ch1-AmDH and *Rs*-AmDH showed to possess a general perfect stereoselectivity (i.e. "*R*-selectivity") for the reductive amination of prochiral ketones with ammonia.[34] However, different points remained unclear at this stage: 1) the molecular discriminants that determine a productive combination between the ketone/aldehyde and the amine donor; 2) the formation of secondary amines with moderate stereoselectivity; 3) the unexpected formation of primary amine in enantiopure form.

Therefore, we performed several computational analyses in the attempt of elucidating these points. First, we generated several models of *Rs*-AmDH in complex with NADH and different protonated imine intermediates (*i.e.* carbonyl compounds: 4'-fluorophenylacetone (**1**), hexanal (**4**), heptanal (**5**), phenylacetaldehyde (**6**), 4-phenyl-butan-2-one (**9**), acetophenone (**10**); amine donors: ammonia (**a**), methylamine (**b**), ethylamine (**c**) and *n*-propylamine (**f**)). Details on the creation of these models are reported in the methods section. Based on the reported catalytic mechanism of the parent wild-type phenylalanine dehydrogenase from *Rhodococcus sp.* M4,[54] we analyzed the models considering two crucial parameters as depicted in **Figure 2**: 1) the distance between the departing hydride of NADH and the prochiral carbon of the imine intermediate (herein referred as "distance 1"); 2) the distance between the negatively charged oxygen
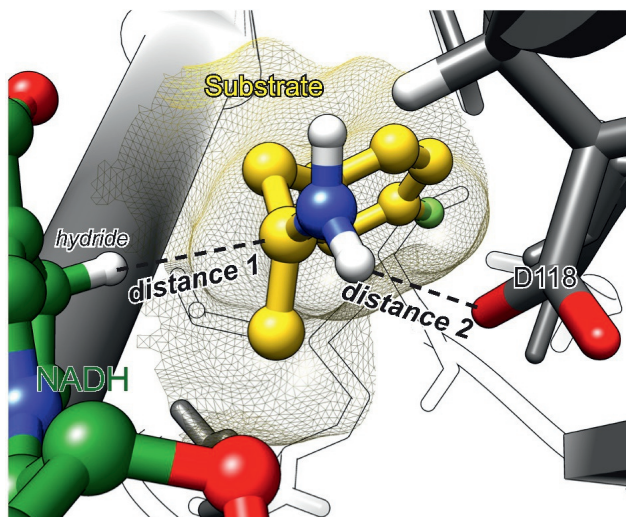
Figure 2. Simplified schematic view of the productive binding mode for the iminium intermediate bound in the active site of the AmDH. For clarity, only the nicotinamide coenzyme in its reduced form (NADH) and the highly conserved amino acid residue Asp 118 (numbering of *Rs*-AmDH) of the enzyme are depicted. The actual spatial positions and orientations of NADH, substrate and Asp 118 in the active site were retained according to our calculated model. The iminium intermediate (**1a***) is depicted. **1a*** is generated by interaction between 4-fluorophenylacetone (**1**) and ammonia (**a**). The crucial distances 1 and 2 are depicted with a dashed black line

atom of the terminal carboxylic group of Asp118 of *Rs*-AmDH and the hydrogen of the positively charged iminium group of the intermediate (herein referred as "distance 2").

Our analysis revealed that highest reactivity (*i.e.* conversion) for the reductive amination is achieved when both above-mentioned distances have an optimal value. The sum of the van der Waals radius [55] of carbon and hydrogen can be considered as the threshold distance, which is ca. 2.9 Å ($r_H^{vdw} = 1.2$ Å, $r_C^{vdw} = 1.7$ Å; for details see methods). Thus, an optimal distance must be around or moderately below 2.9 Å. For instance, the reductive amination of **1** with ammonia (**a**) catalyzed by *Rs*-AmDH was reported to proceed quickly and in quantitative manner.[34] Our model for this reaction with *Rs*-AmDH and the related iminium intermediate (**1a***) displays indeed an optimal "distance 1" of 2.7 Å and an optimal "distance 2" of 1.9 Å (**Figure 3A**). Conversely, the same reaction between **1** and ethylamine (**c**) affords only 4% conversion (**Table 2**, entry 3). In our models for the latter reaction considering the related iminium intermediate **1c***, the "distance 1" is still ideal (2.9 - 3.0 Å), whereas the "distance 2" is significantly larger (4.8 - 6.0 Å), (**Figure 3B** and **3C**). Another interesting example is the reductive amination between acetophenone (**10**) and either ammonia (**a**) or ethylamine (**b**). The reaction with ammonia (**a**) as amine donor afforded only a moderate conversion of 34% after 48 h;[34] our model for this reaction with the related iminium intermediate **10a*** (**Figure 3D**) displays an optimal "distance 1" of 3.0 Å, but "distance 2" is slightly elongated (3.3 Å). Conversely, the reaction between acetophenone (**10**) and ethylamine (**b**) did not occur at all (**Table 1**); in fact, although one of our models for this reaction with iminium intermediate **10b*** displays an optimal "distance 2" of 3.0 Å, "distance 1" is much larger (4.0 Å; **Figure 3E**). Finally, 4-phenyl-butan-2-one (**9**) and ammonia (**a**) react quantitatively within short reaction time.[28,34] Our model for this reaction with iminium

intermediate **9a*** shows both perfect "distance 1" and "distance 2" of 2.8 Å and 3 Å, respectively (**Figure 3G**). In contrast, the reaction between 4-phenyl-butan-2-one (**9**) and ethylamine (**b**) did not occur. Coherently, our models for this reaction with iminium intermediate **9b*** show a longer
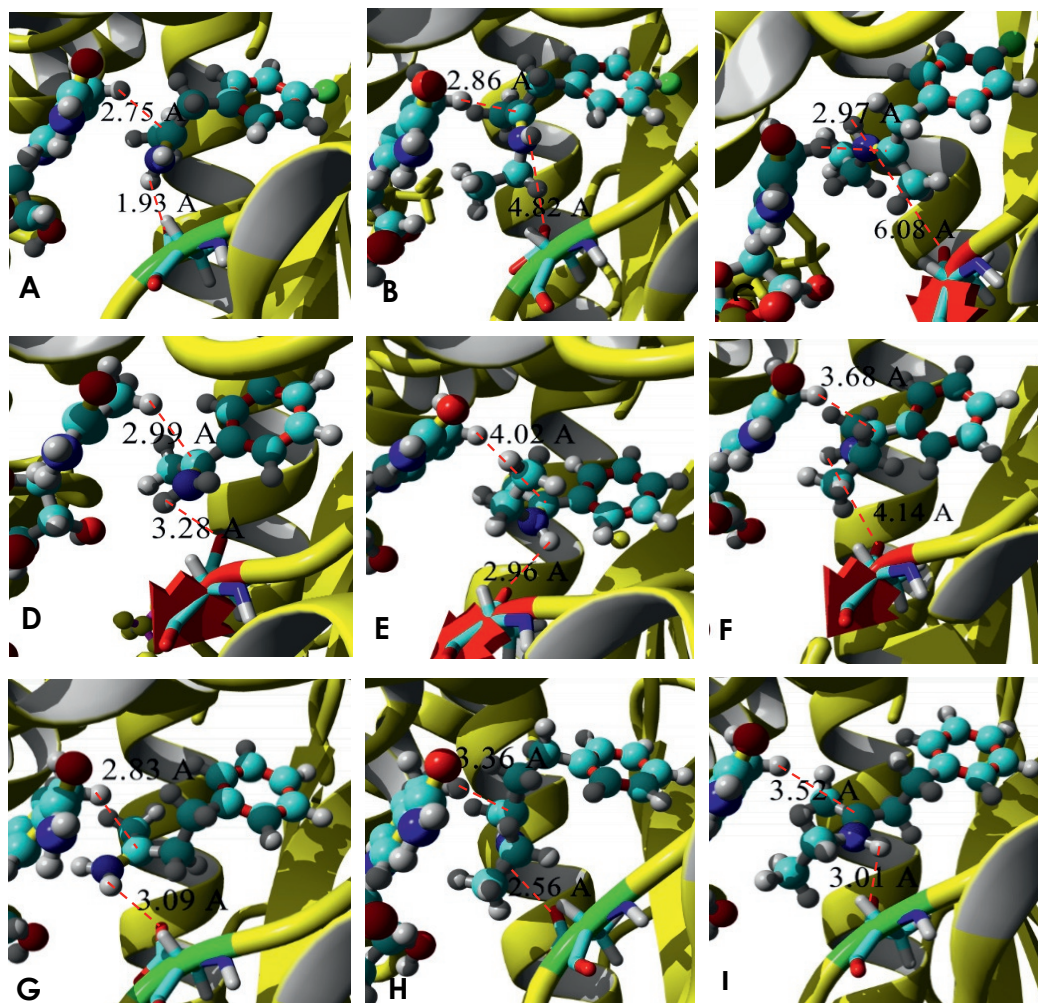
***F*igure 3. Enzyme-substrate calculated binding poses.** Figures rep[resent the active site of *Rs*-AmDH for the imine intermediate formed during the reaction of: **A)** 4'-fluoro-phenylacetone (1) with ammonia (a); **B) and C)** 4'-fluoro-phenylacetone (1) with ethylamine (c) in two different binding poses. Similarly, **D)** acetophenone (10) with ammonia (a); **E) and F)** acetophenone (10) with ethylamine (c) in two different binding poses. **G)** 4-phenyl-2-butanone (9) with ammonia (a); **H) and I)** 4-phenyl-2-butanone (9) with ethylamine (c) in two different binding poses.

"distance 1" ranging from 3.4 Å and 3.5 Å (**Figure 3H and 3I**). A similar study conducted with aldimine as intermediates provided an analogous trend (**Figure 4**). In conclusion, our analysis revealed that the distance between the prochiral iminium carbon of the intermediate and the hydride of NADH (**Figure 2**, distance 1) is the parameter of primary importance for the reaction to occur. Nevertheless, the residue Asp118 (numbering of *Rs*-AmDH) appears to play a role for achieving relevant turnovers (**Figure 2**, distance 2). However, this analysis permits only to rationalise which are the crucial parameters that enable the reduction of the iminium intermediate bound in the active site of an AmDH. Otherwise, the reductive amination of a prochiral ketone with different amine donors (**b-e**) catalysed by AmDHs generates complex reaction mixtures containing secondary amines (**1b-d**, **2b**, **3b**, **4b**, **5e**) with moderate optical purity and the unexpected primary amines in enantiopure form (**1-3a**). This observation suggests the existence of, at least, two stereocomplementary productive binding configurations for the reduction of secondary iminium intermediates.
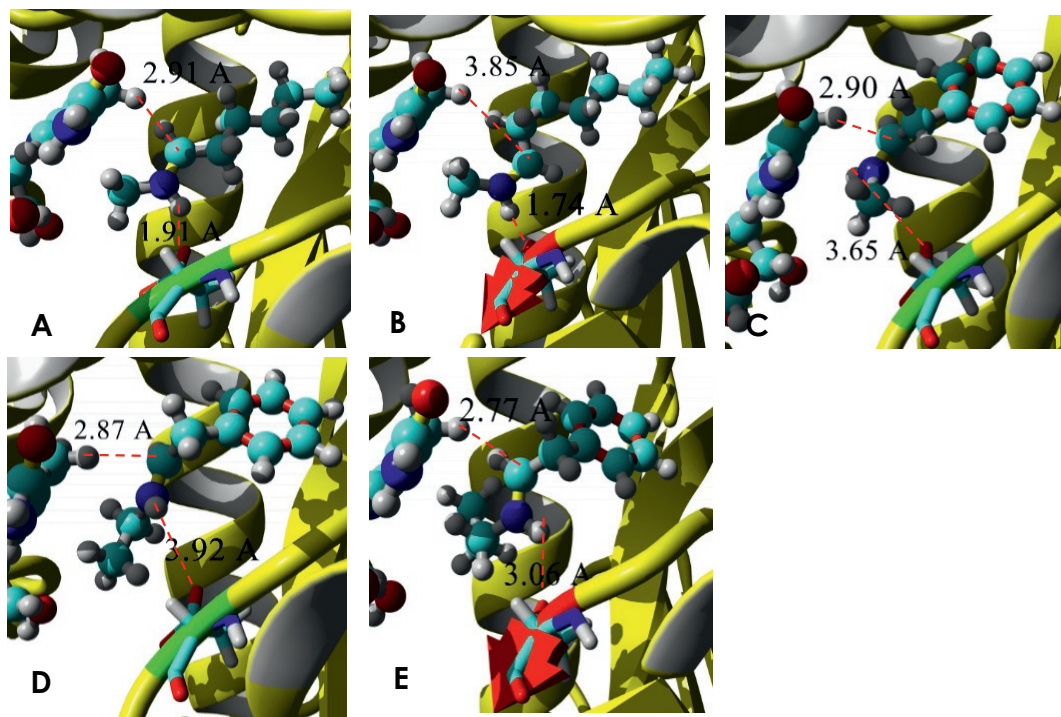
Figure 4. The best enzyme-substrate calculated binding poses. Figures represent the active site of *Rs*-AmDH for the imine intermediate formed during the reaction of: A) hexanal (4) with methylamine (b), B) heptanal (5) with methylamine (b), C) phenylacetaldehyde (6) with methylamine (b), D) phenylacetaldehyde (6) with ethylamine (c) and E) phenylacetaldehyde (6) with n-propylamine (f).

On the other hand, as the unexpected primary amines (**1-3a**) were always obtained in optically pure form (>99% ee, *R*), the promiscuous formation of these products was clearly catalyzed by the AmDHs. At this stage, we envisioned three possible reaction mechanisms that could explain the formation of primary amines (**Scheme 2**).

The first hypothesis (**Scheme 2A**) foresees an oxidative deamination of the amine donor (**b-d**; **d** in the example), which is catalyzed by the AmDH. The free ammonia generated in the first step may serve as the amino donor in a subsequent reductive amination that is always catalyzed by the AmDH. The second hypothesis (**Scheme 2B**) for explaining the formation of the enantiopure primary amine as side-product foresees an unlikely

promiscuous hydrolytic activity of AmDHs. In fact, a polarized water molecule in the active site of AmDH and possessing a proper orientation, may attack the sp^3-carbon in a-position to the nitrogen of the ketiminium intermediate (**1d***** in the example). Although such a hydrolytic step is chemically unlikely, it cannot be excluded beforehand because of the particular catalytic environment in the active site of the AmDH in which a polarised water molecule is normally involved in catalysis.[54] If such a hydrolytic step occurred, a subsequent hydride transfer from NADH would generate a primary amine. Furthermore, only in the case of cyclic intermediates such as **1d***, the same nucleophilic attack of a water molecule may also provoke the opening of the cyclopropyl ring to give an aminol upon reduction (not depicted in **Scheme 2B**). However, this route is also incompatible with the observed mixture of products. The third hypothesis (**Scheme 2C**) is an unprecedented formal transamination reaction. In nature, transamination reactions are catalysed by pyridoxal 5'-phosphate (PLP) dependent aminotransferase through a ping-pong mechanism.[56-59] However, an alternative NAD^+/NADH redox-mediated mechanisms is conceivable. According to this hypothesis, the key catalytic step would be the isomerization of the ketiminium intermediate (**1d*** in the scheme 2c) by the action of NAD^+/NADH, to give the other ketiminium intermediate **1d****.

1ˢᵗ option - *in situ* ᴺᴴ₃ **formation followed by reductive amination of ketone substrate**
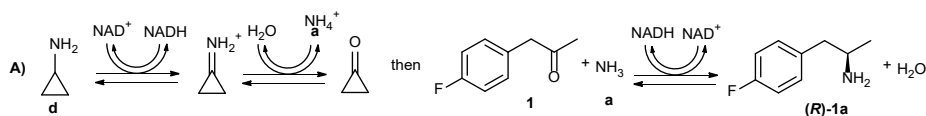
2ⁿᵈ option - $C(sp^3)$-*N*-iminium water attack followed by reductive amination
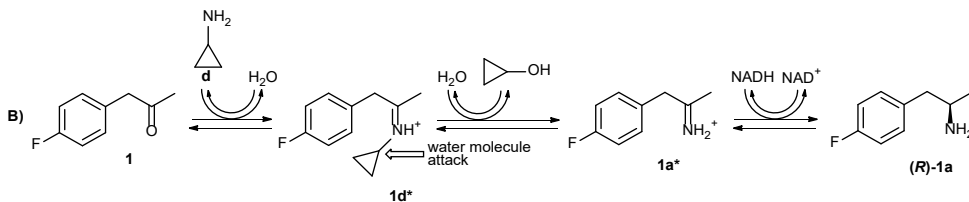
3ʳᵈ option - NAD⁺/NADH redox-mediated formal transamination
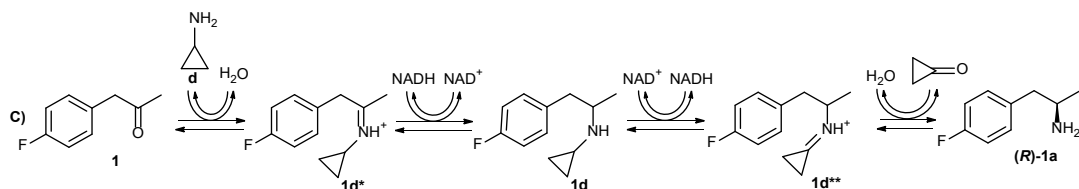
Scheme 2. Possible mechanistic explanations for the promiscuous formation of enantiopure primary amine as by-product.

One could already exclude the first hypothesis (**Scheme 2A**) by considering the analysis of the composition of the reaction mixture after the biocatalytic reductive amination. In fact, the concentration of amine donor (**b-d**) remained constant at nearly 1 M concentration from the beginning until the end of the reaction. This observation indicates a negligible, if any at all, formation of ammonia during the course of the reaction. On the other hand, our research group as well as other groups have shown that a large excess of ammonia (ca. 0.2-1 M) is required in order to drive the reductive amination of ketone substrates (15-50 mM) in aqueous buffer to a significant extent.[27-29,34,39] Moreover, AmDHs such as Ch1-AmDH show a K_M value of ca. 1 M for ammonia.[32] Similarly, with the only exception of the glutamine dehydrogenases from bovine liver, frog liver and *Clostridium* SB₄, the parent wild-type amino acid dehydrogenases are also characterized by elevated K_M values for ammonia (20-500 mM).[60]

Consequently, the biocatalytic reductive amination with ammonia is kinetically disfavored already at significant concentration of ammonia as amine donor. Nonetheless, we investigated this possibility by incubating *Rs*-AmDH (102.8 µM) with cyclopropylamine (**d**, 50 mM) and NAD$^+$ (60 mM) in phosphate buffer at pH 8.5, at 30 °C. The possible formation of ammonia was determined indirectly by analytical quantification of the consumption of **d**. As expected, the concentration of **d** remained constant during 48 h hence excluding any detectable formation of ammonia by oxidative deamination of **d** catalyzed by *Rs*-AmDH.

The second hypothesis foresees the elimination of an alcohol (**Scheme 2B**; cyclopropanol in the example) during the possible catalytic cycle of the enzymatic reductive amination between ketones (1 in the example) and amine donor (**d**, cyclopropylamine in the example). By careful monitoring of the reactions, the formation of cyclopropanol as by-product was never observed. Analysis was accomplished by comparing the GC-MS chromatogram (*i.e.* retention times and fragmentation patterns) of authentical cyclopropanol as reference compound against the GC-MS chromatograms for the enzymatic reductive amination. Crucially, control experiments also revealed that cyclopropanol (used as reference compound) is stable in the reaction buffer (1M, pH 8.5) at 30 °C and within the 48 h reaction time.

The last hypothesis foresees a promiscuous formal transamination via NAD$^+$/NADH redox-mediated iminium isomerization (**Scheme 2C**). Firstly, we ascertained that the presence of the nicotinamide coenzyme was crucial for a possible formal transamination. Hence, *Rs*-AmDH (102.6 µM) and ketone **1** (10 mM) were incubated in aqueous buffer of amine **d** (1M, pH 8.5), but in absence of NADH. As expected, we did not observe any formation of products. Then, in order to exclude any possible classical transamination reaction that is enabled by pyridoxal 5'-phosphate (PLP) as

cofactor, we also repeated the same experiment but in presence of exogenous PLP (0.5 mM). Even in this case, the formation of any product was not observed. Finally, we undertook further experiments for proving the promiscuous enzymatic activity as depicted in **Scheme 3C**. In the first set of experiments, we incubated chemically synthesized racemic *N*-(1-(4'-fluorophenyl)propan-2-yl) cyclopropanamine (**1d**) in aqueous buffer in presence of NAD$^+$ (varied concentration from 2 mM to 20 mM) and *Rs*-AmDH. In this way, we aimed at creating a dynamic equilibrium between all possible oxidative deamination pathways and reductive amination pathways (for schematic details, see **Table 3**). Crucially, control experiments (*i.e.* without AmDH) showed that **1d** is stable under these reaction conditions and no reaction was observed. In contrast, the incubation of **1d** and NAD$^+$ with the AmDH produced measurable amounts of primary amine **1a** (**Table 3**). The concentration of **1a** detected was typically low (ca. 1% conversion) because **1a** is also in equilibrium with **1** (ca. 7% conversion), the latter species being favored because of the aqueous environment. Thus, with these experiments, we proved that the *Rs*-AmDH converts the secondary amine *rac*-**1d** into the primary amine (*R*)-**1a**, which is the second part of the mechanism depicted in **Scheme 3C**.

Table 3. GC-MS conversions obtained after the oxidative deamination of 1d.
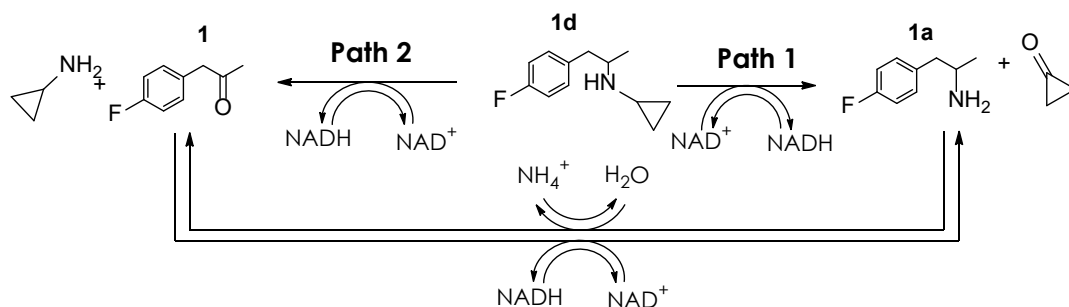
NAD+ [mM]	Compound	Conv. [%]					
		5 min	30 min	90 min	3 h	7 h	24 h
2	Alcohol	N.d.	N.d.	N.d.	N.d.	0.25	1.22
	Ketone (1)	2.86	3.96	3.71	4.07	6.08	7.64
	Prim. Amine (1a)	**N.d.**	**0.66**	**1**	**0.89**	**1**	**0.98**
	Sec. Amine (1d)	97.14	95.38	95.29	95.04	92.67	90.16
4	Alcohol	N.d.	N.d.	N.d.	N.d.	0.10	0.76
	Ketone	2.69	3.09	3.99	4.72	6.32	7.05
	Prim. Amine	**0.44**	**0.64**	**0.84**	**1.02**	**0.82**	**0.97**
	Sec. Amine	95.97	96.23	95.17	94.26	92.76	91.22
6	Alcohol	N.d.	N.d.	N.d.	N.d.	0.14	0.74
	Ketone	2.89	2.83	3.77	4.53	6.59	7.22
	Prim. Amine	**0.61**	**0.87**	**0.70**	**0.88**	**0.94**	**1.05**
	Sec. Amine	96.50	96.30	95.53	94.59	92.33	90.99
10	Alcohol	N.d.	N.d.	N.d.	N.d.	N.d.	0.24
	Ketone	2.75	3.21	3.64	4.34	5.77	6.29
	Prim. Amine	**0.52**	**1.09**	**0.98**	**0.86**	**0.75**	**1.12**
	Sec. Amine	96.73	95.70	95.38	94.80	93.48	92.35
20	Alcohol	N.d.	N.d.	N.d.	N.d.	N.d.	0.24
	Ketone	2.88	3.03	2.96	4.30	5.43	5.50
	Prim. Amine	**0.82**	**1.16**	**1.11**	**1.08**	**0.84**	**1.04**
	Sec. Amine	96.30	95.81	95.93	94.62	93.73	93.22

N.d: Not detected

Further experiments of kinetic resolution (**Table 4**) on *rac*-**1d** catalysed by *Rs*-AmDH and using NAD-oxidase (NOx) for NAD^+ recycling was also performed. Detailed analysis of the composition of the reaction mixture revealed that the enzyme is indeed capable of distinguishing between the two enantiomeric forms of **1d**. In fact, the enantiomeric excess of remaining substrate **1d** increased during the time. After 48 h reaction time, the remaining **1d** was ca. 70% whereas its *ee* was ca. 16% (**Table 4**). If perfect kinetic resolution had occurred, the remaining *ee* should have been instead 30% (*i.e.* 70% remaining **1d** equal to 20% of the 1st enantiomer and 50% of the 2nd enantiomer; hence theoretical *ee* = (50-20) = 30%). Thus, these data demonstrate that, albeit one enantiomer of the secondary amine **1d** is preferred, both enantiomers can be accepted by *Rs*-AmDH.

Table 4. Determination of conversion into 1 and of the ee of the remaining 1d after different reaction times

Experimental conditions: 0.5 mL final volume in Eppendorf tubes, buffer strength: 50 mM KPi, pH 8.5, T: 30 °C, 170 rpm on orbital shaker, [1d]: 20 mM, [NAD$^+$]: 1 mM, [NOx]: 5 µM, [Rs-AmDH]: 102.8 µM; n.m.: not measured
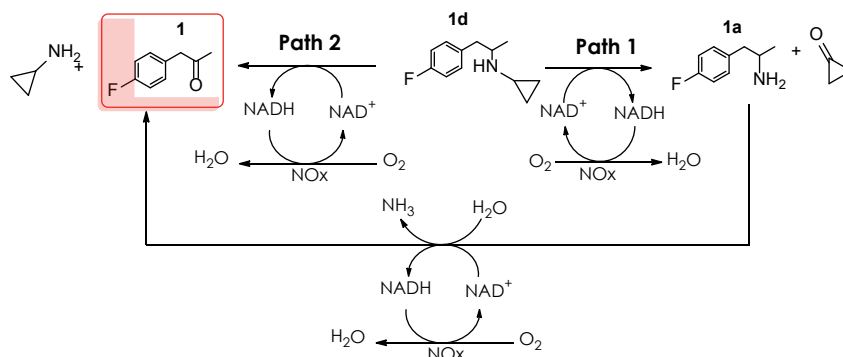
Time	Conversion into **1** [%]	Enantiomeric ratio (er) remaining **1d** [%]	ee [%]
0h	n.m.	50:50	0
1h	n.m.	48:52	4
2h	n.m.	46:54	8
48h, 1st sample	25	43:57	14
48h, 2nd sample	30	42:58	16

In conclusion, considering all the results, the side-product formation of enantiopure primary amines is originated by a non-classical promiscuous transamination activity that is mediated by the nicotinamide coenzyme. The expected ketone by-products such as cyclopropanone, or formaldehyde, or acetaldehyde could not be observed because of their known elevated instability and reactivity in solution.

2.3.4 Elucidation of the stereoselective properties of AmDHs with the aid of computational studies

The models of *Rs*-AmDH, previously discussed, served as starting point towards a deeper understanding on how a given substrate interacts with the active-site residues of the enzyme while adapting its putative reactive pose(s). This information was used in the subsequent molecular modelling of the Ch1-AmDH described in this paragraph. In fact, for the in-depth computational analysis aimed at elucidating the experimental observations regarding the stereoselectivity of the AmDHs, we selected the reaction between ketone (**1**) and methylamine (**b**), which is catalyzed by Ch1-AmDH. This choice was taken because data of conversion and enantiomeric excess for the reaction between **1** and **b** were available (**Table 2**, entry 1 and 2). Therefore, direct comparison between computational data and experimental laboratory data was possible.

Since the crystal structure of Ch1-AmDH is not publicly available, the initial step was to generate a high-quality homology model of this enzyme. The model of Ch1-AmDH was generated in two steps. Firstly, an "exploratory homology modelling run" was executed in order to determine the best suitable template(s) for this enzyme. Secondly, a "productive homology modelling run" was executed only considering the "best" template(s) as candidate(s), (**Table 5**). It is noteworthy that our homology model was created with the enzyme in its reactive conformation (*i.e.* "closed conformation") in which the nicotinamide coenzyme is bound in the active site. That is an important prerequisite for performing molecular docking simulation with these enzymes as described in this work. In contrast, the available crystal structure of opine dehydrogenases (ODHs), which also catalyze the formation of secondary amine functionalities following a formally similar mechanism, are reported in the non-reactive conformation

("open conformation") in which the nicotinamide coenzyme is unfortunately absent.[53]

Table 5. Homology model generation of Ch1-AmDH. The full amino acid sequence was explored. The multimeric state, the selected templates, the excluded templates, and the number of models generated per run are shown. The template that was selected as main contributor to the hybrid model is demarked in bold font. Moreover, the accuracy of the generated models is reported by the use of Z-scores.[61,62] The overall Z-scores for all models have been calculated as the weighted averages of the individual Z-scores (Dihedrals, Packing 1D, and Packing 3D) using the formula Overall = 0.145*Dihedrals + 0.390*Packing1D + 0.465*Packing3D.

run	Multimeric state	Templates	Cofactor	Ligand	Number of models	Overall Z-score (Quality)[a]	Overall Z-score (Quality)[b]
exploratory	monomer	**1LEH**[63], 3VPX[64], 1C1X [54], 1C1D [54], 1BXG [65]	none	none	23	-0.290 (Good)	*ND*
production	monomer	**1C1D** [54]	NADH	*L*-Phe	10	-0.520 (Good)	-0.520 (Good)

ND: Not determined

[a] Z-score and quality of the model after hybrid model generation.

[b] Best Z-score and quality of the model after molecular dynamic refinement.

We initially performed Molecular Docking simulations using the obtained model of Ch1-AmDH as target with the iminium intermediates **1a*** and **1b*** as ligands (*i.e.* **1a*** and **1b*** are generated by the interaction between the ketone **1** with ammonia (**a**) or methylamine (**b**), respectively). The aim was to obtain models of the possible reactive conformations that explain the different stereoselectivity of the reaction, considering the formation of the (*R*)-configured enantiopure primary amine by reaction of **1** with **a** [32,34] or both secondary amine enantiomers by reaction of **1** with **b**. Through the analysis of the structures obtained with molecular docking simulations, we were able to create the putative pro-(*R*) and pro-(*S*) binding modes for both iminium intermediate: **1a*** and **1b***. Comparing the models of Ch1-AmDH possessing **1a*** bound either in pro-(*S*) or in pro-(*R*) *reactive conformation*, the calculated binding energies as well as the

calculated distances between the departing hydride of NADH and the prochiral carbon of the iminium intermediate (distance 1 as defined in **Figure 2**) were similar. A similar scenario was also observed in the models of Ch1-AmDH possessing **1b*** bound either in pro-(*S*) or in pro-(*R*) reactive conformation. For this reason, we executed a set of Molecular Dynamics simulations with the aim of "relaxing" the docked enzyme-substrate complexes and, therefore, allowing for a more accurate re-evaluation of the reactive conformations for **1a*** and **1b*** (**Figure 5** and **Figure 6a-b**). After MD relaxation, it was evident that Ch1-AmDH does not tolerate well **1a*** in the pro-(*S*) binding mode (**Figure 5b and 6d**); hence, the pro-(*R*) binding mode is highly preferred for **1a***. After MD conformational relaxation, the following scenario was observed. **Figure 6c** and **6d** depict: 1) the average relative binding energies for the binding of the imine intermediates (pro-*S* **1a***, pro-*R* **1a***, pro-*S* **1b*** and pro-*R* **1b***) in the active site of Ch1-AmDH; 2) the average distances between the departing hydride of NADH and the pro-chiral carbon of the imine intermediates (distance 1 as previously defined). The pro-(*S*) binding conformation of **1a*** is the less favored compared to all the other binding conformations (**Figure 5b** and **6c**) that appears energetically similar.
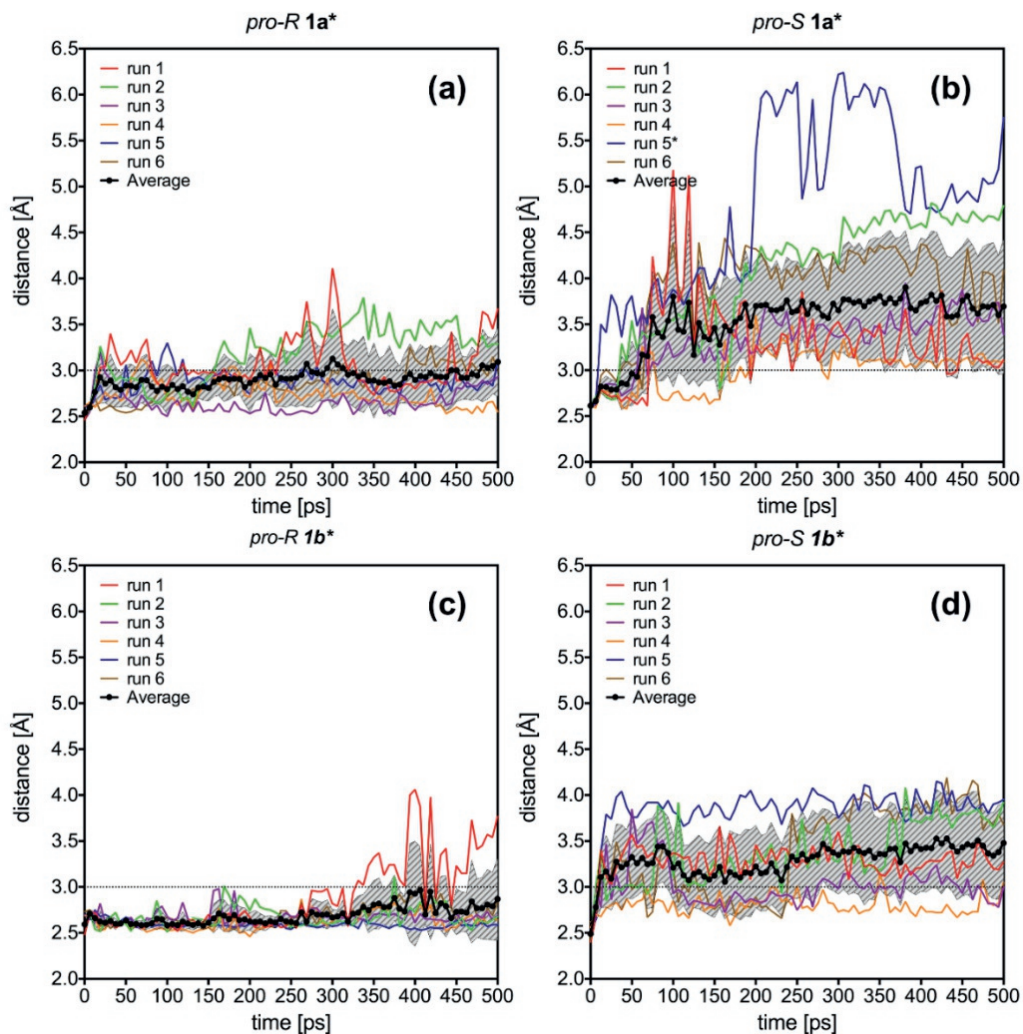
Figure 5. Interatomic distance between the hydride atom of NADH and the pro-chiral carbon atom of the imine intermediates vs. simulation time. The measured distance vs. time per each simulation run is shown. The average value is shown with black traces within a grey area that indicates the standard deviation amongst simulation runs. The simulation run 5 (denoted with an asterisk) of substrate 1a* was not considered for the average calculation due to fact that the substrate moved away from the active site. The threshold distance is indicated with a dotted black line at 3.0 Å.

More instructive is the analysis of the behavior of the distance 1 over the time of the simulations. The substrate intermediate **1a*** in its pro-(*R*) conformation showed an average distance 1 of 2.90±0.20 Å, while in its pro-(*S*) conformation moved

considerably above the threshold distance with an average of 3.74±0.64 Å (**Figure 6d**). A slightly similar behavior was observed for the substrate intermediate **1b***. **1b*** showed an average distance 1 value of 2.69±0.11 Å in its pro-(*R*) conformation, while it showed a higher average distance value of 3.29±0.36 Å in its pro-(*S*) conformation (**Figure 6d**). Nevertheless, it is important to note that distance 1 for pro-(*S*) **1b*** (3.29±0.36 Å) is relatively shorter than the same distance for pro-(*S*) **1a*** (3.74±0.64 Å). This finding indicates that Ch1-AmDH must tolerate better the pro-(*S*) conformation of **1b*** than the pro-(*S*) conformation of **1a***. On the other hand, **1b*** in the pro-(*R*) orientation is still the preferred binding mode by Ch1-AmDH. That can be observed further in **Figure 5c** and **6d**, in which approximately 94% of the MD snapshots (within the simulation time) represent the pro-(*R*) **1b*** intermediate in the active site of Ch1-AmDH with a distance between its prochiral carbon atom and the attacking hydride of NADH (distance 1 as previously defined) below the threshold of 3 Å (required for hydride shift). Thus, there is an elevated probability that the hydride shift from NADH to **1b*** occurs if **1b*** is bound in its pro-(*R*) binding conformation. Conversely, the pro-(*S*) binding conformation of **1b*** is less favorable for hydride shift from NADH because only approximately 32% of the MD snapshots showed a distance 1 below the threshold of 3 Å (**Figure 5d and 6d**).

On the other hand, the relative binding energies of **1b*** on pro-(*R*) and pro-(*S*) conformations respectively seem to be approximately the same (**Figure 6c**). We can therefore conclude that, although tolerated, the pro-(*S*) configuration of **1b*** has a lower probability to react than the pro-(*R*) contra-part. The pro-(*S*) conformation of **1b*** seems to be stabilized by hydrophobic interactions of the methyl-group with residues M75, A298 and C310. The pro-(*R*) binding mode of **1b*** is stabilized as already known from literature for wild-type AADHs.[54] This stabilization involves the previously discussed highly conserved Asp residue (numbering 125 for Ch1-AmDH) in a similar way as depicted in **Figure 2** for *Rs*-AmDH. The described enzyme/substrate contacts for Ch1-AmDH are

depicted in **Figure 6e-f** for both pro-(*R*) and pro-(*S*) binding modes. It is interesting to note that the intermediate **1b*** bound in its reactive pro-(*R*) binding mode was mainly observed assuming the *E* configuration at the C=N double bond (**Figure 6a** and **6e**). In contrast, the intermediate **1b*** bound in its reactive pro-(*S*) binding mode was mainly observed assuming the *Z* configuration (Figure **6b** and **6f**). It is known for literature that *N*-alkylimines can isomerize in solution at ambient temperature by tautomerization and rotation.[66,67] In the case of intermediate **1b***, which bears non-bulky substituents such as hydrogen or methyl groups, the *E* isomer is known to be favored in equilibrium in solution at room temperature.[68] Nonetheless, in our case, the enzyme selects the preferred *E* or *Z* configuration of the intermediate in the active site.
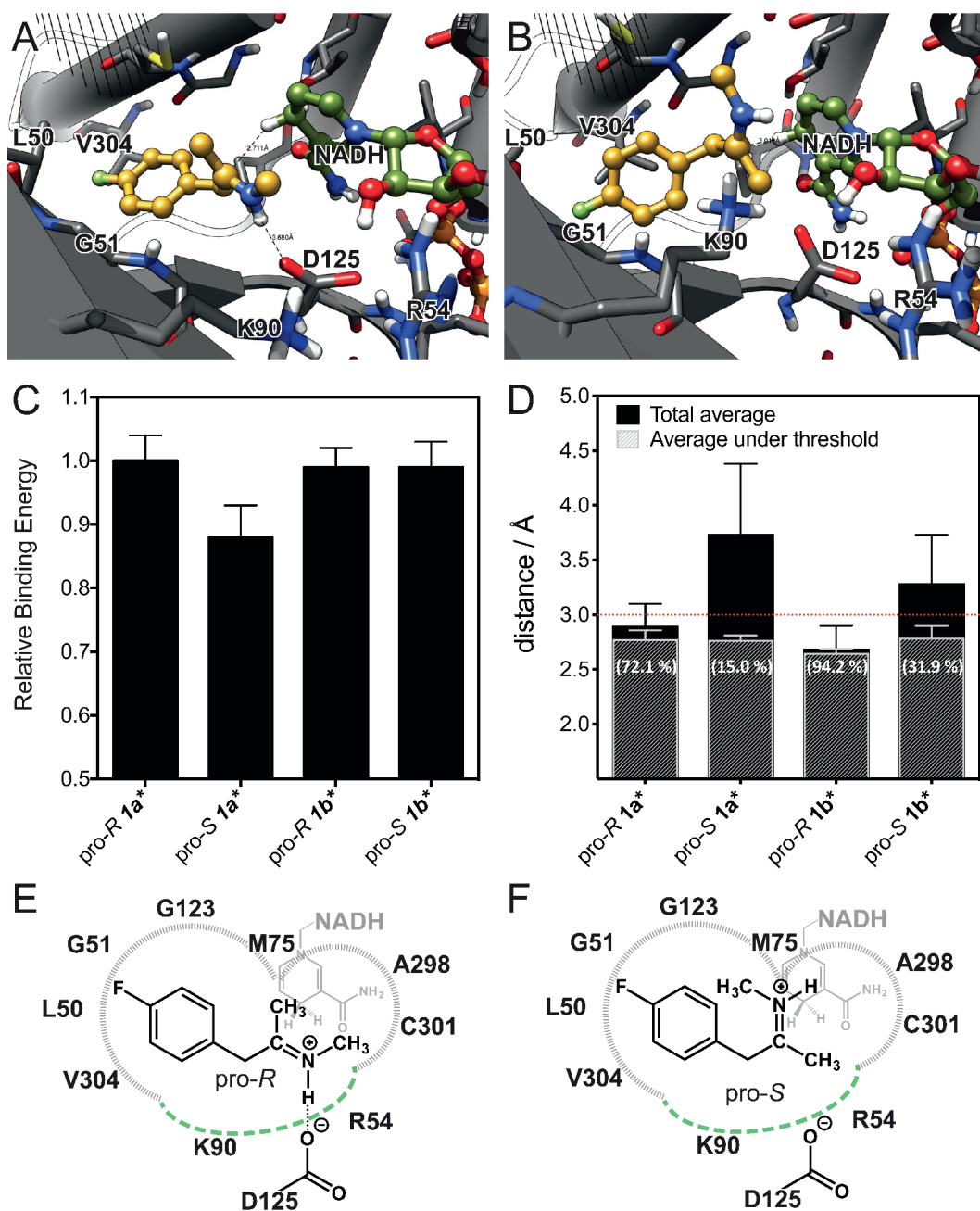
Figure 6. Pro-chiral preferences of Ch1-AmDH. Representative relaxed molecular dynamics snapshots of the 1b* on its pro-(*R*) (a) and pro-(*S*) (b) conformations. The substrate is shown in yellow, while the NADH is shown in green. For clarity, all non-polar hydrogen atoms were

not shown. Panel (c) depicts the relative binding energy for 1a* and 1b* on their pro-(*R*) and pro-(*S*) configuration. All the binding energies are given as relative to the average binding energy of 1a* on its pro-(*R*) conformation. A lower value of relative binding energy means a less favorable binding. Only those snapshots that showed the substrate on its "reactive conformation" were considered for binding energy determination. Panel (d) depicts the distance from the departing hydride of the coenzyme (NADH) to the pro-chiral carbon of the ligand (iminium) for 1a* and 1b* (in both pro-(*R*) and pro-(*S*) configurations). The number in between brackets indicate the percentage of snapshots that contributed with substrates located under the distance threshold (3 Å). Panel (e) and (f) depict the observed enzyme/substrate contacts for 1b* on its pro-(*R*) and pro-(*S*) conformation, respectively. Lines in grey indicate hydrophobic interactions, while the dashed green line indicate hydrophilic interactions. The NADH cofactor is depicted behind the substrate in light-grey.

Additionally, a non-bonding dihedral angle (χ) was defined in order to describe the stereo-binding mode of the substrate in the active site (**Figure 7a**). This dihedral angle was defined following the Cahn–Ingold–Prelog priority rules between the three atoms bonded to the pro-chiral carbon of the substrate and the hydride atom of the NADH cofactor. This dihedral angle was determined for the (*R*)- and (*S*)- configured products (both for **1a** and **1b**) of the reaction, indicating that the (*R*)-configured product shows an average value of 63.85±0.20°, while the (*S*)-configured product shows an average value of -63.95±0.27°.

Figure 7b shows the behavior of the χ angle in function of the time for substrate intermediates **1a*** and **1b*** and starting from both pro-(*R*) and pro-(*S*) binding conformations. Notably, in the case where the intermediate substrate **1a*** is bound in a pro-(*S*) binding mode, a switch to the pro-(*R*) conformation occurred within the simulation time (**Figure 7b**) In particular, 50% of the simulation runs for pro-(*S*) **1a*** (3 out of 6) showed this switch from pro-(*S*) to pro-(*R*) (**Figure 7b**, black line). An additional simulation (run 5) also showed a switch in the conformation but, during this simulation, the substrate moved out of the active-site. Therefore, we did not consider this simulation into the calculation of the average values. Only in 2 cases out of 6, substrate **1a*** maintained the pro-(*S*) binding

conformation (**Figure 7b**, green line). In contrast to the simulation with pro-(*S*) **1a***, a conformational switch was never observed for simulations starting from either pro-(*R*) **1a*** or pro-(*R*) **1b***or pro-(*S*) **1b*** (**Figure 7**). It is important to remark that the average value of the herein defined dihedral angle for pro-(*S*) **1a*** amongst simulation runs has only illustrative value, thus indicating great conformational changes in the active site of Ch1-AmDH.

In summary, the molecular dynamic simulations provide an insight at molecular level on the different stereoselective behavior of the AmDHs in the reductive amination of prochiral ketones with either ammonia or more complex amines. When ammonia is the amine donor, the *reactive* pro-(*R*) conformation of the iminium intermediate is much more favored than the pro-(*S*) conformation explaining why the primary amine product is always experimentally obtained in enantiopure (*R*)-configured form.[34] In the event that a pro-(*S*) binding mode for the primary iminium intermediate is generated in the active site, a conformational switch to pro-(*R*) binding mode (Figure 7b) or even the release of the intermediate from the active site is likely to occur. Conversely, when a primary amine is the amine donor for the reductive amination, both pro-(*R*) and pro-(*S*) binding modes can be generated as reactive conformations so that the secondary amine product is obtained in both enantiomeric forms.
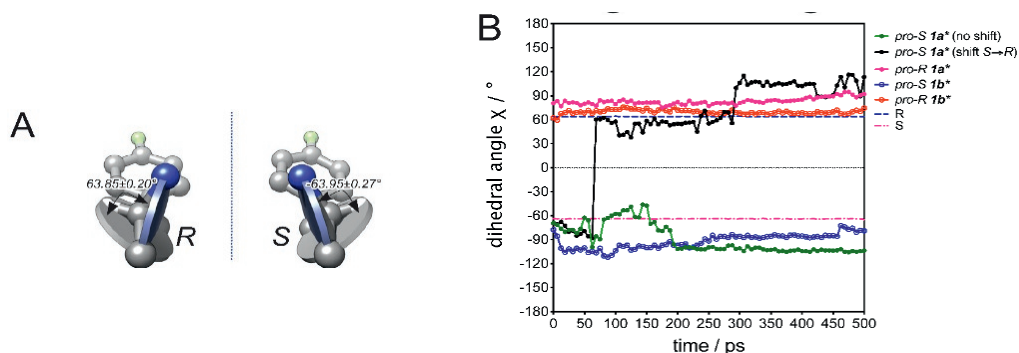
Figure 7. Dihedral angle χ versus time for the Molecular Dynamics Simulations starting from pro-(*R*) 1a*, pro-(*S*) 1a*, pro-(*R*) 1b* and pro-(*S*) 1b*. (a) Illustrative depiction of the χ angle

for the (*R*)- and (*S*)-configured product of the reaction. These values were used as reference for describing the hydride shift from NADH that would afford any of these enantiomers. According to this definition, a positive value of the dihedral angle in the intermediate will lead to the (*R*)-configured amine upon reduction. A negative value will lead to the (*S*)-configured amine upon reduction. (b) The average variation of χ angle over the time is shown for the simulations of pro-(*R*) **1a*** (purple), pro-(*S*) **1a*** (black or green), pro-(*R*) **1b*** (orange) and pro-(*S*) **1b*** (blue). For each system, the depicted line is the average of six independent simulation runs. Only the simulation run number 5 for substrate **1a*** in pro-(*S*) binding conformation was not considered for the average calculation due to fact that the substrate moved away from the active site. For the sake of clarity of the depiction, the error bars of these average simulations have been omitted. The average χ values for the (*R*)-configured (blue) and (*S*)-configured products (purple) are also shown as dashed lines.

2.3.5 Proposed catalytic mechanism

Considering all the results obtained from practical experimental laboratory and computational experiments, we postulated a biocatalytic cycle that illustrates the formation of both secondary and primary amines (**Scheme 3**). The proposed cycle is adapted from the catalytic mechanism of the phenylalanine dehydrogenases from *Rhodococcus sp.* M4 (the wild-type parent of the variant *Rs*-AmDH).[54]
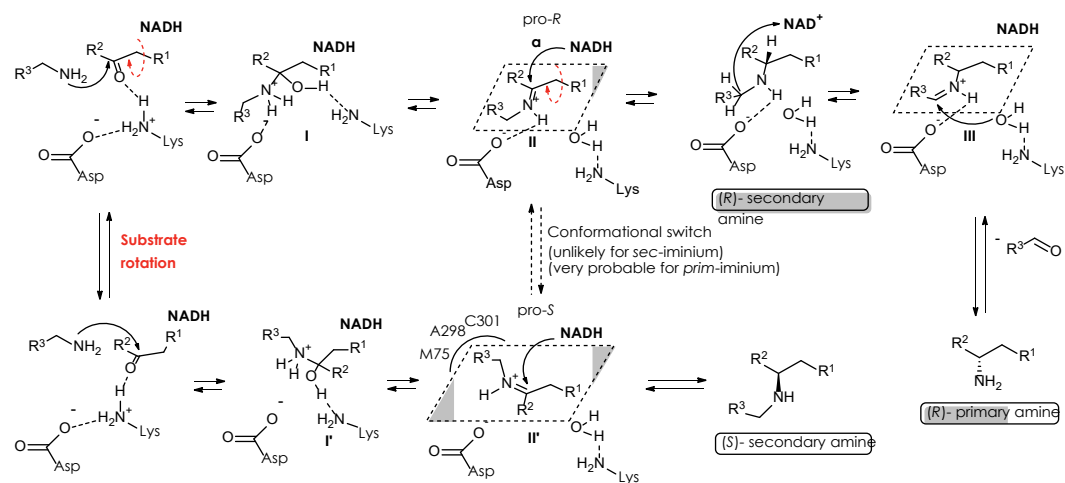
Scheme 3. Proposed catalytic cycle for the reductive amination catalysed by *Rs*-AmDH and Ch1-AmDH with amine donors different from ammonia (adapted from reference 17). Two stereocomplementary binding modes are the most probable: either intermediate **II** (E configuration and pro-(*R*) binding mode) or intermediate **II'** (Z configuration and pro-(*S*) binding mode). Interconversion between **II** and **II'** (and vice versa) was never observed for

secondary iminium intermediates during the time of our simulations. In contrast, interconversion from **II'** to **II** was observed in 50% of the cases in our simulations with primary iminium intermediates. The opposite interconversion (from **II** to **II'**) was never observed. Further reduction of intermediate **II'** by hydride shift from NADH forms the secondary amine product in (*S*)-configuration. Reduction of intermediate **II** by hydride shift from NADH forms the secondary amine product in (*R*)-configuration. However, intermediate **II** can also be oxidized to the iminium isomer **III**. After this formal imine isomerization step, the hydrolysis of intermediate **III** furnishes the primary amine product in (*R*)-configuration.

In the first step, the carbonyl compound and the amine donor generate the geminal amino alcohol (**I** or **I'**) assisted by a protonated Lys and deprotonated Asp residues from the AmDH active site. Intermediate **I** and **I'** can interconvert through a rotation around the carbon-carbon bond that connects the prochiral C-sp^2 of the ketone and the C-sp^3 in its a-position (the latter connected to substituent R^1 in Scheme 3). This rotation appears to be the most probable one since our model structures clearly show that the R^1 substituent (e.g. in this study phenyl, phenylmethyl, alkyl) is tightly accommodated in a hydrophobic cavity in the active site of the AmDH (**Figure 8**).
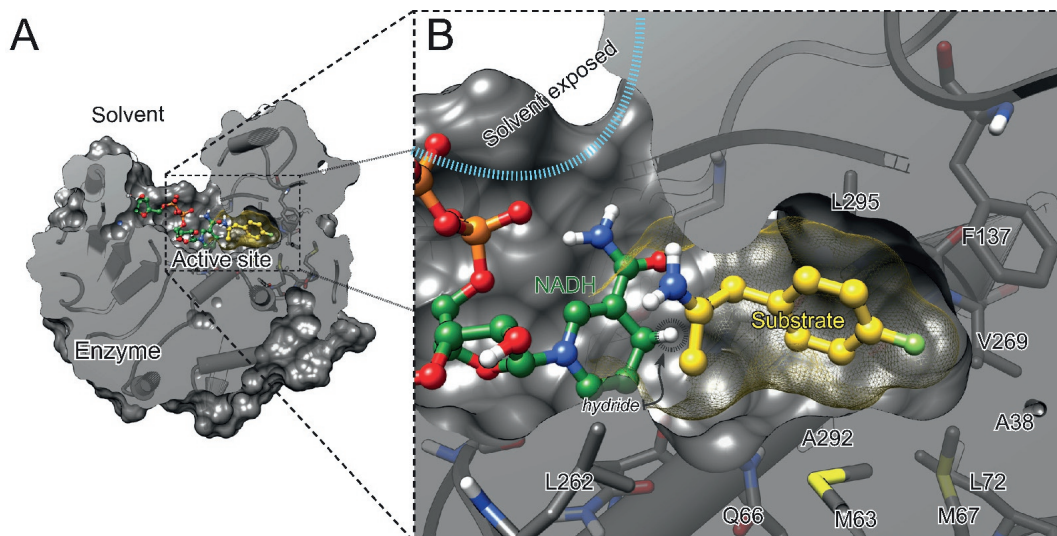
Figure 8. (a) Hydrophobic binding pocket of Rs-AmDH (b) Amino acid residues constituting the hydrophobic binding pocket in the active site of *Rs*-AmDH

Then, assisted by the same Lys residues, a water molecule is released from intermediate **I** or **I'** to generate the iminium intermediate **II** (pro-*R* binding mode) and **II'** (pro-*S* binding mode), respectively. From the analysis of the snapshots of our molecular docking simulations, it appears that the iminium moiety of the intermediate **II** (pro-*R*) is stabilized further by a hydrogen bond with the deprotonated aspartate residue (Figures 3a and 3e; Asp 118 in *Rs*-AmDH or Asp 125 in Ch1-AmDH). In contrast, such a hydrogen bond was not observed with intermediate **II'** since the aspartate residue is too distant from the hydrogen of the iminium moiety. Intermediate **II'** appears to be stabilized by hydrophobic interactions of the methyl group with residues M75, A298, C310 (**Figure 6b** and **6f**). As observed before, intermediate **II** assume the preferred *E* configuration whereas intermediate **II'** assumes the preferred *Z* configuration (in **Scheme 3**, C.I.P. priority: $R^1 > R^2$). Although a conformational switch from pro-(*S*) to pro-(*R*) binding mode (or vice versa) of the secondary imine intermediate was never observed within the time of our simulations, this event cannot be completely ruled out. Hence, this theoretically possible conformational binding switch was depicted as dashed line in **Scheme 3**. In contrast, as previously described, such a conformational binding switch from pro-(*S*) to pro-(*R*) (but not vice versa) is very likely to occur with primary iminium intermediates (**Figure 7b**)

At this stage, hydride shift from NADH to intermediate **II** or **II'** can occur to furnish the secondary amine product in (*R*)-configuration or (*S*)-configuration, respectively. Nonetheless, the amine (*R*)-**1b** obtained by reduction of intermediate **II** can be also subjected to a further promiscuous re-oxidation in the active site by abstraction of the hydride from the other alkyl chain of the amine moiety. This promiscuous formal imine isomerization generates intermediate **III**. Hydrolysis of intermediate **III** by the same water molecule coordinated to the catalytic Lys residue or by another polarized water molecule at proper distance in the active site forms the primary amine product (*R*)-**1b** as single enantiomer.

2.4 Conclusions

The known AmDHs were engineered from amino acid dehydrogenases and therefore they display the highest catalytic activity with ammonia as amine donor. In contrast to the common belief that ammonia is the only possible amine donor, we have demonstrated in this work that the reactivity of AmDHs can be extended to other amine donors. In fact, enantioenriched secondary amines were obtained with conversion up to 43%. However, we observed that the control of the chemo- and stereoselectivity of the reductive amination catalyzed by AmDHs with different amine donors is challenging. This study revealed that the secondary amine products can be obtained just in enantioenriched form, so far. Furthermore, an unprecedented nicotinamide (NAD)-dependent isomerization step may take place in the active site of the enzyme, during the catalytic cycle, ultimately leading to the formation of the structurally related enantiopure primary amine as additional product. To the best of our knowledge, our findings suggest the first example of a formal enzymatic transamination mechanism that is not catalyzed by PLP. By combining practical laboratory experiments and computational experiments and analysis, we could rationalize the formation of all the products observed in the reaction mixture. Finally, a catalytic cycle was postulated based on the known natural catalytic cycle of the wild-type phenylalanine dehydrogenases from *Rhodococcus sp.* M4.

In summary, this study provides an understanding of the molecular discriminants that are crucial for the efficient catalytic activity of AmDHs, and it will contribute to provide the knowledge required for further rational engineering of AmDHs in order to improve activity, stereoselectivity and suppress possible side reactions.

2.5 Methods

2.5.1 General procedure for the biocatalytic amination of carbonyl compounds 1-13 with amine donors b-j.

All buffers were prepared by mixing each amine donor **b-k** with distilled water to obtain a final concentration of 1 M. The pH was adjusted to 8.5 with formic acid. In the case of aniline (**l**), due to solubility issues, saturated solution of aniline (pH 8.5) was used. Both amine dehydrogenases (*Rs*-AmDH and Ch1-AmDH) were tested for the synthesis of secondary or tertiary amines by using all eleven different amine buffers, as well as the carbonyl compounds **1-12** as acceptor substrates (for detailed structures, see **scheme 1**).

Biotransformations were performed in 1.5 mL Eppendorf tubes with a total reaction volume of 0.5 mL. The reaction consisted of NAD$^+$ (1 mM), substrate (10 mM), AmDH (102.8 µM for *Rs*-AmDH and 91.8 µM for Ch1-AmDH) and Cb-FDH (23.5 µM). Reactions were performed at 30 °C for 48 h on orbital shakers (170 rpm) in a horizontal position. The reactions were quenched after 48 h by the addition of aqueous KOH (10 M, 100 µL). Then, the organic compounds were extracted with dichloromethane (CH_2Cl_2, 1 x 600 µL) and dried with magnesium sulphate. The conversions were measured by GC-FID using commercially available or chemically synthesised reference compounds. In the cases where reference compounds were not available, preliminary identification of the desired products (amines) was also done by GC-MS using the same column and method as for GC-FID. The enantiomeric excess was determined after derivatization to acetamido using a solution of DMAP (50 mg) in 1 mL of acetic anhydride (409 mM). In total, 50 µL of this solution was added to each 600 µL dichloromethane contained the amine product. The mixtures were shaken at 25 °C for 30 min. After that 500 µL of water was added for another 30 min with shaking at 25 °C. The samples were centrifuged for 10 min at 14800 rpm and the organic phases were dried with magnesium sulphate prior to the injection in the

Chrompack Chiracel Dex-CB (25 m, 320 µm, 0.25 µm, Agilent), or Hydrodex-β-TBDAC (50m, 0.40 mm, 0.25 mm, Macherey-Nagel).

2.5.2 Disproving *in-situ* generation of ammonia by enzymatic oxidative deamination of amine donor (1st option in Scheme 2).

To demonstrate that free ammonia is not generated as a result of the oxidative deamination of the amine donor (e.g. cyclopropylamine, **d**) catalysed by *Rs*-AmDH, we incubated cyclopropylamine (50 mM) in the presence of *Rs*-AmDH (102.8 µM) and stoichiometric NAD$^+$ (60 mM). The reactions were performed in duplicates for 1 h, 2 h and 7 h. After the reported times, reactions were quenched with KOH and extracted with ethyl acetate supplemented with toluene (10 mM) as internal standard. For each set of reactions the average ratio between the GC areas of cyclopropylamine and toluene was calculated. A blank experiment was also performed in triplicate by incubating cyclopropylamine (50 mM) in the reaction buffer (phosphate buffer pH 8.5). After basic extraction with ethyl-acetate containing the internal standard (toluene, 10 mM), the ratios between cyclopropylamine and toluene areas (d/t) were calculated. Comparison among the values (d/t) obtained from the reactions performed with those obtained from the blank reactions revealed that cyclopropylamine was not consumed by the enzyme over time. Therefore, a possible scenario in which free ammonia is generated by the oxidative deamination of cyclopropylamine by Rs-AmDH and subsequently used by the enzyme to produce the primary amine can be excluded.

2.5.3 Study of oxidative deamination on racemic 1d catalyzed by *Rs*-AmDH

In total 90 µM of *Rs*-AmDH was incubated with NAD$^+$ (2 mM, 4 mM, 6 mM, 10 mM and 20 mM) for six different reaction times (5 min, 30 min, 90 min, 3 h, 7 h and 24 h) in Kpi 100 mM pH 8. The reactions were quenched after the reported times by the addition of aqueous KOH (10 M, 100 µL). Then, the organic compounds were extracted with dichloromethane (CH2Cl2, 1 x 600 µL) and dried with

magnesium sulphate. The conversions were measured by GC-FID using commercially available or chemically synthesized reference compounds.

2.5.4 Computational model of *Rs*-AmDH

The 3D structural model of *Rs*-AmDH was created starting from the crystal structure of the L-phenylalanine dehydrogenase from *Rhodococcus sp.* M4 (PDB code: 1C1D).[54] The *Rs*-AmDH variant differs only for three amino acids positions from the wild-type L-phenylalanine dehydrogenase: namely K66Q, S149G, and N262C.[28] These mutations were *in silico* induced using the YASARA software,[69] utilizing the AMBER 03 force field.[70] The protonation state of all atoms was automatically adjusted, with the exception of those atoms involved in the hydride transfer between the co-factor and the substrate. The protonation state of the latter atoms was adjusted manually accordingly. Every time a mutation was induced a three-step energy minimization was executed. Step one: only the mutated residue was energetically minimized. Step two: the mutated residue plus all those residues within a radius of 6.0 Å from the mutated residue were subjected to energy minimization. Step three: the complete enzyme was submitted to energy minimization. By using this energy minimization protocol, it was assured a gradual adjustment of the complete structure to the new mutation, thus avoiding the production of undesired deformations of the secondary structure.

All selected substrates were generated *in situ* by mimicking the observed position of L-phenylalanine in the crystal structure PDB 1C1D. After substrate generation, the three-steps energy minimization protocol above-described was applied. These models were created for studying the possible reactive poses of *Rs*-AmDH containing the ketimine (**Figure 3**) and aldimine (**Figure 4**) intermediates formed during the catalytic mechanism. Based on the reported catalytic mechanism of the parent wild-type L-phenylalanine dehydrogenase from Rhodococcus sp. M4[54], we analyzed the models considering two crucial parameters: 1) the distance between the attacking hydride of NADH and the pro-chiral carbon of

the iminium intermediate (distance 1); 2) the distance between the negatively charged oxygen atom of the terminal carboxylic group of D118 in *Rs*-AmDH and the hydrogen of the iminium group (distance 2).

2.5.5 Computational model of Ch1-AmDH

Ch1-AmDH chimeric enzyme was previously created in laboratory by domain shuffling of two first generation variants such as *Bb*-AmDH (originated from *Bacillus badius* L-phenylalanine dehydrogenase) and L-AmDH (originated from *Bacillus stearothermophilus* L-leucine dehydrogenase).[32] The Ch1-AmDH model structure was generated in two steps. Firstly, an "exploratory homology modelling run" was executed in order to determine what was (were) the best suitable template(s) for this enzyme. Then, a second homology modelling run was executed only considering the "best" template(s) as candidate(s).

Exploratory homology modelling run. This exploratory run was carried out using the YASARA [69] homology model building protocol,[71,72] which involves multi-template structural model generation. Since the linear amino acid sequence of the target protein was the only given input, the possible templates were identified by running 3 PSI-BLAST[73] iterations to extract a position specific scoring matrix (PSSM) from UniRef90,[74] and then searching the PDB for a match with an E-value below the homology modelling cut-off of 0.005. A maximum of 5 templates was allowed. To aid alignment correction and loop modelling, a secondary structure prediction for the target sequence had to be obtained. This was achieved by running PSI-BLAST to create a target sequence profile and feeding it to the PSI-Pred[75] secondary structure prediction algorithm. For each of the found templates, models were built. Either a single model per template was generated, when the alignment was certain, or a number of alternative models were generated, when the alignment was ambiguous. A maximum of 50 conformations per loop were explored. A maximum of 10 residues were added to the termini. Finally, YASARA attempted to combine the best parts of the generated models to obtain a hybrid model, with the intention of increasing the

accuracy beyond each of the contributors. The quality of the models was evaluated by the use of Z-score[61,62]. A Z-score describes how many standard deviations the model quality is away from the average high-resolution X-ray structure. The overall Z-scores for all models have been calculated as the weighted averages of the individual Z-scores using the formula: Overall = 0.145*Dihedrals + 0.390*Packing1D + 0.465*Packing3D. The overall score thus captures the correctness of backbone- (Ramachandran plot) and side-chain dihedrals, as well as packing interactions.

Production homology modelling run. Based on the results of the exploratory run, it turned out that the generated model showed a reasonably good quality; however, it contained neither the cofactor nor a co-crystalized substrate in its active-site. For this reason, the template 1C1D was only considered for the production run. In fact, the crystal structure of 1C1D was co-crystalized with cofactor and substrate in its active-site.[54] In summary, the production run was carried out using the same parameters used in the exploratory run with exception of the following parameters: only one template was manually selected, a maximum of 100 conformations per loop were explored and a maximum of 2 residues were added to the termini. In order to increase their quality, the obtained models were submitted to 500 picoseconds molecular dynamic refinement simulation using the protocol describe by E. Krieger *et al*.[76] A structural snapshot was saved every 25 picoseconds for further analysis of quality parameters (potential energy, Dihedrals, Packing1D and Packing3D). The model with the best quality was selected for further computational molecular studies. In **Table 5**, the results of homology model generation are reported.

2.5.6 Computational molecular docking and molecular dynamics simulations

The model of Ch1-AmDH obtained in the previous step was used as starting point for the molecular dynamics (MD) simulations. MD simulations were executed using the Yasara software,[69] with the AMBER 03 force field.[70] Prior to this, all

substrates were *in situ* generated starting from the reactive pose of *L*-phenylalanine. After substrate generation, the three-step energy minimization protocol was applied. These models were created representing the reactive pose of Ch1-AmDH with the iminium intermediate. The final relaxed structure was evaluated using the Autodock Vina[77] scoring function in order to assess its binding energy at its reactive pose. Both binding conformations, pro-(R) and pro-(S) obtained, were submitted to MD simulations. A minimum of six independent MD simulations (with random initial velocities) were executed per system. Each MD simulation was run for 500 ps, and a snapshot was taken every 6.25 ps, thus resulting in 81 frames (counting the starting structure) per simulation. These frames were submitted for analysis and several dynamic properties were followed. However, the distance between the departing hydride of NADH and the pro-chiral carbon atom of the imine intermediate substrate was considered as the main descriptor of the reactive pose. The sum of the van der Waal's radius [55] of carbon and hydrogen was considered as the threshold distance, which was set to a rounded value of 3.0 Å (r_H^{vdw} = 1.2 Å, r_C^{vdw} = 1.7 Å; $r_H^{vdw} + r_C^{vdw}$ = 2.9 Å; thus: $d_{CH}^{threshold}$ = 3.0 Å).

2.6 References

1 Khersonsky, O. & Tawfik, D. S. *Annu. Rev. Biochem* **79**, 471-505, doi:10.1146/annurev-biochem-030409-143718 (2010).

2 Nobeli, I., Favia, A. D. & Thornton, J. M. *Nat. Biotechnol.* **27**, 157-167, doi:10.1038/nbt1519 (2009).

3 Humble, M. S. & Berglund, P. *Eur. J. Org. Chem.*, 3391-3401, doi:10.1002/ejoc.201001664 (2011).

4 Hult, K. & Berglund, P. *Trends Biotechnol.* **25**, 231-238, doi:10.1016/j.tibtech.2007.03.002 (2007).

5 Khersonsky, O., Roodveldt, C. & Tawfik, D. S. *Curr. Opin. Chem. Biol.* **10**, 498-508, doi:10.1016/j.cbpa.2006.08.011 (2006).

6 Bornscheuer, U. T. & Kazlauskas, R. J. *Angew. Chem. Int. Ed.* **43**, 6032-6040, doi:10.1002/anie.200460416 (2004).

7 Babtie, A., Tokuriki, N. & Hollfelder, F. *Curr. Opin. Chem. Biol.* **14**, 200-207, doi:10.1016/j.cbpa.2009.11.028 (2010).

8 Kazlauskas, R. J. *Curr. Opin. Chem. Biol.* **9**, 195-201, doi:10.1016/j.cbpa.2005.02.008 (2005).

9 Vilim, J., Knaus, T. & Mutti, F. *Angew. Chem. Int. Ed.*, doi:10.1002/anie.201809411 (2018).

10 Emmanuel, M. A., Greenberg, N. R., Oblinsky, D. G. & Hyster, T. K. *Nature* **540**, 414-417, doi:10.1038/nature20569 (2016).

11 Sandoval, B. A., Meichan, A. J. & Hyster, T. K. *J. Am. Chem. Soc.* **139**, 11313-11316, doi:10.1021/jacs.7b05468 (2017).

12 Garrabou, X., Beck, T. & Hilvert, D. *Angew. Chem. Int. Ed.* **54**, 5609-5612, doi:10.1002/anie.201500217 (2015).

13 Cuetos, A. *et al. Angew. Chem. Int. Ed.* **55**, 3144-3147, doi:10.1002/anie.201510554 (2016).

14 Wetzl, D., Bolsinger, J., Nestl, B. M. & Hauer, B. *ChemCatChem* **8**, 1361-1366, doi:10.1002/cctc.201501244 (2016).

15 Liu, Z., Lv, Y., Zhu, A. & An, Z. *ACS Macro Letters* **7**, 1-6, doi:10.1021/acsmacrolett.7b00950 (2017).

16 Payer, S. E. *et al. Adv. Synth. Catal.* **359**, 2066-2075, doi:10.1002/adsc.201700247 (2017).

17 Coelho, P. S., Brustad, E. M., Kannan, A. & Arnold, F. H. *Science* **339**, 307-310, doi:10.1126/science.1231434 (2013).

18 Roiban, G. D. & Reetz, M. T. *Angew. Chem. Int. Ed.* **52**, 5439-5440, doi:10.1002/anie.201301083 (2013).

19   Miao, Y., Geertsema, E. M., Tepper, P. G., Zandvoort, E. & Poelarends, G. J. *ChemBioChem* **14**, 191-194, doi:10.1002/cbic.201200676 (2013).

20   Wuensch, C. *et al. Angew. Chem. Int. Ed.* **52**, 2293-2297, doi:10.1002/anie.201207916 (2013).

21   Devamani, T. *et al. J. Am. Chem. Soc.* **138**, 1046-1056, doi:10.1021/jacs.5b12209 (2016).

22   Miao, Y., Metzner, R. & Asano, Y. *ChemBioChem* **18**, 451-454, doi:10.1002/cbic.201600596 (2017).

23   Roth, S. *et al. ChemBioChem* **18**, 1703-1706, doi:10.1002/cbic.201700261 (2017).

24   Abrahamson, M. J., Vazquez-Figueroa, E., Woodall, N. B., Moore, J. C. & Bommarius, A. S. *Angew. Chem. Int. Ed.* **51**, 3969-3972, doi: 10.1002/anie.201107813 (2012).

25   Chen, F.-F., Liu, Y.-Y., Zheng, G.-W. & Xu, J.-H. *ChemCatChem* **7**, 3838-3841, doi:10.1002/cctc.201500785 (2015).

26   Chen, F.-F. *et al. ACS Catal.* **8**, 2622-2628, doi:10.1021/acscatal.7b04135 (2018).

27   Abrahamson, M. J., Wong, J. W. & Bommarius, A. S. *Adv. Synth. Catal.* **355**, 1780-1786, doi: 10.1002/adsc.201201030 (2013).

28   Ye, L. J. *et al. ACS Catal.* **5**, 1119-1122, doi:10.1021/cs501906r (2015).

29   Pushpanath, A., Siirola, E., Bornadel, A., Woodlock, D. & Schell, U. *ACS Catal.* **7**, 3204-3209, doi:10.1021/acscatal.7b00516 (2017).

30   Mayol, O. *et al. Catal. Sci. Technol.* **6**, 7421-7428, doi:10.1039/c6cy01625a (2016).

31   Au, S. K., Bommarius, B. R. & Bommarius, A. S. *ACS Catal.* **4**, 4021-4026, doi: 10.1021/cs4012167 (2014).

32   Bommarius, B. R., Schürmann, M. & Bommarius, A. S. *Chem. Commun.* **50**, 14953-14955, doi: 10.1039/C4CC06527A (2014).

33   Mutti, F. G., Knaus, T., Scrutton, N. S., Breuer, M. & Turner, N. J. *Science* **349**, 1525-1529, doi:10.1126/science.aac9283 (2015).

34   Knaus, T., Böhmer, W. & Mutti, F. G. *Green Chem.* **19**, 453-463, doi:10.1039/c6gc01987k (2017).

35   Liu, J., Pang, B. Q. W., Adams, J. P., Snajdrova, R. & Li, Z. *ChemCatChem* **9**, 425-431, doi:10.1002/cctc.201601446 (2017).

36   Knaus, T., Cariati, L., Masman, M. F. & Mutti, F. G. *Org. Biomol. Chem.* **15**, 8313-8325, doi:10.1039/c7ob01927k (2017).

37   Ren, H. *et al. J. Biotechnol.* **241**, 33-41, doi:10.1016/j.jbiotec.2016.11.006 (2017).

38   Thompson, M. P. & Turner, N. J. *ChemCatChem* **9**, 3833-3836, doi:10.1002/cctc.201701092 (2017).

39   Bohmer, W., Knaus, T. & Mutti, F. G. *ChemCatChem* **10**, 731-735, doi:10.1002/cctc.201701366 (2018).

40   Lowe, J., Ingram, A. A. & Groger, H. *Bioorg. Med. Chem.* **26**, 1387-1392, doi:10.1016/j.bmc.2017.12.005 (2018).

41   Schrittwieser, J. H., Velikogne, S. & Kroutil, W. *Adv. Synth. Catal.* **357**, 1655-1685, doi:10.1002/adsc.201500213 (2015).

42   Sharma, M., Mangas-Sanchez, J., Turner, N. J. & Grogan, G. *Adv. Synth. Catal.* **359**, 2011-2025, doi:10.1002/adsc.201700356 (2017).

43   Scheller, P. N., Lenz, M., Hammer, S. C., Hauer, B. & Nestl, B. M. *ChemCatChem* **7**, 3239-3242, doi:10.1002/cctc.201500764 (2015).

44   Huber, T. *et al.* *ChemCatChem* **6**, 2248-2252, doi:10.1002/cctc.201402218 (2014).

45   Wetzl, D. *et al. ChemCatChem* **8**, 2023-2026, doi:10.1002/cctc.201600384 (2016).

46   Matzel, P., Gand, M. & Höhne, M. *Green Chem.* **19**, 385-389, doi:10.1039/c6gc03023h (2017).

47   Aleku, G. A. *et al. Nat. Chem.* **9**, 961-969, doi:10.1038/nchem.2782 (2017).

48   Montgomery, S. L. *et al. Angew. Chem. Int. Ed.* **56**, 10491-10494, doi:10.1002/anie.201705848 (2017).

49   France, S. P. *et al.* *ChemCatChem* **10**, 510-514, doi:10.1002/cctc.201701408 (2018).

50   Codexis-INC *et al.*, WO2013/170050 (2013).

51   Asano, Y., Yamaguchi, K. & Kondo, K. *J. Bacteriol.* **171**, 4466-4471, doi:10.1128/jb.171.8.4466-4471.1989 (1989).

52   Kato, Y., Yamada, H. & Asano, Y. *J. Mol. Catal. B: Enzym.* **1**, 151-160, doi:10.1016/1381-1177(95)00011-9 (1996).

53   K.L. Britton, Y. A., D.W. Rice. *Nat. Struct. Biol.* **5**, 593-601, doi: 10.1038/854 (1998).

54   Brunhuber, N. M. W., Thoden, J. B., Blanchard, J. S. & Vanhooke, J. L. *Biochemistry* **39**, 9174-9187, doi: 10.1021/bi000494c (2000).

55   Rowland, R. S. & Taylor, R. *J. Phys. Chem.* **100,** doi: 10.1021/jp960615b (1996).

56   Mathew, S. & Yun, H. *ACS Catal.* **2**, 993-1001, doi:10.1021/cs300116n (2012).

57   Oliveira, E. F., Cerqueira, N. M., Fernandes, P. A. & Ramos, M. J. *J. Am. Chem. Soc.* **133**, 15496-15505, doi:10.1021/ja204229m (2011).

58   Mehta, P. K., Hale, T. I. & Christen, P. *Eur. J. Biochem.* **214**, 549-561, doi:10.1111/j.1432-1033.1993.tb17953.x (1993).

59   Hwang, B.-Y., Cho, B.-K., Yun, H., Koteshwar, K. & Kim, B.-G. *J. Mol. Catal. B: Enzym.* **37**, 47-55, doi:10.1016/j.molcatb.2005.09.004 (2005).

60   Toshihisa Ohshima, K. S. *Adv. Biochem. Eng./Biotechnol.* **42**, 187-209, (1990).

61   Laskowski, R. A., MacArthur, M. W., Moss, D. S. & Thornton, J. M. *J. Appl. Crystallogr.*, 283-291, doi: 10.1107/S0021889892009944 (1993).

62   Hooft, R. W., Vriend, G., Sander, C. & Abola, E. E. *Nature* **381**, 272-272 doi: 10.1038/381272a0 (1996).

63   Baker, P. J., Turnbull, A. P., Sedelnikova, S. E., Stillman, T. J. & Rice, D. W. *Structure* **3**, 693-705, doi: 10.1016/S0969-2126(01)00204-0 (1995).

64   Zhao, Y., Wakamatsu, T., Doi, K., Sakuraba, H. & Ohshima, T. *J. Mol. Catal. B: Enzym.* **83**, 65-72, doi: 10.1016/j.molcatb.2012.06.018 (2012).

65   Vanhooke, J. L., Thoden, J. B., Brunhuber, N. M. W., Blanchard, J. S. & Holden, H. M. *Biochemistry* **38**, 2326-2339, doi: 10.1021/bi982244q (1999).

66   Jennings, W. B. & Boyd, D. R. *J. Am. Chem. Soc.* **94**, 7187-7188, doi:10.1021/ja00775a073 (1972).

67   Johnson, J. E., Morales, N. M., Gorczyca, A. M., Dolliver, D. D. & McAllister, M. A. *J. Org. Chem.* **66**, 7979-7985, doi:10.1021/jo010067k (2001).

68   Bjørgo, J., Boyd, D. R., Watson, C. G. & Jennings, W. B. *J. Chem. Soc., Perkin Trans. 2*, 757-762, doi:10.1039/p29740000757 (1974).

69   Krieger, E., Koraimann, G. & Vriend, G. *Proteins* **47**, 393-402, doi:10.1002/prot.10104 (2002).

70   Oostenbrink, C., Villa, A., Mark, A. E. & van Gunsteren, W. F. *J. Comput. Chem.* **25**, 1656-1676, doi:10.1002/jcc.20090 (2004).

71   Krieger, E., Nabuurs, S. B. & Vriend, G. *Methods Biochem. Anal.* **44**, 509-523, doi: 10.1007/springerreference_33987 (2003).

72   Venselaar, H. *et al. Eur. Biophys. J.* **39**, 551-563, doi: 10.1007/s00249-009-0531-0 (2010).

73   Altschul, S. F. *et al. Nucleic Acids Res.* **25**, 3389-3402, doi: 10.1093/nar/25.17.3389 (1997).

74   Suzek, B. E., Huang, H., McGarvey, P., Mazumder, R. & Wu, C. H. *Bioinformatics* **23**, 1282-1288, doi: 10.1093/bioinformatics/btm098 (2007).

75   Jones, D. T. *J. Mol. Biol.* **292**, 195-202, doi: 10.1006/jmbi.1999.3091 (1999).

76   Krieger, E., Darden, T., Nabuurs, S. B., Finkelstein, A. & Vriend, G. *Proteins* **57**, 678-683, doi: 10.1002/prot.20251 (2004).

77   Trott, O. & Olson, A. J. *J. Comput. Chem.* **25**, 1656-1676, doi: 10.1002/jcc.21334 (2010).

Chapter 3

Generation of amine dehydrogenases with increased catalytic performance and substrate scope from ε-deaminating *L*-lysine dehydrogenase

3.1 Abstract

Amine dehydrogenases (AmDHs) catalyse the conversion of ketones into enantiomerically pure amines at the sole expense of ammonia and hydride source. Guided by structural information from computational models, we create AmDHs that can convert pharmaceutically relevant aromatic ketones with conversions up to quantitative and perfect chemical and optical purities. These AmDHs are created from an unconventional enzyme scaffold that apparently does not operate any asymmetric transformation in its natural reaction. Additionally, the best variant (LE-AmDH-v1) displays a unique substrate-dependent switch of enantioselectivity, affording (S)- or (R)-configured amine products with up to >99.9% enantiomeric excess. These findings are explained by *in silico* studies. LE-AmDH-v1 is highly thermostable (T_m of 69 °C), retains almost entirely its catalytic activity upon incubation up to 50 °C for several days and operates preferentially at 50 °C and pH 9.0. This study also demonstrates that product inhibition can be a critical factor in AmDH-catalysed reductive amination.

3.2 Introduction

In 2007, when the Roundtable of the American Chemical Society's Green Chemistry Institute identified the most aspirational chemical transformations to challenge the pharmaceutical industry, the reductive amination of prochiral ketones with free ammonia ranked second on the list.[1] Indeed, a-chiral amines constitute approximately 40% of the optically active drugs that are currently commercialised mainly as single enantiomers.[2] These amines are classically synthesised industrially through the asymmetric hydrogenation of activated intermediates such as enamides, enamines, or pre-formed N-substituted imines;[3] however, such strategies lack efficiency because multiple chemical steps are required. Although significant progress in the asymmetric reductive amination of carbonyl-containing compounds has been recently achieved in organometallic catalysis (e.g., using Ir or Ru or Pd-based catalysts) and organocatalysis,[4] a number of enzymatic routes offer more atom-efficient approaches, particularly for the synthesis of active pharmaceutical ingredients (APIs) in enantiomerically pure forms.[5] Furthermore, the often perfect stereoselectivity of enzymes eliminates the need for recrystallization steps to upgrade the chemical purity of the enantiomer product, and there is no concern regarding the removal of traces of toxic heavy metals.

Classical industrially-applied and laboratory scale biocatalytic methods convert a-chiral racemic amines into enantiomerically pure amines via either kinetic resolution (KR) or dynamic kinetic resolution (DKR) using hydrolases,[6] or deracemisation using monoamine oxidases,[7] the latter of which also gives access to optically active secondary and tertiary amines. Although KR is limited to a theoretical maximum of 50% yield, DKR and deracemisation require an additional chemical catalyst or a stoichiometric reagent.[6,7] Emerging enzymatic methods involve the use of ammonia lyases,[8,9] Pictet-Spenglerases,[10,11] or berberine bridge enzymes,[12,13] all of which are active towards valuable types of intermediates for the synthesis of chiral amines; however, their substrate scope is

rather restricted. Direct biocatalytic amination of non-functionalized C-H bonds has been enabled by creating cytochrome P411, which requires tosyl azide as the nitrogen source;[14] however, this challenging strategy is limited to benzylic C-H amination and requires a subsequent deprotection step to remove the tosyl group. As such, asymmetric reductive amination of prochiral ketones and hydroamination of olefins are currently more atom-efficient methods for introducing an α-chiral amine moiety. However, the biocatalytic hydroamination of alkene moieties is restricted to the synthesis of α- and β-amino acids,[8,9] whereas chemocatalytic hydroaminations yield preferentially secondary and tertiary amines with non-perfect enantiomeric excess.[15] The stereoselective conversion of ketones to amines can be accomplished either by a formal reductive amination using ω-transaminases[16] or a truly reductive amination using amine dehydrogenases (AmDHs), imine reductases (IReds) or reductive aminases (RedAms).[17,18] IReds and RedAms are normally employed for the synthesis of secondary and tertiary amines,[17,18] although this property was also recently observed in some cases with AmDHs.[19] Transaminases have proven to be useful and efficient biocatalysts for the stereoselective amination of ketones in laboratory as well as industrial scale settings;[16,20,21] however, their downside is the requirement for supra-stoichiometric amounts of an amine donor and/or more enzymes and cofactors.[16,20-22] In this context, the AmDH-FDH system enables the efficient reductive amination of prochiral ketones (i.e., TONs > 10^3) while requiring only HCOONH$_4$ buffer and catalytic NAD(H).[23] A natural AmDH activity on aliphatic substrates was reported about two decades ago; however, the gene was never identified.[24] Native AmDHs were very recently identified for the reductive amination of aliphatic ketones with (*S*)-stereoselectivity using a genome-mining approach.[25,26] Conversely, known engineered AmDHs have been obtained starting exclusively from *L*-amino acid dehydrogenases (deaminating at the α-amino group) and by mutating the same highly conserved amino acid residues in the active site (i.e., lysine and aspartate).[27-31]

Other AmDHs have been produced either by domain-shuffling or introducing further mutations into these first generation variants.[32,33]

Accordingly, the diversity of substrate scope and activity among these AmDHs is poor because they were engineered from very similar scaffolds and following an identical strategy. For instance, all of the known AmDHs—whether native or engineered enzymes—exhibit mediocre or no activity towards the amination of acetophenones, tetralones, and chromanones, the related enantiomerically pure amines of which are recurrent motives in many pharmaceuticals such as Sertraline, Norsertraline, Rotigotine, Rivastigmine, and Cinacalcet, among others.[3]

Herein, we show that AmDHs can be engineered from a wild-type enzyme that apparently does not operate any asymmetric transformation. This property is revealed for an ε-deaminating L-lysine dehydrogenase from *Geobacillus stearothermophilus* (LysEDH), and it is exploited for the creation of AmDHs that perform the reductive amination of pharmaceutically relevant prochiral ketones with perfect stereo- and chemo-selectivity.

3.3 Results and Discussion

3.3.1 Molecular modelling and preliminary activity studies

The wild-type LysEDH catalyzes the (formally) irreversible oxidative deamination of the ε-amino group of *L*-lysine (**1b**, **Figure 1a, Scheme 1** group B).[34] This apparent irreversibility stems from the subsequent spontaneous cyclization of the ω-oxo amino acid product (**1a**). However, the reverse reaction must be possible if substrates devoid of the a-amine moiety (e.g., 6-oxo hexanoic acid) could be accepted by LysEDH (**2a**, **Scheme 1** group A). Initial experiments on the reductive amination of **2a** (10 mM) in $HCOONH_4/NH_3$ (2 M, pH 9.0) revealed that LysEDH (90 µM) catalyses this reaction (44% analytical yield). The experiment was conducted in the presence of formate dehydrogenase (Cb-FDH) for NADH recycling (**Figure 2a**) as described in methods section.[23,35] Under the same conditions, substrates devoid of the ω-carboxyl moiety such as hexanal (**23a**), heptanal (**24a**), 2-heptanone (**5a**), 2-octanone (**25a**), acetophenone (**8a**), and a-chromanone (**13a**) were not converted (**Scheme 1**) Thus, the a-amino group (i.e., present in *L*-lysine) is not essential for productive substrate binding and amination catalysed by LysEDH, whereas the a-carboxyl group is crucial. These findings motivated us to undertake a structural examination of the active site architecture of LysEDH. Due to the lack of a crystal structure of LysEDH, a homology model was created based on published homologous structures (**Table 1**). After several rounds of homology modelling, in silico modifications, and energy minimisation followed by molecular dynamic refinement, the model of LysEDH was obtained with both coenzyme (NADH) and ligand **1c** bound in the active site in the reactive pose (**Figure 1b**).
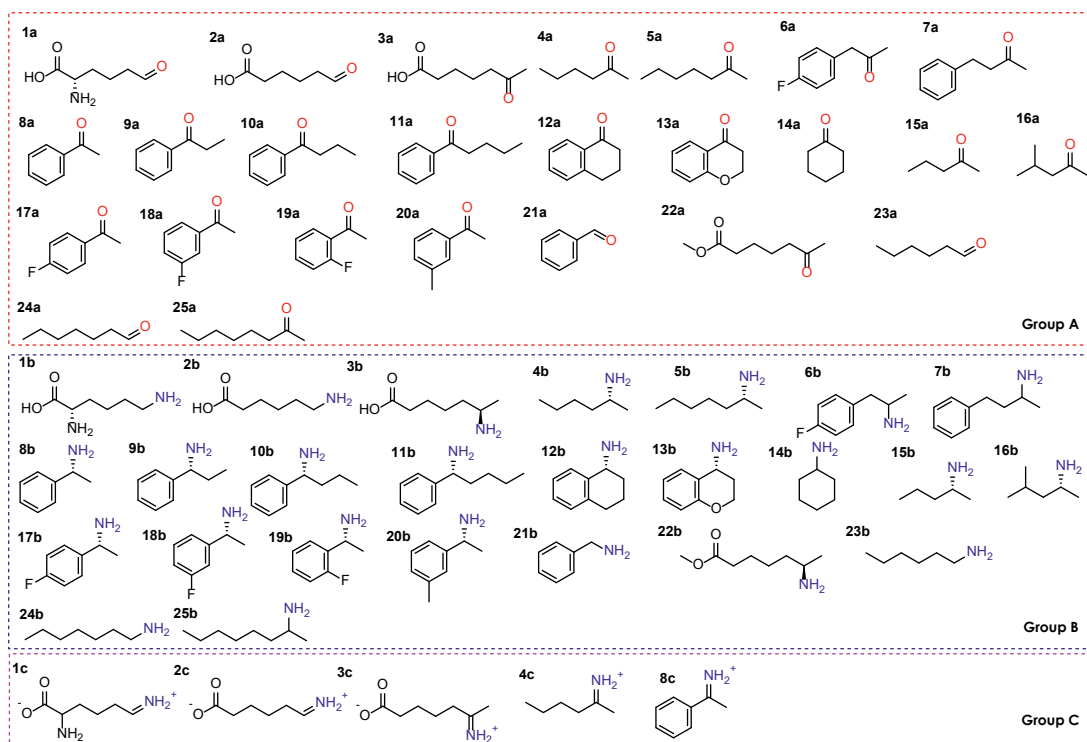
Scheme 1 List of compounds used in this study. Group A: pro-chiral ketones and aldehydes; Group B: products obtained and group C: list of iminium intermediates used for computational simulations

Our analysis of the model identified seven amino acid residues as potential targets for mutagenesis, which can be classified into two categories based on their role in the binding pocket (**Figure 1b**). Group one encompasses residues that are appointed in the binding of the a-amino and a-carboxylic groups of **1b**, namely H181, Y238, and T240 and R242, respectively. These residues create a hydrophilic cavity that accommodates the hydrophilic a-amino acid moiety of **1b**. On the opposite side, residues F173, V172, and V130 create a hindered hydrophobic environment that forces the substrate into its ideal reactive pose and prevents its rotation. In fact, in our model, the distance between the departing hydride of NADH and the pro-chiral carbon of the imine intermediate **1c** is 2.7 Å, which is below the sum of the van der Waals' radii of carbon and hydrogen atoms. Since F173 is the bulkiest hydrophobic residue, we envisioned

that its mutation into a less bulky residue such as alanine or glycine would retain the overall hydrophobic properties of the cavity while also permitting the binding of bulkier substrates in different orientations. Hence, ketones might be accepted besides simpler aldehydes.

Table 1. Homology models of the wild-type LysEDH. The full amino acid sequence was explored. The multimeric state, the selected templates, the excluded templates, and the number of models generated per run are shown. The template that was selected as main contributor to the hybrid model is demarked in bold font. Moreover, the accuracy of the generated models is reported by the use of Z-scores[36,37]. The overall Z-scores for all models have been calculated as the weighted averages of the individual Z-scores (Dihedrals, Packing 1D, and Packing 3D) using the equation described in experimental section

Model	Multimeric state	Templates	Excluded templates	Cofactor	Ligand	Number of models	Overall Z-score (Quality)[a]	Overall Z-score (Quality)[b]
0	dimer	3ABI[38], 2AXQ[39], **4INA**[c], 1E5Q[40], 4RL6[c]	None	NO	NO	25	-1.564 (Satisfactory)	N.d
1	dimer	1E5Q[40], **3ABI[38]**, 2AXQ[39], 3IC5[c], 3WYE[c]	4INA[c], 4RL6[c]	NADH	NO	21	-1.321 (Satisfactory)	N.d
2	monomer	1E5Q[40], **3ABI[38]**, 2AXQ[39],	4INA[c], 4RL6[c]	NADH	NO	15	-1.161 (Satisfactory)	-1.11 (Satisfactory)
2.1	monomer	N.a	N.a	NADH	**1c**	N.a	N.a	-1.14 (Satisfactory)
2.2	monomer	N.a	N.a	NADH	**2c**	N.a	N.a	-1.18 (Satisfactory)

[a].Z-score and quality of the model after hybrid model generation.
[b].Z-score and quality of the model after molecular dynamic refinement.
[c].Crystal structure not yet associated to a publication. Please visit the www.pdb.org website for more information.
N.d: Not determined
N.a: Not applicable
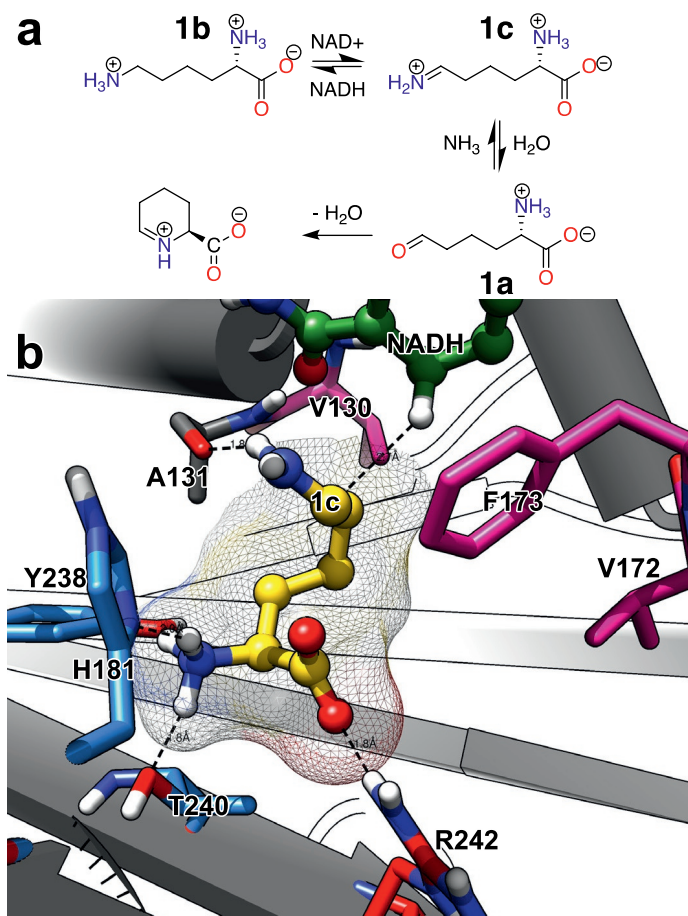
Figure 1 Model of the active site of the ε-deaminating lysine dehydrogenase from *G. stearothermophilus*. (**a**) Schematic representation of the reactions undergone by the natural substrate **1b**. (**b**) Model of the active site containing its natural substrate **1c**. Residues H181, Y238, and T240 (in cyan) appear to stabilize the alpha NH_3^+ group, whereas R242 appears to interact with the COO^- of the substrate. Residues V172, F173, and V130 create a hindered hydrophobic environment. All highlighted residues are amenable targets for protein engineering studies.

As mentioned above, the wild-type LysEDH converted **2a** to **2b** with 44% analytical yield. As **2b** is a terminal (achiral) amine product, information on the reaction's stereoselectivity was not attainable; however, the reductive amination of **3a** as substrate (i.e., the structurally related methyl-ketone of **2a**) would result in an a-chiral amine. Since according to our model, the hydride of

NADH must be transferred towards the *Si*-face of the prochiral carbonyl moiety, this experiment would reveal a possible stereoselectivity of LysEDH in the conversion of **3a**. Indeed, **3b** was produced in an enantiomerically pure *S*-configuration (**3a** 50 mM; LysEDH 90 μM; *ee* >99%) and with 90% analytical yield. When LysEDH F173A (herein referred as LE-AmDH-v1) was tested under the same conditions, **3a** was aminated with >99% analytical yield and high stereoselectivity (*ee* >99% *S*, **Table 4**). Moreover, preparative scale production of **3b** starting from **3a** (150 mg, 1.040 mmol), which aimed at identifying the product's absolute configuration, resulted in 73% isolated yield with *ee* >99% *S* after GC analysis of the corresponding methyl ester (**22b**) (**Scheme 2** and **Methods**).
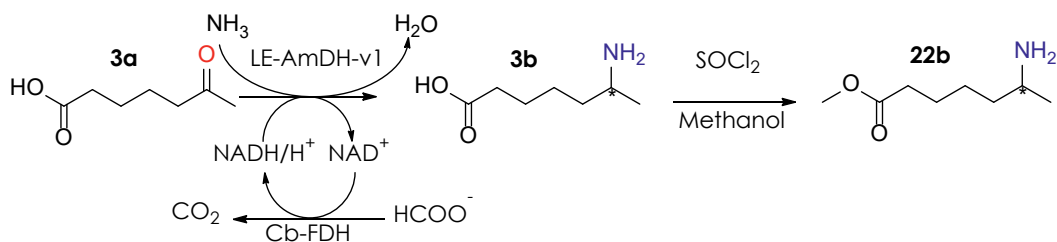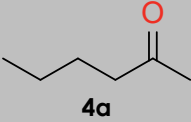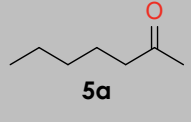
Scheme 2. Schematic representation of the chemoenzymatic synthesis of 22b
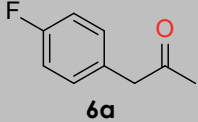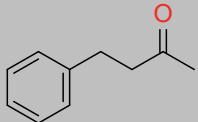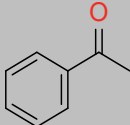
3.3.2 Asymmetric synthesis of amines catalysed by LysEDH variants
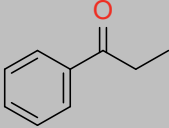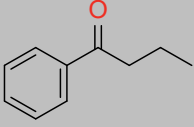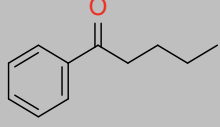
The mutation F173A in the wild-type LysEDH created an additional large hydrophobic binding pocket in the active site, which might favour the binding of aromatic substrates such as **8a**. Analysis of our LysEDH model also evidenced that residues V172, V130 and R242 might be suitable targets for mutagenesis (**Figure 1b**). Therefore, a focused library of 14 variants (LE-AmDH-v1 to v14, **Figure 2d**) was created and screened against a number of aliphatic and aromatic ketones (**Figure 2b, Table 2**) in $HCOONH_4/NH_3$ buffer (pH 9.0, 2 M) using LE-AmDH variants (90 μM), Cb-FDH (19 μM), NAD^+ (1 mM) for 48 h at 30 °C. The screening outcome is summarised in **Figure 2c** (with further details in **Table 2**). Notably, in a large majority of cases, the amine product was obtained in enantiomerically pure form
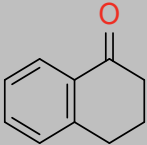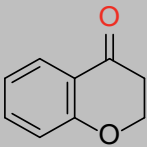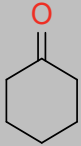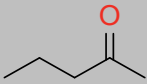
(*ee* >99%), albeit with the opposite configuration (*R*) than that observed for the natural binding mode of *L*-lysine (pro-*S*).
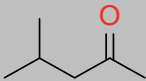
Table 2. Biocatalytic reductive amination reactions performed in this study.

Substrate	*LE-AmDH*	Recovered substrate	Amine	Imine intermediate	Alcohol	Amine
10 mM	**90 µM**	**(%)**		**Conv. (%)ᵃ**		**ee**
	v1	22	78	n.d.	n.d.	>99%
	v2	100	n.d.	n.d.	n.d.	-
	v3	100	n.d.	n.d.	n.d.	-
	v4	100	n.d.	n.d.	n.d.	-
	v5	100	n.d.	n.d.	n.d.	-
	v6	100	n.d.	n.d.	n.d.	-
	v7	100	n.d.	n.d.	n.d.	-
4a	v8	100	n.d.	n.d.	n.d.	-
	v9	100	n.d.	n.d.	n.d.	-
	v10	100	n.d.	n.d.	n.d.	-
	v11	100	n.d.	n.d.	n.d.	-
	v12	37	64	n.d.	n.d.	83%
	v13	100	n.d.	n.d.	n.d.	-
	v14	100	n.d.	n.d.	n.d.	-
	v1	90	10	n.d.	n.d.	>99%
	v2	100	n.d.	n.d.	n.d.	-
	v3	100	n.d.	n.d.	n.d.	-
	v4	100	n.d.	n.d.	n.d.	-
	v5	100	n.d.	n.d.	n.d.	-
	v6	100	n.d.	n.d.	n.d.	-
	v7	100	n.d.	n.d.	n.d.	-
	v8	100	n.d.	n.d.	n.d.	-
	v9	100	n.d.	n.d.	n.d.	-
5a	v10	100	n.d.	n.d.	n.d.	-
	v11	98	2	n.d.	n.d.	*N.m.*
	v12	89	11	n.d.	n.d.	>99%
	v13	100	n.d.	n.d.	n.d.	-
	v14	100	n.d.	n.d.	n.d.	-
	v1	100	n.d.	n.d.	n.d.	-
	v2	100	n.d.	n.d.	n.d.	-
	v3	100	n.d.	n.d.	n.d.	-
	v4	100	n.d.	n.d.	n.d.	-
	v5	100	n.d.	n.d.	n.d.	-
	v6	100	n.d.	n.d.	n.d.	-

Substrate	*LE-AmDH*	Recovered substrate	Amine	Imine intermediate	Alcohol	Amine
6a (F-phenyl acetone)	v7	100	n.d.	n.d.	n.d.	-
	v8	100	n.d.	n.d.	n.d.	-
	v9	100	n.d.	n.d.	n.d.	-
	v10	100	n.d.	n.d.	n.d.	-
	v11	100	n.d.	n.d.	n.d.	-
	v12	100	n.d.	n.d.	n.d.	-
	v13	100	n.d.	n.d.	n.d.	-
	v14	100	n.d.	n.d.	n.d.	-
7a	v1	100	n.d.	n.d.	n.d.	-
	v2	100	n.d.	n.d.	n.d.	-
	v3	100	n.d.	n.d.	n.d.	-
	v4	100	n.d.	n.d.	n.d.	-
	v5	100	n.d.	n.d.	n.d.	-
	v6	100	n.d.	n.d.	n.d.	-
	v7	100	n.d.	n.d.	n.d.	-
	v8	100	n.d.	n.d.	n.d.	-
	v9	100	n.d.	n.d.	n.d.	-
	v10	100	n.d.	n.d.	n.d.	-
	v11	>99	<1	n.d.	n.d.	-
	v12	99	1	n.d.	n.d.	-
	v13	100	n.d.	n.d.	n.d.	-
	v14	100	n.d.	n.d.	n.d.	-
8a (acetophenone)	v1	2	98	n.d.	n.d.	>99%
	v2	70	30	n.d.	n.d.	-
	v3	90	10	n.d.	n.d.	-
	v4	100	n.d.	n.d.	n.d.	-
	v5	88	12	n.d.	n.d.	-
	v6	77	23	n.d.	n.d.	-
	v7	94[c]	6[c]	n.d.	n.d.	-
	v8	>99[c]	<1[c]	n.d.	n.d.	-
	v9	100	n.d.	n.d.	n.d.	-
	v10	100	n.d.	n.d.	n.d.	-
	v11	26	74	n.d.	n.d.	>99%
	v12	6	9	n.d.	n.d.	>99%
	v13	62	38	n.d.	n.d.	>99%
	v14	100	n.d.	n.d.	n.d.	-
	v1	11	89	n.d.	n.d.	>99%
	v2	73	27	n.d.	n.d.	-
	v3	92	8	n.d.	n.d.	-
	v4	100	n.d.	n.d.	n.d.	-
	v5	86	14	n.d.	n.d.	-

Substrate	*LE-AmDH*	Recovered substrate	Amine	Imine intermediate	Alcohol	Amine
9a	v6	82	18	n.d.	n.d.	-
	v7	81	19	n.d.	n.d.	>99%
	v8	100	n.d.	n.d.	n.d.	-
	v9	100	n.d.	n.d.	n.d.	-
	v10	100	n.d.	n.d.	n.d.	-
	v11	35	65	n.d.	n.d.	>99%
	v12	22	78	n.d.	n.d.	>99%
	v13	59	41	n.d.	n.d.	>99%
	v14	100	n.d.	n.d.	n.d.	-
10a	v1	59	41	n.d.	n.d.	>99%
	v2	81	19	n.d.	n.d.	-
	v3	93	7	n.d.	n.d.	-
	v4	n.d.	n.d.	n.d.	n.d.	-
	v5	89	11	n.d.	n.d.	-
	v6	50	6	n.d.	n.d.	-
	v9	100	n.d.	n.d.	n.d.	-
	v10	100	n.d.	n.d.	n.d.	-
	v11	59	41	n.d.	n.d.	>99%
	v12	52	48	n.d.	n.d.	>99%
	v13	62	38	n.d.	n.d.	>99%
	v14	100	n.d.	n.d.	n.d.	-
11a	v1	80	20	n.d.	n.d.	*(R)*[b]
	v2	97	3	n.d.	n.d.	-
	v3	100	n.d.	n.d.	n.d.	-
	v4	100	n.d.	n.d.	n.d.	-
	v5	100	n.d.	n.d.	n.d.	-
	v6	100	n.d.	n.d.	n.d.	-
	v9	100	n.d.	n.d.	n.d.	-
	v10	100	n.d.	n.d.	n.d.	-
	v11	81	19	n.d.	n.d.	*(R)*[b]
	v12	100	n.d.	n.d.	n.d.	-
	v13	100	n.d.	n.d.	n.d.	-
	v14	100	n.d.	n.d.	n.d.	-
	v1	39	61	n.d.	n.d.	>99%
	v2	100	n.d.	n.d.	n.d.	-
	v3	100	n.d.	n.d.	n.d.	-
	v4	100	n.d.	n.d.	n.d.	-
	v5	100	n.d.	n.d.	n.d.	-
	v6	100	n.d.	n.d.	n.d.	-
	v7	>99	<1	n.d.	n.d.	-
	v8	100	n.d.	n.d.	n.d.	-

Substrate	*LE-AmDH*	Recovered substrate	Amine	Imine intermediate	Alcohol	Amine
12a	v9	100	n.d.	n.d.	n.d.	-
	v10	100	n.d.	n.d.	n.d.	-
	v11	92	8	n.d.	n.d.	>99%
	v12	66	34	n.d.	n.d.	>99%
	v13	100	n.d.	n.d.	n.d.	-
	v14	97	3	n.d.	n.d.	>99%
13a	v1	30	70	n.d.	n.d.	>99%
	v2	96	4	n.d.	n.d.	-.
	v3	100	n.d.	n.d.	n.d.	-
	v4	100	n.d.	n.d.	n.d.	-
	v5	100	n.d.	n.d.	n.d.	-
	v6	100	n.d.	n.d.	n.d.	-
	v7	100	n.d.	n.d.	n.d.	-
	v8	100	n.d.	n.d.	n.d.	-
	v9	100	n.d.	n.d.	n.d.	-
	v10	100	n.d.	n.d.	n.d.	-
	v11	64	36	n.d.	n.d.	>99%
	v12	64	36	n.d.	n.d.	>99%
	v13	85	15	n.d.	n.d.	>99%
	v14	100	n.d.	n.d.	n.d.	-
14a	v1	49	51	n.d.	n.d.	*N.a.*
	v3	100	n.d.	n.d.	n.d.	*N.a.*
	v4	100	n.d.	n.d.	n.d.	*N.a.*
	v5	100	n.d.	n.d.	n.d.	*N.a.*
	v6	100	n.d.	n.d.	n.d.	*N.a.*
	v7	100	n.d.	n.d.	n.d.	*N.a.*
	v8	100	n.d.	n.d.	n.d.	*N.a.*
	v9	100	n.d.	n.d.	n.d.	*N.a.*
	v10	100	n.d.	n.d.	n.d.	*N.a.*
	v11	96	4	n.d.	n.d.	*N.a.*
	v12	70	30	n.d.	n.d.	*N.a.*
	v13	100	n.d.	n.d.	n.d.	*N.a.*
	v14	100	n.d.	n.d.	n.d.	*N.a.*
15a	v1	63	26	n.d.	n.d.	89%
	v2	100	n.d.	n.d.	n.d.	-
	v3	100	n.d.	n.d.	n.d.	-
	v4	100	n.d.	n.d.	n.d.	-
	v5	100	n.d.	n.d.	n.d.	-
	v6	100	n.d.	n.d.	n.d.	-
	v7	100	n.d.	n.d.	n.d.	-
	v8	100	n.d.	n.d.	n.d.	-

Substrate	*LE-AmDH*	Recovered substrate	Amine	Imine intermediate	Alcohol	Amine
	v9	100	n.d.	n.d.	n.d.	-
	v10	100	n.d.	n.d.	n.d.	-
	v11	24	2	n.d.	n.d.	-
	v12	58	42	n.d.	n.d.	*77%*
	v13	100	n.d.	n.d.	n.d.	-
	v14	100	n.d.	n.d.	n.d.	-
	v1	42	58	n.d.	n.d.	*97%*
	v2	100	n.d.	n.d.	n.d.	-
	v3	100	n.d.	n.d.	n.d.	-
	v4	100	n.d.	n.d.	n.d.	-
	v5	100	n.d.	n.d.	n.d.	-
16a	v6	100	n.d.	n.d.	n.d.	-
	v7	100	n.d.	n.d.	n.d.	-
	v8	100	n.d.	n.d.	n.d.	-
	v9	100	n.d.	n.d.	n.d.	-
	v10	100	n.d.	n.d.	n.d.	-
	v11	95	5	n.d.	n.d.	n.m.
	v12	62	38	n.d.	n.d.	>99%
	v13	100	n.d.	n.d.	n.d.	-
	v14	100	n.d.	n.d.	n.d.	-

[a] Conversions were determined using a 7890A GC system (Agilent Technologies), equipped with FID detector using H_2 as carrier gas with a DB-1701 column from Agilent (30 m, 250 µm, 0.25 µm)

[b] Unable to determine the ee due to partially overlap of the enantiomers with the method used

[c] Determined by GC-MS

n.d: Not determined

n.a: Not applicable

n.m: Not measured

The mutation F173G (v2) resulted in a significant loss of activity compared to the beneficial F173A (v1). Compared with LE-AmDH-v1, LE-AmDH-v2 showed an approximately three-fold decrease of conversion values for the amination of **8a** and **9a** and a two-fold decrease for the amination of **10a**. Moreover, LE-AmDH-v2 did not convert **4a**, **5a**, **12a**, **15a** and **16a** into the corresponding amines, whereas LE-AmDH-v1 yielded respectively 78%, 10%, 61%, 26%, and 58% conversion for the same substrates (**Table 2**). All variants bearing the mutation

F173G (LE-AmDH-v2, v3 and v4) generally showed very low levels of activity towards the tested substrates, thus indicating that an increase of flexibility in the active site is detrimental. Substitution of the neighbouring V172 either to alanine or glycine while maintaining the beneficial F173A mutation (LE-AmDH-v5 and v6) provoked a dramatic reduction of catalytic activity. Interestingly, the residue R242 appears to be involved in the binding of the a-carboxylic group of *L*-lysine and it is located at the entrance of the active site in a region that is exposed to an aqueous environment. To investigate if R242 regulates accessibility of substrates to the active site, we also created the variants R242M (v14), R242M/F173A (v7), R242M/F173V (v13), and R242W/F173A (v8). LE-AmDH-v7 converted substrates **8a** (6%) and **9a** (19%, *ee* >99% *R*), whereas LE-AmDH-v13 converted **8-10a** and **13a** (38%, 41%, 8%, 15% conversions, *ee* >99% *R,* **Table 2**)**,** thus indicating that increasing the hydrophobicity of the binding pocket at this site, with minimal conformational rearrangement, reduces enzyme activity.

Finally, we investigated if the mutation of V130, which is located on the opposite face of F173A, to a less bulky hydrophobic amino acid residue such as alanine or glycine, would enable a different binding mode for the substrate. LE-AmDH-v1 (F173A) was combined with mutations V130A or V130G to generate LE-AmDH-v11 and v12. LE-AmDH-v11 exhibited a significant level of activity towards **8a** (74% conversion) and **9a** (65% conversion), and all amine products (**8-13b**) were obtained in enantiomerically pure form (*ee* >99% *R*). LE-AmDH-v12 was also stereospecific (*ee* >99% *R*) for the amination of **9a** (78% conversion) and other ketones (**8-9a, 12-13a, 16a**, **Table 2**). Nonetheless, LE-AmDH-v12 also aminated **4a** and **15a** (64% and 42% conversion), albeit with imperfect stereoselectivity (*ee* 83% *R* and 77% *R*). These results indicate that a productive pro-(*S*) binding pose was generated in these two reactions in addition to the favoured pro-(*R*). Architectural modulation of the active site by testing the F173V mutation generated inactive variants (LE-AmDH-v9 and v10). **Figure 2c** shows that the best variant for the reductive amination of the target aromatic ketones

turned out to be LE-AmDH-v1. Accordingly, further studies in this work were conducted with that AmDH.
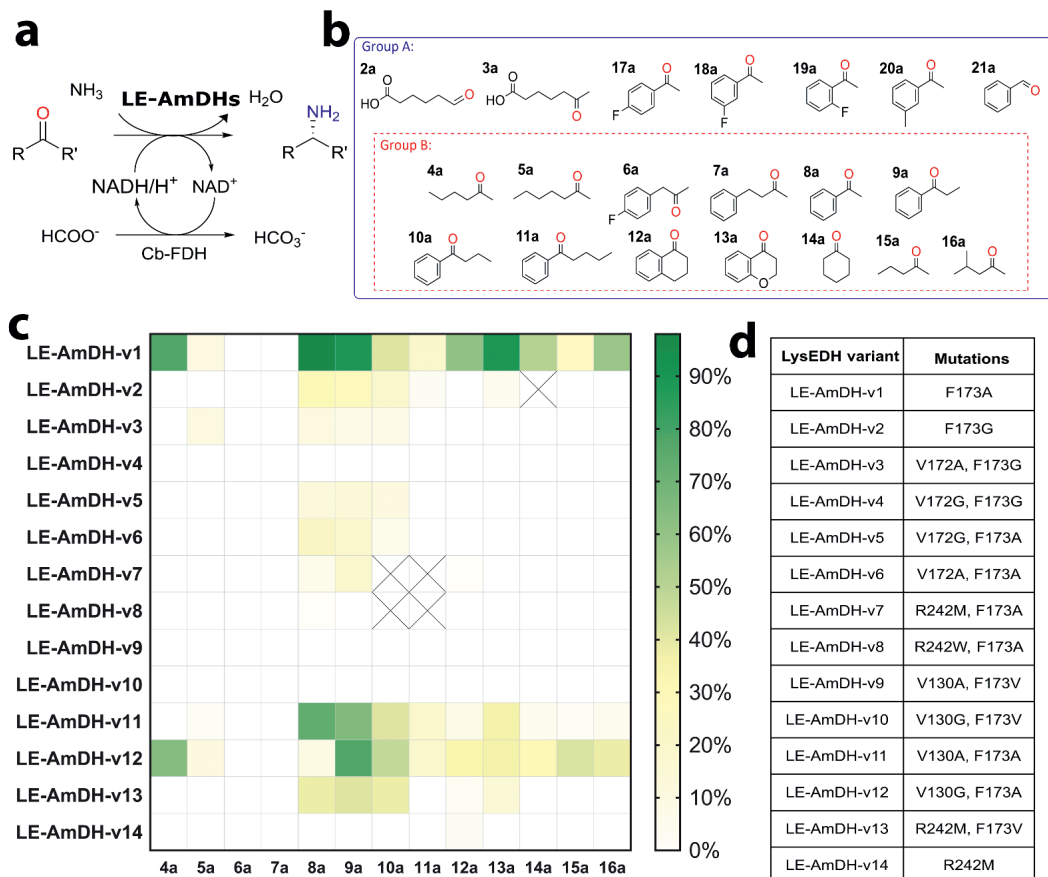
Figure 2. Initial screening with LE-AmDH variants. (**a**) General scheme of the biocatalytic reductive amination performed by LE-AmDH variants. A catalytic amount of NAD⁺ (1 mM) was applied. The reducing equivalents as well as the nitrogen source originated from the buffer of the reaction: HCOONH₄/NH₃ (pH 9.0, 2 M). The substrate concentration was 10 mM. AmDH and Cb-FDH were used in final concentrations of 90 µM and 19 µM, respectively. Reaction volume: 0.5 mL; reaction time: 48 h; temperature: 30 °C; agitation on an orbital shaker at 170 rpm. (**b**) Group B: substrates used for screening of the LysEDH variants reported here. Group A: additional substrates tested with LE-AmDH-v1. (**c**) Heatmap of the screening outcome, in which Group B substrates were tested to reduce screening effort (results expressed in conversion). (**d**) List of mutations introduced in the LysEDH scaffold.

3.3.3 Thermal stability of LE-AmDH-v1

The thermal robustness of LE-AmDH-v1 motivated us to determine its thermostability data at different pH values using $HCOONH_4/NH_3$ buffer (2 M, pH 7.0-9.5) in the presence as well as absence of ligand **8a** and coenzyme (NADH). In all cases, the T_m was found to be 66-67 °C, which indicates no influence of pH in the thermal stability of LE-AmDH-v1 (**Table 3**). Notably, T_m was increased to 69 °C when NADH was present in the mixture. All of these data align with the thermal stability profile of the wild-type LysEDH,[34] thus indicating that the mutation F173A did not affect the stability of LE-AmDH-v1.

Table 3. Melting temperature Tm of LE-AmDH-v1 at different pH values. Error bars represent the standard deviation from three independent experiments.

	T_m (°C)		
buffer		**+ 8a**	**+ NAD+**
2 M HCOONH₄/NH₃ pH 7.5	66 ± <1	N.m.	N.m.
2 M HCOONH₄/NH₃ pH 8.0	67 ± <1	N.m.	N.m.
2 M HCOONH₄/NH₃ pH 8.5	67 ± <1	N.m.	N.m.
2 M HCOONH₄/NH₃ pH 9.0	67± <1	67 ± <1	69 ± <1
2 M HCOONH₄/NH₃ pH 9.5	66 ± <1	N.m.	N.m.

Finally, the long-term stability of LE-AmDH-v1 was tested in $HCOONH_4/NH_3$ (2 M) buffer at pH 9.0 at different temperatures and using various batches of enzyme for a maximum of 7 days (**Figure 3**). Remarkably, no loss of activity was observed within this time period for samples incubated at 4 °C and at room temperature. Samples incubated at 40 °C exhibited a consistent residual activity between 80% and 90% after 7 days, whereas samples incubated at 50 °C showed an average residual activity of ca. 60% and a maximum residual activity of 80% after 7 days. Notably, the sample incubated at 60 °C (close to the T_m) still showed a residual

activity of ca. 50% after 7 days. These data further support the real applicability of LE-AmDH-v1 in organic synthesis.
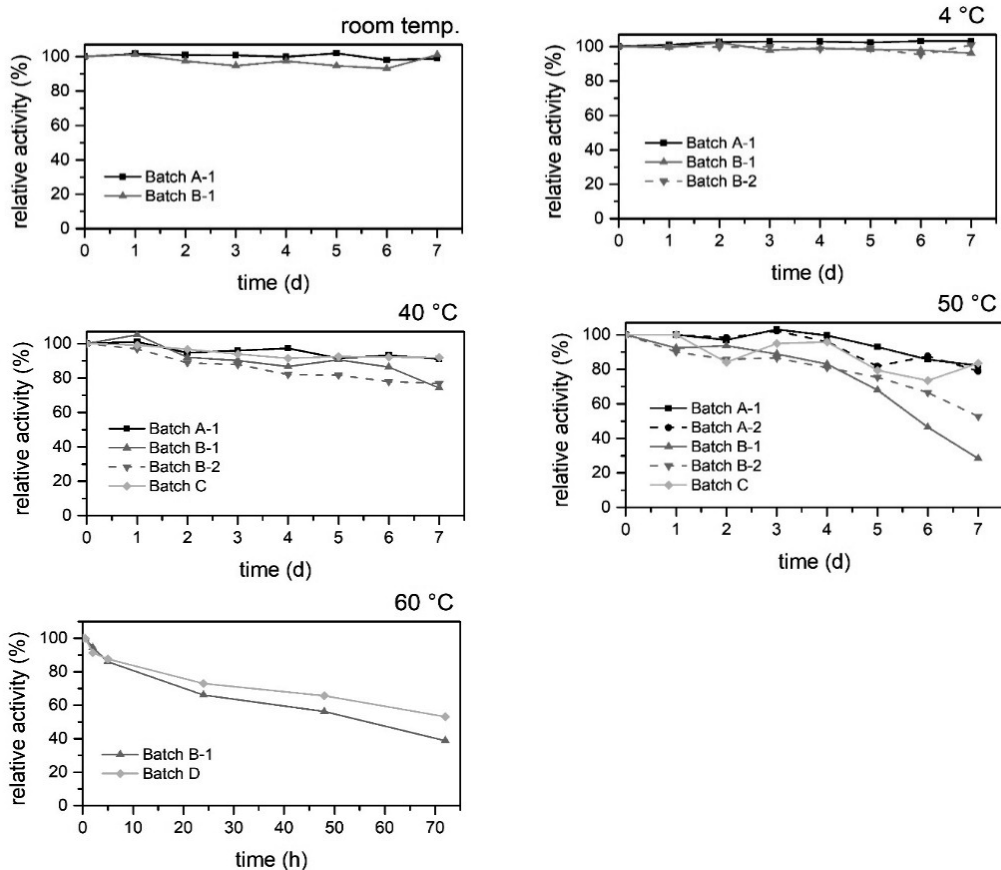
Figure 3. Long-term stability studies of LE-AmDH-v1. In each assay, the residual enzyme activity after incubation of the enzyme at different times (up to 7 days) and temperatures (4 °C, room temp., 40 °C, 50 °C and 60 °C, respectively) was determined at 60 °C by following the oxidation of NADH (250 µM) at 360 nm (ε = 4250 M^{-1} cm^{-1}) using a Shimadzu UV-1800 UV-vis spectrophotometer

3.3.4 Biocatalytic optimization studies on LE-AmDH-v1

The temperature dependence and influence of the pH value were investigated for the reductive amination catalysed by LE-AmDH-v1 using **8a** as test substrate. As it originates from the thermophile bacterium *Geobacillus stearothermophilus*, the wild-type LysEDH displays high stability and activity at elevated temperatures.[34] The same features were observed for the LE-AmDH-v1 variant.

Figure 4a shows that conversions of **8a** were above 90% after 16 h for reactions performed in the range of 30-60 °C. Remarkably, at 50 °C and 60 °C, conversions were found to already be 80% and 90%, respectively, after the first 4 h. Conversely, the conversion at 20 °C did not exceed 90% even after 32 h. A subsequent evaluation of the influence of buffers (HCOONH$_4$/NH$_3$ 2 M) at different pH values revealed the highest conversions at pH 9.0–9.5 (**Figure 4b**).

3.3.5 Substrate scope of LE-AmDH-v1

LE-AmDH-v1 exhibited a significantly extended and complementary substrate scope for aromatic substrates compared with the currently available AmDHs (**Table 4**). Specifically, Rs-AmDH, Bb-AmDH, and Cal-AmDH can efficiently aminate 4-phenylbutan-2-one (and derivatives) and/or phenylacetone (and derivatives),[23,28,29,31] whereas other AmDHs such as Ch1-AmDH, LeuDH, AmDH4, MsmeAmDH, MicroAmDH, CfusAmDH and EsLeuDH enzymes exhibit particularly high activity towards aliphatic substrates.[23,25,27,30,33,41] In contrast, elevated biocatalyst loading of the previously described Ch1-AmDH (130 µM) poorly aminated a 50 mM solution of **8a** (34% conversion), derivatives thereof (**17-20a**, 9-43% conversion), and **9a** (8% conversion) within 48 h.[23] Bulky-bulky ketones such as **10a** and **11a** were not accepted at all by Ch1-AmDH.[23] In another case, an elevated concentration of an AmDH engineered from *Exigobacterium sibiricum* (EsLeuDH, 1.45 mM; concentration calculated from a reportedly amount of 10 U mL^{-1}, activity of 0.17 U mg$_{enzyme}$$^{-1}$ and MW$_{enzyme}$ 40.5 kDa) was necessary to reach ca. 80% conversion of **8a** in 100 h.[42] In contrast, LE-AmDH-v1 (90 µM) converted the above-mentioned acetophenone and derivatives thereof (**8a** and **17-20a**, 50 mM) with conversions up to 98% within 48 h (**Table 4**). Propiophenone (**9a**) was accepted (50 mM, 95% conversion), as well as the more bulky substrates **10a** (50 mM, 65%) and **11a** (50 mM, 26%). Moreover, neither Ch1-AmDH[23,32] nor other previously reported AmDHs (e.g., Cal-AmDH)[23,25,27-31,33,41] are capable of aminating either a-tetralone (**12a**) or a-chromanone (**13a**) to any synthetically useful extent. In contrast, LE-AmDH-v1 exhibited conversions above 50% for the

amination of these substrates (50 mM, **Table 4**). Additionally, LE-AmDH-v1 proved to be a versatile biocatalyst, such that aliphatic ketones (**4a**, **14-16a**, 50 mM) were also accepted (53-84% conversion) and benzaldehyde (**21a**, 50 mM) was quantitatively aminated. Lastly, LE-AmDH-v1 is a high stereoselective catalyst that produces either (*S*)-configured ω-amino acid **3a** or (*R*)-configured a-chiral amines in elevated enantiomeric excess (**Table 4**).

Table 4. **Reductive amination of a panel of ketones employing LE-AmDH-v1.** Reaction conditions: substrate (10 mM or 50 mM), LE-AmDH-v1 (90 µM), Cb-FDH (19 µM), NAD$^+$ (1 mM), HCOONH$_4$/NH$_3$ buffer (2 M, pH 9.0), T 50 °C, agitation orbital shaker 170 rpm, reaction time 48 h. n.d.: could not be determined; n.a.: not applicable.

Substrate	10 mM (Conv. %)	50 mM (Conv. %)	ee (%)[a]
2a	>99	>99	n.a.
3a	>99	>99	>99 (*S*)[b]
4a	87	71	99 (*R*)
8a	>99	98	>99.9 (*R*)[b]
9a	98	95	>99.9 (*R*)[b]
10a	87	65	99.8 (*R*)
11a	36	26	n.d.
12a	79	50	>99 (*R*)[b]
13a	82	55	99.4 (*R*)
14a	86	84	n.a.
15a	86	81	89 (*R*)
16a	76	53	97 (*R*)
17a	99	92	>99.8 (*R*)[b]
18a	99	96	>99.7 (*R*)[b]
19a	>99	98	>99.8 (*R*)[b]
20a	88	73	>99 (*R*)[b]
21a	>99[c]	>99[c]	n.a.

[a] In some analytical scale reactions, it was possible to determine the *ee* values with an accuracy equal or superior to 99.7% due to the elevated conversion and the high response GC factor of the amine product. The 99.7% *ee* threshold value is important, as it is set by law for the manufacture and commercialisation of APIs (i.e., max 0.15% total impurities, with

the minor enantiomer being considered as impurity). High stereoselectivity was also confirmed in the preparative scale reactions.

[b] In these cases, the level of precision depends on instrumental detection limits rather than the intrinsic stereoselectivity of the enzyme. Indeed, the (*S*)-enantiomer was never observed.

[c] Reaction in HCOONH$_4$/NH$_3$ buffer (2 M, pH 7.8)

3.3.6 Reaction intensification

Using the optimum pH value (pH 9.0), a panel of ketones (**8a**, **9a, 13a, 17-19a, and 21a**) was tested for reductive amination from 10 mM up to 100 mM final substrate concentrations at two different temperatures (30 °C and 50 °C), since higher temperatures may affect the stability of the enzyme under process reaction conditions (e.g., shaking). The conversions and productivities are displayed in **Figure 4c to 4i**. The highest productivity was observed at 50 °C and 100 mM substrate concentration for aminations of **8a** (84 mM), **9a** (89 mM), and **18a** (58 mM). The highest productivity for amination of **17a** (at 50 °C) was observed with 50 mM of substrate concentration resulting in 46 mM of the corresponding amine product. LE-AmDH-v1 could also produce 69.6 mM of **19b** (at 50 °C) and 38.3 mM of **13b** (at 30 °C) starting from 75 mM of **19a** and **13a**, respectively. Finally, the highest activity was observed with benzaldehyde (**21a**), which was fully converted by LE-AmDH-v1 at 200 mM scale at 50 °C.
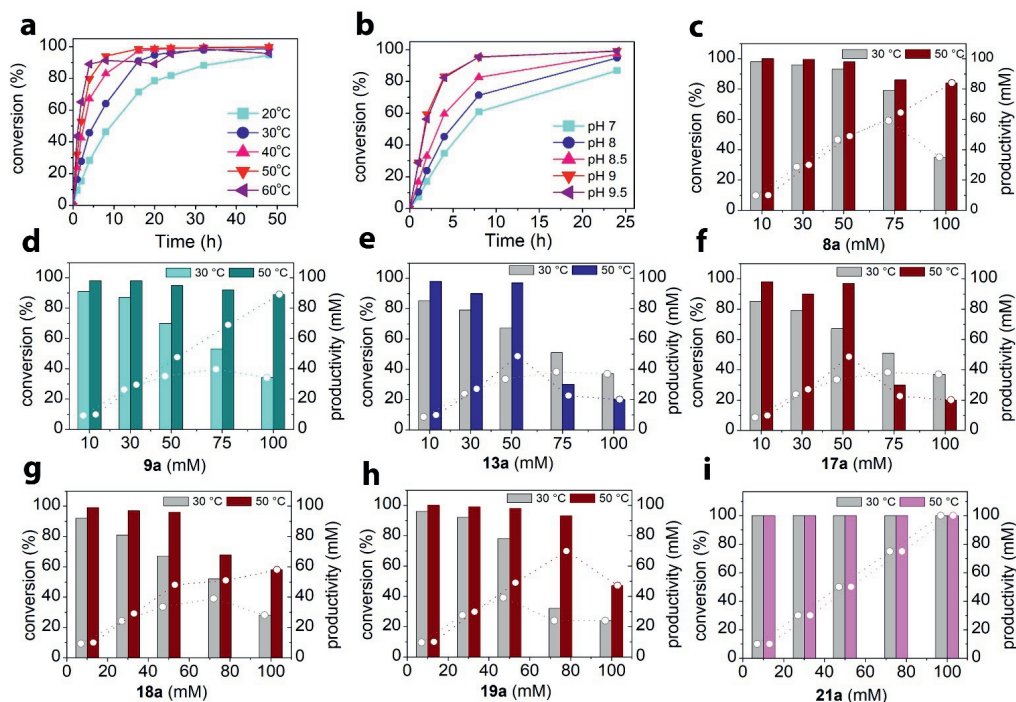
Figure 4. Optimization studies employing LE-AmDH-v1. Reaction conditions: 0.5 mL final volume; buffer: HCOONH₄/NH₃ 2 M pH 7.0-9.5; 170 rpm on orbital shaker; [substrate]: 10-100 mM; [NAD⁺]: 1 mM; [LE-AmDH-v1]: 90 µM; [Cb-FDH] = 19 µM; reaction time: 1-48 h (a-b) and 48 h (c-i) (**a**) Influence of the temperature (20 to 60 °C) on the reductive amination of **8a** in HCOONH₄/NH₃ 2 M pH 9.0 buffer. (**b**) Influence of the pH values using HCOONH₄/NH₃ buffer at 50 °C on the reductive amination of **8a**. (**c-i**) Effect of the substrate concentration on conversions (left y-axis; columns) and productivities (right y-axis; dashed lines with symbols) at two different temperatures: 30 and 50 °C.

3.3.7 Reductive amination reactions in preparative scale

In order to confirm the potential usefulness of LE-AmDH-v1 for the manufacturing of APIs, we performed preparative scale reductive amination reactions (100 mL reaction volume) starting from **8a** (600 mg, 5 mmol) and **9a** (671mg, 5 mmol), which were converted into (*R*)-**8b** and (*R*)-**9b** with >99% and 97% conversion, respectively. The unreacted ketone substrate was removed by extraction with MTBE under acidic conditions. After basification, the amine products (*R*)-**8b** and (*R*)-**9b** were extracted with MTBE in 82% and 65% isolated yields, respectively. No further purification was required. By considering the detection limit of the GC

measurement and concentration of the analytical samples (**Table 5**), we could conclude that (*R*)-**8b** and (*R*)-**9b** were obtained in >99.9% ee and total impurities were below the detection limit (i.e., surely <0.15%); these values comply with the requirement for API commercialisation.

Table 5. Experimentally determined ee values

		GC Area (*R*)	GC Area (S)	% (R)	% (S)	ee [%]
(*R*)-**8b**	reference compound	19584	97	99.51	0.49	99.0
(*S*)-**8b**	reference compound	82	19421	0.42	99.58	99.2
(*R*)-**8b**	preparative scale	16473	n.d.[a]	>99.98	<0.012	**>99.9**
(*R*)-**9b**	reference compound	6909	91	98.70	1.3	97.4
(*S*)-**9b**	reference compound	31	12038	0.26	99.74	99.5
(*R*)-**9b**	preparative scale	8492	n.d.[a]	>99.97	<0.023	**>99.9**

[a] For calculation of the ee, a GC peak area of 2 was used as threshold value, as this is clearly detectable with our equipment.

3.3.8 Steady state kinetic data and inhibition studies

LE-AmDH-v1 was characterized with respect to its kinetic properties for the amination of **8a** and **21a**. First, steady-state kinetics were determined for the amination of **8a** at different temperatures; the most elevated catalytic profile was observed at 60 °C (**Table 6**, **Figure 5**). Therefore, all other enzymatic assays were performed at 60 °C. LE-AmDH-v1 exhibited both the highest k_{cat} value and the lowest K_M for **21a** (**Table 6**, **Figure 5**).

With the aim of rationalizing the higher conversion of **8a** into **8b** that LE-AmDH-v1 exhibits over Ch1-AmDH, we also determined the kinetic parameters of Ch1-AmDH for the reductive amination of **8a** (**Table 6**, **Figure 5**). Surprisingly, despite the much higher conversion for the amination of **8a** (50 mM) catalysed by LE-AmDH-v1 (>99%, 90 µM enzyme) compared with Ch1-AmDH (34%, 130 µM enzyme) after 48 h[23], Ch1-AmDH possesses ca. two-fold higher k_{cat} and similar K_M values of those of LE-AmDH-v1 for the amination of **8a** at 60 °C (**Table 6**). Therefore, we hypothesized that the reductive amination of **8a** catalyzed by

Ch1-AmDH could be affected by severe product inhibition, as has also been observed with other aminating enzymes such as ω-transaminases.[16,43,44] We remark that steady-state k_{cat} and K_M values are commonly determined at an initial zero concentration of the product of the reaction. As such, solely considering these parameters for the evaluation of the catalytic effectiveness of a biocatalyst can lead to wrong conclusions, particularly when product inhibition occurs, as reviewed elsewhere.[45,46]

Table 6. Steady state kinetic data and inhibitory effects obtained for LE-AmDH-v1 and Ch1-AmDH.

Enzyme	Substrate	T (°C)	k_{app} (min^{-1})	K_M (mM)	IC$_{50}$[15] (mM)[b]	K_I (mM)[c]	K_M^{eff} (mM)[c]	k_{app}/K_M^{eff} (M min^{-1})
LE-AmDH-v1	**8a**	60	7.1 ± 0.2	5.5 ± 0.5	20	4.480	467	15
		50	7.0 ± 0.1	7.2 ± 0.4				
		40	5.7 ± 0.1	9.6 ± 0.6				
Ch1-AmDH[a]	**8a**	60	17.7 ± 0.4	5.6 ± 0.4	1	0.120	16838	1
		50	13.1 ± 0.5	8.5 ± 0.8				
		40	7.7 ± 0.3	11.6 ± 0.9				
LE-AmDH-v1	**21a**	60	43.6 ± 1.7	4.9 ± 0.5				

[a] The determination of the catalytic parameters of Ch1-AmDH by Bommarius and coworkers (Ref. [32]) are very similar to those obtained in this study: k_{app} 14.4 min^{-1} (60 °C), 10.8 min^{-1} (50 °C) and 7.2 min^{-1} (40 °C); K_M 5.2 mM (60 °C). ± represent the error (n=2 independent experiments using two different enzyme batches).
[b] Determined at a concentration of 15 mM **8a**
[c] (R)-**8b** was used as inhibitor. Following Fox *et al*. (Ref. [45]), K_M^{eff} was calculated based on the determined K_I, [S]$_0$=100 mM and c=99%.
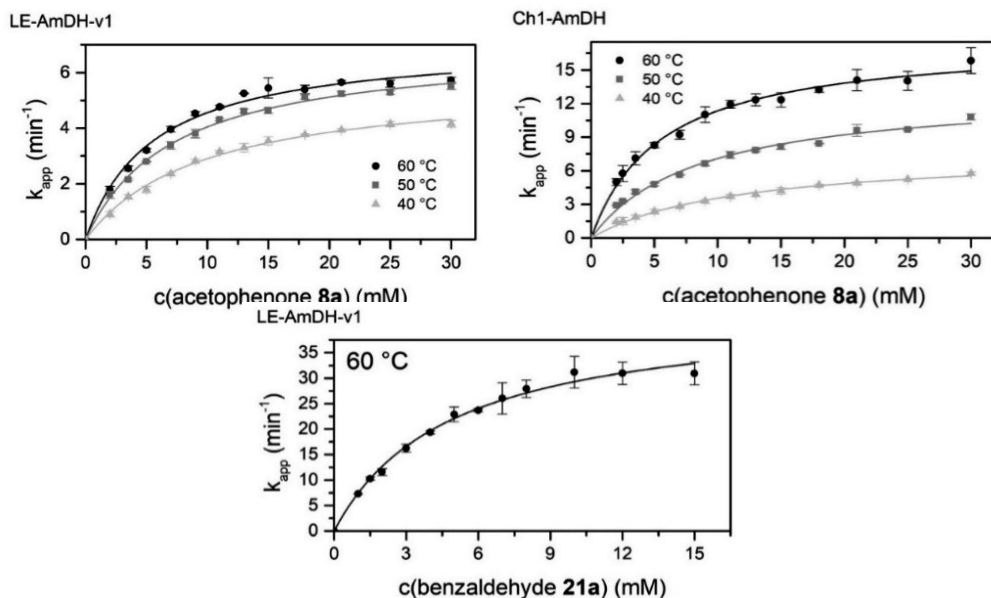
Figure 5. Hyperbolic fit of the reaction rates obtained for the reductive amination of 8a by LE-AmDH-v1 and Ch1-AmDH at different temperatures and for the reductive amination of 21a by LE-AmDH-v1 at 60 °C.

Initially, we studied the potential inhibitory effect of the amine product (*R*)-**8b** on LE-AmDH-v1 and Ch1-AmDH at a 15 mM concentration of **8a** by determining the IC$_{50}$ values, which were indeed 20 mM for LE-AmDH-v1 and 1 mM for Ch1-AmDH (**Figure 6b** and **Table 6**). A subsequent set of in-depth kinetic experiments on competitive product inhibition followed by Lineweaver-Burk analysis (**Figs. 6c-e**)[47] revealed that Ch1-AmDH is ca. 38-fold more inhibited than LE-AmDH-v1 (**Table 5**, see *K*$_I$ values). The evaluation of the overall catalytic performance (k$_{app}$/K_M^{eff}) according to Fox *et al.*,[45] demonstrated that LE-AmDH-v1 is ca. 15-fold more efficient than Ch1-AmDH (**Table 6**). In this evaluation, K_M^{eff} acts as the time-averaged and effective value for the K_M over the course of the reaction, thus including the competitive product inhibition phenomenon. Notably, an extremely high value of K_M^{eff} for the conversion of **8a** with Ch1-AmDH indicates that the theoretical v$_{max}$ (i.e., k$_{app}$)—although mathematically higher—already becomes physically unattainable at the beginning of the reaction. In conclusion,

our kinetics explain the superior catalytic performance of LE-AmDH-v1 in the reductive amination of **8a**. Notably, LE-AmDH-v1 is also capable of converting prochiral ketones that are not accepted by other AmDHs at all.
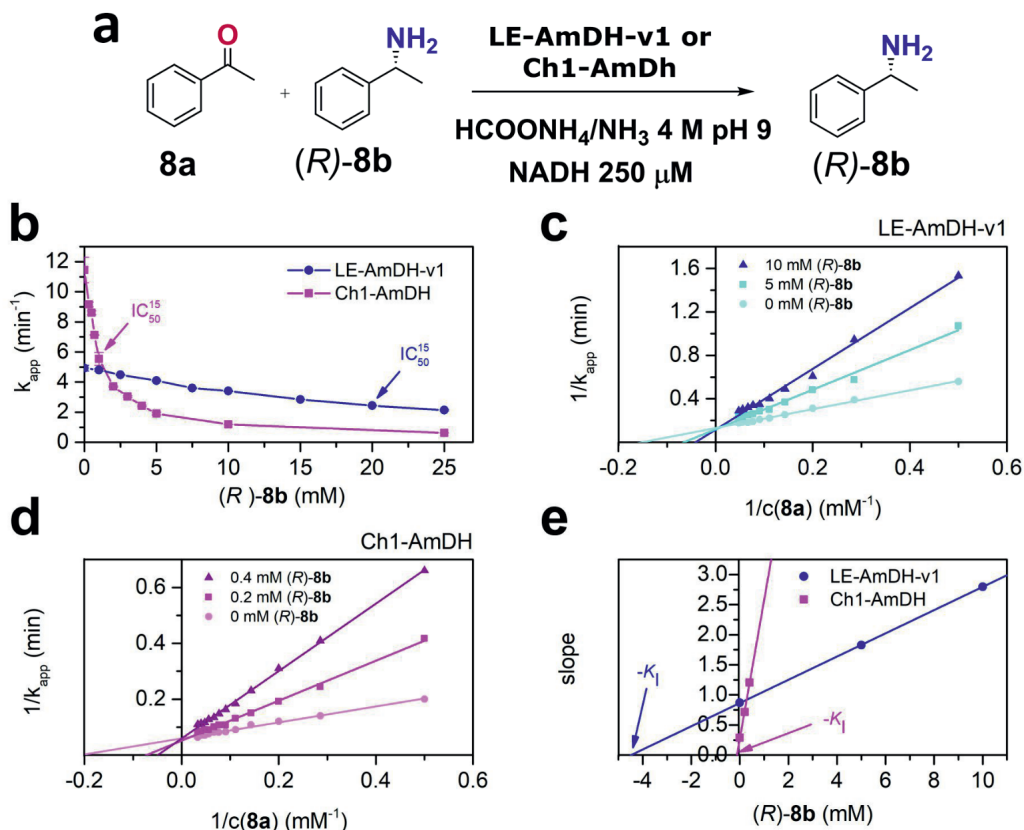
Figure 6.   Product inhibition studies employing LE-AmDH-v1 and Ch1-AmDH. (**a**) Overall scheme of the kinetic experiments, in which **8a** is used as substrate and (*R*)-**8b** as competitive inhibitor. (**b**) Inhibitory effect (IC$_{50}$[15]) of the amine product (*R*)-**8b** at 15 mM of substrate concentration **8a**. (**c** and **d**) Primary double reciprocal plots for competitive inhibition according to Lineweaver-Burk analysis for LE-AmDH-v1 and Ch1-AmDH, respectively. (**e**) Secondary plots of the slopes obtained from the primary Lineweaver-Burk plots vs. inhibitor concentrations. The absolute value of the intercept with the x-axis provides the competitive inhibition constant (K_I). Data points of Figure 6b are the average of n=2 independent measurements, but the deviation is so low that the error bar is smaller than the dots; the only visible error bar is for the pink line at k$_{app}$ ca. 5. **Figures 6c, d** are based on single measurements. **Figure 6e** is a secondary plot derived from **Figures 6c, d**.

3.3.9 Computational studies

The final refined model of LE-AmDH-v1 (**Figure 1b**) was used for in-depth computational studies aimed at explaining the stereoselective outcome of the reactions. We have shown that linear or aromatic ketones (e.g. **4a**, **8a**) can be quantitatively aminated with perfect stereoselectivity (*ee* >99% *R*). Conversely, the amination of **3a** proceeded quantitatively with opposite stereoselectivity (*ee* >99% *S*). A substrate-dependent switch of the enantioselectivity enabled by introducing a single mutation (as the F173A in LE-AmDH-v1) has been observed in very rare cases in enzyme catalysis such as with an ene-reductase,[48] a naphthalene dioxygenase[49], a lipase,[50] and an ω-transaminase.[51] However, a substrate-dependent switch of enantioselectivity has been observed only in the latter two cases, albeit the resulting enantiomeric excess was poor (ca. 58%).[50,51] Therefore, LE-AmDH-v1 is the first example of a biocatalyst possessing substrate-dependent stereo-switchable selectivity while always affording perfect enantiopurity of the products. Other examples from the literature describe either more mutations and consequent major structural alterations,[52] or starting from scaffolds with poor selectivity,[53,54] or changing the reaction medium.[55] To explain this singular feature, the iminium intermediates **4c**, **8c** and **3c (Scheme 1)** were docked into the active site of the enzyme. Via molecular docking and molecular dynamics simulations, we were able to identify the putative productive pro-(*R*) and pro-(*S*) binding modes for all three iminium intermediates. The two parameters to consider are:[19] *i)* the distance between the departing hydride of NADH and *pro-chiral* carbon of the iminium intermediate; and *ii)* the behavior of a dihedral angle as defined by the three atoms bonded to the *pro-chiral* carbon of the iminium intermediate and the hydride atom of the NADH. This angle determines the optical configuration of the amine product. The data are summarized in **Figure 7a**.
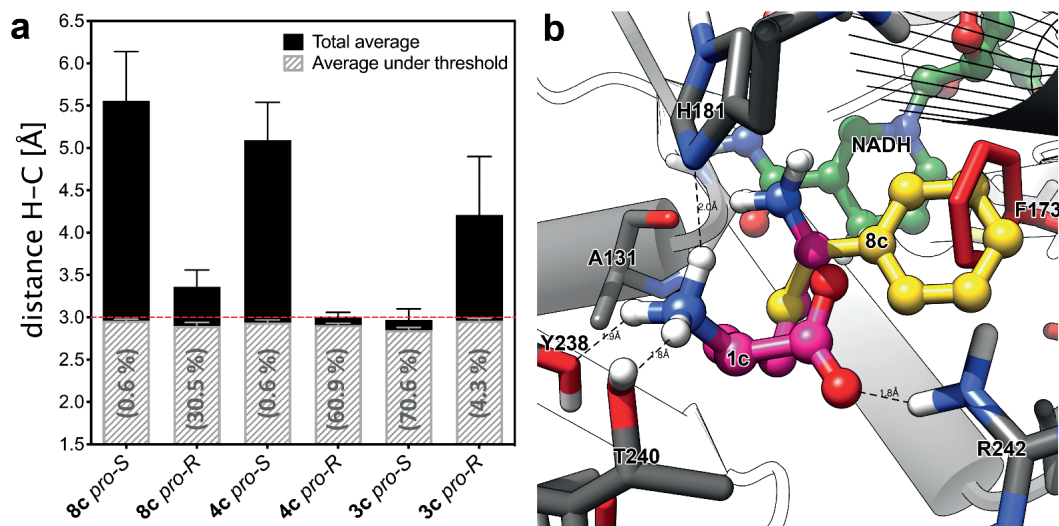
Figure 7. Pro-chiral preferences of LE-AmDH-v1. (**a**) Total average hydride/pro-chiral carbon distance over a minimum of 6 MD simulations and average under the distance threshold (3 Å). The percentiles indicate how often the average distance was under the given threshold. (**b**) Superposition of the natural substrate and **8c** in the active site of the wild type enzyme. The natural intermediate **1c** is depicted in magenta, whereas the iminium of acetophenone (**8c**) is depicted in yellow. The mutation point (F173A) is marked in red and the cofactor NADH is depicted in green. It can be observed that once the mutation F173A is introduced, the aromatic ring of **8c** gets accommodated into the newly created hydrophobic cavity, which was previously occupied by the phenyl group of F173; that produces an inversion of the chiral preferences of this mutant towards aromatic substrates and towards substrates with (relatively) short hydrophobic chains. Error bars represent the standard deviation of six independent experiments.

In the case of the iminium intermediate (**8c**) generated from **8a**, the pro-(R) conformation is highly favoured with 30.5% of the MD snapshot (within the simulation time) below the threshold distance of 3.0 Å between the hydride of NADH and prochiral carbon of **8c**. Starting from the pro-(S) conformation of **8c**, only 0.6% of MD snapshot is favourable for reduction. The same scenario occurs for the iminium intermediate **4c** (generated from **4a**). As expected, the situation is reversed for the reduction of **3c** (generated from **3a**). In this case, the pro-(S) conformation assumes a value below the threshold distance at 70.6% of the simulation time compared with at only 4.30% of the time for the pro-(R).

Figure 7b represents a superposition of the structure of the wild-type LysEDH and the LE-AmDH-v1 (i.e., F173A variant) with bound iminiums of *L*-lysine (**1c**) and acetophenone (**8c**). Ligand **8c** is oriented to have its phenyl ring in the new cavity created by the mutation F173A. This binding is not possible in the wild-type enzyme due to a steric clash with the side chain of F173. In contrast, **1c** always assumes the "natural" conformation as reported in the initial homology model (**Figure 1b**).

3.3.10 Enzymatic synthesis of a-chiral amines as reference compounds using ωTAs

Synthesis of non-commercially available reference compounds was performed employing ωTAs.[56-58] Three (*R*)-selective ωTAs (*Hyphomonas neptunium* Hn-ωTA, *Aspergillus terreus* At-ωTA and *Arthrobacter sp.* As-ωTA), as well as six (*S*)-selective ωTAs (*Bacillus megaterium* Bm-ωTA, *Chromobacterium violaceum* Cv-ωTA, *Paracoccus denitrificans* Pd-ωTA, *Pseudomonas fluorescens* Pf-ωTA, *Vibrio fluvialis* Vf-ωTA and *Arthrobacter citreus* Ac-ωTA) were used according to **Scheme 3**. Moreover, The (*R*)-selective ωTA: As*R*mut11[57] was employed for the reductive amination of **10a-13a** according to **Scheme 4**. Results are summarized in **Table 7.**
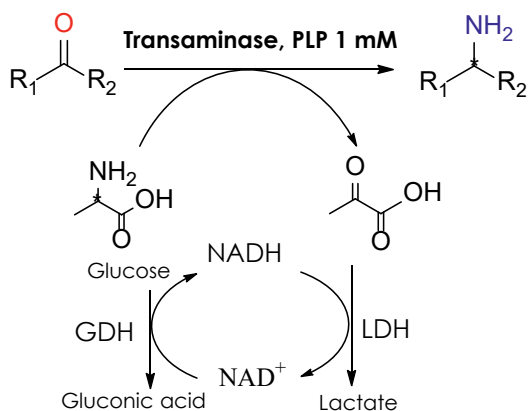
Scheme 3. Schematic representation of the biocatalytic reactions performed by ωTAs. Reaction conditions for ωTAs. substrate (50 mM or 10 mM), alanine (250 mM, D-alanine for *R*-selective ωTAs and L-alanine for (*S*)-selective ωTAs), KPi buffer (pH 7.0, 100 mM), PLP (1 mM), freeze-dried *E. coli* cells containing overexpressed ωTA (20 mg), LDH (LDH-101, 60 U mg^{-1}), GDH (GDH-901, 50 U mg^{-1}), NAD+ (1 mM), glucose (150 mM); reaction volume: 1 mL; reaction time: 24 h; temperature: 30 °C; agitation on an orbital shaker at 170 rpm.
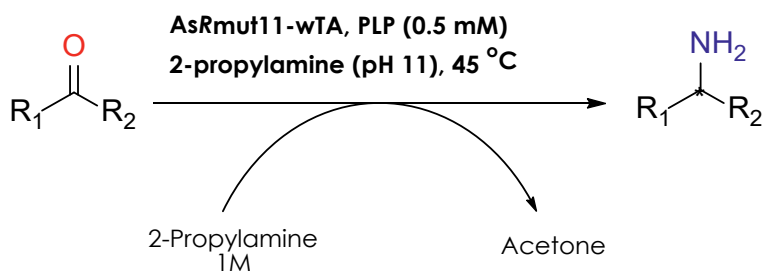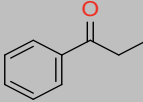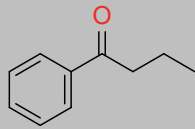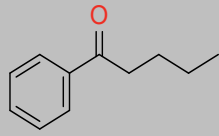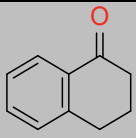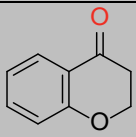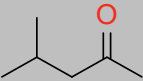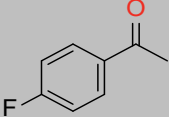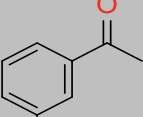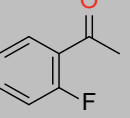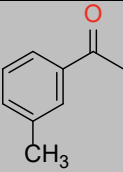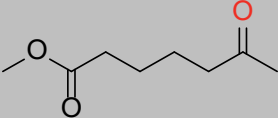
Scheme 4. Schematic representation of the biocatalytic reactions performed by AsRmut11 ωTA. Reaction conditions for AsRmut11-ωTA: H$_2$O, 2-propylamine (1 M), PLP (0.5 mM), adjusted to pH 11.0 with aqueous HCl, freeze-dried *E. coli* cells containing overexpressed ωTA (20 mg), substrate (50 mM or 10 mM). Reaction volume: 1 mL; reaction time: 24 h; temperature: 45 °C; agitation on an orbital shaker 170 rpm.

Table 7. Results for the biocatalytic reactions performed by ωTAs.

Substrate	Enzyme	Recovered substrate (%)	Amine product[a] Conv (%)	Alcohol (%)	Reported Selectivity
9a	As-ωTA	94	6	-	(R)
	At-ωTA	97	3	-	(R)
	Hn-ωTA	>99	-	-	(R)
	Ac-ωTA	98	2	-	(S)
	Bm-ωTA	3	97	-	(S)
	Cv-ωTA	70	30	-	(S)
	Pd-ωTA	47	53	-	(S)
	Pf-ωTA	47	53	-	(S)
10a	As-ωTA	100	-	-	(R)
	At-ωTA	100	-	-	(R)
	Hn-ωTA	100	-	-	(R)
	AsRmut11-ωTA	85	15	-	(R)
	Ac-ωTA	100	-	-	(S)
	Bm-ωTA	87	13	-	(S)
	Cv-ωTA	>99	<1	-	(S)
	Pd-ωTA	96	4	-	(S)
	Pf-ωTA	>99	<1	-	(S)
11a	Vf-ωTA	6	14	-	(S)
	As-ωTA	100	-	-	(R)
	At-ωTA	100	-	-	(R)
	Hn-ωTA	100	-	-	(R)
	AsRmut11-ωTA	97	3	-	(R)
	Ac-ωTA	100	-	-	(S)
	Bm-ωTA	92	8	-	(S)
	Cv-ωTA	>99	<1	-	(S)
	Pd-ωTA	99	1	-	(S)
12a	AsRmut11-ωTA	52	48	-	(R)
	Vf-ωTA	32	68	-	(S)
13a	AsRmut11-ωTA	26	74	-	(R)
	Vf-ωTA	69	25	6	(S)
	As-ωTA	100	-	-	(R)

Substrate	Enzyme	Recovered substrate (%)	Amine product[a] Conv (%)	Alcohol (%)	Reported Selectivity
16a	At-ωTA	100	-	-	*(R)*
	Hn-ωTA	73	27	-	*(R)*
	Ac-ωTA	89	11	-	*(S)*
	Bm-ωTA	44	56	-	*(S)*
	Cv-ωTA	11	89	-	*(S)*
	Pd-ωTA	89	11	-	*(S)*
	Pf-ωTA	66	34	-	*(S)*
	Vf-ωTA	77	23	-	*(S)*
17a	As-ωTA	13	85	2	*(R)*
	At-ωTA	83	11	6	*(R)*
	Hn-ωTA	90	1	8	*(R)*
	Ac-ωTA	48	47	5	*(S)*
	Bm-ωTA	16	80	4	*(S)*
	Cv-ωTA	7	91	2	*(S)*
	Pd-ωTA	4	93	3	*(S)*
	Pf-ωTA	43	50	7	*(S)*
	Vf-ωTA	2	97	1	*(S)*
18a	As-ωTA	3	96	1	*(R)*
	At-ωTA	27	70	3	*(R)*
	Hn-ωTA	76	7	17	*(R)*
	Ac-ωTA	21	75	4	*(S)*
	Bm-ωTA	13	81	6	*(S)*
	Cv-ωTA	2	97	1	*(S)*
	Pd-ωTA	1	98	1	*(S)*
	Pf-ωTA	14	82	4	*(S)*
	Vf-ωTA	1	98	1	*(S)*
19a	As-ωTA	1	98	1	*(R)*
	At-ωTA	2	96	2	*(R)*
	Hn-ωTA	61	19	20	*(R)*
	Ac-ωTA	11	85	4	*(S)*
	Bm-ωTA	3	93	4	*(S)*
	Cv-ωTA	<1	99	<1	*(S)*
	Pd-ωTA	1	99	-	*(S)*
	Pf-ωTA	14	76	10	*(S)*
	Vf-ωTA	<1	99	-	*(S)*
	As-ωTA	13	85	2	*(R)*
	At-ωTA	27	71	2	*(R)*
	Hn-ωTA	86	9	5	*(R)*

Substrate	Enzyme	Recovered substrate (%)	Amine product[a] Conv (%)	Alcohol (%)	Reported Selectivity
20a	Ac-ωTA	87	8	5	*(S)*
	Bm-ωTA	83	8	9	*(S)*
	Cv-ωTA	4	93	3	*(S)*
	Pd-ωTA	66	25	9	*(S)*
	Pf-ωTA	7	90	3	*(S)*
	Vf-ωTA	13	85	2	*(S)*
22a	As-ωTA	10	90	-	*(R)*
	At-ωTA	27	73	-	*(R)*
	Hn-ωTA	69	31	-	*(R)*
	Ac-ωTA	63	37	-	*(S)*
	Bm-ωTA	32	68	-	*(S)*
	Cv-ωTA	12	88	-	*(S)*
	Pf-ωTA	86	14	-	*(S)*
	Vf-ωTA	32	68	-	*(S)*

[a] Conversions were determined using a 7890A GC system (Agilent Technologies), equipped with FID detector using H_2 as carrier gas with a DB-1701 column from Agilent (30 m, 250 μm, 0.25 μm)

3.4 Conclusions

In summary, guided by structural information obtained from computational studies, we have generated AmDHs starting from an enzyme that does not operate any apparent asymmetric transformation in its natural reaction. The best variant (LE-AmDH-v1) is highly thermostable (T_m: 69 °C), also exhibiting highly retained catalytic activity (>99% at RT, 90% at 40 °C and 80% at 50 °C) upon incubation for 7 days. LE-AmDH-v1 operates preferentially at 50 °C and pH 9.0, thus affording pharmaceutically relevant amines such as **8b** (and derivatives), **12b**, **13b**, and **9b** in enantiomerically pure (*R*)-configurations and elevated productivities. Such biocatalytic performance is in part due to a remarkably reduced product inhibition, as investigated for the amination of **8a**. LE-AmDH-v1 also quantitatively aminated **3a** into an (*S*) configured product (*ee* >99%), thus providing a rare example of substrate-dependent stereo-switchable selectivity. Finally, *in silico* studies provided insight into the role of the mutations upon ligand binding and explained the enantioselective preferences of LE-AmDH-v1.

3.5 Methods

3.5.1 Biocatalytic reductive amination in analytical scale

LysEDH variant (90 µM, 4 mg mL^{-1}), NAD$^+$ free acid (1 mM), formate dehydrogenase from *Candida boidinii* (Cb-FDH, 19 µM, 0.81 mg mL^{-1}) and substrate (**4-21a**, 10-200 mM) were added to an ammonium formate buffer (HCOONH$_4$/NH$_3$ 0.5 mL, 2 M, pH 9). Biotransformations were performed at various temperatures and for different lengths of time in Eppendorf tubes in a horizontal position on orbital shakers (170 rpm). The reactions were quenched by the addition of aqueous 10 M KOH (100 µL) and extracted with dichloromethane (1 x 600 µL). After centrifugation, the organic phase was dried with MgSO$_4$ and the conversion was measured by GC-FID. Prior to injection into a chiral column for the determination of the *ee*, derivatisation of the samples was performed by the addition of 4-dimethylaminopyridine in acetic anhydride (50 µL of stock solution 50 mg mL^{-1}, 409 mM). The samples were shaken in an incubator at RT for 30 min, after which water (500 µL) was added and the samples were shaken for an additional 30 min. After centrifugation, the organic layer was dried with MgSO$_4$. Enantiomeric excess was determined by GC with a variant Chiracel DEX-CB column.

In the cases of **2a** and **3a**, the reactions were quenched by the addition of 100 µL HCl (3 M) and the samples were centrifuged (15 min, 21.1 g). The supernatants were analysed by RP-HPLC.

3.5.2 Biocatalytic reductive amination in preparative scale

Preparative scale reactions of **8a** (50 mM, 600 mg, 5 mmol) and **9a** (50 mM, 671 mg, 5 mmol) were performed in a total volume of 100 mL of HCOONH$_4$/NH$_3$ buffer (2 M, pH 9.0) at 50 °C in 250 mL Erlenmeyer flasks containing LE-AmDH-v1 (90 µM, 4 mg mL^{-1}), FDH (16 µM, 0.68 mg mL^{-1}), NAD$^+$ (1 mM). After 48 h, a >99% conversion was obtained for **8a** and a 63% was obtained for **9a**. For the latter reaction, additional aliquots of FDH (8 µM) and NAD$^+$ (1 mM) were added and

the reaction was incubated for another 48 h, thus obtaining 97% conversion. The reactions were acidified with concentrated HCl (6 mL) and unreacted starting material was extracted with MTBE (2 x 80 mL). After the addition of KOH (10 M, 12 mL), the amine products were extracted with MTBE (2 x 120 mL). The combined organic layers were dried over MgSO$_4$ and concentrated under reduced pressure. Avoiding any further purification step, (*R*)-**8b** and (*R*)-**9b** were obtained with 82% (colourless liquid, 495 mg, 4 mmol) and 65% (clear, yellow liquid, 437 mg, 3 mmol) isolated yields. The purity of the products was analyzed by ^{1}H-NMR (400 MHz in CDCl$_3$) and GC equipped with chiral column.

3.5.3 Chemoenzymatic synthesis of methyl-6-aminoheptanonate (22b)

Step 1, **3a** to **3b** :

The biocatalytic reaction (21 mL final volume) consisted of HCOONH$_4$/NH$_3$ (1 M, pH 9.0), LE-AmDH-v1 (90 µM), NAD$^+$ (1 mM), Cb-FDH (19 µM) and **3a** (50 mM, 150 mg, 1.040 mmol). The reaction was run at 30 °C for 48 h in an orbital shaker (170 rpm) before quenching by the addition of concentrated HCl (to pH 1). Aliquots of 2 mL were centrifuged in Eppendorf tubes (14.800 rpm, 20 min). The pellets were re-dissolved in water, centrifuged (14.800 rpm, 20 min) and all supernatants combined and freeze-dried overnight. The dry product was dissolved in HCl (0.1 M, 9 mL) and purified by cation exchange chromatography using a Dowex ® 50WX8 hydrogen form 100-200 mesh resin (Sigma Aldrich).

The resin (3 mL) was equilibrated by washing with 4 column columns (CV) of HCl (1 M, 12 mL), followed by 10 CV of HCl (0.1 M, 30 mL). The sample was loaded on the column and washed with H$_2$O (5 CV, 15 mL). Elution of **3b** was performed with NH$_4$OH (10%, 20 mL) in 5 mL aliquots. Fractions were freeze dried overnight and dissolved in water. Fractions containing the product were verified by TLC (ninhydrin staining, violet colour), combined and freeze dried. Pure **3b** was obtained as white solid in 73% yield (110 mg, 0.757 mmol).

Step 2, **3b** to **22b** :

75 mg (0.516 mmol) of **3b** obtained from step 1 were dissolved in methanol (3 mL) and HCl (2 M, ~150 µL) in a round bottom flask and the mixture was stirred on ice. Thionylchloride (SOCl$_2$, 2 eq., 1.03 mmol, 74.8 µL) was added dropwise and the reaction stirred at room temperature for 8 h. MeOH was removed under reduced pressure affording the crude product as an orange/red oil. K$_2$CO$_3$ (saturated solution, 3.5 mL) was added, thoroughly mixed, and the product was extracted with DCM (3 x 3 mL) and dried over MgSO$_4$. The solvent was removed under reduced pressure and **22b** was obtained as an orange oil in 73% yield (55 mg, 0.345 mmol).

The structures of **3b** before and after purification as well as of 22b were confirmed by ^{1}H-NMR.

Finally, the enantiomeric excess of **22b** was determined to be >99% (*S*) by comparing its retention time with the retention times of the products obtained by enzymatic transformation of **22a** using the As-ωTA and Cv-ωTA after derivatization.

3.5.4 In silico modifications

All *in silico* modifications were performed using YASARA (version 17.1.28) as software,[59] and selecting AMBER 03 as force field[60]. Prior to the introduction of any *in silico* mutation into the model structure, the protonation state of all the atoms was corrected automatically with the exception of the atoms involved in the hydride shift from the cofactor to the substrate. The protonation state of these atoms was corrected manually upon visual inspection. After the introduction of a mutation, the energy of the system was minimized following a three-step protocol that enables the adjustment of the model structure without creating any possible unwanted deformation. In step one, only the atoms constituting the mutated amino acid residue were subjected to energy minimization. In step two, the process for energy minimization was repeated by including all the atoms of the amino acid residues that are located within 6.0 Å distance from the mutated residue. In step three, the energy of the overall structure was minimised.

3.5.5 Homology modelling generation

The generation of homology models was carried out using the YASARA[59] homology model building protocol,[61] which involves multi-template structural model generation. Since the linear amino acid sequence of the target protein was the only given input, the possible templates were identified by running 3 PSI-BLAST[62] iterations to extract a position specific scoring matrix (PSSM) from UniRef90,[63] and then searching the PDB for a match with an E-value below the homology modelling cut-off 0.005. A maximum of 5 templates was allowed. To aid alignment correction and loop modelling, a secondary structure prediction for the target sequence had to be obtained. This was achieved by running PSI-BLAST to create a target sequence profile and feeding it to the PSI-Pred[64] secondary structure prediction algorithm. For each of the found templates, models were built. Either a single model per template was generated, when the alignment was certain, or a number of alternative models were generated, when the alignment was ambiguous. A maximum of 100 conformations per loop were explored. A maximum of 10 residues were added to the termini. Finally, YASARA tried to combine the best parts of the generated models to obtain a hybrid model, with the intension of increasing the accuracy beyond each of the contributors. The quality of the models was evaluated by use of Z-score.[36,37] A Z-score describes how many standard deviations the model quality is away from the average high-resolution X-ray structure. The overall Z-scores for all models have been calculated as the weighted averages of the individual Z-scores using the formula:

equation 1 $\text{Overall} = 0.145 * \text{Dihedrals} + 0.390 * \text{Packing1D} + 0.465 * \text{Packing3D}$

The overall score thus captures the correctness of backbone- (Ramachandran plot) and side-chain dihedrals, as well as packing interactions. In order to increase their quality, the obtained models were submitted to 500 ps molecular dynamic refinement simulation using the protocol describe by E. Krieger *et al.*[65]

A structural snapshot was saved every 25 ps for further analysis of quality parameters (potential energy, Dihedrals, Packing1D and Packing3D).

Amino acid sequence of the wild-type L-lysine epsilon-dehydrogenase from *Geobacillus stearothermophilus* (LysEDH):

```
MKVLVLGAGLMGKEAARDLVQSQDVEAVTLADVDLAKAEQTVRQLHSKKLAAVRVDAGDPQQLA
AAMKGHDVVVNALFYQFNETVAKTAIETGVHSVDLGGHIGHITDRVLELHERAQAAGVTIIPDL
GVAPGMINILSGYGASQLDEVESILLYVGGIPVRPEPPLEYNHVFSLEGLLDHYTDPALIIRNG
QKQEVPSLSEVEPIYFDRFGPLEAFHTSGGTSTLSRSFPNLKRLEYKTIRYRGHAEKCKLLVDL
TLTRHDVEVEINGCRVKPRDVLLSVLKPLLDLKGKDDVVLLRVIVGGRKDGKETVLEYETVTFN
DRENKVTAMARTTAYTISAVAQLIGRGVITKRGVYPPEQIVPGDVYMDEMKKRGVLISEKRTVH
SLE
```

The first homology model generation delivered model 0, which does not contain cofactor or ligand in its active site. Therefore, a second run was carried out excluding templates 4INA, 4RL6 for not containing cofactor or confirmation of the desired activity. This run yielded model 1 (dimeric) containing only the cofactor NADH but not ligand. In order to eliminate possible crystal contact artefacts, a third run was carried out also excluding templates 4INA, 4RL6 and allowing only the monomeric model to be generated. This run produced model 2 that contains the desired cofactor. In order to include the substrate, the intermediate model created with template 1E5Q, which contains not only the cofactor but also a ligand (saccharopine), was combined with model 2 and saccharopine was *in silico* modified into compound **1c** (model 2.1) and subsequently into **2c** (model 2.2). These three last models (2, 2.1 and 2.2 from **Table 1**) were submitted to molecular dynamic refinement.

3.5.6 Molecular docking

The molecular dockings were performed using Autodock Vina,[66] both as standalone engine or as tool incorporated into YASARA. The pre-selection and analysis of the obtained docked conformations were executed using the standard Vina's scoring function implemented into in-house-scripts. This analysis resulted in a number of selected docking poses that were finally inspected

visually. The refined analysis resulted in the selection of the reactive docking poses, which were used for the molecular dynamics (MD) simulations.

3.5.7 Molecular dynamics simulations

MD simulations were executed using the YASARA software,[67] with the AMBER03 force field.[68] In order to generate equilibrated starting structures for the MD simulations, each system (containing the desired mutations, co-factor and substrate) was placed in a rectangular box of simple point charge (SPC) water, to which approximately 100 mM NaCl (including neutralizing counter-ions) was added to simulate physiological salinity.[69] The protonation state of all atoms was automatically adjusted, with the exception of those atoms involved in the hydride transfer between co-factor and the substrate which were usually inspected and manually altered accordingly. The protonation state of the histidine residues and the orientation of asparagine and glutamine residues was automatically determined by its environment (hydrogen-bond network) using the graph-theory algorithm included in YASARA.[70-72] The walls of the simulation box were located at least 5.0 Å from the surface of the protein, following energy minimization (steepest descents) where a-carbon atoms, co-factor and substrate were kept frozen. Each of the systems was equilibrated in two-step protocol, with position restraints applied to the protein heavy atoms throughout, co-factor and substrate. The first phase involved simulating for 100 ps under a constant volume (NVT) ensemble. The complete system was coupled to temperature coupling baths, and temperature was maintained at 298 K using the V-rescale coupling method[73]. Following NVT equilibration (phase 2 of the equilibration), 500 ps of constant pressure (NPT) equilibrations were performed, also using weak coupling to maintain pressure isotropically at 1.0 bar. All productions MD simulations were carried out under NPT conditions with 2.5 fs step size (YASARA fast protocol).[74] The LINCS algorithm[75] was used to constrain the lengths of hydrogen containing bonds; the waters were restrained using the SETTLE algorithm.[76] Van der Waals forces were treated using a 12.0 Å cut-off.

Long-range electrostatic forces were treated using the particle mesh Ewald method (PME).[77] Both binding conformations, pro-(R) and pro-(S), were submitted to MD simulations. MD simulations were executed considering both the pro-(R) and pro-(S) binding conformations of the three iminium substrate intermediates (**3c**, **4c**, and **8c**). The following parameters were selected for the MD simulations: 1) the minimum number of independent simulations with random initial velocities was 6; 2) the time for each simulation was 500 ps; 3) analysis was performed by taking one snapshot every 6.25 ps. Thus, 81 frames (counting also the starting structure) were collected for each simulation. Among all the inspected properties, the most important ones resulted to be: 1) the distance between the departing hydride of the coenzyme NADH and the prochiral carbon of the iminium intermediate; 2) a dihedral angle (χ) that allows us to define the stereoselective outcome of the reaction based on the binding mode of the substrate in the active site.[19] In the case of the first parameter, the threshold distance for a productive hydride shift was set to the sum between the van der Walls radii of the carbon and hydrogen atoms, which is equal to ca. 3.0 Å ($r_H^{vdw} =$ 1.2 Å, $r_C^{vdw} = 1.7$ Å; $r_H^{vdw} + r_C^{vdw} = 2.9$ Å; thus: $d_{CH}^{threshold} = 3.0$ Å).[78] In the case of the second parameter, the dihedral angle was defined using the Cahn–Ingold–Prelog priority and considering the hydride of the NADH coenzyme along with the three atoms of the iminium substrates that are bound to the prochiral carbon. In our model system, an angle of 63.88±0.21° leads to the formation of the (R)-configured amine product, whereas an angle of -63.97±0.29° leads to the formation of the (S)-configured amine product.

3.5.8 Determination of NADH saturation for steady-state kinetics

All kinetic experiments were conducted using a Shimadzu UV-1800 UV-vis spectrophotometer in $HCOONH_4/NH_3$ buffer (4 M, pH 9) and following the oxidation of NADH at λ of 360 nm ($\varepsilon = 4250$ M^{-1} cm^{-1}) for 1 min (λ of 360 nm was selected due to an overlap of the absorption of **8a** and NADH at the most frequently selected λ of 340 nm).

The saturation concentration of NADH for Ch1-AmDH and LE-AmDH-v1 was determined with **8a** as substrate. Measurements at 60 °C were performed in two sets of independent experiments and using two different charges of purified protein.

A fixed concentration of **8a** (25 mM; from 500 mM main stock in DMSO which was further diluted to 350 mM in buffer) was added to a preincubated buffer (70 °C) and further incubated at 60 °C for 2 min in the thermostatic-controlled cuvette holder of the UV-vis spectrophotometer. The enzyme was added (2.0 µM for Ch1-AmDH and 5.2 µM for LE-AmDH-v1) and the solution was incubated for a further 20 sec at the desired temperature. Then, the reaction was initiated by the addition of coenzyme (0-270 µM; from 50 mM main stock in 50 mM KPi buffer at pH 8.0, which was further diluted to 10 mM in a reaction buffer).

The initial velocities were calculated from the linear range of the fitted trend line of the progress curve and were then plotted against the NADH concentration to obtain the K_M values. The Michaelis-Menten equation fitted well with the experimental determination.

3.5.9 Steady-state kinetics

Two sets of independent measurements were performed using two different charges of purified protein. Varied substrate concentrations (from 500 mM main stock in DMSO, which was further diluted to 350 mM in buffer) were added to a preincubated buffer (with an incubation temperature 10 °C higher than the measuring temperature) and further incubated at the desired measuring temperature in the thermostatic controlled cuvette holder of the UV-vis spectrophotometer for 2 min. The enzyme was added and the solution was incubated for a further 20 sec, after which the reaction was initiated by the addition of NADH (250 µM; from 50 mM main stock in 50 mM KPi buffer at pH 8.0, which was further diluted to 10 mM in a reaction buffer).

The initial velocities were calculated from the linear range of the fitted trend line of the progress curve and were then plotted against the substrate concentration to obtain the kinetic parameter.

3.5.10 Determination of the IC_{50}[15]

Product inhibition studies were performed in duplicate at 60 °C. A fixed concentration of **8a** (15 mM; from 500 mM main stock in DMSO, which was further diluted to 350 mM in buffer) and varied concentrations of product (*R*)-**8b**, (inhibitor, 0-25 mM; from 500 mM main stock in DMSO, which was further diluted to 350 mM in buffer) were added to a preincubated buffer (70 °C) and further incubated at 60 °C for 2 min in the thermostatic-controlled cuvette holder of the UV-vis spectrophotometer. The enzyme was added (2.1-10.7 μM for Ch1-AmDH and 4.9 μM for LE-AmDH-v1) and the solution was incubated at the desired temperature for a further 30 sec, after which the reaction was initiated by the addition of coenzyme (250 μM; from 50 mM main stock in a 50 mM KPi buffer at pH 8.0, which was further diluted to 10 mM in a reaction buffer).

The initial velocities were calculated from the linear range of the fitted trend line of the progress curve and were then plotted against the inhibitor concentration to obtain IC_{50} at a fixed substrate concentration (this value represents the amount of amine product that correlates with a decrease of 50% of the initial catalytic activity due to product inhibition at 15 mM **8a**.

3.5.11 Determination of the K_I for (*R*)-8b

Varied concentrations of substrate **8a** (0-30 mM, from 500 mM main stock in DMSO, which was further diluted to 350 mM in buffer) and inhibitor (*R*)-**8b** (0, 5 and 10 mM for LE-AmDH-v1 and 0, 0.2, and 0.4 mM for Ch1-AmDH, from 500 mM main stock in DMSO, which was further diluted to 350 mM in buffer) were added to a preincubated buffer (70 °C) and further incubated at 60 °C for 2 min in the thermostatic controlled cuvette holder of the UV-vis spectrophotometer. The enzyme was added (4.5-9 μM for LE-AmDH-v1 and 2.9-6.4 μM for Ch1-AmDH) and

the solution was incubated for a further 30 sec, after which the reaction was initiated by the addition of NADH (250 µM; from 50 mM main stock in 50 mM KPi buffer at pH 8.0, which was further diluted to 10 mM in a reaction buffer).

The initial velocities were calculated from the linear range of the fitted trend line. Primary double reciprocal Lineweaver-Burk plots were generated for each set of experiments at different inhibitor concentrations (**Figs. 6c** and **d**). The slopes obtained from these primary plots were plotted against the inhibitor concentration to obtain K_I (**Figure 6e**).[47] $K_M{}^{eff}$ was determined according to the equation:

$$K_M^{eff} = K_M \cdot 4.61 \cdot \left(1 + [S_0] \cdot \frac{0.78}{K_I}\right) 45.$$

3.6 References

1   Constable, D. J. C. *et al. Green Chem.* **9**, 411-420, doi:10.1039/b703488c (2007).

2   Ghislieri, D. & Turner, N. J. *Top. Catal.* **57**, 284-300, doi:10.1007/s11244-013-0184-1 (2013).

3   Nugent, T. C. in *Chiral amine synthesis: Methods, Developments and Applications*   (ed T. C. Nugent) (Wiley-VCH, Weinheim, 2010).

4   Wang, C. & Xiao, J. in *Stereoselective Formation of Amines* Vol. 343 (eds Wei Li & Xumu Zhang) 261-282 (Springer-Verlag 2014).

5   Kohls, H., Steffen-Munsberg, F. & Hohne, M. *Curr. Opin. Chem. Biol.* **19**, 180-192, doi:10.1016/j.cbpa.2014.02.021 (2014).

6   Mata-Rodríguez, M. & Gotor-Fernández, V. in *Science of Synthesis, Biocatalysis in Organic Synthesis 1*   (eds K. Faber, W.-D. Fessner, & N. J. Turner) 189-222 (Georg Thieme Verlag KG, 2015).

7   Pollegioni, L. & Molla, G. in *Science of Synthesis, Biocatalysis in Organic Synthesis 3* (eds K. Faber, W.-D. Fessner, & N. J. Turner) 235-284 (Georg Thieme Verlag KG, 2015).

8   Bartsch, S. & Vogel, A. in *Science of Synthesis, Biocatalysis in Organic Synthesis 2*   (eds K. Faber, W.-D. Fessner, & N. J. Turner) 291-311 (Georg Thieme Verlag KG, 2015).

9   Li, R. F. *et al. Nat. Chem. Biol.* **14**, 664-670, doi:10.1038/s41589-018-0053-0 (2018).

10   Ilari, A., Bonamore, A. & Boffi, A. in *Science of Synthesis, Biocatalysis in Organic Synthesis 2*   (eds K. Faber, W.-D. Fessner, & N. J. Turner) 159-175 (Georg Thieme Verlag KG, 2015).

11   Lichman, B. R., Zhao, J. X., Hailes, H. C. & Ward, J. M. *Nat. Commun.* **8**, 14883, doi:ARTN 14883a10.1038/ncomms14883 (2017).

12   Schrittwieser, J. H. *et al. Angew. Chem. Int. Ed.* **53**, 3731-3734, doi:10.1002/anie.201400027 (2014).

13   Schrittwieser, J. H. *et al. Angew. Chem. Int. Ed.* **50**, 1068-1071, doi:10.1002/anie.201006268 (2011).

14   Prier, C. K., Zhang, R. K., Buller, A. R., Brinkmann-Chen, S. & Arnold, F. H. *Nat. Chem.* **9**, 629-634, doi:10.1038/nchem.2783 (2017).

15   Reznichenko, A. L., Nawara-Hultzsch, A. J. & Hultzsch, K. in *Stereoselective Formation of Amines*   (eds W. Li & X. Zhang) 191-260 (Springer, 2014).

16   Slabu, I., Galman, J. L., Lloyd, R. C. & Turner, N. J. *ACS Catal.* **7**, 8263-8284, doi:10.1021/acscatal.7b02686 (2017).

17   Sharma, M., Mangas-Sanchez, J., Turner, N. J. & Grogan, G. *Adv. Synth. Catal.* **359**, 2011-2025, doi:10.1002/adsc.201700356 (2017).

18   Aleku, G. A. *et al. Nat. Chem.* **9**, 961-969, doi:10.1038/Nchem.2782 (2017).

19   Tseliou, V., Masman, M. F., Böhmer, W., Knaus, T. & Mutti, F. G. *ChemBioChem* **20**, 800-812, doi:10.1002/cbic.201800626 (2019).

20   Fuchs, M., Farnberger, J. E. & Kroutil, W. *Eur. J. Org. Chem.*, 6965-6982, doi:10.1002/ejoc.201500852 (2015).

21   Savile, C. K. *et al. Science* **329**, 305-309, doi:10.1126/science.1188934 (2010).

22   Mutti, F. G., Sattler, J., Tauber, K. & Kroutil, W. *ChemCatChem* **3**, 109-111, doi:10.1002/cctc.201000349 (2011).

23   Knaus, T., Böhmer, W. & Mutti, F. G. *Green Chem.* **19**, 453-463, doi:10.1039/c6gc01987k (2017).

24   Itoh, N., Yachi, C. & Kudome, T. *J. Mol. Catal. B: Enzym.* **10**, 281-290, doi: 10.1016/S1381-1177(00)00111-9 (2000).

25   Mayol, O. *et al. Catal. Sci. Technol.* **6**, 7421-7428, doi:10.1039/C6CY01625A (2016).

26   Mayol, O. *et al. Nat. Catal.* **2**, 324-333 doi:10.1038/s41929-019-0249-z (2019).

27   Abrahamson, M. J., Vazquez-Figueroa, E., Woodall, N. B., Moore, J. C. & Bommarius, A. S. *Angew. Chem. Int. Ed.* **51**, 3969-3972, doi: 10.1002/anie.201107813 (2012).

28   Abrahamson, M. J., Wong, J. W. & Bommarius, A. S. *Adv. Synth. Catal.* **355**, 1780-1786, doi:10.1002/adsc.201201030 (2013).

29   Ye, L. J. *et al. ACS Catal.* **5**, 1119-1122, doi:10.1021/cs501906r (2015).

30   Chen, F.-F., Liu, Y.-Y., Zheng, G.-W. & Xu, J.-H. *ChemCatChem* **7**, 3838-3841, doi:10.1002/cctc.201500785 (2015).

31   Pushpanath, A., Siirola, E., Bornadel, A., Woodlock, D. & Schell, U. *ACS Catal.* **7**, 3204-3209, doi:10.1021/acscatal.7b00516 (2017).

32   Bommarius, B. R., Schürmann, M. & Bommarius, A. S. *Chem. Commun.* **50**, 14953-14955, doi:10.1039/c4cc06527a (2014).

33   Chen, F.-F. *et al. ACS Catal.* **8**, 2622-2628, doi:10.1021/acscatal.7b04135 (2018).

34   Heydari, M., Ohshima, T., Nunoura-Kominato, N. & Sakuraba, H. *Appl. Environ. Microbiol.* **2004**, 937-942, doi: 10.1128/AEM.70.2.937-942.2004 (2004).

35   Knaus, T., Cariati, L., Masman, M. F. & Mutti, F. G. *Org. Biomol. Chem.* **15**, 8313-8325, doi:10.1039/c7ob01927k (2017).

36   Laskowski, R. A., MacArthur, M. W., Moss, D. S. & Thornton, J. M. *J. Appl. Crystallogr.* **26**, 283-291, doi:10.1107/s0021889892009944 (1993).

37   Hooft, R. W., Vriend, G., Sander, C. & Abola, E. E. *Nature* **381**, 272, doi:10.1038/381272a0 (1996).

38   Yoneda, K., Fukuda, J., Sakuraba, H. & Ohshima, T. *J. Biol. Chem.* **285**, 8444-8453, doi:10.1074/jbc.M109.084384 (2010).

39   Andi, B., Cook, P. F. & West, A. H. *Cell Biochemistry and Biophysics* **46**, 17-26, doi:10.1385/cbb:46:1:17 (2006).

40   Johansson, E., Steffens, J. J., Lindqvist, Y. & Schneider, G. *Structure* **8**, 1037-1047, doi: 10.1016/S0969-2126(00)00512-8 (2000).

41   Au, S. K., Bommarius, B. R. & Bommarius, A. S. *ACS Catal.* **4**, 4021-4026 doi: (10.1021/cs40121672014).

42   Lowe, J., Ingram, A. A. & Groger, H. *Bioorg. Med. Chem.* **26**, 1387-1392, doi:10.1016/j.bmc.2017.12.005 (2018).

43   Shin, J.-S. & Kim, B.-G. *Biotechnol. Bioeng.* **65**, 206-211, doi:10.1002/(sici)1097-0290(19991020)65:2<206::aid-bit11>3.0.co;2-9 (1999).

44   Truppo, M. D., Rozzell, J. D. & Turner, N. J. *Org. Process Res. Dev.* **14**, 234-237, doi:10.1021/op900303q (2010).

45   Fox, R. J. & Clay, M. D. *Trends Biotechnol.* **27**, 137-140, doi:10.1016/j.tibtech.2008.12.001 (2009).

46   Eisenthal, R., Danson, M. J. & Hough, D. W. *Trends Biotechnol.* **25**, 247-249, doi:10.1016/j.tibtech.2007.03.010 (2007).

47   Segel, I. H. *Enzyme Kinetics: Behavior and Analysis of Rapid Equilibrium and Steady-State Enzyme Systems.* 100ff (Wiley, 1993).

48   Pompeu, Y. A., Sullivan, B. & Stewart, J. D. *ACS Catal.* **3**, 2376-2390, doi:10.1021/cs400622e (2013).

49   Parales, R. E. *et al.* *J. Bacteriol.* **182**, 5495-5504, doi:10.1128/jb.182.19.5495-5504.200 (2000).

50   Magnusson, A. O., Takwa, M., Hamberg, A. & Hult, K. *Angew. Chem. Int. Ed.* **44**, 4582-4585, doi:10.1002/anie.200500971 (2005).

51   Svedendahl, M., Branneby, C., Lindberg, L. & Berglund, P. *ChemCatChem* **2**, 976-980, doi:10.1002/cctc.201000107 (2010).

52   Pratter, S. M. *et al. Angew. Chem. Int. Ed.* **52**, 9677-9681, doi:10.1002/anie.201304633 (2013).

53   Sun, Z. *et al. Angew. Chem. Int. Ed.* **54**, 12410-12415, doi:10.1002/anie.201501809 (2015).

54   Reetz, M. T. *Angew. Chem. Int. Ed.* **50**, 138-174, doi:10.1002/anie.201000826 (2011).

55   Jongejan, J. A. in *Organic Synthesis with Enzymes in Non-Aqueous Media* (eds Giacomo Carrea & Sergio Riva) 25-46 (Wiley, 2008).

56   Koszelewski, D., Goritzer, M., Clay, D., Seisser, B. & Kroutil, W. *ChemCatChem* **2**, 73-77, doi:10.1002/cctc.200900220 (2010).

57   Mutti, F. G., Fuchs, C. S., Pressnitz, D., Sattler, J. H. & Kroutil, W. *Adv. Synth. Catal.* **353**, 3227-3233, doi:10.1002/adsc.201100558 (2011).

58   Mutti, F. G. *et al. Eur. J. Org. Chem.* **2012**, 1003-1007, doi:10.1002/ejoc.201101476 (2012).

59   Krieger, E., Koraimann, G. & Vriend, G. *Proteins* **47**, 393-402, doi:10.1002/prot.10104 (2002).

60   Oostenbrink, C., Villa, A., Mark, A. E. & van Gunsteren, W. F. *J. Comput. Chem.* **25**, 1656-1676, doi:10.1002/jcc.20090 (2004).

61   Venselaar, H. *et al. Eur. Biophys. J.* **39**, 551-563, doi:10.1007/s00249-009-0531-0 (2010).

62   Altschul, S. *Nucleic Acids Res.* **25**, 3389-3402, doi:10.1093/nar/25.17.3389 (1997).

63   Suzek, B. E., Huang, H., McGarvey, P., Mazumder, R. & Wu, C. H. *Bioinformatics* **23**, 1282-1288, doi:10.1093/bioinformatics/btm098 (2007).

64   Jones, D. T. *J. Mol. Biol.* **292**, 195-202, doi:10.1006/jmbi.1999.3091 (1999).

65   Krieger, E., Darden, T., Nabuurs, S. B., Finkelstein, A. & Vriend, G. *Proteins* **57**, 678-683, doi:10.1002/prot.20251 (2004).

66   Trott, O. & Olson, A. J. *J. Comput. Chem.* **31**, 455-461, doi:10.1002/jcc.21334 (2010).

67   Krieger, E. *et al. Proteins: Structure, Function, and Bioinformatics* **77**, 114-122, doi:doi:10.1002/prot.22570 (2009).

68   Duan, Y. *et al. J. Comput. Chem.* **24**, 1999-2012, doi:10.1002/jcc.10349 (2003).

69   Berendsen, H. J. C., Postma, J. P. M., van Gunsteren, W. F. & Hermans, J. in *Intermolecular Forces: Proceedings of the Fourteenth Jerusalem Symposium on Quantum Chemistry and Biochemistry Held in Jerusalem, Israel, April 13–16, 1981* (ed Bernard Pullman) 331-342 (Springer Netherlands, 1981).

70   Hooft, R. W. W., Sander, C. & Vriend, G. *Proteins: Structure, Function, and Bioinformatics* **26**, 363-376, doi:doi:10.1002/(SICI)1097-0134(199612)26:4<363::AID-PROT1>3.0.CO;2-D (1996).

71   Word, J. M., Lovell, S. C., Richardson, J. S. & Richardson, D. C. *J. Mol. Biol.* **285**, 1735-1747, doi: 10.1006/jmbi.1998.2401 (1999).

72   Canutescu, A. A., Shelenkov, A. A. & Dunbrack Jr., R. L. *Protein Sci.* **12**, 2001-2014, doi: 10.1110/ps.03154503 (2003).

73   Bussi, G., Donadio, D. & Parrinello, M. *J. Chem. Phys.* **126**, 014101, doi:10.1063/1.2408420 (2007).

74   Berendsen, H. J. C., Postma, J. P. M., Gunsteren, W. F. v., DiNola, A. & Haak, J. R. *J. Chem. Phys.* **81**, 3684-3690, doi:10.1063/1.448118 (1984).

75   Hess, B., Bekker, H., Berendsen, H. J. C. & Fraaije, J. G. E. M. *J. Comput. Chem.* **18**, 1463-1472, doi: 10.1002/(SICI)1096-987X(199709)18:12<1463::AID-JCC4>3.0.CO;2-H (1997).

76   Miyamoto, S. & Kollman, P. A. *J. Comput. Chem.* **13**, 952-962, doi: 10.1002/jcc.540130805 (1992).

77   Darden, T., York, D. & Pedersen, L. *J. Chem. Phys.* **98**, 10089-10092, doi:10.1063/1.464397 (1993).

78   Bondi, A. *J. Phys. Chem.* **70**, 3006-3007, doi:10.1021/j100881a503 (1966).

Chapter 4

Kinetic resolution of racemic primary amines using *Geobacillus stearothermophilus* amine dehydrogenase variant

4.1 Abstract

The high enantioselectivity of the AmDHs can be used for the preparation of valuable enantiomerically pure amines. The most well studied approach is the reductive amination of ketones. However, kinetic resolution (KR) of racemic amines can also be used for the preparation of amines with excellent optical purity. Herein, the NAD(H)-dependent engineered AmDH from *Geobacillus Stearothermophilus* LE-AmDH-v1 was applied together with NAD-oxidase from *Streptococcus mutans* (NOx) for the kinetic resolution of pharmaceutical relevant racemic a-chiral primary amines. The pH optimum for the oxidative deamination reaction was determined to be 7.4 using Britton–Robinson's universal buffer. In this pH optimum, the influence of different types of buffer was investigated for the oxidative deamination of racemic a-methylbenzylamine. Increasing the temperature of the reaction resulted in faster resolution of a-methyl-benzylamines under the optimized conditions. Pharmaceutical relevant racemic amines were successfully resolved after 24h (ee >99 %) using these optimized conditions. Increased concentration of a-methylbenzylamine (up to 75 mM) resulted in successful resolution using the same amount of catalyst due to the decreased inhibition of LE-AmDH-v1 compare with previously reported AmDHs. Finally, the dynamic kinetic resolution of a-methylbenzylamine was attempted using amine boranes. In all cases, only the racemic substrate was recovered indicating a possible inhibition of LE-AmDH-v1 by these complexes. Moreover, Implementation of LE-AmDH-v1 into deracemization cascades employing (*S*)-selective ω-transaminases resulted in low to moderate ee values.

4.2 Introduction

a-Chiral amines are fundamental building blocks for the manufacturing of many active pharmaceutical ingredients (APIs), fine chemicals, and agrochemicals.[1-4] An increasing number of newly approved drugs contain an a-chiral amine core, and the legislative regulations for their commercialisation are stringent in terms of chemical and enantiomerical purity (i.e., total impurity amount < 0.15%). In this context, several biocatalytic methods to obtain enantiopure a-chiral amines have been developed, including asymmetric synthesis from prochiral ketones using either ω-transaminases (ωTA),[5-12] or dehydrogenases (i.e., reductive aminases (RedAm), imine reductases (IRed), amine dehydrogenases(AmDH);[13-33] from alkenes using either ammonia lyases[34,35] or engineered cytochrome c;[36] and from alkanes using engineered cytochrome P411 monooxygenases.[15,37] Enantiomerically pure amines can also be obtained from a racemic mixture by applying one among several available deracemisation strategies.[38] Kinetic resolution (KR) is the simplest among these deracemisation methods, as it is based on the use of an enantioselective catalyst that acts exclusively on one enantiomer while leaving the other untouched. Additionally, KR is a practical approach to assess the efficiency of a biocatalyst that can possibly then be implemented in another deracemisation method. For instance, KR can be combined with a racemisation catalyst (i.e., dynamic KR using e.g., Pd/C, Pd/AlO(OH), $VOSO_4$, Ru or Ir complexes) or a hydride transfer reagent (e.g., $NaCNBH_3$, $NaBH_4$).[38-40] The applicability of KR and DKR for chiral amine synthesis has been demonstrated using hydrolases,[39] ωTAs,[5-7,9,10,41] and monoamine oxidases (MAOs),[42-50] as well as with AmDHs or RedAms in combination with either a NADH oxidase or an alanine dehydrogenase.[51-53]

Complementary strategies include deracemisation cascades in which stereocomplementary AmDH and ωTA, or vice versa, perform stereoselective oxidative deamination followed by stereoselective reductive amination.[54]

The KR of a-chiral amines can be performed using AmDHs in combination with a H_2O-forming NADH oxidase (NOx), thereby maximising the atom-economy, as

dioxygen acts as an oxidant and water is the by-product. However, the restricted substrate scope of AmDHs imposes a limitation on the applicability of the AmDH-NOx system, as most of the currently available AmDHs were engineered starting from structurally related wild-type enzymes and using a similar engineering approach. However, we recently reported a highly stereoselective AmDH (LE-AmDH-v1), which was engineered starting from a wild-type enzyme that does not catalyse any apparent asymmetric transformation in its natural reaction, namely the ε-deaminating L-lysine dehydrogenase (LysEDH) from *Geobacillus stearothermophilus*[27] LE-AmDH-v1 exhibited excellent activity and stereoselectivity in the asymmetric synthesis of pharmaceutically relevant (*R*)-configured a-chiral amines, including (*R*)-a-methylbenzylamines, (*R*)-1-aminotetraline, and (*R*)-4-aminochromane. Notably, the previously discovered AmDHs do not possess this property.[13,15,23-33] Herein, we report the harnessing of the catalytic and stereoselective properties of LE-AmDH-v1 to carry out the KR (i.e., enantioselective oxidative deamination) of pharmaceutically relevant a-chiral amines starting from a racemic mixture of a-methyl- and a-ethyl-benzylamines, 1-aminotetralin, 4-aminochromane, and 1-aminoindan.

4.3 Results and discussion

4.3.1 Response factors

For an accurate determination of the obtained conversions of the racemic amines into the corresponding ketones, we determined the response factors of amines **1-7a** and ketones **1-7b** by comparing the corresponding GC peak areas at different concentrations of analyte (**Table 1**). Using the obtained slopes the conversion of the KR of a racemic compound into its corresponding ketone was determined as described in methods section (section 4.5.2).

Table 1. Response factors of the substrates and products used.
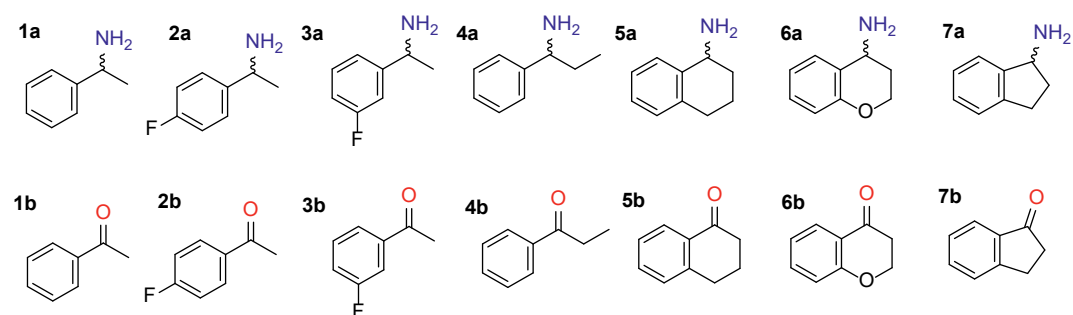
Entry	DMSO stock	Conc. (mM)	Area extracted of		Slope (R²)		Response factor	
			1a	**1b**	**1a**	**1b**	**1a/1b**	**1b/1a**
		5	504	626				
		7.5	739	884				
1	1 M	10	1047	1075	104.87 (0.99)	111.99 (0.99)	0.94	1.06
		15	1553	1592				
		20	2136	2295				
			2a	**2b**	**2a**	**2b**	**2a/2b**	**2b/2a**
		5	715	814				
		7.5	994	1138				
2	1 M	10	1459	1572	140.51 (0.99)	151.45 (0.99)	0.93	1.08
		15	2105	2267				
		20	2805	2989				
			3a	**3b**	**3a**	**3b**	**3a/3b**	**3b/3a**
3	1 M	5	437	396	104.14 (0.98)	117.89 (0.95)	0.88	1.13
		7.5	657	587				

Entry	DMSO stock	Conc. (mM)	Area extracted of		Slope (R²)		Response factor	
		10	852	770				
		15	1285	1187				
		20	1523	1434				
			4a	**4b**	**4a**	**4b**	**4a/4b**	**4b/4a**
		5	606	569				
		7.5	899	851				
4	1 M	10	1202	1102	123.51 (0.99)	114.63 (0.99)	1.08	0.93
		15	1840	1715				
		20	2510	2323				
			5a	**5b**	**5a**	**5b**	**5a/5b**	**5b/5a**
		5	398	532				
		7.5	628	766				
5	1 M	10	831	978	84.51 (0.99)	98.37 (0.99)	0.86	1.16
		15	1288	1495				
		20		1935				
			6a	**6b**	**6a**	**6b**	**6a/6b**	**6b/6a**
		5	463	371				
		7.5	666	540				
6	1 M	10	849	665	88.65 (0.99)	68.93 (0.99)	1.28	0.78
		15	1370	1075				
		20	1756	1344				
			7a	**7b**	**7a**	**7b**	**7a/7b**	**7b/7a**
		5	593	540				
		10	1307	1168				
7	1 M	15	1811	1632	123.8 (0.99)	110.97 (0.99)	1.08	0.93
		20	2449	2205				
		25	3122	2785				

4.3.2 Influence of the pH in the oxidative deamination of a-methyl-benzylamine

Initially, we determined the optimum pH for the biocatalytic oxidation using **1a** as substrate. The rate of the oxidative deamination reaction of **1a** (10 mM) was investigated in a pH range from 2.5 to 9.8 using Britton–Robinson's universal buffer using LE-AmDH-v1 (45 μM), NAD+ (1 mM) and NAD-oxidase (NOx, 3 μM) from

Streptococcus mutans for cofactor recycling (**Figure 1A**). The study was performed at 40 °C due to the reported thermal stability of NOx that is limited up to 52 °C. Conversely, we have previously demonstrated that LE-AmDH-v1 is a thermostable enzyme (T_m: 69 °C). **Figure 1** shows that the reaction rate was the highest at pH 7.4 (56.2 µM/min). Although, we have previously shown that LE-AmDH-v1 better performed the reductive amination at pH 9-9.5, in the oxidative deamination direction, more basic pH reduced the reaction's rate. For instance, at pH 9.2 the rate of the reaction was determined to be 34.6 µM min^{-1} or 18.3 µM min^{-1} at pH 9.7, respectively.
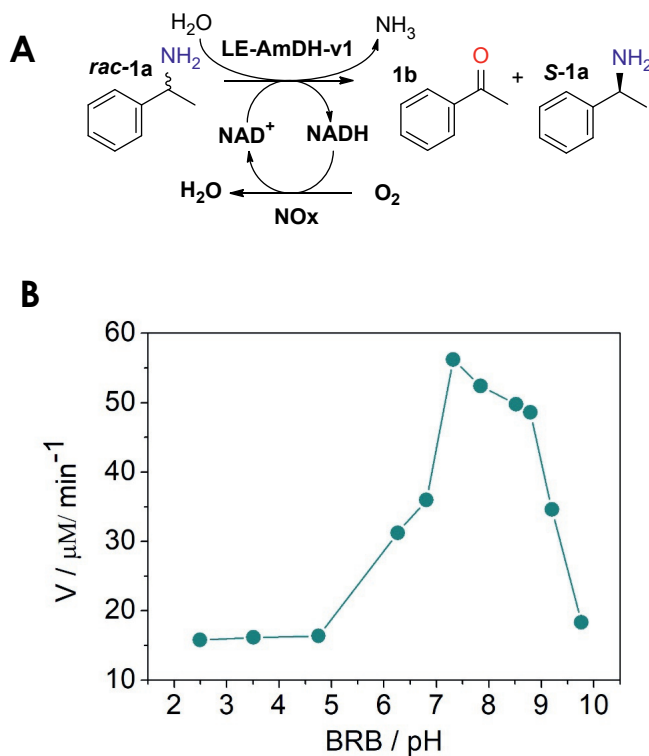
Figure 1. (A) Schematic representation of the reactions performed. (B) Reaction rate of the oxidative deamination of *rac*-1a at different pH values using Britton–Robinson's universal buffer. Catalytic amount of NAD$^+$ (1mM) was applied and recycled using the NOx (3 µM). All reactions (0.5 mL) were performed at 40 °C using 10 mM of **1a** and 45 µM of LE-AmDH-v1. Reaction times varied from 5 to 40 min.

4.3.3 Influence of the type of buffer

Next, we investigated the influence of different types of buffer for the oxidative deamination of **1a** (10 mM) catalyzed by LE-AmDH-v1 (45 µM) in presence of NOx (3µM). The temperature was reduced to 30 °C to avoid any evaporation of the product at longer reaction times as was partially observed in the previous set of experiments. Conversion and *ee* values obtained were acquired for the KR at the optimum pH of 7.4 in 50 mM Tris-HCl, 100 mM KPi, 100 mM MOPS and 100 mM HEPES buffers. Results are summarized in **Figure 2**. In general, biocatalytic transformations proceeded equally well and reached the highest conversion of 48 % and 49% after 24 h in 50 mM Tris/HCl and 100 mM KPi buffers, respectively. In both cases the reaction reached completion after this time as *ee* was more than 99% for the (*S*)-configured product. A more detailed study showed that enantiopure (*S*)-**1a** was obtained after 16 h using both buffers, thus indicating that prolonging the reaction time is unnecessary. In contrast, the LE-AmDH-v1 performed less efficiently in 100 mM MOPS buffer; a maximum conversion of only 35% was obtained after 24 h (*ee* = 57% *S*). A similar scenario was observed when using a HEPES buffer (100 mM pH 7.4), which provided a maximum conversion of 36% (*ee* = 61% *S*) after 24 h.
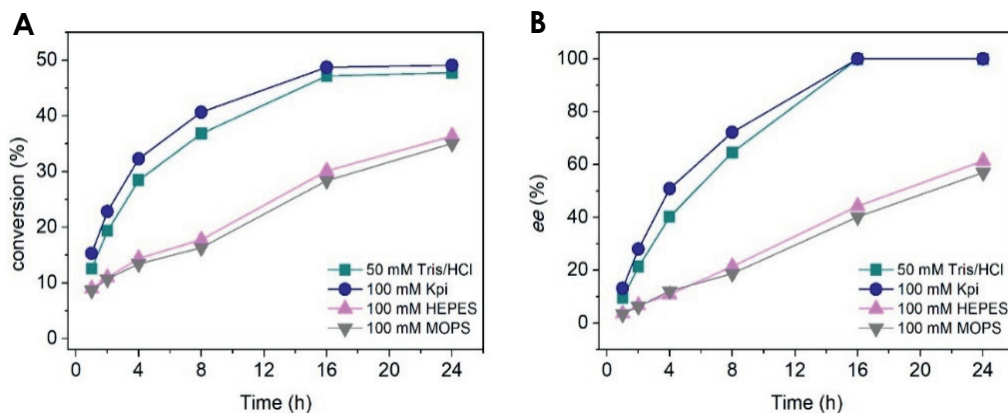
Figure 2. KR of *rac*-1a (10 mM) catalyzed by LE-AmDH-v1 (45 µM) and using different types of buffers with NAD+ (1 mM) and NOx (3 µM) at 30 °C. (A) Progress of the KR over the time. (B) Variation of the ee of the unreacted enantiomer over the time.

4.3.4 Influence of the temperature into the stereoselective outcome

With the aim of investigating the influence of the temperature on the oxidative KR of **1a**, we monitored the progress of enantiomeric excess at different temperatures (30 °C, 40 °C and 50 °C). Reactions were performed in 50 mM Tris/HCl pH 7.4 comprising LE-AmDH-v1 (90 µM), NOx (10 µM), and analyzed after 2h, 4h, 8h, 16h and 24h. **Figure 3** shows that complete KR of **1a** (*ee* >99% *S*) was obtained after 16h at 30 °C or 40 °C. However, the KR proceeded at higher rate at 40 °C as the *ee* reached already 99.1% after 8 h, whereas it was 95.2% at 30 °C after the same time. At 50 °C, the KR proceed even faster and only (*S*)-**1a** remained in the reaction mixture after 8 h. However, due to the reported mesophilic thermal stability of NOx (Tm 52 °C), we decided to attempt the KR of *rac*-**2-7a** at 30 °C (**Table 2**) and eventually to increase the temperature only in those cases in which resolution would not reach completion at 30 °C within 24 h.
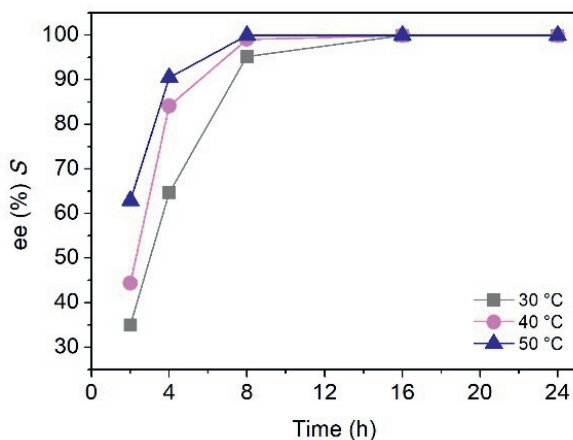
Figure 3. Progress of the KR of *rac*-**1a (10 mM) at different temperatures (30 °C- 50 °C) catalyzed by LE-AmDH-v1 (90 μM) with NAD+ (1 mM) and NOx (10 μM).**

4.3.5 Kinetic resolution of pharmaceutical relevant *racemic* amines employing LE-AmDH-v1

On the basis of the investigation performed for compound **1a**, the LE-AmDH-v1 was applied for the kinetic resolution of racemic amines **2**-**6a**. Normalized conversions using the response factors (**Table 1**) as well as the *ee* of the obtained amines are reported in **Table 2**. In all cases, the production of enantiopure amines was achieved by the biocatalytic kinetic resolution using LE-AmDH-v1 under the reported conditions with the exception of fluoro substituted α-methylbenzylamines. Starting from these racemic amines, the *ee* values of **2a** and **3a** were respectively 94% and 77% (*S*), thus indicating that the reaction did not reach completion at 30 °C after 24 h. Longer reaction times (48 h) allowed the KR to reach completion in the case of **2a** (*ee*: >99%), whereas **3a** was obtained in higher enantioenriched form (*ee*: 95%). The same results were observed when *rac*-**2a** and *rac*-**3a** were resolved at 50 °C for 24 h, thereby affording ee values of >99% and 95%, respectively. These results indicate that higher temperatures can indeed accelerate the kinetics of the reaction, as previously reported for reductive amination of ketones catalyzed by

LE-AmDH-v1. Finally, LE-AmDH-v1 was able to resolve **5-7a** at 30 °C after 24 h; these bicyclic aromatic enantiopure amines are motives in many important pharmaceuticals, such as Rotigotine (a dopamine agonist), Norsertraline (a selective serotonin reuptake inhibitor, SSRI), and Resagiline (an irreversible inhibitor of monoamine oxidase-B).

Table 2. Kinetic resolution of racemic amines 1-7a employing LE-AmDH-v1. Reaction conditions: [substrate]: 10 mM, [NAD+]: 1 mM, [LE-AmDH-v1]: 90 μM, [NOx]: 10 μM, Temperature: 30 °C, Time: 24h

Substrate	Time (h)	Conv. (%)[a]	ee [c]
1a	24	49.84	>99.3 % (S)
2a [b]	48	49.72	>99.2 % (S)
3a [b]	48	46.12	94.9 % (S)
4a	24	50.37	>99.4 % (S)
5a	24	49.44	>99.5 % (S)
6a	24	49.86	>99.3 % (S)
7a	24	50.40	>99.6 % (S)

[a] conversion reported here are normalized based on the response factors of the obtained amines: ketones as describe in the **Table 1**.

[b] reaction time: 48h.

[c] In some analytical scale reactions, it was possible to determine the ee values with an accuracy superior to 99.2 % due to the elevated conversion and the high response GC factor of the amine product. In these cases, the (*R*)-enantiomer was never observed.

4.3.6 Influence of the substrate concentration in the kinetic resolution of a-methyl-benzylamine

In a previous work by Yun's group the kinetic resolution of *rac* **1a** was attempted using the cFL1-AmDH that was previously engineered by Bommarius and co-workers.[25] However, due to significant inhibitory effect of **1a** in the activity of cFL1-AmDH as we have previously demonstrated,[27] the authors had to use a large amount of whole cells (100 mg$_{DCW}$ mL^{-1}) co-expressing cFL1-AmDH and an NADH oxidase (NOx) *Lactobacillus brevis*[55] in order to resolve 20 mM of **1a**. We have previously determined that LE-AmDH-v1 possess 20-fold reduced IC$_{50}$ and 38-fold reduced K_I values for **1a** as inhibitor compare with cFL1-AmDH; therefore we investigated the kinetic resolution of **1a** at higher substrate concentrations

while keeping constant the amount of LE-AmDH-v1 present in the reaction mixture (90 µM). **Figure 4** shows that 90 µM of LE-AmDH-v1 were sufficient for resolving 50 mM of *rac*-**1a** after 24 h, leading to enantiopure (*S*)-**1a** (conv. 50%) at 30 °C. Elevated *ee* (95% S) and conversion into **1b** (48%) were also obtained at 75mM of **1a**, while KR was not effective at 100 mM of the same substrate (*ee*: 11% *S*) with the conversion into the corresponding ketone to be 14%. Increasing the temperature to 40 °C resulted in full resolution of 75 mM of *rac*-**1a** after 24 h using the same amount of LE-AmDH-v1. The resolution of 100 mM of *rac*-**1a** was also improved by increasing the temperature from 30 °C to 40 °C as the conversion increased from 14% to 57%.
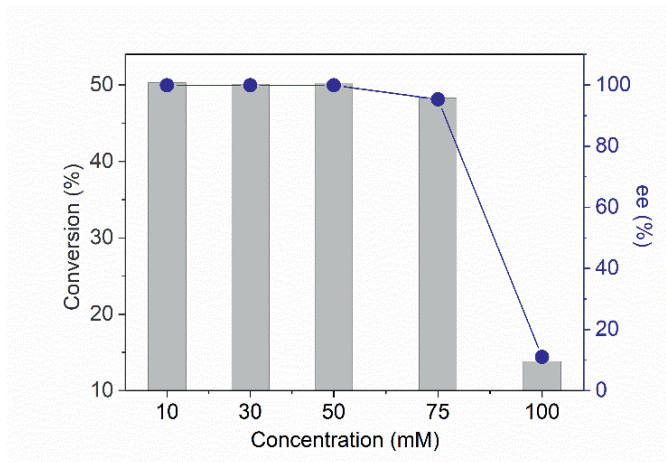
Figure 3. Investigation on the influence of the substrate concentration in the oxidative kinetic resolution of 1a. Reactions were performed at 30 °C using 10 mM of **1a**, 1 mM of NAD+, 90 µM of LE-AmDH-v1 and 10 µM of NOx.

4.3.7 Kinetic resolution in semi-preparative scale.

Finally, the potential usefulness of the LE-AmDH-v1/ NOx system was tested in semi-preparative scale amination starting from 100 mg of *rac*-**1a** (50mM). After 24h, the KR reached completion and resulted in 49.81% conversion into the corresponding ketone **1b**. The ketone formed was removed by extraction with

MTBE under acidic conditions. After basification, the (*S*)-**1a** was obtained with 43.6% isolated yield (theoretical maximum is 50%) and with 99.2% *ee*.

4.3.8 Dynamic kinetic resolution of α-methyl-benzylamine using amine boranes

In this set of reactions, we applied the LE-AmDH-v1 for the DKR of **1a** by using H_3NBH_3 as a racemization catalyst. Starting either from 10 mM or 50 mM of *rac*-**1a** and by adding 4 or 8 eq., of H_3NBH_3 in the reaction mixture we observed no conversion into the corresponding ketone (**1b**). In fact, the amine **1b** was obtained in racemic form (*ee*: 0.8% *S*) indicating no activity by LE-AmDH-v1 at all, possibly due to inhibitory effects of ammonia borane into the activity of LE-AmDH as previously reported for berberine bridge enzyme.[3] As last attempt, we followed a sequential one-pot, two-step procedure in which the KR of **1a** was performed using the optimized process for 24h to yield (*S*)-**1b** (50% conv., >99% *ee*), following by addition of 8 eq. NH_3-BH_3 for another 24h as described in the methods. After that time only **1a** was present in the reaction mixture which was obtained in enantiopure (*S*)-configuration (*ee* >99%). However, analysis of the reaction mixture revealed the ammonia borane complex reduced the remaining ketone to alcohol indicating that the second step was unsuccessful. Incubation of 25 mM **1b** in Tris-HCl pH 7.4 with 4 or 10 equivalents of ammonia borane for 1 h at 30 °C resulted in alcohol formation indicating that the alcohol observed, was formed from the reduction of the remaining ketone by the ammonia-borane after the first 24 h. In another study,[1] more bulky or less water soluble boranes (e.g. morpholine-BH_3 or Me_3N-BH_3) found to also compatible with enzymes employed in deracemization cascades. Therefore we also tested 4 or 8 eq of morpholine borane for the DKR of 50 mM *rac*-**1a**. In both cases the reaction proceeded with 0-10 % *ee* for the (*S*)-configured **1a**. As always, the positive control (without addition of morpholine borane complex) resulted in >99% for (*S*)-**1a** after the reaction time indicating that morpholine borane has a negative effect in the activity of LE-AmDH-v1.

4.3.9 Biocatalytic deracemization cascades employing LE-AmDH-v1 and (S)-selective ω-TAs

Finally we employed the *R* selective LE-AmDH-v1 together with the (*S*)-selective *Vf*-ωTA originated from *Vibrio fluvialis*[4] in the deracemization cascades shown in **scheme 1**. The first cascade requires LDH for cofactor recycling while transforming the pyruvate produced by the ω-TA to L-lactate (**Scheme 1A**). Similarly in the second cascade (**Scheme 1B**), Ala-DH recycles the cofactor while converting the produced pyruvate to L-alanine which is required by the ω-TA. Since *Vf*-ωTA is (*S*)-selective, the remaining 50 % ketone will be converted to the (*S*)-configured amine. These enzymatic cascades were performed using 90 μM of AmDH and 50 μM of ω-TA at substrate concentrations of 25 or 50 mM. After the reported times (see Methods 4.5.5) the reaction mixture of the first cascade contained 19 % or 16 % of the ketone starting from 25 or 50 mM *rac*-**1a**, respectively, while the amine was obtained with 28% or 15% ee for the (*S*)-configured **1a**. A similar scenario was observed with the second case. Starting from 50 mM of *rac*-**1a** the one-pot system proceeded with 15% conversion into **1b**. Analysis of the stereoselective outcome of the cascade revealed the **1a** was obtained in nearly racemic form (*ee* 3% *R*).
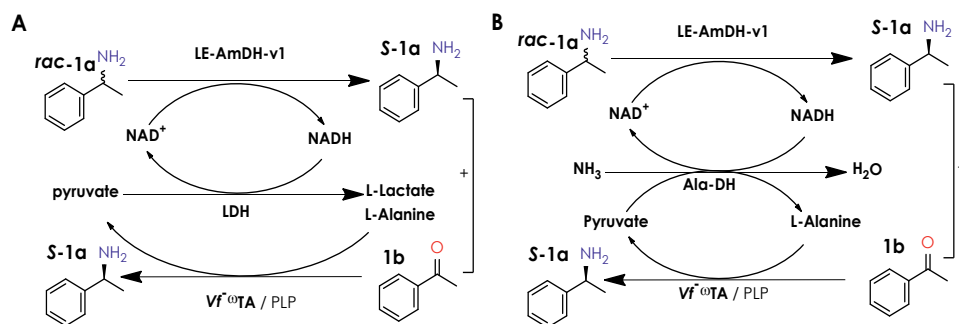
Scheme 1. Enzymatic cascades applied for the deracemization of 1a. (A) Reaction conditions: [substrate]: 25 or 50 mM, [NAD+]: 1 mM, [PLP]: 1 mM [LE-AmDH-v1]: 90 μM, [Vf-ωTA]: 50 μM. [LDH]: 1 mg mL⁻¹, 100 mM Tris-HCl pH 7.3 supplemented with 5 eq. L-alanine, Temperature: 30 °C, Time: 24 h. (B) Reaction conditions: [substrate]: 50 mM, [NAD+]: 1 mM, [PLP]: 1 mM [LE-AmDH-v1]: 90 μM, [Vf-ωTA]: 50 μM. [Ala-DH]: 20 μM, 100 mM KPi pH 7.3 supplemented with 150 mM L-alanine and 100 mM HCOONH₄, Temperature: 30 °C, Time: 24 h.

4.4 Conclusions

In summary, we have applied the recently engineered LE-AmDH-v1 for the kinetic resolution of a selection of substrates that proved to be challenging for the other available AmDHs so far. For instance, only low activities were observed for the reductive amination of **5b** using *Bb*-AmDH, cFL1-AmDH and *Cal*-AmDH[24,25,28] while no activity towards **6b** or **7b** was reported with any of the AmDHs developed up to date. Similarly, cFL1-AmDH performed the reductive amination of respective ketones **1-4b** yielding from poor to moderate conversion after 48 h,[56] and low activity was observed with *Es*-LeuDH (AmDH) for the reductive amination of **1b** and **4b**.[31] In the oxidative deamination direction (KR), only few a-methylbenzylamines could be resolved but at the expense of a large amount of whole cells biocatalysts,[51] and by using a less atom-efficient pyruvate/AlaDH system for NAD$^+$ recycling.[52] Herein, we used the LE-AmDH-v1/NOx system to access pharmaceutically relevant optically active amines in (*S*)-configuration starting from the respective racemic mixtures. The oxidative kinetic resolution proceeded efficiently at the optimum pH of 7.4 in 50 mM Tris-HCl or 100 mM KPi. At 30 °C the KR reached completion after 16 h and the increase of the reaction temperature from 30 °C to 50 °C resulted in the resolution of **1a** within 8 h. Using these optimal conditions the kinetic resolution of a-methylbenzylamines, 1-aminotetralin, 1-aminoindan and 4-aminochroman was complete in all cases with the exception of **3a** which proceeded with 95% ee after 48 h. LE-AmDH-v1 could not be combined with any chemical reducing agent (ammonia borane or morpholine borane) to achieve quantitative yield most possibly due to inhibition of the biocatalyst with these amine borane complexes. In addition, application of LE-AmDH-v1 with the (*S*)-selective ω-transaminase *Vf*-ωTA in deracemization cascades resulted in amine product with low ee.

4.5 Methods

4.5.1 General procedure for biocatalytic oxidative kinetic resolution

Biotransformations were performed in 1.5 mL Eppendorf tubes with a total reaction volume of 0.5 mL. The optimized reaction consisted of NAD$^+$ (1 mM), substrate (10 mM), LE-Am-DHv1 (90 µM) and NOx (10 µM). Reactions were performed at 30 °C for 24 h on orbital shakers (170 rpm) in a horizontal position. The reactions were quenched after 24 h by the addition of aqueous KOH (10 M, 100 µL), the organic compounds were extracted with dichloromethane or ethyl-acetate (2 x 550 µL), dried with magnesium sulfate and the conversions were measured by GC-FID.

4.5.2 Determination of response factors and calculation of final conversions

The Response factors of amines **1-7a** and ketones **1-7b** were determined by GC-FID by comparing the corresponding GC peak areas of amine and ketones at different concentrations of analyte. For a given final concentration (e.g., 5 mM) both the amine and its corresponding ketone (e.g., **1a** and **1b**) were pipetted into the same reaction tube containing the reaction buffer (1 mL, 50 mM Tris-HCl pH 7.34) and incubated at 25 °C for 1 h. After that the mixture was basified with 100 µL of 10 M KOH and split into equal volumes (2 x 500 µL). Each aliquot was extracted with 550 µL of dichloromethane. The organic phases were combined, dried over MgSO$_4$ and analyzed by GC-FID. The obtained areas were plotted against the concentration used. The response factors were calculated by divided the obtained slopes (**Table 1**). Conversions of racemic amines into the corresponding ketones were finally normalized using the response factor of amine:ketone. For instance, the KR of a-chromamine resulted in 43.73 % conversion to a-chromanone. The response factor of a-chromanine to a-chromanone was determined to be 1.28. Multiplying the initial conversion of ketone with the response factor (amine: ketone) resulted in 56.24% as normalized conversion into a-chromanone. The final conversion was calculated by dividing this normalized conversion with the sum of the amine left in the reaction mixture

(%) and the normalized conversion of the ketone (%). The resulted number was multiplied by 100.

4.5.3 pH study for the oxidative kinetic resolution of 1a catalyzed by LE-AmDH-v1

Biocatalytic reactions were performed for different times (0-40 min). In all cases, only data points for which the conversion was below 20 % were considered in order to ensure that the reaction rate was always in the linear range. The product produced (mM) at different times was calculated based on the conversions and plotted versus the time. The velocity of the reaction ($\mu M\ min^{-1}$) was calculated from the obtained slope. Reactions were performed with 10 mM of substrate, 1 mM NAD^+, 45 μM of LE-AmDH-v1 and 3 μM of NOx, in Britton–Robinson's universal buffer (pH 2.5-9.2, 0.5 mL final volume).

4.5.4 Dynamic kinetic resolution using amine boranes

The DKR reactions were performed in 1.5 mL Eppendorf tubes with a total reaction volume of 0.5 mL. The reaction buffer Tris-HCl (50 mM pH 7.3) consisted of NAD^+ (1 mM), substrate (50 mM, 3.029 mg, 0.025 mmol), LE-Am-DH-v1 (90 μM) and NOx (10 μM). In the cases of the two-step one-pot reactions, the reactions were performed at 30 °C for 24 h on orbital shakers (170 rpm) to allow kinetic resolution to reach completion. After that time, the ammonia borane complex was added (4 eq., 3.087 mg, 1 mmol or 8 eq., 6.174 mg, 2 mmol) and the reaction was run for another 24 h. For the reaction with morpholine borane, 10.1 mg (4 eq.) or 20.2 mg (8 eq.) were added into the reaction mixture (0.5 mL, 50 mM of substrate) and the reactions were run for 24 h. The amine borane complexes were quenched by the addition of concentrated HCl (~ 300 μL) and after basification with 10 M KOH (pH >10) the reaction mixture was extracted with ethyl acetate (2 x 500 μL).

4.5.5 Biocatalytic deracemization cascades employing LE-AmDH-v1 and S selective ω-TAs

For the deracemization cascade shown in **scheme 1A**, reactions of 1 mL consisted of 100 mM Tris-HCl buffer pH 7.3 supplemented with NAD^+ (1 mM), PLP

(0.5 mM), L-alanine 150 mM and *rac*-**1a** (25 or 50 mM). The (*S*)-selective *Vf-ωTA* (50 µM), and the *R* selective LE-AmDH-v1 were added together with LDH (1 mg mL^{-1}) and the reactions were run at 30 °C for 24 h on orbital shakers (170 rpm) in a horizontal position. For the deracemization cascade shown in **scheme 1B** reactions of 1 mL consisted of 100 mM KPi buffer pH 7.3 supplemented with HCOONH$_4$ (100 mM), L-alanine (150 mM), NAD$^+$ (1 mM) and PLP (0.5 mM). *Vf-ωTA* and LE-AmDH-v1 were added at the final concentrations of 50 µM and 90 µM, respectively. Finally, Ala-DH (20 µM) was added and the reactions were run at 30 °C for 24 h on orbital shakers (170 rpm) in a horizontal position. The organic compounds were extracted with dichloromethane or ethyl-acetate (2 x 500 µL), dried with magnesium sulfate and the conversions were measured by GC-FID.

4.5.6 Analytical methods for the determination of conversions and of the absolute configurations

The conversions for the enantioselective oxidative deamination (KR) were determined by GC using a 7890A GC system (Agilent Technologies), equipped with a FID detector using H$_2$ as carrier gas and a DB-1701 column from Agilent (30 m, 250 µm, 0.25 µm). The following method was used: constant pressure 6.9 psi, split ratio 40:1, T injector 250 °C. Temperature Program: T initial 60 °C, hold 6.5 min, gradient 20 °C/min up to 100 °C; hold 1 min, gradient 20 °C/min up to 280 °C; hold 1 min.

After the extraction of the obtained amines, a solution of DMAP (50 mg) in 1 mL of acetic anhydride was prepared. In total, 50 µL of this solution were added to the organic phase containing 25 mM of the obtained amine(*i.e.* for reactions with 50 mM of *rac* amine substrate). The mixtures were shaken at 25 °C for 30 min. After that, 500 µL of water was added and shaken for another 30 min at 25 °C. The samples were centrifuged for 10 min at 14.800 rpm and the organic phases were dried with magnesium sulfate prior to injection in a Chrompack Chiracel Dex-CB column (length 25 m, internal diameter 0.32 mm). The following method was used: constant Flow: 1.4 mL/min, split ratio 40:1, T injector 200 °C. Temperature Program: T initial 100 °C, hold 2 min, gradient 1°C/min up to 130 °C;

hold 5 min, gradient 10 °C/min up to 170 °C; hold 10 min, gradient 10 °C/min up to 180 °C; hold 1 min

4.5.7 Dynamic kinetic resolution in semi-preparative scale

Preparative scale reactions of 1a (50 mM, 100 mg, 0.825 mmol) was performed in a total volume of 16.5 mL of Tris-HCl buffer (50 mM, pH 7.4) at 30 °C. The reaction mixture contained LE-AmDH-v1 (90 µM, 4 mg mL^{-1}), NOx (10 µM, 0.5 mg mL^{-1}), NAD$^+$ (1 mM). After 24 h, a 49.81% conversion was obtained for **1b.** The reaction was acidified with concentrated HCl (~1 mL) the ketone formed was extracted with MTBE (2 x 20 mL). After the addition of KOH (10 M, ~1 mL), the amine products were extracted with MTBE (3 x 20 mL). The combined organic layers were dried over MgSO$_4$ and concentrated under reduced pressure. Avoiding any further purification step, (*S*)-**1b** was obtained with 43.6% isolated yield (colorless liquid, 43.1mg, 0.356 mmol) and with 99.2% ee.

4.6 References

1   Wittcoff, H. A., Rueben, B. G. & Plotkin, J. S. *Industrial Organic Chemicals, 2nd ed.*, (Wiley-Interscience, New York, 2004).

2   Ghislieri, D. & Turner, N. J. *Top. Catal.* **57**, 284-300, doi:10.1007/s11244-013-0184-1 (2013).

3   Constable, D. J. C. *et al. Green Chem.* **9**, 411-420, doi:10.1039/b703488c (2007).

4   Nugent, T. C. *Chiral amine synthesis: Methods, Developments and Applications*. (Wiley-VCH, 2010).

5   Slabu, I., Galman, J. L., Lloyd, R. C. & Turner, N. J. *ACS Catal.* **7**, 8263-8284, doi:10.1021/acscatal.7b02686 (2017).

6   Guo, F. & Berglund, P. *Green Chem.* **19**, 333-360, doi:10.1039/c6gc02328b (2017).

7   Kelly, S. A. *et al. Chem. Rev.* **118**, 349-367, doi:10.1021/acs.chemrev.7b00437 (2018).

8   Gomm, A. & O'Reilly, E. *Curr. Opin. Chem. Biol.* **43**, 106-112, doi:10.1016/j.cbpa.2017.12.007 (2018).

9   D. Patil, M., Grogan, G., Bommarius, A. & Yun, H. *Catalysts* **8**, 254, doi:10.3390/catal8070254 (2018).

10   Fuchs, M., Farnberger, J. E. & Kroutil, W. *Eur. J. Org. Chem.*, 6965-6982, doi:10.1002/ejoc.201500852 (2015).

11   Savile, C. K. *et al. Science* **329**, 305-309, doi:10.1126/science.1188934 (2010).

12   Pavlidis, I. V. *et al. Nat. Chem.* **8**, 1076-1082, doi:10.1038/nchem.2578 (2016).

13   Sharma, M., Mangas-Sanchez, J., Turner, N. J. & Grogan, G. *Adv. Synth. Catal.* **359**, 2011-2025, doi:10.1002/adsc.201700356 (2017).

14   Mangas-Sanchez, J. *et al. Curr. Opin. Chem. Biol.* **37**, 19-25, doi:10.1016/j.cbpa.2016.11.022 (2017).

15   Patil, M. D., Grogan, G., Bommarius, A. & Yun, H. *ACS Catal.*, 10985-11015, doi:10.1021/acscatal.8b02924 (2018).

16   Dong, J. *et al. Angew. Chem. Int. Ed.* **57**, 9238-9261, doi:10.1002/anie.201800343 (2018).

17   Aleku, G. A. *et al. Nat. Chem.*, **10**, 961-967, doi:10.1038/nchem.2782 (2017).

18   Wetzl, D. *et al. ChemCatChem* **8**, 2023-2026, doi:10.1002/cctc.201600384 (2016).

19   Scheller, P. N., Lenz, M., Hammer, S. C., Hauer, B. & Nestl, B. M. *ChemCatChem* **7**, 3239-3242, doi:10.1002/cctc.201500764 (2015).

20   Roiban, G.-D. *et al. ChemCatChem* **9**, 4475-4479, doi:10.1002/cctc.201701379 (2017).

21   Schober, M. *et al. Nat. Catal.* **2**, 909-915, doi:10.1038/s41929-019-0341-4 (2019).

22   Matzel, P., Gand, M. & Höhne, M. *Green Chem.* **19**, 385-389, doi:10.1039/c6gc03023h (2017).

23   Abrahamson, M. J., Vazquez-Figueroa, E., Woodall, N. B., Moore, J. C. & Bommarius, A. S. *Angew. Chem. Int. Ed.* **51**, 3969-3972, doi:10.1002/anie.201107813 (2012).

24   Abrahamson, M. J., Wong, J. W. & Bommarius, A. S. *Adv. Synth. Catal.* **355**, 1780-1786, doi:10.1002/adsc.201201030 (2013).

25   Bommarius, B. R., Schurmann, M. & Bommarius, A. S. *Chem. Commun.* **50**, 14953-14955, doi:10.1039/c4cc06527a (2014).

26   Knaus, T., Böhmer, W. & Mutti, F. G. *Green Chem.* **19**, 453-463, doi:10.1039/c6gc01987k (2017).

27   Tseliou, V., Knaus, T., Masman, M. F., Corrado, M. L. & Mutti, F. G. *Nat. Commun.* **10**, 3717, doi:10.1038/s41467-019-11509-x (2019).

28   Pushpanath, A., Siirola, E., Bornadel, A., Woodlock, D. & Schell, U. *ACS Catal.* **7**, 3204-3209, doi:10.1021/acscatal.7b00516 (2017).

29   Chen, F.-F. *et al. ACS Catal.* **8**, 2622-2628, doi:10.1021/acscatal.7b04135 (2018).

30   Ye, L. J. *et al. ACS Catal.* **5**, 1119-1122, doi:10.1021/cs501906r (2015).

31   Lowe, J., Ingram, A. A. & Groger, H. *Bioorg. Med. Chem.* **26**, 1387-1392, doi:10.1016/j.bmc.2017.12.005 (2018).

32   Mayol, O. *et al. Nat. Catal.* **2**, 324-333, doi:10.1038/s41929-019-0249-z (2019).

33   Mayol, O. *et al. Catal. Sci. Technol.* **6**, 7421-7428, doi:10.1039/c6cy01625a (2016).

34   Bartsch, S. & Vogel, A. in *Science of Synthesis, Biocatalysis in Organic Synthesis 2, Chapter 2.3.3 Addition of Ammonia and Amines to C=C Bonds* (eds K. Faber, W.-D. Fessner, & N. J. Turner) 291-311 (Georg Thieme Verlag KG, 2015).

35   Li, R. *et al. Nat. Chem. Biol.* **14**, 664-670, doi:10.1038/s41589-018-0053-0 (2018).

36   Cho, I. *et al. Angew. Chem. Int. Ed.* **58**, 3138-3142, doi:10.1002/anie.201812968 (2019).

37   Prier, C. K., Zhang, R. K., Buller, A. R., Brinkmann-Chen, S. & Arnold, F. H. *Nat. Chem.* **9**, 629-634, doi:10.1038/nchem.2783 (2017).

38   Musa, M. M., Hollmann, F. & Mutti, F. G. *Catal. Sci. Technol.* **9**, 5487-5503, doi:10.1039/c9cy01539f (2019).

39   Verho, O. & Backvall, J. E. *J. Am. Chem. Soc.* **137**, 3996-4009, doi:10.1021/jacs.5b01031 (2015).

40   Schrittwieser, J. H., Velikogne, S., Hall, M. & Kroutil, W. *Chem. Rev.* **118**, 270-348, doi:10.1021/acs.chemrev.7b00033 (2018).

41   Shin, J.-S. & Kim, B.-G. *Biotechnol. Bioeng.* **60**, 534-540, doi:10.1002/(sici)1097-0290(19981205)60:5<534::aid-bit3>3.0.co;2-l (1998).

42   Turner, N. J. *Curr. Opin. Chem. Biol.* **14**, 115-121, doi:10.1016/j.cbpa.2009.11.027 (2010).

43   Dunsmore, C. J., Carr, R., Fleming, T. & Turner, N. J. *J. Am. Chem. Soc.* **128**, 2224-2225, doi:10.1021/ja058536d (2006).

44   Ghislieri, D. *et al.* *J. Am. Chem. Soc.* **135**, 10863-10869, doi:10.1021/ja4051235 (2013).

45   Yasukawa, K., Nakano, S. & Asano, Y. *Angew. Chem. Int. Ed.* **53**, 4428-4431, doi:10.1002/anie.201308812 (2014).

46   Heath, R. S., Pontini, M., Bechi, B. & Turner, N. J. *ChemCatChem* **6**, 996-1002, doi:10.1002/cctc.201301008 (2014).

47   Li, G. *et al.* *ACS Catal.* **4**, 903-908, doi:10.1021/cs401065n (2014).

48   Leisch, H., Grosse, S., Iwaki, H., Hasegawa, Y. & Lau, P. C. K. *Can. J. Chem.* **90**, 39-45, doi:10.1139/v11-086 (2012).

49   Herter, S. *et al.* *Bioorg. Med. Chem.* **26**, 1338-1346, doi:10.1016/j.bmc.2017.07.023 (2018).

50   Batista, V. F., Galman, J. L., G. A. Pinto, D. C., Silva, A. M. S. & Turner, N. J. *ACS Catal.* **8**, 11889-11907, doi:10.1021/acscatal.8b03525 (2018).

51   Jeon, H. *et al.* *Catalysts* **7**, 251, doi:10.3390/catal7090251 (2017).

52   Patil, M. D. *et al.* *Catalysts* **9**, 600, doi:10.3390/catal9070600 (2019).

53   Aleku, G. A. *et al.* *ChemCatChem* **10**, 515-519, doi:10.1002/cctc.201701484 (2018).

54   Yoon, S. *et al.* *ChemCatChem*, **11**, 1898-1902, doi:10.1002/cctc.201900080 (2019).

55   Geueke, B., Riebel, B. & Hummel, W. *Enzyme Microb. Technol.* **32**, 205-211, doi: 10.1016/S0141-0229(02)00290-9 (2003).

56   Knaus, T., Böhmer, W. & Mutti, F. G. *Green Chemistry* **19**, 453-463, doi:10.1039/C6GC01987K (2017).

Chapter 5

Exploiting the catalytic promiscuity of *L*-lysine-ε-dehydrogenase for the enzymatic synthesis of primary alcohols and (a)chiral amines

5.1 Abstract

L-lysine-ε-dehydrogenase (LysEDH) from *Geobacillus stearothermophilus* naturally catalyzes the oxidative deamination of the ε-amino group of *L*-lysine. Recently, this enzyme was found to be capable of converting aromatic aldehydes into primary alcohols. Herein, we exploited the promiscuous catalytic activity of LysEDH and created enzymes that exhibit increased activity for the reduction of a wide range of benzylic aldehydes to primary alcohols. Interestingly, these novel engineered alcohol dehydrogenases (ADHs) also catalyzed the reductive amination of a variety carbonyl containing compounds with excellent enantioselectivity. We envisioned that the bi-functionality of the enzymes could be harnessed for the direct conversion of alcohols to amines. As a proof of principle, we were able to perform an unprecedented one-pot hydrogen-borrowing cascade of benzyl alcohol to benzylamine using a single enzyme (5% analytical yield). Conducting the same biocatalytic cascade in the presence of cofactor recycling enzymes (NADH-oxidase and formate dehydrogenase), increased the yields up to 34%. This work provides the first examples of enzymes showing 'alcohol aminase' activity.

5.2 Introduction

During the past decades, catalytic enzyme promiscuity has been exploited for the generation of novel enzymes that are able to catalyse alternative chemical reactions than the 'natural' ones.[1-4] These promiscuous enzymes served as excellent starting points for the evolution of enzymes possessing novel catalytic activities.[5,6] Indeed, it was shown that even a few point mutations can enhance a promiscuous activity by several orders of magnitude.[7] In the past, we and others have studied this phenomenon. For instance, we have exploited the catalytic promiscuity of amine dehydrogenases (AmDHs) for the synthesis of secondary or tertiary amines.[8] In another work by our group, we have also shown that the promiscuous activity of galactose oxidase enables the efficient synthesis of nitriles,[9] although this enzyme was engineered for the oxidation of alcohols.

Oxidation of alcohols to aldehydes or ketones can be accomplished using alcohol dehydrogenases (ADHs). ADHs are NAD(P)H dependent oxidoreductases that catalyze the reversible reduction of aldehydes and ketones to their corresponding alcohols.[10-12] ADHs have been commonly studied for the asymmetric reduction of ketones to the corresponding chiral alcohols, for the deracemization of secondary alcohols via stereoconversion;[13] furthermore, they have been applied in cascade processes that entail a ketone intermediate formed by ADH-catalyzed oxidation.[14,15] However, the use of ADHs for the aerobic oxidation of primary alcohols has not been frequently applied possibly due to the scarce availability of primary ADHs although this reaction is also gaining more interest recently.[12] In the past, the conversion of aromatic aldehydes to primary alcohols (and vice versa) has been achieved with engineered or wild-type ADHs mainly originating from *Bacillus stearothermophilus,*[16] *Saccharomyces cerevisiae*,[17] *Acinetobacter calcoaceticus*,[18] *Sulfolobus solfataricus*[19] and horse livers.[20] The applicability of these enzymes has also been demonstrated in the hydrogen borrowing amination of alcohols when combined with AmDHs.

Amine dehydrogenases (AmDHs) catalyze the reductive amination of carbonyl compounds at the sole expense of ammonia and a hydride source. Because of their impressive enantioselectivities they have been applied for the synthesis of enantiopure a-chiral amines.[21-23] Since the pioneering work of Bommarius and coworkers,[24] the toolbox of AmDHs have been significantly expanded either by engineering L- amino acid dehydrogenases or by the discovery of native AmDHs (nat-AmDHs) using metagenomic data.[24-29] We have recently created an AmDH by introducing the F173A mutation into *L*-lysine-(ε-deaminating)-dehydrogenase (LysEDH) scaffold that normally catalyzes the oxidative ε-deamination of *L*-lysine.[30] This single mutation created a new hydrophobic cavity capable of accommodating small aromatic ketones that were converted into a-chiral amines. However, we recently observed that the *wild type* LysEDH is also able to produce primary alcohols starting from aromatic aldehydes.

Herein, starting from this promiscuous enzyme scaffold, we were able to obtain enzymes that showed both AmDH and ADH activity. The additional mutations introduced in the scaffold of *L*-lysine-(ε-deaminating)-dehydrogenase resulted either in AmDHs with increased catalytic performance for the reductive amination of carbonyl-containing compounds compared with the previously reported AmDH from the same scaffold (LE-AmDH-v1) or in ADHs with superior catalytic activity for the reduction of aldehydes to alcohols compared with the wild type enzyme. Notably, by controlling the conditions of the reactions, these variants could produce exclusively either amines or alcohols. As amine dehydrogenases, these enzymes were highly enantioselective and afforded (*R*)-configured amines with >99% *ee*. As ADHs, the enzymes proved to be excellent catalysts for the synthesis of primary alcohols. This bi-functional role of the enzymes was harnessed for the direct conversion of benzyl alcohol to benzylamine using two cascades. As a proof of principle we were able to obtain the amine product confirming an unprecedented 'alcohol aminase' behavior by these catalysts.

5.3 Results and discussion

5.3.1 Substrate selection

A range of carbonyl containing compounds were tested in this study. Group A (**Scheme 1**) consists of aromatic aldehydes and was tested both in the reductive amination reaction and in the reduction to the corresponding alcohols (**1-19a**). Group B, aromatic and aliphatic ketones, were tested in the reductive amination reaction. The aldehydes of Group A (**1-19b**), their corresponding alcohols (**1-19a**) and amines (**1-19c**) were first tested if they could be extracted from aqueous media; this evaluation was accomplished by comparing the obtained response factors (area of the compound divided with the area of internal standard) with the response factors obtained from reference compounds directly prepared in organic solvent. Due to their known high volatility after prolonged incubation as during the biocatalytic reaction, these compounds were incubated in the reaction buffer for 24 h and, after extraction, the obtained response factors were compared with the ones obtained from the reference compounds directly prepared in organic solvent. A possible interaction of these compounds with the residues of the enzyme was also excluded by preparing the same reference compounds in the presence of the enzyme. As always, the obtained response factors were compared with the response factors initially obtained. Only those aldehydes that showed response factors ≥60% (compare with the response factors of the same compounds directly prepared in to the organic solvents) were used; these compounds are depicted in **Scheme 1.** All results are summarized in **Table 1** (for more details about the preparation of the reference compounds and data analysis see methods, section 5.5.2).
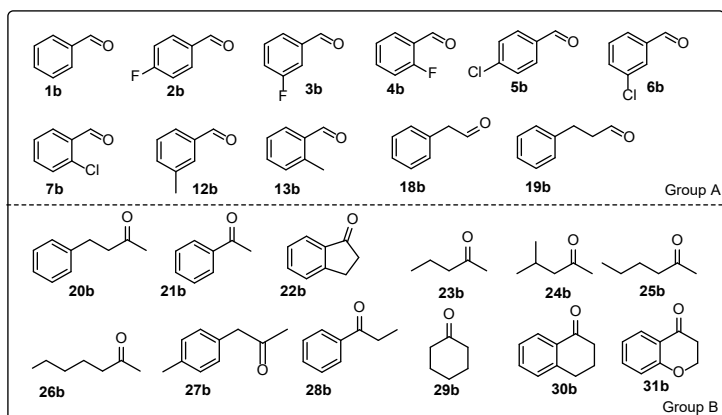
Figure 1. List of compounds used in this study. Group A was used for the reductive amination and the reduction to alcohols, while group B was used only for the reductive amination reactions.

Table 1. Response factors in percentage calculated for aldehydes (group A) under different conditions. The response factor of the references directly prepared in organic solvent is considered as 100%.

Compound	Response factor (RF)			
	Prepared in Organic solvent	Extracted from buffer	Incubated for 24 h	In presence of enzyme
1a	1.18 (100%)	1.12 (95%)	1.09 (92%)	1.11 (94%)
1b	1.01 (100%)	0.97 (96%)	0.86 (86%)	0.88 (88%)
1c	0.88 (100%)	0.75 (85%)	0.77 (88%)	0.79 (90%)
2a	1.16 (100%)	1.12 (96%)	1.12 (96%)	1.12 (97%)
2b	1.04 (100%)	0.98 (94%)	0.88 (85%)	0.91 (87%)
2c	1.09 (100%)	1.14 (104%)	1.12 (102%)	1.14 (104%)
3a	1.01 (100%)	1.03 (103%)	1.05 (104%)	1.05 (104%)
3b	0.98 (100%)	0.95 (97%)	0.83 (85%)	0.83 (85%)
3c	1.10 (100%)	1.10 (99%)	1.06 (96%)	1.08 (98%)
4a	1.11 (100%)	1.09 (99%)	1.09 (98%)	1.14 (103%)
4b	0.93 (100%)	0.89 (97%)	0.76 (82%)	0.75 (81%)
4c	1.05 (100%)	1.02 (97%)	1.01 (96%)	1.01 (96%)

Compound	Response factor (RF)			
	Prepared in Organic solvent	Extracted from buffer	Incubated for 24 h	In presence of enzyme
5a	1.09 (100%)	1.12 (103%)	1.16 (107%)	1.15 (106%)
5b	1.04 (100%)	1.04 (100%)	0.79 (76%)	0.76 (73%)
5c	1.17 (100%)	1.18 (100%)	1.13 (97%)	1.16 (99%)
6a	0.98 (100%)	0.97 (98%)	0.95 (96%)	0.98 (99%)
6b	0.54 (100%)	0.52 (98%)	0.33 (62%)	0.34 (63%)
6c	N.D.	N.D.	N.D.	N.D.
7a	1.14 (100%)	1.19 (104%)	1.18 (103%)	1.18 (103%)
7b	1.01 (100%)	0.97 (95%)	0.53 (53%)	0.58 (57%)
7c	N.D.	N.D.	N.D.	N.D.
12a	1.32 (100%)	1.34 (102%)	1.34 (102%)	1.37 (104%)
12b	1.19 (100%)	1.15 (96%)	0.78 (66%)	0.81 (68%)
12c	1.19 (100%)	1.24 (104%)	1.24 (104%)	1.27 (106%)
13a	1.15 (100%)	1.18 (103%)	1.11 (97%)	1.11 (97%)
13b	1.08 (100%)	1.04 (96%)	0.72 (66%)	0.76 (70%)
13c	1.32 (100%)	1.29 (98%)	1.24 (94%)	1.26 (95%)
18a	1.09 (100%)	0.91 (84%)	1.01 (93%)	1.01 (93%)
18b	0.99 (100%)	0.85 (86%)	0.72 (73%)	0.46 (46%)
18c	1.28 (100%)	1.06 (83%)	1.04 (81%)	1.09 (85%)
19a	1.15 (100%)	1.04 (90%)	1.10 (95%)	1.11 (96%)
19b	1.06 (100%)	0.96 (90%)	0.96 (90%)	0.73 (69%)
19c	1.44 (100%)	1.47 (102%)	1.48 (103%)	1.47 (102%)

N.D.: Not determined

5.3.2 Reductive aminations of aldehydes

The reductive amination of aldehydes was performed using the WT LysEDH, the LE-AmDH-v1[30]—that showed high activity for the reductive amination of

benzaldehyde—and four other variants that were originally designed to accommodate bulky-bulky ketones in different binding poses. These variants were obtained by mutation of the residues involved in the interaction of the enzyme's active site with the amino group of the natural substrate L-lysine (Y238A and/or T240A). Combining these mutations with the F173A or F173S resulted in variants: Y238A/F173A   (LE-AmDH-v22),   Y238A/F173S   (LE-AmDH-v24), Y238A/T240A/F173A (LE-AmDH-v25), Y238A/T240A/F173S (LE-AmDH-v27). The F173A mutation was included in order for the enzymes to retain the previously engineered amine dehydrogenase activity, while serine was introduced further in order to investigate the effects of a hydrophilic, yet not bulky residue in this position. In all of the reactions, two blank samples were included. Only the cofactor but no enzymes were present in blank 2, whereas in the blank 1 the FDH was also present to exclude any product (amine) or by byproduct (e.g., alcohol) formation as a result of the action of the cofactor-recycling enzyme alone. All biocatalytic reactions with aldehydes as substrates were analyzed using internal standards as described in methods. Therefore, both the conversions and the analytical yields could be accurately determined based on these response factors. **Table 2** summarizes the results obtained for the reductive aminations reactions. It is evident that all variants bearing the F173A mutation performed better in the reductive amination of aldehydes than variants containing the F173S mutation. Among these variants, LE-AmDH-v22 possess the highest catalytic activity followed by LE-AmDH-v1. Among the variants containing the F173S mutation, the highest analytical yields for the amine formation were obtained with the double variant LE-AmDH-v24. No amine formation was observed in any of the blank reactions, thus indicating that the LE-AmDHs catalyze the reductive aminations. In some cases, we observed that the wild type LysEDH as well as both variants containing the F173S mutation, produced alcohols as by-products. In contrast, none of the reactions with LE-AmDHs variant possessing the F173A mutation resulted in any alcohol formation; alcohol formation was also not observed in the blank samples hence indicating that the introduction of F173S favored the formation of alcohols. This was further

confirmed in biocatalytic reactions that were performed in ammonia-free environment as described later in this chapter.

Table 2. Reductive amination of aromatic aldehydes catalyzed by LE-AmDHs variants.

Enzyme		1b	2b	3b	4b	5b	12b	13b	18b	19b
WT	Conversion (%)	62	70	19	22	17	1	0	16	54
	Amine yield (%)	17	23	0	2	0	0	0	0	0
	Alcohol yield (%)	35	28	12	0	0	0	0	0	20
LE-AmDH-v1	Conversion (%)	>99	>99	85	>99	19	3	97	15	50
	Amine yield (%)	>99	90	74	98	3	6	91	0	0
	Alcohol yield (%)	0	0	0	0	0	0	0	0	11
LE-AmDH-v22	Conversion (%)	>99	>99	>99	>99	26	15	97	19	43
	Amine yield (%)	>99	89	99	>99	11	13	92	0	0
	Alcohol yield (%)	0	0	0	0	0	0	0	0	9
LE-AmDH-v24	Conversion (%)	94	58	28	71	16	2	3	18	49
	Amine yield (%)	80	34	11	54	1	0	6	0	0
	Alcohol yield (%)	0	0	6	0	4	0	0	0	15
LE-AmDH-v25	Conversion (%)	>99	>99	85	>99	16	6	92	19	31
	Amine yield (%)	>99	91	74	>99	5	8	87	0	0
	Alcohol yield (%)	0	0	0	0	0	0	0	0	0
LE-AmDH-v27	Conversion (%)	97	84	46	63	44	8	3	22	65
	Amine yield (%)	52	36	4	44	0	0	6	0	0
	Alcohol yield (%)	22	28	30	0	18	0	0	0	33
Blank 1	Conversion (%)	9	0	3	4	0	2	0	17	14
	Amine yield (%)	0	0	0	0	0	0	0	0	0
	Alcohol yield (%)	0	0	0	0	0	0	0	0	0
Blank 2	Conversion (%)	1	0	0	2	0	0	0	15	0
	Amine yield (%)	0	0	0	0	0	0	0	0	0

Enzyme	1b	2b	3b	4b	5b	12b	13b	18b	19b
Alcohol yield (%)	0	0	0	0	0	0	0	0	0

Experimental conditions: 1 mL final volume in Eppendorf tubes; buffer: ammonium formate 2 M pH 8.2-9.0; T: 30 °C; reaction time: 24 h; agitation orbital shaker (170 rpm); [substrate]: 20 mM; [NAD$^+$]: 1 mM; [LysEDH]: 45 µM; [Cb-FDH]: 16 µM. Blank 1: reaction without LE-AmDH, Blank 2: reaction without LE-AmDH and FDH

The conversion and yield depicted here are the average values obtained from four independent experiments.

5.3.3 Reductive amination of ketones

The applicability and stereoselectivity of the LE-AmDHs were further investigated in the reductive amination of ketones (**Scheme 1**, group B). Ketones are known to be more stable and less volatile than aldehydes, therefore the use of reference compounds for the determination of the response factors was not strictly necessary in these cases (i.e., response factors of ketone and related amine are very similar when using GC-FID analysis). In this set of reactions, the four variants: LE-AmDH-v22, -v24, -v25 and –v27 were tested for the reductive amination of a diverse panel of ketones. The LE-AmDH-v1 was already tested for the reductive amination of most of these compounds in our previous study. These results are also included here for comparison (**Table 3**). The reactions were performed at 50 °C for 48 h, since we have shown that LE-AmDH-v1 is highly thermostable and its kinetics are accelerated at higher temperatures.[30] We therefore assumed that the other variants would also exhibit similar thermostable behavior. In agreement with the results obtained for the reductive amination of aldehydes, **Table 3** shows that LE-AmDH-v22 was the most active variant for the reductive amination of ketones, exhibiting similar or even higher conversions than LE-AmDH-v1. In fact, LE-AmDH-v22 showed the highest catalytic activity among all variants tested. Interestingly the LE-AmDH-v25, containing the same mutations as LE-AmDH-v22 and the additional mutations T240A, led to lower conversions for the ketones tested. This is likely due to the larger volume of the active site of this variant that enables a higher flexibility of the substrate into the binding pocket of LE-AmDH-v25. The increased flexibility possibly affects the crucial distance

between the prochiral carbon of the substrate and the hydride of the cofactor. This hypothesis is supported further by the fact that this variant was the only one capable of aminating the larger substrate **27b**, albeit with low conversion (5%). Notably, all variants bearing the F173S mutation (LE-AmDH-v24 and LE-AmDH-v27) showed a dramatic decrease of the conversion for the prochiral ketones tested, thus indicating that the introduction of the hydrophilic serine in this new binding cavity has a major impact in the accommodation of small hydrophobic substrates. In all cases in which we were able to obtain information about the stereoselective outcome of these reactions, the amines were always obtained with >99% ee for the (*R*)-configured product.

Table 3. Reductive amination of ketones catalyzed by LE-AmDHs variants.

		20b	21b	23b	24b	25b	26b	27b	28b	29b	30b	31b
LE-AmDH-v1	Conv.(%)	0	>99	86	76	87	-	0	99	-	79	82
	ee (%) R	N.D.	>99.9	89	97	>99			>99.9		>99	99.4
LE-AmDH-v22	Conv.(%)	0	97	52	83	93	13	0	97	85	80	99
	ee (%) R	N.D.	>99	>99	>99	>99	N.D.	N.D.	>99	N.A.	>99	>99
LE-AmDH-v24	Conv.(%)	0	50	3	0	8	0	0	50	5	9	41
	ee (%) R	N.D.	>99	N.D.	N.D.	N.D.	N.D.	N.D.	>99	N.A.	>99	>99
LE-AmDH-v25	Conv.(%)	0	84	32	53	53	10	5	84	75	64	85
	ee (%) R	N.D.	>99	>99	>99	>99	N.D	N.D.	>99	N.A.	>99	>99
LE-AmDH-v27	Conv.(%)	0	34	1	0	0	0	1	34	7	12	27
	ee (%) R	N.D.	>99	N.D.	N.D.	N.D.	N.D.	N.D.	>99	N.A.	>99	>99
Blank 1	Conv.(%)	0	0	0	0	0	0	0	0	0	0	0
	ee (%) R	N.D.	N.D.	N.D.	N.D.	N.D.	N.D.	N.D.	N.D.	N.D.	N.D.	N.D.
Blank 2	Conv.(%)	0	0	0	0	0	0	0	0	0	0	0
	ee (%) R	N.D.	N.D.	N.D.	N.D.	N.D.	N.D.	N.D.	N.D.	N.D.	N.D.	N.D.

Experimental conditions: 0.5 mL final volume in Eppendorf tubes; buffer: ammonium formate 2 M pH 9.0; T: 50 ºC; reaction time: 48 h; agitation orbital shaker (170 rpm);

[substrate]: 10 mM; [NAD⁺]:1 mM; [LysEDH]: 90 µM; [Cb-FDH]: 16 µM. Blank 1: reaction without LE-AmDH, Blank 2: reaction without LE-AmDH and FDH
N.D.: Not determined, N.A.: Not applicable

5.3.4 Investigation of the optimal reaction conditions for the reduction of aldehydes to alcohols

As reported before, when the WT LysEDH and variants LE-AmDH-v24 and -v27 were tested for the reductive amination of aldehydes, we observed formation of alcohols. LE-AmDH-v27 produced the highest amount of alcohol among all enzymes tested. We envisioned that this promiscuous activity could be increased in an ammonia free environment under the optimized conditions. Therefore the LE-AmDH-v27 was applied in a series of optimization studies for the reduction of benzaldehyde to benzylalcohol. Initially, the pH optimum for this biocatalytic transformation was investigated using the Britton-Robinson's universal buffer in pH range values 6.5-9.0. Results (**Figure 1**) showed that the highest velocity (µM min⁻¹) was obtained at pH 7.0. In contrast, we have previously reported that the reductive amination reaction proceeds better at increased pH values (pH 9.0-9.5).[30] However, at this pH, the rate of the reduction of benzaldehyde to benzylalcohol was reduced approx. 4 times compared with the rates obtained at pH 7.0.
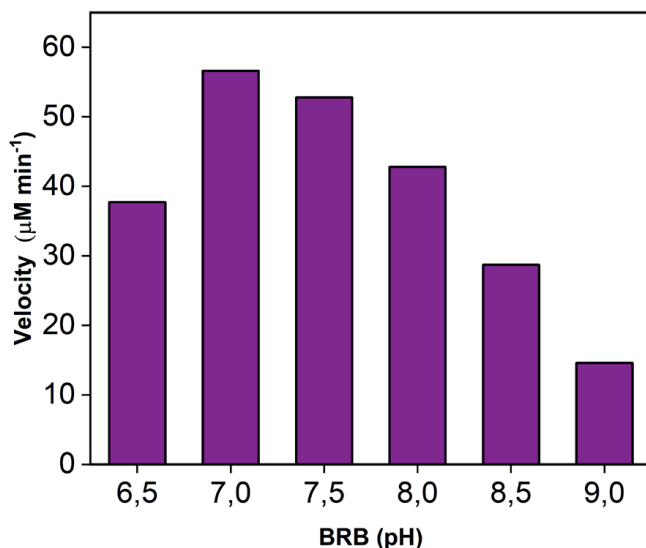
Figure 2. pH optimum for the reduction of benzaldehyde to benzylalcohol using the LysEDH variant.

In the next step, the progress of the reduction of benzaldehyde to benzylalcohol was monitored using several buffers all prepared at pH 7 (see methods). In total, five different buffers (HEPES, Tris, MOPS, KPi, NaH_2PO_4) were tested, all prepared at 100 mM and pH 7.0. **Figure 3** summarizes the analytical yield (expressed in mM) of the produced alcohol. These results show that the reactions proceeded almost equally well in all buffers tested. The enzyme showed no preference for a certain type of buffer since the reactions always resulted in ≥98.6% conversion and ≥18.84 mM of benzyl alcohol produced after 24h. Therefore, the KPi buffer was chosen for further experiments.
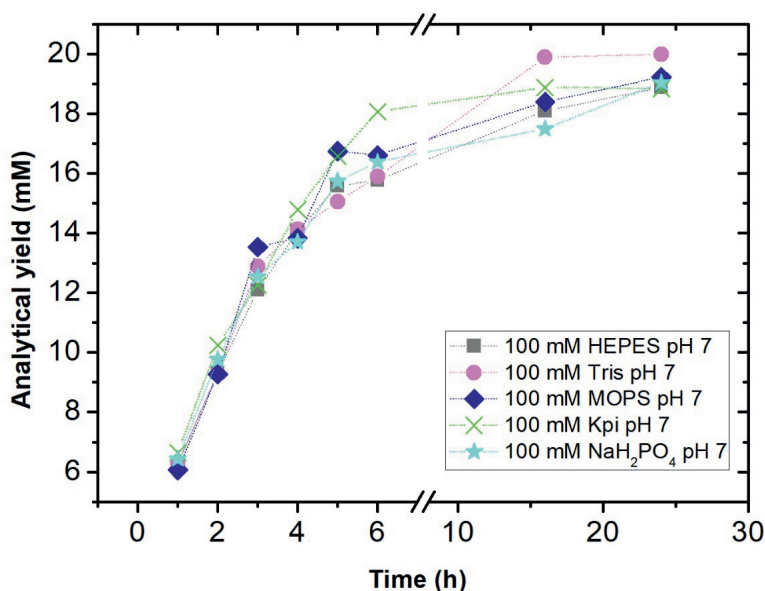
Figure 3 Progress of the reduction of benzaldehyde to benzylalcohol at different types of buffers.

5.3.5 Reduction of aldehydes to alcohols

After amine dehydrogenase (AmDH) activity was confirmed, we investigated the promiscuous ADH activity of the LE-AmDHs. The six selected enzymes were tested for the reduction of aromatic ketones or aldehydes (**Figure 1**, group A) to their corresponding alcohols. All results are presented in **Table 4**. Substrates **1-3b** were well accepted by all enzymes, resulting in moderate to high conversions (62-100%). Interestingly, for substrate **4b** only LE-AmDH-v27 was able to produce the corresponding alcohol in moderate yield (40%) possibly because the *ortho*-fluoro substituent may cause unfavorable electronic effects that negatively affect the activity of the enzymes. This trend was not observed for the reductive amination reactions of *para*- and *meta*-substituted fluorobenzaldehyde. For substrates **5b** and **12b**, LE-AmDH-v27 yielded full conversion to the corresponding alcohols (>99% yield). In contrast, LE-AmDH-v22

and -v25 in particular, were less active towards these two substrates. Unlikely to the *meta*-methylbenzaldehyde (**12b**), *ortho*-methylbenzaldehyde (**13b**) was not accepted by any of the enzymes tested (0% yield of **13a**). Remarkably, in the reductive amination reaction, the *ortho*-substituted substrate was favored by LE-AmDH-v1, -v22 and -v25. For substrate **18b**, only LE-AmDH-v27 was capable of producing the corresponding alcohol in low yield (4%). Notably, aldehyde **19b**, in which the carbonyl moiety is located a carbon further than **18b**, was converted to alcohol in high yields (67-68%). However, a similar yield (61%) was obtained in the blank sample containing Cb-FDH, indicating that the cofactor-recycling enzyme is probably responsible for this transformation. Ketones **20-22b** could not be reduced by any LE-AmDHs (0% analytical yield) and therefore we were not able to determine the stereoselectivity of these enzymes. Among all of the six LE-AmDHs, the variant LE-AmDH-v27 was the most active in the reduction of aldehydes to primary alcohols (**Table 4**). Notably, this enzyme showed relatively high activity towards substrate **4b** (40% yield) compare with all LE-AmDHs used. The wild-type enzyme (LysEDH) also exhibited considerable ADH activity (59-84% yield of products **1**-**3a**, **5a** and **12a**). In general, the variants with the F173S mutation (LE-AmDH-v24 and LE-AmDH-v27) were more active than the variants with an alanine at the same position (v22 and v25). Interestingly, in the reductive amination reaction this trend was reversed (**Table 2**). Comparing the results obtained by LE-AmDH-v24 and LE-AmDH-v27 is evident that the alanine mutation in position 240 (T240A) caused an increase in alcohol dehydrogenase activity.

Table 4. Reduction of aromatic aldehydes to alcohols by LE-AmDHs.

Enzyme		1b	2b	3b	4b	5b	12b	13b	18b	19b
WT	Conv (%)	95	92	98	24	89	70	0	28	81
	Yield (%)	82	74	83	11	84	59	0	0	67
Le-AmDH-v1	Conv (%)	90	84	98	23	73	63	0	30	80
	Yield (%)	76	64	85	11	65	52	0	0	68
Le-AmDH-v22	Conv (%)	73	77	94	18	40	37	0	28	79
	Yield (%)	54	59	80	7	24	28	0	0	68
Le-AmDH-v24	Conv (%)	85	71	98	21	69	60	0	26	81
	Yield (%)	66	53	84	9	59	51	0	0	67
Le-AmDH-v25	Conv (%)	76	62	94	18	40	42	0	25	80
	Yield (%)	56	46	79	7	21	33	0	0	68
Le-AmDH-v27	Conv (%)	>99	99	>99	68	99	99	0	28	81
	Yield (%)	77	80	86	40	>99	>99	0	4	67
Blank 1	Conv (%)	16	20	29	9	5	5	0	7	77
	Yield (%)	7	5	18	1	0	1	0	0	61
Blank 2	Conv (%)	6	11	7	6	0	3	0	0	1
	Yield (%)	0	0	0	0	0	0	0	0	0

Experimental conditions: 1 mL final volume in Eppendorf tubes; buffer: KPi 100 mM pH 7.0; T = 30 °C; reaction time: 24 h; agitation orbital shaker (170 rpm); [substrate]: 20 mM; [NAD$^+$]: 1 mM; [LysEDH]: 45 μM; [Cb-FDH]: 16 μM. Blank 1: reaction without LE-AmDH, Blank 2: reaction without LE-AmDH and FDH.
The conversion and yield depicted here are the average values obtained from four independent experiments.

5.3.6 Reduction of benzaldehyde at higher concentrations.

In this set of reactions the influence of benzaldehyde concentration (10-100 mM) to the analytical yield of the obtained product was investigated. The LysEDH concentration was 90 μM, FDH concentration was 16 μM; reactions were run in

100 mM KPi buffer pH 7.0 supplemented with 100 mM of HCOONa. Results are summarized in **Figure 4**. After 24 h, 90% of 100 mM benzaldehyde was converted to benzyl alcohol (76% analytical yield). In general only a small influence in the analytical yield of benzylalcohol as observed by increasing the concentration of benzaldehyde even 10 folds (from 95% to 76%).
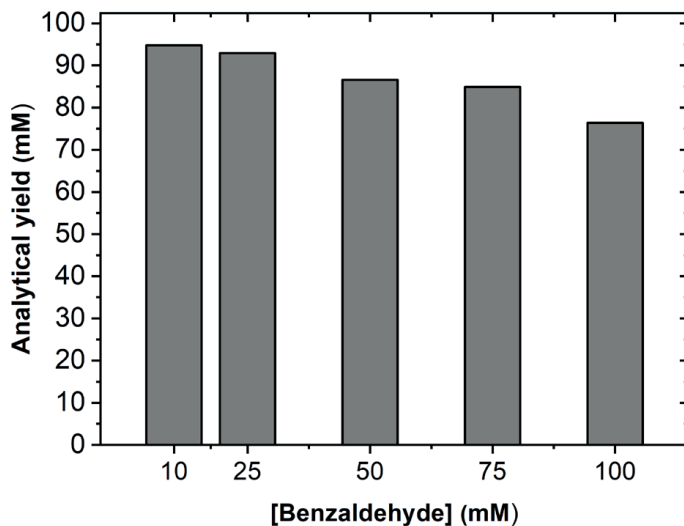
Figure 4 Influence of benzaldehyde concentration in the analytical yield of the alcohol product. Experimental conditions: buffer: KPi 100 mM pH 7.0; T: 30 ∘C; reaction time: 24 h; agitation orbital shaker (170 rpm); [substrate]: 10-100 mM; [NAD$^+$]: 1 mM; [LysEDH]: 45 μM; [*Cb*-FDH]: 16 μM.

5.3.7 Investigation of the oxidation of benzyl alcohol to benzaldehyde

The oxidation of alcohols to aldehydes or ketones often proceeded better in different reaction conditions than those favor the opposite direction. Therefore, we performed a time study in different buffers with the aim of investigating the potential influence of different factors (e.g., type of buffer, pH) for the oxidation of benzylalcohol to benzaldehyde. **Figure 5** summarizes the progress of the analytical yield over the time for this reaction catalyzed by LE-AmDH-v27 in different buffers. The LE-AmDH-v27 was chosen because of its high catalytic

activity in the opposite direction. Results showed that there is a high variation among the different buffers tested. Increasing the pH of the reaction correlated with an increase in the obtained yield of benzaldehyde with the highest to be 66% after 24 h using 100 mM Tris-HCl pH 9.0. In contrast at the same pH using 2 M ammonium formate buffer the analytical yield was reduced to 7% after the same time. The lower formation of alcohol observed in the ammonium formate buffer, compared with the other buffers tested, may be explained by the interaction of the ammonia with some residues in the active site of the enzyme, and/or significant proportion of iminium intermediate formed.
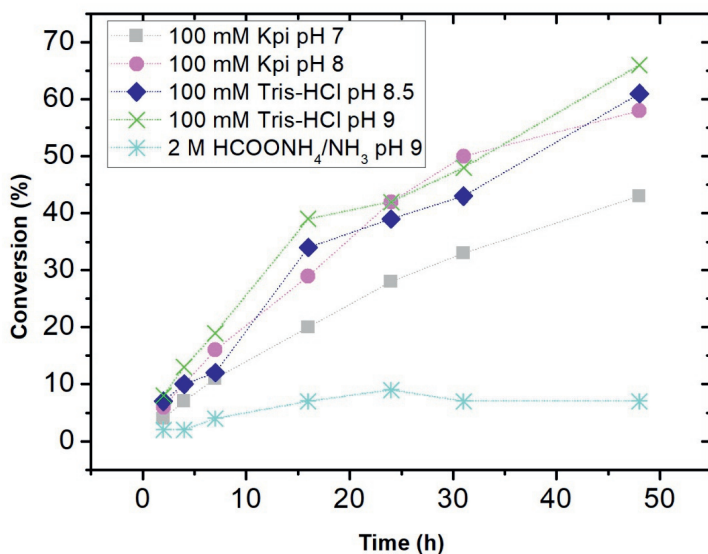
Figure 5. Progress of the conversion of benzylalcohol into benzaldehyde in different buffers using LE-AmDH-v27. Experimental conditions: 0.5 mL final volume in Eppendorf tubes; KPi and Tris-HCl buffer are 100 mM; ammonium formate (AF) buffer is 2 M; enzyme: LE-AmDH-v27 (F173S_Y238A_T240A); T: 30 °C; agitation orbital shaker (170 rpm); [substrate]: 10 mM; [NAD$^+$]: 1 mM; [LysEDH]: 90 μM; [NOx]: 10 μM.

Using the 100 mM Tris-HCl pH 9.0 buffer the oxidation of benzylalcohol to benzaldehyde was tested with all variants (**Figure 6**). All enzymes were capable of producing benzaldehyde (**1b**) in moderate to high yields (44-86%). Notably, blank reactions with NOx (**blank 1**) afforded the desired product (**1b**) in 31% yield.

Only the LE-AmDH-v27 was able to achieve higher yields (86%) than the wild-type enzyme (66% yield). Considering both the oxidation and the reduction experiments, this variant displayed the highest alcohol dehydrogenase activity. Generally, substituting F173 with serine (F173S) instead of an alanine increased the activity towards the formation of benzylalcohol. This is especially evident, when comparing the two triple mutants: LE-AmDH-v25 (44% yield) with LE-AmDH-v27 (86% yield). Compared with LE-AmDH-v24, the additional T240A mutation in LE-AmDH-v27 resulted in increased activity.
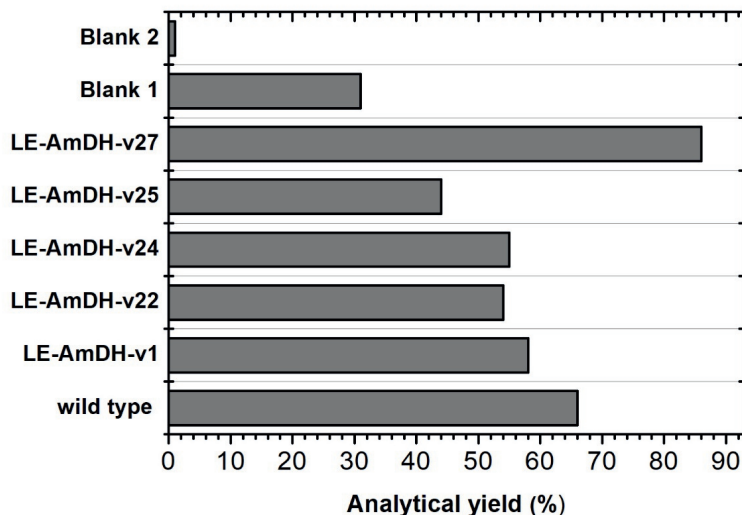
Figure 6. Oxidation of alcohol 1a using six LE-AmDHs. The analytical yield (%) depicted here is the average values obtained from two independent experiments. Blank 1 did not contain LysEDH. In blank 2, LysEDH and NOx were not present. Experimental conditions: 0.5 mL final volume in Eppendorf tubes; buffer: Tris-HCl 100 mM pH 9.0; T: 30 °C; agitation on orbital shaker (170 rpm); reaction time: 48 h; [substrate 1a]: 10 mM; [NAD$^+$]: 1 mM; [LysEDH]: 90 µM; [NOx]: 10 µM

5.3.8 Investigation of direct conversion of benzylalcohol to benzylamine

We have shown that by altering the reaction conditions the catalytic activities of the LE-AmDHs can also be altered, thereby behaving either as highly enantioselective amine dehydrogenases or as primary alcohol dehydrogenases. We envisioned that this catalytic promiscuity can be harnessed for the direct

conversion of benzylalcohol into benzylamine *via* a one-enzyme oxidation-reductive amination cascade. Such a cascade was first reported by Mutti and coworkers[31] but using two different enzyme families: an ADH and an AmDH. In this scenario, the LE-AmDH has a bi-functional role, acting both as ADH and as AmDH. Still the cofactor can be added in catalytic amounts and regenerated by the same enzyme in an "auto-recycling" fashion. Even though the LE-AmDH variants that were most active in the oxidation of benzylalcohol showed decreased activity in the reductive amination (and vice versa), as well as that benzaldehyde (formed as intermediate) can be reduced back to benzylalcohol, we attempted this one-pot single-enzyme hydrogen-borrowing cascade using all LE-AmDHs. In a previous experiment we have shown that this reaction did not result in any amine formation when we used 2 M ammonium formate buffer (**Figure 4**); therefore, a set of different ammonia/ammonium containing buffers (ammonium acetate, ammonium formate, ammonium chloride, ammonium citrate, ammonium sulfate, all prepared at 1M, pH 9) were tested. Additionally, we have shown that the oxidation of benzylacohol proceeded better in Tris-HCl pH 9.0 (**Figure 5**). Therefore, we performed the same reaction in 100 mM Tris-HCl supplemented with 500 mM NH_4OH. Notably, as a proof of principle, we were able to obtain 5% analytical yield of benzylamine using 100 mM Tris-HCl supplemented with 500 mM ammonia solution (**Figure 7**, cascade 1). The highest yield was observed with LE-AmDH-v1 (5%) followed by LE-AmDH-v22 (4%). Both variants were the most active in the reductive amination direction (**Table 2**). Varying the NAD^+ concentration (1, 5 and 10 mM) as well as the substrate concentration (10, 50 and 100 mM, respectively) while maintaining the molar ratio of NAD^+ to substrate (1: 10), resulted in increased yield of benzylamine (0.4, 2.1 and 2.5 mM, respectively). To avoid any possible thermodynamic equilibrium limitation, the concept of single-enzyme, two-step amination of benzyl alcohol was investigated by uncoupling the oxidative and the reductive steps using NOx (for the first step) and Cb-FDH (for the second step)
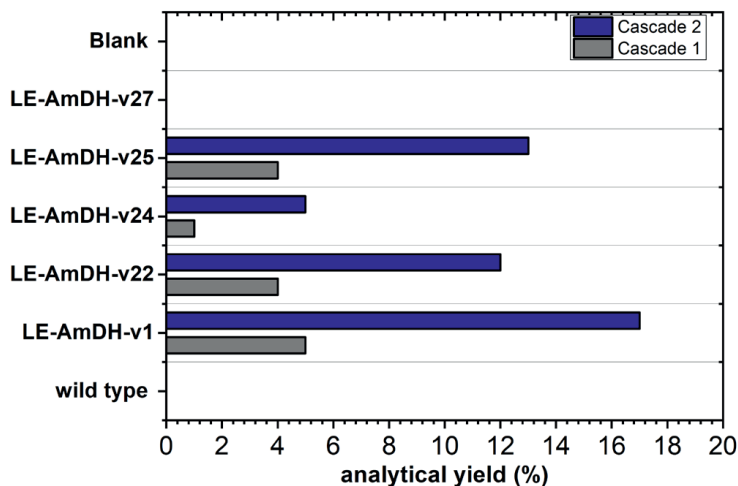
Figure 7. Amination of benzyl alcohol using a single enzyme for oxidation and reduction steps. All LE-AmDHs were tested. Cascade 1: buffer: Tris-HCl (100 mM) suppl. with NH$_4$OH (1 M) pH 9.0; T: 30 °C; reaction time: 48 h; agitation orbital shaker (170 rpm); [1a]: 10 mM; [NAD$^+$]: 1 mM; [LysEDH]: 90 µM. Cascade 2: Tris-HCl (100 mM) suppl. with NH$_4$OH (1 M) pH 9.0; T: 30 °C; reaction time: 48 h; agitation orbital shaker (170 rpm); [substrate 1a]: 10 mM; [NAD$^+$]: 1 mM; [NOx]: 10 µM; [LysEDH]: 90 µM; added after 24 h: [HCOONa]: 100 mM and [FDH]: 16 µM.

as cofactor recycling enzymes (**Figure 7**, cascade 2), as previously shown by Knaus *et al.*[15] Due to the fact that the enzymes use NAD(H) in both steps, the benzaldehyde formed in the first step can be used for reductive amination to the corresponding alcohol by the same enzyme, upon addition of FDH and formate. Indeed, higher analytical yield of benzylamine was observed using this cascade. In fact, LE-AmDH-v1 was capable of producing most of benzylamine (17% anal. yield) among all LE-AmDHs tested. Finally, using the same enzyme, we were able to obtain 34% analytical yield for the amine product when the first step of the cascade (cascade 2) was performed in Tris-HCl buffer pH 9 containing no ammonia. After 24 h, the ammonia solution was added (NH$_4$OH, 0.5 M) as well as HCOONa (100 mM) and FDH (16 µM) and the reaction was run for another 24 h. This result is in a good agreement with the results shown in **Figure 5** (light blue line) that shows that the oxidation of benzyl alcohol to benzaldehyde is highly unfavorable in an ammonia containing buffer. Moreover, performing the same

cascade using in the first step the most active variant for the oxidation of **1a** (LE-AmDH-v27), did not increase the analytical yield of the obtaining amine **1c**, which was obtained in 32% analytical yield using the combination of LE-AmDH-v27 with LE-AmDH-v1.

5.4 Conclusions

In this study, we exploited the catalytic promiscuity of *L*-lysine-(ε-deaminating)-dehydrogenase (LysEDH) from *G. stearothermophilus*. Starting from this scaffold, we created enzymes that show both ADH activity as well as AmDH activity towards benzylic substrates. By optimizing and controlling the reactions, these enzymes were used either for the preparation of a-chiral amines or primary alcohols with high efficiency. The three engineered LysEDHs containing the F173A mutation (LE-AmDH-v1, -v22 and -v24) were the most active variants in the reductive amination of aldehydes and ketones. On the other hand, LE-AmDH-v27 (F173S/Y238A/T240A) displayed the highest alcohol dehydrogenase activity, both in the reduction of aromatic aldehydes and in the oxidation of primary alcohols. As we only obtained achiral alcohols, the stereoselectivity of these ADHs could not be determined. Reductive amination of ketones afforded the corresponding amines in enantiomerically pure (*R*)-configuration (>99% *ee*). Notably, some of the LysEDH variants were able to catalyze the single-enzyme hydrogen-borrowing amination of benzyl alcohol to benzylamine (≤5% yield), providing the first examples of 'alcohol aminase' behavior. Performing the same biocatalytic cascade in the presence of NOx and FDH as recycling enzymes, benzylamine was obtained in yields up to 34%.

5.5 Methods

5.5.1 Enzyme expression and purification

All the enzymes in this study carry an *N*-terminal His$_6$-tag. *E. coli* BL21(DE3) competent cells, harboring the plasmids (pET-28bvar) with the genes for the expression of the proteins, were used as expression strain. Glycerol stock solutions of the corresponding *E. coli* cells were prepared in advance. Firstly, LB broth (Luria/Miller) was prepared according to the standard recipe (25 g LB powder to 1 L demi-water). The resulting LB medium was sterilized. A single colony of *E. coli* was used to inoculate the LB broth (ONC). The cells were grown overnight at 37 °C and 170 rpm in a shaker incubator. Next day, 800 µL kanamycin solution (50 mg mL^{-1}) was added to 800 mL sterilized LB broth, resulting in a final kanamycin concentration of 50 µg mL^{-1}. The cultures were inoculated by the addition of 15 mL overnight culture and incubated at 37 °C in a shaker incubator (170 rpm). The cell growth was checked by measuring the optical density at 600 nm (OD$_{600}$). When the absorbance was 0.6-1.0 (after 2-3 h), the synthesis of the enzymes was induced by the addition of 400 µL of 1M isopropyl β-D-thiogalactoside (IPTG) solution (final IPTG concentration = 0.5 mM). Expression was performed at 25 °C and 170 rpm, overnight. The following day, the OD$_{600}$ value was checked again, applying a 1:5 dilution. Before and after induction a small sample of each culture was taken in order to verify the expression level with SDS-PAGE. The cells were harvested by centrifugation (4500 rpm; 4 °C; 15 min; IEC FL40R centrifuge from Thermo Electron Corporation). After resuspending the cells in lysis buffer (50 mM KH$_2$PO$_4$; 300 mM NaCl; 10 mM imidazole; pH 8.0), centrifugation was performed (4500 rpm; 4 °C; 30 min). Then, the supernatant was removed and the cell wet weight was determined. The pellet was stored in the freezer at -20 °C.

The wet cells were suspended in lysis buffer (5-10 mL buffer added for 1 g of cell wet weight). *E. coli* cells were disrupted by sonication (amplitude = 45%; pulse ON = 10 s; pulse OFF = 10 s; total sonication time = 10-20 min). Sonication was performed until the suspension became darker and less viscous. During

sonication, the enzyme solutions were constantly cooled to prevent the loss of activity. The disrupted cells were centrifuged at 16000 rpm (4 °C) for 60 min (Beckman J2-21 centrifuge), and the supernatant was collected and filtered through a 0.45 µm filter. A small sample of the pellet (insoluble part) as well as of the filtrate (soluble part) was taken for SDS-PAGE analysis. Protein purification was performed by column chromatography using pre-packed Ni-NTA Histrap™ HP columns (5 mL) according to the manufacturer's instructions. All solutions utilized during chromatography had been filtered and degassed for 1 h. Firstly, the column was washed with demi water (25 mL) and conditioned with lysis buffer (50 mL). Then, the filtrated supernatant was loaded twice on the column. After that, the column was washed with 25 mL lysis buffer and sufficient amounts (~70 mL) of washing buffer (50 mM KH_2PO_4; 300 mM NaCl; 25 mM imidazole; pH 8.0). The protein content of the washing fractions was checked using the colorimetric Bradford assay. Finally, the enzymes were recovered with elution buffer (50 mM KH_2PO_4; 300 mM NaCl; 300 mM imidazole; pH 8.0). Both the washing and elution fractions were analyzed by SDS-PAGE. Fractions containing sufficient purified protein were pooled and dialyzed overnight against potassium phosphate buffer (50 mM; pH 8.0; 4 °C). The resulting protein solution was concentrated using a Vivaspin® centrifugal concentrator (centrifuge: Eppendorf 5430R). The final enzyme concentrations were determined spectrophotometrically by measuring the absorption at 280 nm and using the extinction coefficient (ε) of the enzymes). Finally, purity of the enzyme solution was judged by SDS-PAGE

5.5.2 Compound selection.

Several reference samples were prepared to determine if the compounds could be used for the biocatalytic reactions: (i) samples in which the compounds (substrate and product) were directly pipetted in EtOAc (***inj***), (ii) samples in which substrate and product were first pipetted in the reaction buffer and then extracted using the identical extraction procedure as the reaction samples (***ext***), (iii) samples prepared as *ext*, but which were incubated for 24 h prior to

extraction (*inc*), and (iv) samples prepared as *inc* in the presence of Ch1-AmDH (*enz*). The extraction (*ext*), incubation (*inc*) and enzyme (*enz*) references were used to determine the extractability, volatility and protein adsorption, respectively. Measurements were performed in triplicate. KPi buffer (100 mM; pH 7.0) was prepared by adding K_2HPO_4 (3.74 g; 21.5 mmol) and KH_2PO_4 (2.52 g; 18.5 mmol) to distilled water (final volume = 0.4 L). The pH was increased to 7.0 by the addition of 10 M KOH. Ammonium formate buffer (2 M; pH 8.2) was prepared by dissolving $HCOONH_4$ (23.96 g, 0.38 mol) in water (200 mL). Then, NH_4OH (2.47 mL; 8.1 M) was added to the solution and the pH was adjusted to 8.2 with formic acid. Alcohols and aldehydes /ketones were incubated in KPi buffer, whereas amines were added to ammonium formate buffer. In each case, 20 mM of compound was pipetted into buffer solution (final volume 1 mL, in 2 mL Eppendorf tubes). Additionally, 45 µM of Ch1-AmDH was added to the enzymatic samples (*enz*). Then, the mixtures were incubated at 30 °C in orbital shakers (170 rpm). Prior to extraction, 200 µL of 10 M KOH was added to the samples containing amines. Extraction was performed using EtOAc (supplemented with 20 mM toluene) as extraction solvent. The *ext* samples were extracted after 20 minutes, while the *inc* and *enz* samples were both extracted after 24 h incubation. The *inj* samples were prepared by adding 20 µL of the compound to 980 µL extraction solvent and served as the samples in which the RF was considered 100%. Analysis was performed with GC-FID using split ratio 1:20. After the peak areas of toluene (A_{IS}) and compound **x** (A_x) were determined, the response factor (RF) was calculated from the ratio A_x/A_{IS}. The calculated RF of each sample was compared with the *inj* sample (=100%). When for a specific set of compounds the RF-value of the *inc* reference was too low in comparison with the *inj* reference (<65%), this compound was not used for biotransformations.

5.5.3 Determination of pH optimum for the reduction of benzaldehyde to benzylalcohol by LE-AmDH-v27

Britton-Robinson universal buffer (BRB) was prepared using acetic acid (17.4 M), H_3PO_4 (14.7 M) and boric acid (solid MW: 61.83 g/mol) in the final concentration of 80 mM. 10 mL of this "master" stock solution was titrated with 200 mM NaOH to give the desirable pH value. Then dH_2O was added until the final volume of 20 mL resulted in 40 mM final concentration. Using this procedure, buffers with varied pH values were prepared. The biocatalytic reactions were performed using 45 µM of enzyme, 14 µM of FDH, 100 mM HCOONa, 1 mM of NAD^+ and 20 mM of substrate. The final volume of the reactions was 500 µL. For each pH value of the BRB buffer, several reactions were prepared and run for different times (10-80 min), at 30 °C using an orbital shaker (170 rpm). Extraction was performed using EtOAc (2 x 500 µL) supplemented with 10 mM toluene as internal standard. The organic phases were combined dried with $MgSO_4$ and injected in GC. Determination of the product produced (mM of alcohol) in each reaction sample was performed using the following procedure: first reference benzyl alcohol (20 mM, maximum theoretical yield) was added to BRB buffer pH 7.0 (0.5 mL) and extracted after 80 min with EtOAc (2 x 0.5 mL) containing 10 mM of toluene as internal standard. This sample was prepared in triplicate. For each sample, the area of alcohol was plotted against the area of toluene and the obtained values (for the three reference samples) were averaged. This final number served as reference response factor (RF_{ref}). After extraction of the reaction samples, the obtained area of alcohol was plotted against the area of toluene giving the sample response factor (RF_{sample}). Finally the product produced (mM) after the enzymatic reaction was calculated by multiply the concentration of the substrate used with the RF_{sample} and divided the obtained number with RF_{ref} [mM produced = (RF_{sample} x 10)/ RF_{ref}].

5.5.4 Progress of the reduction of benzaldehyde to benzylalcohol in different types of buffers

For the enzymatic transformations of benzaldehyde to benzylalcohol several types of buffer were tested: 100 mM HEPES pH 7.0, 100 mM Tris pH 7.0, 100 mM MOPS pH 7.0, 100 mM KPi pH 7.0 and 100 mM NaH$_2$PO$_4$. Reactions (1 mL) were performed using 90 µM of the LysEDH variant, 16 µM of FDH, 20 mM of benzaldehyde, 100 mM of HCOONa, and 1 mM of NAD$^+$. The biocatalytic reactions were run at 30 °C using an orbital shaker (170 rpm) for different times (1-24 h). After the reported times, reactions were extracted with EtOAc (2 x 500 µL) supplemented with 10 mM of toluene as internal standard. The organic phases were combined and analyzed by GC. Both conversion (based of the mM of the remaining starting material) and analytical yield (based of the mM of benzylalcohol produced) were determined using the following procedure. Three reference samples were prepared by adding 20 mM of benzaldehyde and 20 mM of benzylalcohol (from 1M stock in DMSO) to 100 mM KPi buffer pH 7.0 (1 mL). These samples were run at 30 °C for 24h. After this time the samples were extracted with EtOAc (2 x 0.5 mL) containing 10 mM of toluene as internal standard. These samples were analyzed by GC. In each sample the area of the aldehyde was plotted against the area of toluene and the response factor (RF) was obtained. All the response factors obtained by the three samples were averaged. This averaged number was used as reference response factor for aldehyde (RF$_{ref/ald}$). In a similar way by plotting the area of alcohol with the area of toluene, the response factor for the alcohol was determined (RF$_{ref/alc}$). The (RF$_{ref/ald}$) was used to calculate the conversions while the RF$_{ref/alc}$ was used to calculate the analytical yields. After extraction of the enzymatic reactions and injection in GC the response factors of the reactions (RF$_{sample/ald}$ and RF$_{sample/alc}$) were calculated using the same procedure as before. The amount (mM) of benzaldehyde left in the reaction mixture was calculated using the formula: mM = (RF$_{sample/ald}$ x 20)/ RF$_{ref/ald}$. This number was used to calculate the amount (mM) of benzaldehyde consumed (20 mM – mM remained) and therefore the conversion. For the calculations of the analytical yield the mM of benzyl alcohol

produced were calculated using the formula: mM produced = (RF$_{sample/alc}$ x 20)/ RF$_{ref/alc}$).

5.4.6 Influence of the substrate concentration in the conversion of benzaldehyde to benzylalcohol

The reactions at varied concentrations of benzaldehyde were performed in 1 mL KPi buffer pH 7.0. Reactions consisted of 90 µM of the LysEDH variant, 16 µM of FDH, 10-100 mM of benzaldehyde, 100 mM of HCOONa, and 1 mM of NAD$^+$. The reactions were extracted with EtOAc (2 x 0.5 mL) supplemented with 10 mM toluene as internal standard. For the calculation of conversions and analytical yields the same procedure was followed as described before. This time for the calculation of RF$_{ref/ald}$ and RF$_{ref/alc}$ the concentration of benzaldehyde and benzyl alcohol in the reference samples was prepared to be the same as the concentration in the reaction samples. Therefore, for each different concentration of benzaldehyde used three replicates of reference samples were prepared with the same concentration.

5.5.5 Determination of conversion and analytical yield in the biocatalytic reductive amination or reduction of aldehydes to alcohols

In each experiment, calculations are based on response factors (RF) of extracted (***ext***) or incubated references (***inc***). For example, when a reaction was performed with 20 mM substrate, reference samples were prepared containing 20 mM of substrate or product. The reference samples were extracted with the same extraction procedure as the reaction samples. By using GC-FID, the peak areas of toluene (A$_{IS}$) and compound **x** (A$_x$) were determined. Next, the response factor (RF) was calculated from the ratio A$_x$/A$_{IS}$. By relating the response factors of the reaction samples to the response factors of the reference samples, the conversions and yields were calculated as described before.

5.5.6 General procedure for the reductive amination of aldehydes and ketones

Ammonium formate buffer (2 M; pH 8.2) was prepare by dissolving HCOONH$_4$ (23.84 g, 0.378 mol) in water (final volume = 200 mL). Then, 2.72 mL of 8.1 M NH$_4$OH

was added and the pH was adjusted to 8.2 with formic acid. The biocatalytic transformations (performed in duplicate) were conducted in a final volume of 1.0 mL (2 mL Eppendorf tubes). Reactions were started by adding NAD^+ (1 mM), Cb-FDH (16 µM), LysEDH (45 µM) and aldehyde (20 mM) in consecutive order. Two different blank reactions were prepared. Blank 1 did not contain any LysEDH, while in blank 2 both LysEDH and Cb-FDH were absent. During the same day of the execution of the reductive amination experiment, new incubation references (*inc*) were measured. These reference samples (also measured in duplicate) were prepared by pipetting 20 mM of compound **x** in ammonium formate buffer (1 mL final volume). All samples, also the references, were incubated at 30 °C in orbital shakers (170 rpm). After 24 h incubation, 20 µL formic acid was added which lowered the pH to 4.5-5.0. Then, extraction was performed with EtOAc (supplemented with 20 mM toluene) according to the standard procedure. The pH of the remaining water layer was increased to 13-14 by the addition of 300 µL of 10 M KOH. Another extraction step was performed using EtOAc (supplemented with 20 mM toluene). Both the acidic extract and the basic extract were dried with $MgSO_4$ and analyzed as separate samples with GC-FID (split ratio 1:20). Peak areas of alcohols and aldehydes were measured in the acidic extract, whereas the amine peak area could be quantified in the basic extract. Response factors of alcohols and aldehydes were calculated by using the peak area of toluene in the acidic extract. In contrast, RF-values of amines were determined with the peak area of toluene in the basic extract.

For the reductive amination of ketones, the NAD^+ (1 mM), Cb-FDH (16 µM), LysEDH (90 µM) and ketone (10 mM) were added in 0.5 mL ammonium formate buffer. The reactions were run at 50 °C for 48 h at 170 rpm in orbital shakers. After the reported time, the reaction mixture was basified (100 µL of 10 M KOH) and the extraction was performed with EtOAc (1 x 600 µL). The organic phases were dried with $MgSO_4$ and analyzed by GC.

5.5.7 Derivatization of chiral amines to determine the absolute configuration

50 mg 4-dimethylaminopyridine (DMAP) was dissolved in 1 mL acetic anhydride. Depending on the amine concentration, either 30 µL or 50 µL of this solution was added to the samples. The mixtures were shaken in an incubator (30 °C; 1000 rpm) for 30 minutes. After addition of distilled water (500 µL), the samples were shaken for an additional 30 min (30 °C 1000 rpm). Then, the mixtures were centrifuged for 5 minutes at 14800 rpm and 4 °C . The top layer (organic phase) was removed and transferred to another Eppendorf tube. Subsequently, the organic layer was dried with $MgSO_4$ and centrifuged at 14800 rpm for 5 min (4 °C). Enantiomeric excess was determined by GC-FID using a CP-Chirasil Dex-CB column.

5.5.8 Investigation of the oxidation of benzyl alcohol to benzaldehytde

During this study five different buffer solutions were tested: KPi pH 7.0 (100 mM); KPi pH 8.0 (100 mM); Tris-HCl pH 8.5 (100 mM); Tris-HCl pH 9.0 (100 mM); ammonium formate pH 9.0 (2 M). The biotransformations (single replicates) were performed in 0.5 mL (1.5 mL Eppendorf tubes) in the presence of NAD^+ (1 mM), NOx (10 µM), LysEDH (90 µM) and alcohol **1a** (10 mM). Only one enzyme was employed: LE-AmDH-v27 (F173S_Y238A_T240A). A blank sample was included, which did not contain LE-AmDH-v27. On the same day, new incubation references (triplicate) were prepared by pipetting 10 mM of compound **1a** and 10 mM of compound **1b** in KPi buffer pH 7.0 (final volume = 500 µL). All mixtures, including the incubation references, were incubated at 30 °C in orbital shakers (170 rpm). Seven different incubation times were applied: 2, 4, 7, 16, 24, 31 and 48 h. When a time-point was reached, the samples were extracted with EtOAc (containing 10 mM toluene) following the standard protocol. GC-FID (split ratio 1:10) was used for analysis.

5.5.9 Screening of LE-AmDHs for the oxidation of benzyl alcohol to benzaldehyde

Tris-HCl (pH 9.0; 100 mM) was prepared by dissolving 2.42 g Tris base (20 mmol) in 150 mL demi water. After adjusting the pH to 9.0 with concentrated HCl, the volume was increased to 200 mL by adding more water. Biocatalytic

transformations were carried out in duplicate in 500 μL reaction buffer (1.5 mL Eppendorf tubes). The reactions were started by adding NAD$^+$ (1mM), NOx (10 μM), LysEDH (90 μM) and substrate **1a** (10 mM) in consecutive order. Two blanks were included: blank 1 did not contain LysEDH, while in blank 2 both LysEDH and NOx were absent. In addition, new incubation references (duplicate) were made by pipetting 10 mM of compound **1a** and **1b** in Tris-HCl buffer (final volume = 0.5 mL). After 48 h incubation at 30 °C in orbital shakers (170 rpm), the samples were extracted with EtOAc (supplemented with 5 mM toluene). Finally, the extracts were analyzed with GC-FID (split ratio 1:10; injection volume = 2 μL). Calculations of conversion and yield are based on response factors (RF) of incubated references as described above.

5.5.10 Investigation of direct conversion of benzylalcohol to benzylamine

For the cascade 1, Tris-HCl (100 mM) supplemented with NH$_4$OH (1 M) pH 9.0 was used in this study. Firstly, 1 M Tris-HCl pH 9.0 was prepared. After slow addition of a 8.1 M solution of NH$_4$OH (1 M final concentration), the pH was lowered to 9.0 by addition of concentrated HCl. The solution was then diluted until the desired concentrations were obtained. Biocatalytic reactions (single replicates; 1.0 mL final volume; 2.0 mL Eppendorf tubes) were performed in the presence of NAD$^+$ (1 mM), LysEDH (90 μM) and benzyl alcohol **1a** (10 mM). All six variants were employed. In addition to blank reactions (without LysEDH), new incubation references were prepared by adding 10 mM of compound **1a-c** to buffer 1 (final volume = 1.0 mL). All samples were incubated at 30 °C in orbital shakers (170 rpm) for 48 h. Prior to extraction, 200 μL of 10 M KOH was added to each tube. Extraction was carried out with EtOAc (supplemented with 10 mM toluene) following the general extraction procedure. Then, GC-FID (split ratio 1: 10) was used for analysis. Calculations of conversion and yield are based on response factors (RF) of incubated references.

For the cascade 2, the same buffer solutions and incubation references were used. Biocatalytic transformations (single replicates) were carried out in 1.0 mL reaction buffer (2.0 mL Eppendorf tubes). Reactions were started by adding

NAD$^+$ (1mM), NOx (10 µM), LysEDH (90 µM) and substrate **1a** (10 mM) in consecutive order. All six LysEDH enzymes were utilized and a blank was included (without LysEDH). Incubation was conducted at 30 °C in orbital shakers (170 rpm). After 24 hours incubation, HCOONa (100 mM) and Cb-FDH (16 µM) were added. Then, the mixtures were incubated for another 24 h. After adding 200 µL of 10 M KOH, the samples were extracted with EtOAc (2x500 µL; supplemented with 10 mM toluene) according to the general procedure. The final extracts were analyzed with GC-FID (split ratio 1:10). Calculations of conversion and yield are based on response factors of incubated references as described above.

5.5.11 Analytical methods

Conversions and yields were determined by gas chromatography using an Agilent 7890B chromatograph, equipped with a FID detector. An Agilent J&W DB1701 (30 m, 250 µm, 0.25 µm) column was used and H$_2$ was applied as carrier gas. Depending on the substrate concentration, a specific split ratio (e.g. 1:20) was chosen. Unless stated otherwise, the injection volume was 1 µL. All measurements were performed with Method B:

- Constant pressure = 6.9 psi; Flow = 1.05 mL/min; T injector = 250 °C.
- Temperature program: T initial = 60 °C; hold 6.5 min; gradient 20 °C min^{-1} up to 100 °C; hold 1 min; gradient 20 °C min^{-1} up to 280 °C; hold 1 min.

Enantiomeric excess of the derivatized amines was measured with the same chromatograph using a CP-Chirasil Dex-CB column (25 m, 320 µm, 0.25 µm). Method:

- Constant pressure = 3.8 psi; Flow = 1.4 mL/min; T injector = 200 °C. Split ratio 1:20
- Temperature program: T initial = 100 °C; hold 2 min; gradient 1 °C min^{-1} up to 130 °C; hold 5 min; gradient 10 °C min^{-1} up to 170 °C; hold 10 min; gradient 10 °C min^{-1} up to 180 °C; hold 1 min.

5.6 References

1   Copley, S. *Curr. Opin. Chem. Biol.* **7**, 265-272, doi:10.1016/s1367-5931(03)00032-2 (2003).

2   Nobeli, I., Favia, A. D. & Thornton, J. M. *Nat. Biotechnol.* **27**, 157-167, doi:10.1038/nbt1519 (2009).

3   Babtie, A., Tokuriki, N. & Hollfelder, F. *Curr. Opin. Chem. Biol.* **14**, 200-207, doi:10.1016/j.cbpa.2009.11.028 (2010).

4   Copley, S. D. *Curr Opin Struct Biol* **47**, 167-175, doi:10.1016/j.sbi.2017.11.001 (2017).

5   Khersonsky, O. & Tawfik, D. S. *Annu. Rev. Biochem* **79**, 471-505, doi:10.1146/annurev-biochem-030409-143718 (2010).

6   Kazlauskas, R. J. *Curr. Opin. Chem. Biol.* **9**, 195-201, doi:10.1016/j.cbpa.2005.02.008 (2005).

7   Khersonsky, O., Roodveldt, C. & Tawfik, D. S. *Curr. Opin. Chem. Biol.* **10**, 498-508, doi:10.1016/j.cbpa.2006.08.011 (2006).

8   Tseliou, V., Masman, M. F., Bohmer, W., Knaus, T. & Mutti, F. G. *ChemBioChem* **20**, 800-812, doi:10.1002/cbic.201800626 (2019).

9   Vilim, J., Knaus, T. & Mutti, F. G. *Angew. Chem. Int. Ed.* **57**, 14240-14244, doi:10.1002/anie.201809411 (2018).

10   Nealon, C. M., Musa, M. M., Patel, J. M. & Phillips, R. S. *ACS Catal.* **5**, 2100-2114, doi:10.1021/cs501457v (2015).

11   Kroutil, W., Mang, H., Edegger, K. & Faber, K. *Adv. Synth. Catal.* **346**, 125-142, doi:10.1002/adsc.200303177 (2004).

12   Liu, J., Wu, S. & Li, Z. *Curr. Opin. Chem. Biol.* **43**, 77-86, doi:10.1016/j.cbpa.2017.12.001 (2018).

13   Voss, C. V. *et al.* *J. Am. Chem. Soc.* **130**, 13969-13972, doi:10.1021/ja804816a (2008).

14   Tauber, K. *et al.* *Chem. Eur. J.* **19**, 4030-4035, doi:10.1002/chem.201202666 (2013).

15   Knaus, T., Cariati, L., Masman, M. F. & Mutti, F. G. *Org. Biomol. Chem.* **15**, 8313-8325, doi:10.1039/c7ob01927k (2017).

16   Cannio, R., Rossi, M. & Bartolucci, S. *Eur. J. Biochem.* **222**, 345-352, doi:10.1111/j.1432-1033.1994.tb18873.x (1994).

17   Pal, S., Park, D. H. & Plapp, B. V. *Chem. Biol. Interact.* **178**, 16-23, doi:10.1016/j.cbi.2008.10.037 (2009).

18   MacKintosh, R. W. & Fewson, C. A. *The Biochemical journal* **255**, 653-661 (1988).

19   Giordano, A. *et al. Biochemistry* **38**, 3043-3054, doi:10.1021/bi982326e (1999).

20   Shearer, G. L., Kim, K., Lee, K. M., Wang, C. K. & Plapp, B. V. *Biochemistry*
        32, 11186-11194, doi:10.1021/bi00092a031 (1993).

21   Patil, M. D., Grogan, G., Bommarius, A. & Yun, H. *ACS Catal.* **8**,
        10985-11015, doi:10.1021/acscatal.8b02924 (2018).

22   Sharma, M., Mangas-Sanchez, J., Turner, N. J. & Grogan, G. *Adv. Synth.
        Catal.* **359**, 2011-2025, doi:10.1002/adsc.201700356 (2017).

23   Knaus, T., Böhmer, W. & Mutti, F. G. *Green Chem.* **19**, 453-463,
        doi:10.1039/C6GC01987K (2017).

24   Abrahamson, M. J., Vazquez-Figueroa, E., Woodall, N. B., Moore, J. C. &
        Bommarius, A. S. *Angew. Chem. Int. Ed.* **51**, 3969-3972,
        doi:10.1002/anie.201107813 (2012).

25   Abrahamson, M. J., Wong, J. W. & Bommarius, A. S. *Adv. Synth. Catal.*
        355, 1780-1786, doi:10.1002/adsc.201201030 (2013).

26   Ye, L. J. *et al. ACS Catal.* **5**, 1119-1122, doi:10.1021/cs501906r (2015).

27   Pushpanath, A., Siirola, E., Bornadel, A., Woodlock, D. & Schell, U. *ACS
        Catal.* **7**, 3204-3209, doi:10.1021/acscatal.7b00516 (2017).

28   Chen, F.-F. *et al. ACS Catal.* **8**, 2622-2628, doi:10.1021/acscatal.7b04135
        (2018).

29   Mayol, O. *et al. Nat. Catal.* **2**, 324-333, doi:10.1038/s41929-019-0249-z
        (2019).

30   Tseliou, V., Knaus, T., Masman, M. F., Corrado, M. L. & Mutti, F. G. *Nat.
        Commun.* **10**, 3717, doi:10.1038/s41467-019-11509-x (2019).

31   Mutti, F. G., Knaus, T., Scrutton, N. S., Breuer, M. & Turner, N. J. *Science*
        349, 1525-1529, doi:10.1126/science.aac9283 (2015).

Chapter 6

Development of a screening methodology for idenification of (S)-selective amine dehydrogenases

The project described in this chapter is in progress

6.1 Abstract

Amine dehydrogenases (AmDHs) represent one of the most rapidly developed enzyme family for the synthesis of a-chiral amines. However, most of the AmDHs developed up to date display (*R*)-selectivity. Engineering of new (*S*)-selective AmDHs is one of the main challenges. In this study, we have developed a screening assay for the identification of (*S*)-configured amines in solution that can be applied for screening novel (*S*)-selective AmDHs. After expression and purification of the potential AmDHs in the 96-deep well blocks, the variants can be screened for the desirable reductive amination direction. The high enantioselectivity of this assay relies on a monoamine oxidase (MAO) capable of oxidizing exclusively (*S*)-configured amines to their corresponding imines producing H_2O_2. The H_2O_2 formed is subsequently used by a horseradish peroxidase (HRP) to form a colored product that can be identify both by eye and spectrophotometrically. Amines with (*R*)-configuration or samples with no amines did not result in any coloration of the sample significantly reducing the possibility of false positive results. It is expected that the assay will be apply for identification of novel (*S*)-selective AmDHs in the future.

6.2 Introduction

Amine dehydrogenases (AmDHs) catalyze the reductive amination of carbonyl compounds at the sole expense of ammonia and a hydride source yielding a-chiral amines with excellent enantioselectivity. When combined with cofactor recycling enzymes (e.g., FDH, GDH), AmDHs represent an enzyme family that displays increased atom economy for the synthesis of chiral amines. Therefore, AmDHs has been the subject of extensive investigation during the last years, In fact, since 2012, fourteen AmDHs are now available, using genome mining or semi-rational approaches as discussed in the first chapter. Apart from the recently discovered (*S*)-selective native AmDHs (nat-AmDHs),[1] all other members have been created starting from L-amino acid dehydrogenases (L-AADHs) by targeting residues that interact with the a-carboxyl-moiety of the substrate. For instance, *Bs*-AmDH,[2] *Bb*-AmDH,[3] *Rs*-AmDH,[4] *cal*-AmDH,[5] *Es*-AmDH,[6] *Lf*-AmDH[7] and *Bsp*-AmDH (displaying *R*-selectivity) were all engineered from L-PheDH or L-LeuDH by substituting the two highly conserved residues that interact with the carboxyl group of the substrate (i.e., lysine and aspartate). Moreover, we have recently created (*R*)-selective AmDHs (LE-AmDHs) starting from L-lysine-(ε-deaminating)dehydrogenase (LysEDH) that does not catalyze any apparent asymmetric transformation on its natural reaction/substrate but displayed (*S*)-selectivity when interrogated for the amination of 6-oxo-hexanoic acid, which is structurally related to the natural substrate (*L*-Lysine).[8] As a result, until now nine out of fourteen available AmDHs display (*R*)-selectivity. These (*R*)-selective AmDHs are capable of transforming a wide range of carbonyl compounds into the corresponding amines. In contrast, the (*S*)-selective nat-AmDHs are all active towards a similar substrates, practically limited to small aliphatic ketones and cycloalkanones.[1]

One of the major limitations of the AmDHs is the limited availably of (*S*)-selective members. This is due to the similar scaffolds and approach that have been used for engineering of new AmDHs as well as due to the lack of a screening assay for the detection of (*S*)-configured amines. So far, the identification of AADH variants as potential AmDHs have been performed using an NAD+ auto fluorescence

assay. Fluorescence-relative quantification of NAD^{+} produced after reductive amination could be monitored at high pH (pH >13) and ranked based upon the differential increase in fluorescence over a background reaction. The long reaction times and the low signal to noise ratio are two major limitations of this assay.[2] A formazan-based assay have been also used for screening of AmDHs.[2,4] This assay is based on the methodology developed by Chen *et al.*[9] The enzymatic deamination activity is related to the conversion of NAD^{+} to NADH, which is reoxidized to NAD^{+} by phenazine ethosulfate (PES). The resulting reduced PES subsequently reduces 2-(4-iodophenyl)-3-(4-nitrophenyl)-5-phenyltetrazolium chloride hydrate (INT) to create formazan. Formazan creates a deep red color, which can be monitored at 495 nm. However, it is expected that not all AmDHs that are able to perform the reductive amination are sufficiently active in the opposite direction (or even are not active at all) as known for alcohol dehydrogenases. As a results, active variants for the reductive amination may never be detected using this assay and, very regretfully, discarded as false negatives. Another limitation reported is the increased number of false positive samples. To eliminate these false positive readings another spectrophotometric assay has been developed by comparing the samples' absorbance in two different wavelengths (340 nm and 600 nm) over a background plate at the same wavelengths.[2,5] The increased absorbance at 340 nm corresponds to the production of NADH in the deamination direction, while absorbance at 600 nm estimates the amount of biomass present. This simple assay can only be applied for the deamination reaction. It should also mentioned that the amine substrate or the ketone product may interfere with the detection if absorbance occurs in wavelengths close to NADH absorbance.

Herein, we reported the development of a screening methodology for the detection of (*S*)-configured amines. Both expression and purification can be performed in 96-deep well blocks using Ni-NTA coated magnetic beads. Purification with Ni-NTA coated magnetic beads is optional. The amines can be detected in aqueous solutions without the need for extraction. Moreover, the potential AmDHs can be screened in the desirable, reductive amination,

direction. One of the main advantages of this colorimetric assay is its high enantioselectivity, since in the presence of (*R*)-configured amines the samples did not result in any coloration. Moreover, in the absence of the amine product, the reaction did not occur, thus eliminating the possibility to obtain false positive results. This assay will be applied for the screening of D-AADH variants as potential (*S*)-selective AmDHs.

6.3 Results and discussion

6.3.1 Electrocompetent cells and electroporation

The electrocompetent cells were prepared based on BioRad MicroPulser application guide as describe in methods (section 6.5.1). The electrocompetent BL21(DE3) cells were used for high efficiency electrotransformation of the plasmid encoding for D-AADH[10] using MicroPulser electroporation apparatus (BioRad) and following manufacturer's instructions (see methods 6.5.1). Aliquots of 100 μL of the 1 mL transformed cells were spread in large petri dishes (approx. 100 mL), and grown at 37 °C overnight. Next day more than 1000 colonies were observed in each petri dish indicating that the method is suitable for the preparation of large number of colonies (~ 30.000) for screening purposes.

6.3.2 Development of an expression and purification assay in 96-deep well blocks

In this assay the Ch1-AmDH[11] was chosen as tested enzyme because of its high expression yield in order to exclude any limitation of the methodology due to enzyme's poor expression. Cultures of Ch1-AmDH were performed in 1 or 2 mL 96-deep well blocks, in order to find the best cultivation volume. In both conditions the enzyme expressed well using the reported methodology (see methods 6.5.2). Higher expression yield was observed in 2 mL cultures in relation to the 1 mL cultures. The lysis of the cells with the reported procedure resulted in enough amount of protein in the soluble fraction for downstream applications.

Purification of the 96-deep well blocks were performed after optimization of the procedure reported by manufacturer using Ni-NTA coated magnetic beads. Optimization was performed by purification trials of known concentration of Ch1-AmDH. The aim was to find the best relationship between the amount of the enzyme that the beads can bind and that can be eluted in one fraction. In order to achieve this, five parameters were tested and adjusted: the quantity of protein that can be bound to a specific volume of beads, the induction time of the sample with beads, the imidazole concentration in the elution buffer as well as the number and volume of elution fractions. After a series of experiments, we

obtained approximately 300 µg of the Ch1-AmDH in the first elution fraction when eluted with 500 mM imidazole (50 µL, 6 mg/mL). Incubation time of the sample with the beads was 20 min and elution time was 5 min. Using these conditions, the supernatants obtained from the *E. coli* cultures of the 2 mL and 1 mL 96-deep well blocks were purified and analyzed by SDS-PAGE. In both cases the enzyme was obtained in high purity at the first elution fraction. Moreover, the purification yield was consistent among the different wells of the same plate.

In order to investigate a possible variation of the conversion levels for the amination catalyzed by the AmDH enzyme obtained from different positions within the same plate, we performed biocatalytic reactions using the eluted enzymes. The substrate *para*-fluoro-phenylacetone was chosen as it is known to be fully converted by Ch1-AmDH to the corresponding amine after 24 h using 90 µM of enzyme.[12] More specifically, the reaction shown in **Figure 1** was performed for 3 h and for 24 h. After 3 h, almost 40% conversion was observed in all different samples tested; after 24 h, all samples tested gave full conversion (**Figure 1**), thus confirming the reproducibility of the assay.
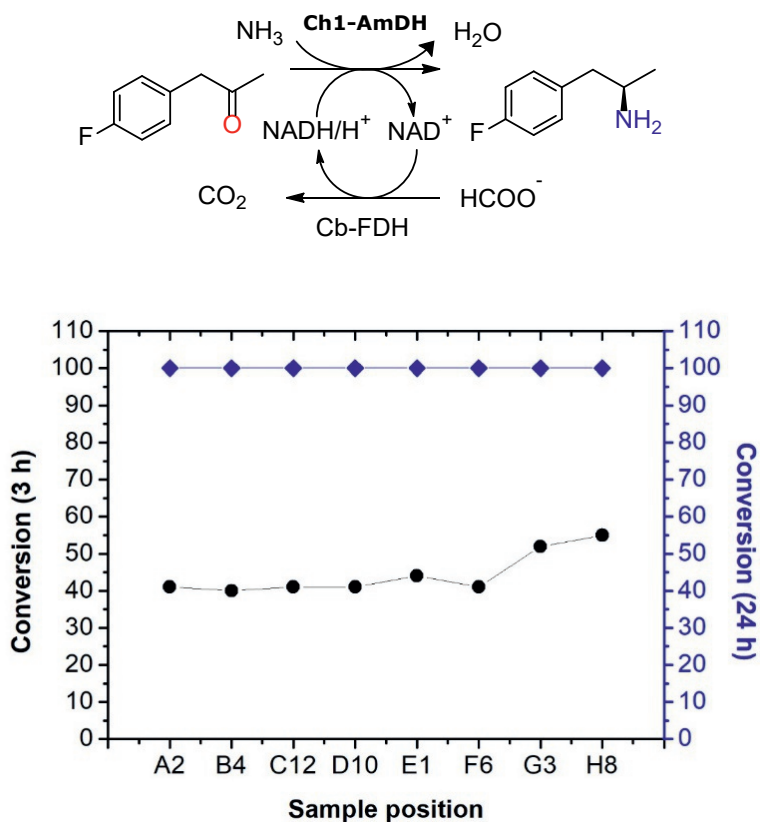
Figure 1. Biocatalytic reactions performed with Ch1-AmDH obtained after expression and purification in 96- deep well blocks.

6.3.3 Small scale expression and purification of D-AADH

The D-AADH has been reported to catalyze the reductive amination of D-amino acids.[10] However the enzyme showed no activity for the reductive amination of ketones or aldehydes tested (2-heptanone, 2-octanone, *para*-fluoro-phenylacetone, phenylacetaldehyde, hexanal, heptanal) but it was found to be active with phenyl-pyruvate. Therefore, the D-AADH was used as a starting template for the construction of library of potential (*S*)-selective AmDHs. This library was constructed by saturation mutagenesis (using NBT degenerated codons) of the enzyme's amino acid residues that are involved in the interaction with the substrate's carboxyl group (Asn244, Asn270, Ser149). For 95% coverage of the library, a screening of 5175 colonies was calculated to be required (i.e.,

including codon usage bias). Prior to the screening of the colonies, the applicability of the assay was tested using the parental enzyme.

Expression and purification were performed with 0.5 mM IPTG, overnight at 25 °C in 2 mL 96-deep well blocks (see methods 6.5.3) as in the case of Ch1-AmDH. These conditions resulted in high expression of the enzyme (**Figure 2**, line 2), while no enzyme was observed before induction (**Figure 2**, line 1). Cell disruption was performed with 900 µL B-PER bacterial protein extraction reagent supplemented with lysozyme (9.6 mg mL^{-1}) and DNAse (0.04 mg mL^{-1}) for 90 min at 25 °C. This lysis protocol resulted in high levels of enzyme in the soluble fraction, thus indicating efficient cell lysis (**Figure 2**, line 3), while only a minor part of the enzyme was observed in the insoluble fraction (**Figure 2**, line 4). The flow-through sample (after incubation of the Ni-NTA beads with the lysate) showed that almost all of the enzyme was bound into the beads (**Figure 2,** line 5). Remarkably, almost all the enzyme was eluted under the reported conditions in the first elution fraction (**Figure 2, line 6**).
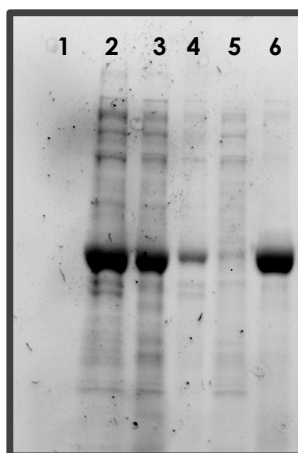
Figure 2. SDS page analysis of the expression, solubility and purification of D-AADH with magnetic beads. (1) Sample before induction; (2) sample after induction); (3) soluble fraction; (4) insoluble fraction; (5) sample after incubation of the enzyme with magnetic beads; (6) elution fraction.

Since the purified enzyme was in imidazole-containing buffer that absorbs at 280 nm, the concentration of the enzyme could not be determined

spectrophotometrically and therefore was calculated using the Bradford method. The calibration curve for the Bradford solution was calculated using BSA (see methods 6.5.3). On average 0.5 mg mL^{-1} of enzyme was present in each elution sample (50 µL, 25 µg in total).

6.3.4 Assay for the detection of (*S*)-configured amines using chromotropic acid

After purification of D-AADH variants (50 µL), they will be tested for the reductive amination of 2-hexanone. The 2-hexanone was chosen as substrate because of the reported high activity of D-AADH with 2-oxo-heptanoic acid. We hypothesize that the more hydrophobic active site of the engineered D-AADH variants will favor the acceptance of 2-hexanone. Furthermore, 2-hexylamine is accepted by the MAO-D5 in the next step of the screening procedure, which is graphically summarized in **scheme 1**.
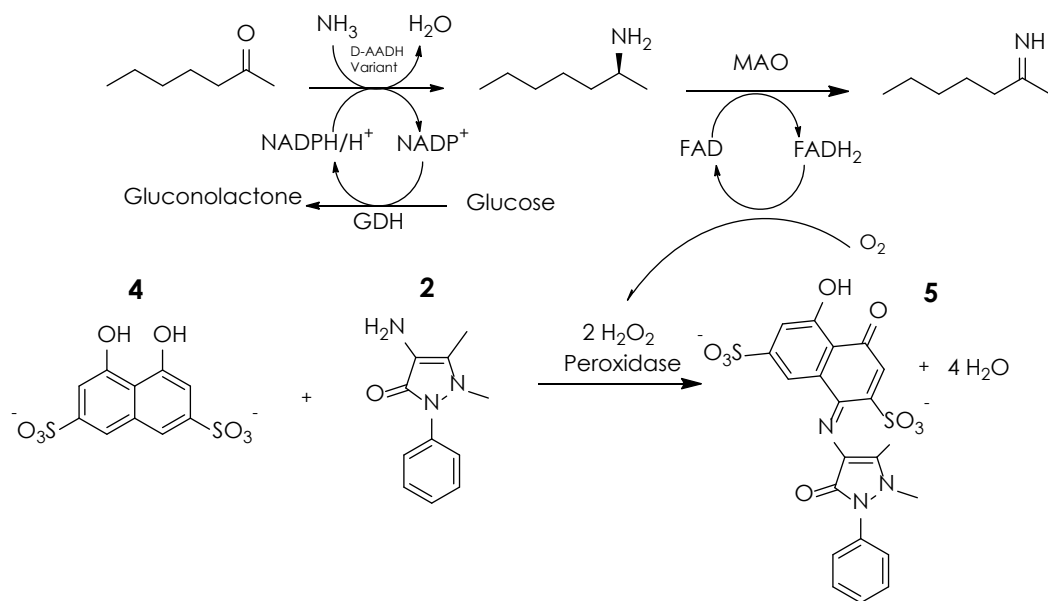
Scheme 1. Propose screening assay for D-AADH variants using chromotropic acid.

This assay is based on the peroxidase assay reported by Wong *et al*.[13] After the reductive amination of 2-hexanone by D-AADH variants, the MAO-D5[14]—which accepts only (*S*)-configured amines—will be used for oxidizing (*S*)-2-hexylamine to its corresponding imine.[15] The hydrogen peroxide formed from this reaction will

be used by the horseradish peroxidase (HRP) to conjugate compounds **4** and **2** forming compound **5** (**Scheme 1**). This compound (**5**) can be easily identified by eye (deep blue) or spectrophotometrically at 590 nm.

Initially the assay was tested with the reported conditions using 100 mM sodium phosphate buffer pH 6.5, 3 mM 4-aminoantipyrine (AAP, compound **2**) and 15 mM chromotropic acid (CTA, compound **4**) as well as 10 mM H_2O_2. In this assay, 5 mM of (*S*)-2-heptylamine were added and the reaction started by addition of HRP (10 µg mL^{-1}). **Figure 3** shows an intensive blue color that is formed after 5 min in the reaction samples (A2-C2). In contrast, the non-protein-containing control (NPC without MAO) did not result in any coloration of the samples (A1-C1).
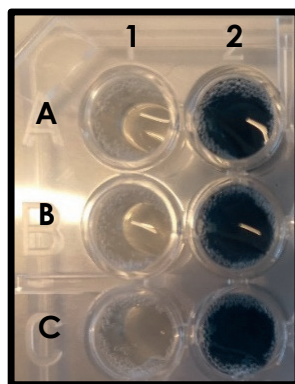
Figure 3. Initial test of the colorimetric assay using chromotropic acid.

Another set of reactions were prepared using 100 mM KPi 7.6, which is the preferred buffer by MAO-D5.[15] Indeed, after 5 min the reactions performed in KPi buffer also became blue. All reactions (both in sodium phosphate and in KPi) were measured spectrophotometrically at 590 nm. Results are shown in **Table 1**. In general, the reactions showed higher absorption values in KPi pH 7.6 compared with sodium phosphate after 5 min. Moreover, in KPi the absorption values at 590 nm for the negative controls remained low (i.e., <0.25) even after 30 min.

Table 1. Absorption values at 590 nm of the colorimetric assay in different buffers.

100 mM Sodium Phosphate pH 6.5				100 mM KPi pH 7.6			
Abs 590 nm				Abs 590 nm			
5 min		30 min		5 min		30 min	
NPC	Reaction	NPC	Reaction	NPC	Reaction	NPC	Reaction
0.17	0.84	0.50	3.6	0.08	1.03	0.2	3.4
0.13	0.86	0.51	3.6	0.12	0.83	0.22	3.3
0.13	0.90	0.56	3.5	0.11	0.90	0.19	3.3

NPC: Non protein control

In the next step, the sensitivity of the assay at low concentrations of H_2O_2 was investigated. The amount of H_2O_2 is related with amount of (*S*)-configured amine produced from the first step of the screening process (reductive amination of ketone). To investigate the lowest amount of H_2O_2 that will still result to measurable amounts of compound **5**, the reactions were performed with 0.1-5 mM of H_2O_2. **Table 2** summarizes the absorption values obtained from the reactions performed after 5 min reaction time. It is evident that the assay can be used even at concentrations of H_2O_2 as low as 0.1 mM. At this concentration the values obtained are still significantly higher than the negative control (0 mM H_2O_2) thereby confirming the sensitivity of the assay. The absorption values above 2 mM of H_2O_2 were observed to be 3.4 because of the saturation of the reaction above this concentration.

Table 2. Absorption values at 590 nm of the colorimetric assay at different concentrations of H_2O_2.

[H_2O_2] mM	Reaction Time (min)	Abs 590 nm
0.0	5	0.15
0.1	5	0.35
0.2	5	0.86
0.3	5	1.30
0.4	5	1.70
0.5	5	2.13
1	5	3.35
2	5	3.4
3	5	3.4
4	5	3.4
5	5	3.4

All results using the CTA assay were obtained with external addition of H_2O_2. However, the activity of MAO may be influenced by CTA. Therefore, in another set of reactions, the assay was performed without any external addition of H_2O_2. The amount of H_2O_2 required was *in situ* produced by the oxidation of (*S*)-2-heptylamine to its corresponding imine by the action of MAO (see methods part 6.5.4 for expression of MAO-D5). The reactions were performed with 15 µL of MAO-D5 (cell free extract) and using different concentrations of (*S*)-2-heptylamine. Unfortunately, no color was observed in any of these reactions, indicating that MAO is possibly inhibited by CTA. A positive control using the 2,4,6-tribromo-3-hydroxybenzoic acid was also included and it was ensured that MAO was active. Therefore, this assay was not investigated any further.

6.3.5 Assay for the detection of (*S*)-configured amines using 2,4,6-tribromo-3-hydroxybenzoic acid

An alternative assay for the detection of (*S*)-configured amines, which is schematically shown in **Scheme 2**, has been developed. The

2,4,6-tribromo-3-hydroxybenzoic acid (**Scheme 2**, compound **1**) was used instead of chromotropic acid (CTA). This compound is commonly used to evaluate the activity of the MAOs for screening both enzyme and substrate libraries.[15] The conjugated product (**Scheme 2**, compound **3**) produces an intensive magenta color and can be determined spectrophotometrically at 510 nm.
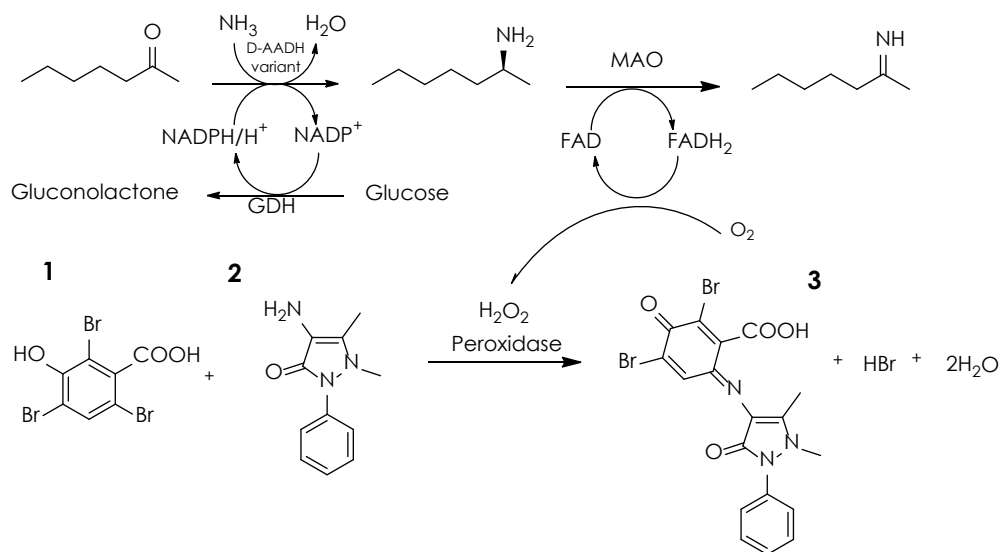
Scheme 2. Colorimetric assay with 2,4,6-tribromo-3-hydroxybenzoic acid for the detection of (S)-configured amines.

In the first set of reactions, it was ensured that MAO-D5 is active in the presence of 2,4,6-tribromo-3-hydroxybenzoic acid using (*S*)-configure a-methylbenzylamine. The a-methylbenzylamine has been reported to be accepted by MAO-D5.[14,15] Reactions were performed with 5 mM (*S*)-configured a-methylbenzylamine with different amounts of MAO-D5 (5-15 µL cell free extract). In all cases the reaction mixture became colored (magenta) after the first 10 min. The same assay was also performed using the (*R*)-configured a-methylbenzylamine. These reactions remained uncolored indicating no activity of MAO-D5 at all, even after 24h. In all cases, a non-protein-containing control (NPC), which did not contain MAO-D5, was also included; thus, it was

ensured that the reaction does not occur in the absence of MAO-D5 due to the required H_2O_2 for the HRP. Next, the acceptance of *rac*-2-hexylamine was tested using the same assay since this is the target compound for screening of the library. Reactions were performed at different concentrations of *rac*-2-hexylamine from 0.1-5 mM. Results showed that after 20 min a magenta color was visible in the reactions samples containing the substrate, the exception being the reaction performed with 0.1 mM substrate; this latter sample required approximately 3 h for the color to be visible by eye.

For the screening of the library of variants of D-ADDH, two separated reaction steps are performed after purification of the biocatalyst. The first step is the addition of the reaction mixture (**RM**, 50 µL) into the purified enzyme (50 µL). The reaction mixture contains: ketone (10 mM), GDH (2 mg/mL), D-glucose (100 mM), and $NADP^+$ (2 mM) in 400 mM NH_4Cl buffer pH 9 supplemented with 100 mM K_2CO_3 as previously reported for this enzyme.[10,16] The second step is the addition of 200 µL of assay solution (**AS**) containing 0.54 mM of compound **1**, 0.75 mM of compound **2** (**Scheme 2**), 15 µL MAO-D5 (15 µL) and HRP (10 µg/ mL) in 500 mM KPi pH 7.6. To simulate the above mentioned conditions in a hypothetical scenario in which D-AADH converted 50% of 2-hexanone substrate at initial 10 mM concentration, 5 mM of 2-hexanone and 5 mM of 2-hexylamine were added into the reaction mixture; next, 50 µL of this mixture were added into 50 µL of elution buffer containing 1 mg/mL DAADH. After that, 200 µL of the assay solution was added. This reaction was performed in triplicate (**Figure 4**, S2-S4). Another reaction was prepared without addition of amine and used as a negative control (**Figure 4**, S1). Finally, two positive controls (**Figure 4** S5 and S6) were prepared containing 5 mM of 2-hexylamine in the assay solution (**AS**). These controls were prepared without any addition of D-AADH and without addition of the reaction mixture (**RM**). Additionally, in the sample (S5) 2-hexanone (5 mM) was added in order to investigate any effect of the unreacted starting compound in the reaction. Results (**Figure 4**) show that after 24h all reactions became colored (S2-S4) while the negative control remained uncolored (S1). The positive control without ketone also gave the expected magenta color (**S6**).

Unexpectently, the positive control containing both ketone and amine did not result in any coloration (**S5**) after this time which colored after longer reaction time (~48h).

Figure 4. Assay for the detection of amines under screening conditions.
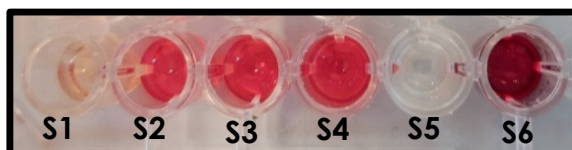
6.4 Conclusions

The scarce availability of (*S*)-selective AmDHs is one of the major limitations of this class of enzymes. This can be partly overcome using highly enantioselective assays for screening of new (*S*)-selective AmDH variants. In most of the reported cases, engineering new AmDHs have been achieved by screening libraries in the oxidative deamination direction leading to a decreased possibility to identify active variants in the reductive amination reaction. Moreover, the variants were used as cell free extracts and therefore consumption of the cofactor by other enzymes produced by the host organism may lead to false positive results. Herein, we have developed an assay for the screening of (*S*)-selective AmDHs. Expression and purification can be performed in 96-deep well blocks using NI-NTA coated magnetic beads that bind to the His-tagged variants. After optimization of the purification procedure, we were able to obtain most of the enzyme in the first elution fraction. The enzymes were screened for the desirable reductive amination direction. The formation of (*S*)-configured amines can be detected by eye using two enzymes: a monoamine oxidase (MAO) and a peroxidase (HRP). The first enzymes oxidizes exclusively (*S*)-configured amines into the corresponding imines producing H_2O_2, which can be subsequently used by the second enzyme that produces a colored product. The HRP was tested for the conjugation reaction using both chromotropic acid (CTA) and 2,4,6-tribromo-3-hydroxybenzoic with 4-aminoantipyrine (AAP). Although the HRP was found to be active in all reactions tested, the presence of MAO negatively affected the reaction between CTA and AAP. In contrast the reactions with 2,4,6-tribromo-3-hydroxybenzoic and AAP resulted in coloration of the samples in the presence of MAO without any external addition of H_2O_2. Moreover, in the presence of (*S*)- but not (*R*)-configured amines the reaction samples were colored, indicating that the enzymes producing the desirable (*S*)-configured product (with or without perfect enantioselectivity) can be identified using this assay.

6.5 Methods

6.5.1 Electrocompetent cells and electroporation

For the preparation of electrocompetent cells, a glycerol stock of BL21(DE3) cells containing no plasmid, was used for streaking an antibiotic free LB-agar plate, grown overnight at 37 °C. Next day, a single colony was used to inoculate an overnight culture (ONC) containing LB medium (5 mL). This ONC was used to inoculate the main culture (500 mL). When the OD was ~ 0.7-1, the main culture was chilled on ice for 20 min. After this time, the main culture was transferred under flame to 10 sterile falcon tubes (10 x 50 mL) on ice. The falcon tubes were centrifuged for 15 min at 4500 rpm (4000g). The supernatants were removed and it was ensured that no supernatant remained into the falcon tubes that could affect the transformation efficiency. The harvested cells were gently resuspended under flame in 50 mL ice cold 10% glycerol (sterile) and the samples were centrifuged for another 15 min at 4500 rpm. The supernatants were removed and the pellets were resuspended in another 25 mL of 10% ice cold glycerol. After another round of centrifugation (4500 rpm) and removal of the supernatants, the cells were finally resuspended in 2 mL 10% ice cold glycerol under sterile conditions. Aliquots of 40 μL were prepared and the electrocompetent cells were store at –80 °C. For the electroporation, an aliquot of 40 μL of cells was used and gently mixed with 1.5 μL of the plasmid encoding for the D-AADH (pET28b). The mixture was cooled on ice for 1 min and transferred to a pre-cooled cuvette (sterile, 0.2 cm) under flame. The cuvette was inserted into the slide of the shocking chamber and a single pulse was delivered with the optimal voltage of 2.5 kV. The cuvette was removed from the chamber and 1 mL of SOC medium was immediately added to the cuvette. The cells were gently resuspended and transferred to a 17 x 100 mm polypropylene tube which was incubated for 1h at 37 °C.

6.5.2 Development of an expression and purification assay in 96-deep well blocks

For the development of the high throughput screening method in 96-deep well blocks, modifications of the protocol reported by Bougioukou *et al.*[17] were made in order to optimize the process. The Ch1-AmDH was used as the testing enzyme because of its favorable properties. Aliquots of 100 µL ONC were used to inoculate new 96-deep well block containing 400 µL of LB medium (in the case of 1 mL 96-well plate) or 900 µL of LB medium (in the case of 2 mL 96-well plate), supplemented with 50 µg mL^{-1} kanamycin. After 3 h incubation at 37 °C with shaking at 390 rpm another 500 µL (for the 1 mL blocks) or 1 mL (for the 2 mL blocks) of LB medium supplemented with 50 µg mL^{-1} kanamycin and 1 mM isopropyl-thiol –β-D-galactoside (IPTG) were added (final concentration of IPTG is 0.5 mM) and the plate were incubated at 25 °C overnight. The expression levels were observed by SDS-PAGE. The next day, the plate was centrifuged and the supernatants were discarded. The pellets were frozen at -20 °C for at least one hour following by thawing and resuspension in 150 µL washing buffer (phosphate buffer pH 7.0, NaCl, Tween 20, 0.04% NaN$_3$, IMAC purification kit). The plate was then shock frozen with liquid nitrogen and immediately thawed with warm water for five times. The lysis of the cells was finally completed by the addition of lysozyme (2 mg mL^{-1}) for 2 h at 4 °C and shaking in an orbital shaker (390 rpm). After incubation, the lysate was centrifuged at 5600 rpm for 45 minutes and the supernatants were collected for purification.

Purification was performed with QuickPick IMAC kit protocol using PickPen 8-M, after modifications of manufacturer's instructions: 100 µL of magnetic beads transferred to 150 µL regeneration buffer (Aqueous NiSO$_4$ solution, Tween 20, 0.02% NaN$_3$) and were washed with washing 1 buffer (phosphate buffer pH 7.0, NaCl, Tween 20, 0.04% NaN$_3$). After that, the beads were transferred to the sample (150 µL) and incubated at RT for 20 min with shaking at 700 rpm using an orbital shaker. After one washing step with washing 2 buffer (100 mM phosphate buffer pH 7.0, 250 mM NaCl, Tween 20, 0.04% NaN$_3$, 20 mM imidazole) the protein was eluted with 100 µL elution buffer (50mM sodium phosphate buffer, 300 mM

imidazole, 500 mM NaCl, pH 8.0). The final imidazole concentration of 500 mM was chosen after purification trials of known quantity Ch1-AmDH by varying its final concentration (300 mM and 500 mM) in the elution buffer and the elution volume (50 µL, 70 µL, 140 µL) in order to obtain as much protein possible in one elution fraction. The incubation time of the sample with the magnetic beads (2-20 min.) as well as the time the beads were been incubated into the elution buffer (1- 10 min) also was adjusted after a series of experiments with the aim to find the optimum incubation times.

For the high-throughput biocatalytic reactions, the enzymes were immediately used after purification. First a mixture was prepared containing $HCOONH_4/NH_3$ buffer (2M, pH 8.5), 2 mM NAD^+, FDH (3mg 10 mL^{-1}) and 10 mM of substrate (*fluoro*-phenylacetone) diluted in DMSO. The mixture was then splited in each well, until the volume of the reaction was 200 µL (100 µL of the mixture and 100 µL of the purified enzyme). The reactions were performed at 30 °C, overnight. The reactions were quenched after 24 h by the addition of aqueous 10M KOH (100 µL) and the extraction was performed with dichloromethane (CH_2Cl_2, 1 x 250 µL) followed by centrifugation. The organic phases were dried with magnesium sulfate and the conversions were measured by GC and determined on an Agilent GC system equipped with an Agilent J&W DB-1701 column (30 m, 320 µm, 0.25 µm); GC program parameters: injector 250 °C; constant pressure 6.9 psi; temperature program: 60 °C/hold 6.5 min; 100 °C/rate 20 °C min^{-1}/hold 5 min; 280 °C/rate 20 °C min^{-1}/hold 1 min.

6.5.3 Small scale expression and purification of D-AADH

For the expression of D-AADH in 96-deep well blocks (2 mL) an ONC was prepared (10 mL LB supplemented with 50 µg mL^{-1} kanamycin). For each well of the plate, 100 µL of this ONC were used to inoculate 900 µL of LB supplemented with 50 µg mL^{-1} kanamycin. This main culture was grown at 37 °C for 3 h. After this time, a 1 mL LB supplemented with 50 µg mL^{-1} kanamycin and 1 mM IPTG was added and the culture was grown at 25 °C overnight. The next day, the plate was centrifuged at 5600 rpm for 1h. The supernatants were removed and the

pellets were resuspended in 150 µL lysis buffer buffer (pH 8.0, 50 mM KH$_2$PO$_4$, 300 mM NaCl). In total 50 µL from a home-made cell lysis reagent (900 µL B-PER bacterial protein extraction reagent, 96 µL lysozyme of 100 mg/mL (concentration of stock solution) and 4 µL DNAse of 10 mg mL^{-1} (concentration of stock solution)) were added to each sample and incubated at 25 °C for 90 min to allow for enough time for cell disruption. The lysates were centrifuged for 90 min at 5700 rpm and the supernatants were transferred in a flat-bottom 96-well plate for downstream purification.

Purification was performed with 50 µL of beads using the following procedure. For each sample (well) to be purified, 50 µL of beads were transferred to a 96-well plate. This plate was put on top of a home-made magnetic plate to keep the beads on the bottom of the plate and the liquid phase (storage solution) could be easily removed. 250 µL of lysis buffer was added to the well containing the beads. The beads were incubated in lysis buffer for 1 min. After that the lysis buffer was removed and 100 µL of regeneration buffer were added to the beads and incubated for another minute. After the incubation time, the regeneration buffer was removed and another 250 µL of lysis buffer were added to the beads. After another minute, the lysis buffer was removed following by the addition of the 200 µL lysate. The lysate was incubated with the Ni-charged magnetic beads for 10 min at 4 °C. After that time the 96-well plate containing the beads was placed on the top of the magnetic plate and the liquid phase was removed. 250 µL of wash buffer (pH 8.0, 50 mM KH$_2$PO$_4$, 300 mM NaCl, 30 mM imidazole) were added and incubated for 2 min. Finally the enzyme was eluted with 50 µL elution buffer (pH 8.0, 50 mM KH$_2$PO$_4$, 300 mM NaCl, 500 mM imidazole) after incubation of another 5 min. After this step, the elution buffer containing the enzyme was stored and the beads were incubated into the 200 µL elution buffer to remove any traces of bound enzyme.

The enzyme concentration was determined using the Bradford assay. A BSA stock (10 mg/mL) was prepared. Using this stock, samples with different concentrations of BSA (0.15-0.5 mg/ mL) were prepared. 20 µL of each sample were added in 980 µL of Bradford solution and the absorbance at 595 nm was

determined. Based on the obtained values, a calibration curve was determined with slope 0.791 (R^2: 0.993). A diluted sample (1:2) of the purified D-AADH was made and 20 µL of this sample were added into 980 µL Bradford solution and the absorbance at 595 nm was measured. In order to calculate the concentration of the enzyme (mg/mL), the obtained value was divided with the slope and multiply by the dilution factor (2).

6.5.4 Expression of MAO-D5

E. coli cells (glycerol stocks) harboring pET-28a plasmids encoding for the MAO-D5 and MAO-D9 were used to prepare ONCs (5 mL LB supplemented with ampicillin 100 µg mL^{-1}). Next day, 100 µL of the ONCs were used to inoculate 10 mL of LB supplemented with ampicillin 100 µg mL^{-1} . This small main culture was grown in 30 °C until the OD_{600} ~ 0.7-1. After the required time, 8 mL of this culture were used to inoculate the main large culture (800 mL LB supplemented with ampicillin 100 µg/mL) which was grown at 30 °C overnight. The next day, the cells were harvested by centrifugation (15 min 4.500 rpm at 4 °C) and the pellet was resuspended in 50 mM KPi buffer, pH 7.6. Lysis of the cells was performed with ultrasonication (total sonication time 10 min). After centrifugation the soluble part was stored in -80 °C supplemented with FAD$^+$ and used as cell free extract in all reactions performed.

6.5.5 Colorimetric assays for the detection of (*S*)-configured amines.

2,4,6-tribromo-3-hydroxybenzoic acid based assay

In this assay, 15 µL of the supernatant (cell free extract) containing MAO-D5 supplemented with FAD was used. Using 0.75 mM of 4-aminoantipyrine (AAP, 1 M stock in DMSO) and 0.54 mM of 2,4,6-tribromo-3-hydroxybenzoic acid (stock 2% w v^{-1} in DMSO) an assay solution was prepared in 100 mM KPi pH 7.6. The reaction consisted of 180 µL of assay solution,15 µL of MAO-D5 cell free extract and 5 µL of horseradish peroxidase (HRP) solution (HRP stock 1 mg mL^{-1}). The reaction was started by the addition of amine (stock 1 M) at the desirable concentration.

Chromotropic acid based assay

1M of 4-aminoantipyrine (AAP, compound 2) and 500 mM of chromotropic acid (CTA, compound **4**) were prepared as stock solution in DMSO. In addition, 1M H_2O_2 stock solution in dH_2O was freshly prepared. The assay solution 2 (1 mL) was prepared by adding 3 mM AAP, 15 mM CTA and 10 mM H_2O_2 in either 100 mM sodium phosphate buffer pH 6.5 or 100 mM KPi buffer pH 7.6. The substrate (5 mM) was added from a stock solution 1 M in DMSO. Reaction was started by the addition of 10 µg mL^{-1} HRP. Reactions were measured spectrophotometrically using a fluorometer with excitation filter A-590 and no emission filter.

6.6 References

1   Mayol, O. *et al. Nat. Catal.* **2**, 324-333, doi:10.1038/s41929-019-0249-z (2019).

2   Abrahamson, M. J., Vazquez-Figueroa, E., Woodall, N. B., Moore, J. C. & Bommarius, A. S. *Angew. Chem. Int. Ed.* **51**, 3969-3972, doi:10.1002/anie.201107813 (2012).

3   Abrahamson, M. J., Wong, J. W. & Bommarius, A. S. *Adv. Synth. Catal.* **355**, 1780-1786, doi:10.1002/adsc.201201030 (2013).

4   Ye, L. J. *et al. ACS Catal.* **5**, 1119-1122, doi:10.1021/cs501906r (2015).

5   Pushpanath, A., Siirola, E., Bornadel, A., Woodlock, D. & Schell, U. *ACS Catal.* **7**, 3204-3209, doi:10.1021/acscatal.7b00516 (2017).

6   Chen, F.-F., Liu, Y.-Y., Zheng, G.-W. & Xu, J.-H. *ChemCatChem* **7**, 3838-3841, doi:10.1002/cctc.201500785 (2015).

7   Chen, F.-F. *et al. ACS Catal.* **8**, 2622-2628, doi:10.1021/acscatal.7b04135 (2018).

8   Tseliou, V., Knaus, T., Masman, M. F., Corrado, M. L. & Mutti, F. G. *Nat. Commun.* **10**, 3717, doi:10.1038/s41467-019-11509-x (2019).

9   Chen, S. & Engel, P. C. *J. Biotechnol.* **142**, 127-134, doi: 10.1016/j.jbiotec.2009.03.005 (2009).

10   Vedha-Peters, K., Gunawardana, M., Rozzell, J. D. & Novick, S. J. *J. Am. Chem. Soc.* **128**, 10923-10929, doi:10.1021/ja0603960 (2006).

11   Bommarius, B. R., Schurmann, M. & Bommarius, A. S. *Chem. Commun.* **50**, 14953-14955, doi:10.1039/c4cc06527a (2014).

12   Knaus, T., Böhmer, W. & Mutti, F. G. *Green Chem.* **19**, 453-463, doi:10.1039/C6GC01987K (2017).

13   Wong, R. C., Ngo, T. T. & Lenhoff, H. M. *Int. J. Biochem.* **13**, 159-163, doi: 10.1016/0020-711X(81)90151-8 (1981).

14   Dunsmore, C. J., Carr, R., Fleming, T. & Turner, N. J. *J. Am. Chem. Soc.* **128**, 2224-2225, doi:10.1021/ja058536d (2006).

15   Batista, V. F., Galman, J. L., G. A. Pinto, D. C., Silva, A. M. S. & Turner, N. J. *ACS Catal.* **8**, 11889-11907, doi:10.1021/acscatal.8b03525 (2018).

16   Parmeggiani, F. *et al. Adv. Synth. Catal.* **358**, 3298-3306, doi:10.1002/adsc.201600682 (2016).

17   Bougioukou, D. J., Kille, S., Taglieber, A. & Reetz, M. T. *Advanced Synthesis & Catalysis* **351**, 3287-3305, doi:10.1002/adsc.200900644 (2009).

Summary

a-Chiral amines are of great relevance in pharmaceutical manufacturing as these amines are involved in a variety of biological activities. Over the past years, their importance as building blocks in many Active Pharmaceutical Ingredients (APIs) was highlighted in a large number of scientific reports. It is estimated that a-chiral amines constitute approximately 40% of the optically active drugs that are currently commercialized mainly as single enantiomers. Their share is expected to increase due to stringent regulations for market approval concerning safety and efficiency, which are both directly related to the (enantio)purity of the compounds. Asymmetric synthesis of a-chiral amines is hard to achieve using traditional synthetic chemistry that involves multiple synthetic steps and often requires the use of toxic transition-metal-based catalysts. Consequently, various enzymatic methods have been developed that provide sustainable synthetic alternatives. Among them, amine dehydrogenases (AmDHs) constitute a recently developed enzyme family that possesses tremendous potential for the synthesis of a-chiral amines due to the elevated atom economy of the enzymatic reductive amination and exquisite enantioselectivity of AmDHs. The diversity of substrate scope, reactivity and enantioselectivity among the known engineered AmDHs is, however, poor. Overcoming these limitations are the main objectives of this thesis. Using a computational based rational approach, we were able to create novel AmDHs with increased and complementary substrate scope than the ones developed so far. The new AmDHs developed showed impressive enantioselectivity, increased thermal stability, and were applied for the asymmetric synthesis of chiral amines (APIs intermediate) at large scale (≥500 mg). Moreover, in contrast to the common belief that AmDHs accept only ammonia as amino donor, we have shown that AmDHs enable the synthesis of secondary and tertiary amines in enantioenriched form using small aliphatic or cyclic-aliphatic amines as amino donors. Through the combination of practical lab experiments and computational simulations, we gained new insights into the catalytic mechanism

of these AmDHs, thus revealing new aspects related to their applicability and current limitations in organic synthesis. The applicability of AmDHs in the kinetic resolution of racemic mixtures of amines was also demonstrated using an optimized AmDH-NOx system to give access to pharmaceutically relevant optically active amines possessing (S)-configuration. Starting from a promiscuous amino acid dehydrogenase scaffold (L-lysine-(ε-deaminating)-dehydrogenase from *G. stearothermophilus*), we were able to create enzymes that show both ADH activity as well as AmDH activity towards benzylic substrates. By optimizing and controlling the conditions of the biocatalytic transformation, these enzymes were used either for the preparation of a-chiral amines or primary alcohols with high efficiency. Amination of benzylalcohol to benzylamine was achieved by a single enzyme providing the first example of biocatalyst showing alcohol aminase activity. Finally, the scarce availability of (S)-selective AmDHs motivated us to develop a high-throughput screening methodology to detect (S)-configured amines in aqueous solution. This strategy possesses several advantages over the previously reported screening methodologies as it is highly enantioselective, can be used for the screening in the more desirable reductive amination reaction direction, and allows *in situ* purification of the biocatalyst. The latter feature enables to avoid any possible interference of other enzymes produced by the host organism as one of the steps of the assay. These features significantly reduce the possibility to obtain false positive results. This assay is expected to be used for screening potential (S)-selective AmDHs in the future.

Samenvatting

Chirale a-amines zijn betrokken bij een verscheidenheid aan biologische activiteiten. Om die reden zijn ze van groot belang bij de productie van geneesmiddelen. Gedurende de afgelopen jaren is de rol van chirale a-amines als bouwstenen van actieve farmaceutische grondstoffen (ook wel Active Pharmaceutical Ingredients - API´s) benadrukt in een groot aantal wetenschappelijke artikelen. Naar schatting vormen chirale a-amines ongeveer 40% van de optisch actieve geneesmiddelen die momenteel hoofdzakelijk als enkele enantiomeren worden verkocht. Er wordt verwacht dat hun aandeel zal toenemen als gevolg van strenge voorschriften voor marktgoedkeuring omtrent veiligheid en efficiëntie, die beide rechtstreeks verband houden met de (enantiomere) zuiverheid van de verbindingen. Asymmetrische synthese van chirale a-amines is moeilijk te bereiken met behulp van traditionele synthetische chemie. Vaak zijn er meerdere synthesestappen nodig en is het gebruik van giftige overgangsmetaal-katalysatoren vereist. Als gevolg hiervan zijn er verschillende enzymatische methodes ontwikkeld die duurzame synthetische alternatieven bieden. Amine dehydrogenases (AmDHs) vormen een recent ontwikkelde enzymfamilie met een enorm potentieel voor de synthese van chirale a-amines vanwege de hoge atoomeconomie van de enzymatische reductieve aminering en de uitstekende enantioselectiviteit. Echter, de substraatomvang, reactiviteit en enantioselectiviteit van alle bekende AmDHs vertonen maar weinig diversiteit. Het overwinnen van deze beperkingen is het hoofddoel van dit proefschrift. Met behulp van een computationeel gebaseerde rationele benadering waren we in staat om nieuwe AmDHs te creëren met een grotere en complementaire substraatomvang in vergelijking met de AmDHs die tot nu toe zijn ontwikkeld. De nieuwe AmDHs vertoonden indrukwekkende enantioselectiviteit, verhoogde thermische stabiliteit en werden toegepast voor de asymmetrische synthese van chirale amines (APIs intermediair) op grote schaal (≥500 mg). Bovendien hebben we, ondanks de algemene overtuiging dat AmDHs alleen ammoniak als aminodonor

accepteren, aangetoond dat onze AmDHs de synthese van secundaire en tertiaire amines in enantio-verrijkte vorm mogelijk maken door kleine alifatische of cyclisch-alifatische amines te gebruiken als aminodonoren. Door een combinatie van praktische laboratoriumexperimenten en computationele simulaties hebben we nieuwe inzichten verkregen in het katalytische mechanisme van deze AmDHs. Hierdoor zijn nieuwe aspecten onthuld met betrekking tot de toepasbaarheid en de huidige beperkingen van deze enzymen in organische synthese. De toepasbaarheid van AmDHs in de kinetische resolutie van racemische mengsels van amines werd aangetoond met behulp van een geoptimaliseerd AmDH-NOx systeem. Dit enzymatische systeem gaf toegang tot farmaceutisch relevante optisch actieve amines met (*S*)-configuratie. Uitgaande van een promiscue aminozuur dehydrogenase scaffold (*L*-lysine-(ε-deaminerende)-dehydrogenase van *G. stearothermophilus*) hebben we enzymen gecreëerd die zowel ADH activiteit als AmDH activiteit vertonen richting benzylische substraten. Door de omstandigheden van de biokatalytische transformatie te optimaliseren en te beheersen, konden deze enzymen worden gebruikt voor de efficiënte productie van chirale α-amines of primaire alcoholen. Dezelfde enzymen werden benut voor de directe aminering van benzyl alcohol tot benzylamine door een enkel enzym. Hiermee leverden we het eerste voorbeeld van een biokatalysator die 'alcohol aminase' activiteit vertoont. Ten slotte motiveerde de schaarse beschikbaarheid van (*S*)-selectieve AmDHs ons om een high-throughput screeningmethode te ontwikkelen voor de detectie van (*S*)-geconfigureerde amines in waterige oplossing. Onze strategie heeft verschillende voordelen ten opzichte van de eerder gepubliceerde screeningsmethodes, aangezien deze zeer enantioselectief is, kan worden gebruikt voor de screening in de meer gewenste reductieve aminering reactie richting en *in situ* zuivering van de biokatalysator mogelijk maakt. Het laatste kenmerk stelt ons in staat om elke mogelijke tussenkomst van andere enzymen te voorkomen, waardoor de kans op vals-positieve uitslagen aanzienlijk kleiner is. Naar verwachting zal deze assay in de toekomst worden gebruikt voor het screenen van potentiële (*S*)-selectieve AmDHs.

Acknowledgements

First and foremost, I would like to thank my supervisor, prof. Francesco G. Mutti, who gave me the opportunity of being a member of his research group. I highly appreciate his continuous support and guidance throughout my time in his laboratory and I am thankful for his inspirational mentorship that influenced my scientific development over the past 4 years. I am proud of being a member of his group that has been remarkably contributed in the field of biocatalysis in a short period of time.

I would like to thank prof. Jan van Maarseveen. His valuable advice, wide spectrum of knowledge and positive attitude have helped me to overcome many scientific challenges that I have faced during my research, have been showed me how to approach scientific questions from different directions and inspired me to develop a general interest in various scientific fields.

Besides my advisors, I would like to express my appreciation to the rest of the committee members; prof. Wever R., prof. Grossmann T.N., prof. Brul S., prof. Pavlidis I., prof. Fernández Ibáñez M.A., for the helpful advice, the time that they dedicated to evaluate my thesis, the fruitful discussions and for agreeing to be part as committee members during my PhD defence ceremony.

The completion of the work presented herein would not have been possible without the valuable efforts of many people, thus I would like to thank all the co-authors (also colleagues and friends), who contributed to the results presented in this dissertation. In particular, I would like to thank Dr. Tanja Knaus for her continuous help and support, since I started this PhD. Together we achieved great things of significant scientific impact, and we were able to smoothly work as a strong team. Besides that, we had a lot of moments of fun, often accompanied with her delicious glühwein. Special thanks to Maria-Luisa Corrado for the tremendous help that generously offered me from the first day that she started in the group. With our everyday collaboration we were able to learn from each other and be co-authors in a publication. Our endless chats certainly made my PhD life enjoyable. Outside the working environment we also

had an uncountable amount of funny moments and we have developed a strong friendship that will last for years. It has been a great pleasure working with Jan Vilim. The enormous amount of alcohol that we drunk together in Amsterdam, Prague and Rhodes, the close collaboration that we had in the lab, part of which also led to a publication, the extensive exchange of realistic and unrealistic ideas during these years, are only a few of the pleasant moments that we have shared. However, the majority of your jokes require great improvement to be considered as 'jokes'. I thank my colleague Wesley Bohmer for being a supportive lab mate by providing his help whenever he was asked for. Our collaboration is clearly highlighted by a nice publication. The times that we spend together out of the lab, both in Amsterdam and in Rhodes were very special. I definitely owe my special appreciation to Dr. Marcelo Masman that generously offered me an endless scientific and moral support. His vital help during our close collaboration in the last four years, has definitely contributed to the quality of this thesis and resulted in many publicly available research papers. I am especially thankful for his immense patience during teaching of the computational methodologies, most of which are presented herein.

I am grateful to all BSc and MSc students that worked with me during these four years. In particular, I would like to thank Martina Manzotti, Don Schilder and Sophie Evers. They all made a great piece of work and I hope that they can recognize themselves in some parts of this thesis. The ideal collaboration that we had, not only helped me completing this thesis but also made me a more responsible person. I am highly confident that you will all have a great future in your scientific career and I am especially happy that I can see that this is the case for most of you.

I would like to thank my best friends: Vasilis N., Iefteris K., Giannis P., Giannis L., Giorgos T., Kostas X., Kostas S., Christos Papas., Christos Papan., Nikos L., Lefteris F., and Loukas K., for their constant support not only during these four years but also during my whole life. These people are a great example of what the term 'true friends' really means. I can confidently state that no feeling coming from a PhD tittle or any other tittle can be compared with the feeling of having them as

friends. Many thanks to all my friends that I have met here in Amsterdam: Yolanda, Marissa, Wen-Liang, Piotr, Agnezkia, Flip, Simone, Kananat and to those that I may forget, for all funny moments that we have spent together and helpful discussions. Special thanks to my friends: Gaston and Roel. Meeting you in the first month of my PhD, it was certainly one of the best things happened to me in Amsterdam. Together we spend a lot of nice moments both in Amsterdam and in Rhodes and you have both helped me settle in Amsterdam. I am sure that this was only the beginning of a true friendship.

I am grateful to my parents: Giorgos T. and Anastasia B. and to my uncle Tharrenos B. who always encouraged and supported me (emotionally and financially) to pursue my dreams. Their unconditional love and altruistic acts made me strong to deal with any situation. I would like to thank my sister Despoina T., for guidance whenever the situation was becoming unclear and complicated and for all nice moments that we have spent together. Another person that I would like to thank is my cousin Sofia P. Her spontaneous attitude has shown me many times a different aspect of how to deal with various situations. Doing things together with you is full of fun and interest.

Finally, I would like to thank Nena P., a person inseparable with my personal and scientific life and development during the last years. I can certainly say that I would not be able to start or complete this PhD without your help and support. Your unique skills of analyzing complex situations and seeing things that I could not, makes you not only a great group leader but also a great partner who have helped me to take the right decisions, make smart choices and become mature and strong.

List of publications

Published:

1. **Kinetic resolution of racemic primary amines using *Geobacillus stearothermophilus* amine dehydrogenase variant**
Vasilis Tseliou, Tanja Knaus Jan Vilím, Marcelo F. Masman and Francesco G. Mutti
ChemCatChem 2019, 12, 1-6
DOI: 10.1002/cctc.201902085

2. **Generation of amine dehydrogenases with increased catalytic performance and substrate scope from ε-deaminating L-lysine dehydrogenase**
Vasilis Tseliou, Tanja Knaus, Marcelo F. Masman, Maria L. Corrado and Francesco G. Mutti
Nature Communications 2019, 10, 3717
DOI: 10.1038/s41467-019-11509-x
   - **Patent application filed '*L-Lysine epsilon-dehydrogenase variants and uses thereof*'**
   application number EP19157237.9

3. **Mechanistic insight into the catalytic promiscuity of amine dehydrogenases: asymmetric synthesis of secondary and primary amines**
Vasilis Tseliou. Marcelo F. Masman, Wesley Böhmer, Tanja Knaus and Francesco G. Mutti
ChemBioChem 2019, 20, 1–14
DOI: 10.1002/cbic.201800626

4. **A biocatalytic method for the chemoselective aerobic oxidation of aldehydes to carboxylic acids**
Tanja Knaus, **Vasilis Tseliou**, Luke D. Humphreys, Nigel S. Scrutton and Francesco G. Mutti
Green Chemistry 2018, 20, 3931-3943
DOI: 10.1039/C8GC01381K

5. **Molecular characterization of pyrethroid resistance in the olive fruit fly *Bactrocera oleae***
Nena Pavlidi Anastasia Kampouraki, **Vasilis Tseliou**, Nicky Wybouw, Wannes Dermauw, Emmanouil Roditakis, Ralf Nauen, Thomas van Leeuwen and John Vontas
Pesticide Biochemistry and Physiology 2018, 148, 1–7
DOI: 10.1016/j.pestbp.2018.03.011

6. Functional characterization of glutathione (*S*)-transferases associated with insecticide resistance in *Tetranychus urticae*.

Nena Pavlidi, **<u>Vasilis Tseliou</u>**, Maria Riga, Ralf Nauen, Thomas van Leeuwen, Nicolaos Labrou and John Vontas

Pesticide Biochemistry and Physiology 2015, 121, 53–60

DOI: 10.1016/j.pestbp.2015.01.009

In preparation

1. Exploiting the catalytic promiscuity of L-lysine-ε-dehydrogenase for the synthesis of primary alcohols and (a)chiral amines

Tseliou *et al*.

In preparation for Chemistry: A European Journal

2. Substrate scope, applications and structural insights of amine dehydrogenases in asymmetric synthesis of a-chiral Amines

Tseliou *et al*.

In preparation as a review for ACS catalysis